Author/s:
Liu, Lin

Title:
Characterization of new regulators in TNFR1-mediated death signalling

Date:
2020

Persistent Link:
https://hdl.handle.net/11343/252728

Characterization of new regulators in TNFR1-mediated death signalling

Lin Liu

ORCID: 0000-0003-2729-1410

Doctor of Philosophy
August 2020

The Walter and Eliza Hall Institute of Medical Research
Department of Medical Biology
The University of Melbourne

Thesis submitted to the University of Melbourne in total fulfilment of the requirements for the degree of Doctor of Philosophy

Abstract

Tumor necrosis factor (TNF) is a master inflammatory cytokine that can, depending on the circumstances, promote survival and proliferation or induce cell death. Anti-TNF drugs have proven strikingly successful in treating inflammatory diseases such as rheumatoid arthritis (RA), psoriasis and inflammatory bowel disease (IBD) but it is still unclear exactly why. For a long time, it was thought that they work solely by preventing TNF induced transcription of other inflammatory cytokines, but more recently it has been proposed that one of their major anti-inflammatory functions is to prevent TNF induced death. Therefore, understanding the mechanism by which TNF induced death is regulated may enable the conceptualization of newer or improved approaches in treating a variety of inflammation-associated pathologies.

Binding of TNF to its receptor TNFR1 leads to the formation of two distinct signalling complexes. While most previous studies have focused on the membrane-bound, transcription-activating complex (complex-1), the composition and post-translational modifications of the cytosolic, caspase-8-containing, death-inducing complex (complex-2) remain far less well defined.

To analyse TNFR1 complex-2 composition at endogenous levels, we decided to generate FLAG tagged caspase-8 knock-in mouse strains. The reagents for the FLAG tag enable very efficient and specific purification and identification of a FLAG tagged protein and its partners. After some preliminary tests and trials, I decided to use a 3x FLAG tag which has been reported to be 20–200 times more sensitive than other FLAG tags in immunoprecipitation and detection assays. Before generating the mouse strains, in **Chapter 3** I performed extensive *in vitro* comparison of N-terminally or C-terminally 3x FLAG-tagged caspase-8 using a doxycycline (Dox)-inducible stably integrated lentiviral system. The results suggested that when expressed above endogenous levels, the expression and killing activity of caspase-8 was unaffected by a 3x FLAG tag. Interestingly, when expressed at physiological levels, C-terminally 3x FLAG tagged caspase-8 appeared to be equivalent to untagged caspase-8 and marginally more efficient in mediating TNF-induced death and complex-2 formation compared to N-terminally 3x FLAG tagged caspase-8. In addition, I immunoprecipitated TNFR1 complex-2 from cells expressing endogenous levels of 3x FLAG tagged caspase-8 and performed a mass spectrometry (MS) analysis. According to this analysis, Tankyrase-1 (TNKS1/PARP5a/

ARTD5), a member of the poly ADP-ribose polymerase (PARP) superfamily, appears to be a novel interactor of complex-2.

Based on our *in vitro* data, we generated N-terminally or C-terminally 3x FLAG tagged caspase-8 knock-in mice using CRIPSR/Cas9 technology and these mice were characterized in **Chapter 4**. Homozygous N-terminally or C-terminally 3x FLAG tagged caspase-8 knock-in mice were viable, fertile and developed normally, indicating that N-terminally or C-terminally 3x FLAG tagged caspase-8 were expressed and active *in vivo*, at least to heterozygous caspase-8 levels. As expected, the expression of N-terminal or C-terminal 3x FLAG tagged caspase-8 was detectable in tissue and cells from knock-in mice by Western blot and immunofluorescence stain using an anti-FLAG M2 antibody. The 3x FLAG tagged caspase-8 displayed similar tissue distribution and comparable expression levels as endogenous caspase-8. The cell death assay suggested that the primary cells and transformed cells from 3x FLAG tagged caspase-8 knock-in mice responded similarly as wild-type cells to apoptotic and necroptotic stimulations. Moreover, by performing anti-FLAG immunoprecipitation, I successfully purified endogenous TNFR1 complex-2 from knock-in mice derived cells. These data indicated that 3x FLAG tagged caspase-8 knock-in mouse strains are useful tools to study caspase-8 and caspase-8-containing protein complexes at physiological levels.

In **Chapter 5**, I characterized tankyrases-mediated poly(ADP-ribosyl)ation (PARsylation) as a novel checkpoint that limits TNF-induced cytotoxicity. Using primary cells from the 3x FLAG tagged caspase-8 knock-in mice described in Chapter 4, I found that the enzyme tankyrase-1 (TNKS1/TNKS/PARP5a/ARTD5), which was identified by mass spectrometry in Chapter 3, is recruited to the endogenous TNFR1 complex-2. Western blot data indicates that tankyrase-2 (TNKS2/PARP5b/ARTD6) may also be recruited. Tankyrases are poly ADP-ribose polymerases and belong to an ancient group of enzymes that post-translationally modify proteins with ADP-ribose. I found that during TNF signalling, complex-2 becomes poly(ADP-ribosyl)ated (PARsylated) in a tankyrases-dependent manner. Furthermore, tankyrases-specific inhibitors sensitized cells to TNF-induced cell death, which correlated with increased levels of complex-2. This suggested that normally tankyrases help limit TNF induced death. Mechanistically, I showed that tankyrases may modulate the stability of complex-2 by recruiting the E3 ubiquitin ligase RNF146, that in turn promotes ubiquitylation and degradation of complex-2. Moreover, inactivation of tankyrases dramatically increased the killing of the clinical Smac-mimetic (SM) birinapant in a primary acute myeloid leukemia (AML) model.

Taken together, this thesis describes 3x FLAG tagged caspase-8 knock-in mice as new tools to study caspase-8 and caspase-8-containing protein complexes at physiological levels. Furthermore, this study identifies tankyrases-mediated PARsylation as a novel checkpoint in TNF signalling that expands our understanding of how TNF induced death is regulated and provides a rationale to use tankyrases inhibitors for cancer therapy.

Declaration

This is to certify that:

(i) this thesis comprises only my original work,

(ii) due acknowledgement has been made in the text to all other material used,

(iii) the thesis is less than 100,000 words in length, exclusive of tables, maps, bibliographies and appendices.

Lin Liu
22/08/2020

Acknowledgements

First and foremost, I would like to thank my supervisors Prof. John Silke and Dr. Najoua Lalaoui for giving me the opportunity to complete my PhD within the Silke Lab at WEHI. I'm so grateful to have you as my supervisors during this period of my life. Your incredible support, trust and encouragement are something I value hugely. Both of you are extremely busy but you meet with me weekly, making sure that everything is on track. Both of you are top scientists but you encourage me to ''challenge'' you. Your supervision has enabled me to have a very pleasant PhD journey, making me more confident. The most important thing I've learned from you is the correct attitude towards science. It is by no means just to generate data and get it published but is to discover the truth and expand people's knowledge. John, thank you for your amazing knock-in mice strategy. Without this extremely creative design I wouldn't be able to make such interesting discoveries. Nij, thank you for teaching me critical thinking, and being so supportive throughout my PhD, like a sister, in the work and in my life.

I would like to express my appreciation towards my previous supervisors A/Prof. Oliver Sieber, Dr. Sheng Liu and Dr. Anu Sakthianandeswaren. Thank you for giving me the opportunity to study at WEHI, training me with logical thinking and basic skills during the first 1.5 years of my PhD. Oliver, thank you for supporting me to pursue my own research interest and for all your help throughout my PhD.

I would like to acknowledge my PhD committee including Dr. Kate Sutherland, Dr. Tracy Putoczki and A/Prof. Marco Herold for valuable suggestions and kind words of encouragement. I'd like to thank Dr. Keely Bumsted-Obrien for the help and support during my lab switch.

To Silke lab members, past and present, thank you for making Silke lab such an amazing place to do research. Everyone is extremely friendly, approachable and supportive. I feel that Silke lab is like a big family where I've learned how to collaborate with people efficiently. I'd like to thank in particular Diep Chau, Valentin Heim, Zhaoqing Hu, Holly Anderton, Gabriela Brumatti, Natasha Silke and Nima Etemadi. Diep held my hand through the first experiment at Silke lab and many important experiments and had been a continuous source of comfort and support. Valentin, thank you for developing the anti-FLAG immunoprecipitation protocol and being so generous in sharing with me all your tricks in every experiment. Zhaoqing was an extremely talented undergraduate student from INSPIRE program who helped me produce lots

of data in just two months! Holly, thank you for training me with the mouse work and thank you Gabi for the help with AML model and every piece of your nice advice. I'd like to say a big thank you to Natasha, who is a master of cloning. It is unbelievable that she could generate a construct in a week which I'd tried thousands of times but didn't work. Thank you Nima for being so supportive, like a brother, during my PhD and all your kind words.

To my collaborators, thank you all for making the pursuit of science so enjoyable and stimulating. I would like to acknowledge Dr. Andrew Kueh and Dr. Jarrod Sandow. Without your amazing knock-in mice and excellent mass spectrometry skill, I wouldn't be able to make any discoveries in my projects. Thank you for always being extremely patient in answering every of my questions. I'd like to express my appreciation to Prof. Michael O. Hottiger and Dr. Deena Leslie Pedrioli from the University of Zurich. Thank you so much for kindly providing PARG as a gift and collaborating with us in ribosylation mass spectrometry.

I would like to acknowledge the entire previous Cell Signalling and Cell Death Division and the current Inflammation Division. I have been privileged to work amongst such creative thinkers, diligent scientists and generous collaborators. I would also like to thank many people from WEHI, who generously offer help whenever I need.

I'd like to thank everyone in Bioservices, in particular Carmen Epifanio, Carmen Gatt, Marina Patsis and Tracey Ballinger, for taking care of my mouse strains. I'd like to say thank you to WEHI FACS lab, histology lab, purchasing and shipping. There is no way I would have been able to produce this body of work without their assistance.

I thank the Walter and Eliza Hall Institute and the University of Melbourne for hosting my PhD. I thank the Australian Government for the scholarship funding. This generous support has enabled me to pursue my scientific passion.

On a personal note, I want to thank my entire family, whom have showered me with their endearing support and pride throughout my life. Also, I'd like to express my love and appreciation towards my Dog, Bella. Thank you for always being there with me and sharing my worries and success.

Table of Contents

List of Figures

Chapter 1

Chapter 3

Chapter 4

Chapter 5

List of Tables

Chapter 1

Chapter 3

Appendices

Abbreviations

ADPR	ADP-ribose
AML	Acute myeloid leukaemia
ARC	ankyrin repeat cluster
ARTD	ADP-ribosyl transferase
BCL10	B cell lymphoma 10
BER	base-excision repair
BMDM	bone marrow derived macrophage
Cas9	CRISPR-associated protein 9
Casp8	caspase-8
Casp3	caspase-3
cFlip	cellular FLICE inhibitory protein
CHX	cycloheximide
cIAP	cellular inhibitor of apoptosis
CRIA	cleavage-resistant autoinflammatory syndrome
CRISPR	clustered regularly interspaced short palindromic repeats
CYLD	cylindromatosis
DAMPs	damage-associated molecular patterns
DD	death domain
DED	death effector domain
DISC	death-inducing signalling complex
DMEM	Dulbecco's Modified Eagle Medium
DNA	deoxyribonucleic acid
Dox	Doxycycline
DSBs	double-strand breaks
DUB	deubiquitylating enzyme
ECL	enhanced chemiluminescence
EGF	epidermal growth factor
FACS	fluorescence-activated cell sorter
FADD	Fas-associated protein with a death domain
FasL	Fas ligand
FCS	foetal calf serum
FDA	U.S Food and Drug Administration
GFP	green fluorescent protein
GST	glutathione S-transferase
HDR	homology-direct repair
HPS	histidine, proline and serine-rich
HRP	horseradish peroxidase
HUWE1	HECT, UBA And WWE Domain Containing E3 Ubiquitin Protein Ligase 1
IBD	inflammatory bowel disease
IF	immunofluorescence
IgG	immunoglobulin G

IL-3	interleukin 3
IKK	IκB kinase
IP	immunoprecipitation
JNK	c-Jun N-terminal kinase
kDa	kilodalton
LPS	lipopolysaccharide
LUBAC	linear ubiquitin chain assembly complex
MAPK	mitogen-activated protein kinases
MAR	mono(ADP-ribose)
MDFs	mouse dermal fibroblasts
MEFs	mouse embryonic fibroblasts
MIB2	Mind Bomb-2
MK2	MAPK-activated protein kinase 2
MLKL	mixed-lineage kinase domain like
MS	mass spectrometry
NAD	nicotinamide adenine dinucleotide
Nec-1s	Necrostatin-1s
NF-κB	nuclear factor-kappa B
PAGE	polyacrylamide gel electrophoresis
PAMPs	pathogen-associated molecular patterns
PAR	poly(ADP-ribose)
PARP	poly(ADP-ribose) polymerase
PARG	poly(ADP-ribose) glycohydrolase
PBS	phosphate-buffered saline
PBST	phosphate-buffered saline+ Tween20
PCD	programmed cell death
PCR	polymerase chain reaction
PLK1	polo-like kinase 1
PTM	post-translational modification
PVDF	polyvinylidene fluoride or polyvinylidene difluoride
RA	rheumatoid arthritis
RANKL	receptor activator of NF-κB ligand
RDA	RIPK1 kinase-dependent apoptosis
RIPK1	receptor interacting serine/threonine protein kinase 1
RIPK3	receptor interacting serine/threonine protein kinase 3
RHIM	RIP homotypic interaction motif
RNA	ribonucleic acid
ROS	reactive oxygen species
SAM	sterile α-motif
SDS	sodium dodecyl sulphate
SEM	standard error of the mean
SHARPIN	SHANK-associated RH domain-interacting protein
SIRS	systemic inflammatory response syndrome

SM	Smac-mimetic
Smac	second mitochondria-derived activator of caspases (DIABLO)
SSBs	single-strand breaks
TAB	TAK1 binding protein
TAK1	transforming growth factor-β-activated kinase 1
TBK1	TANK Binding Kinase
TLR	Toll-like receptor
TNKS	tankyrase-1
TNF	tumor necrosis factor
TNFR1	tumor necrosis factor receptor 1
TNFSF	tumor necrosis factor superfamily
TRADD	TNFR1-associated death domain protein
TRAIL	tumor necrosis factor-related apoptosis-inducing ligand
TRAF2	TNF receptor-associated factor 2
TWEAK	tumor necrosis factor-like weak inducer of apoptosis
Ub	ubiquitin
UBA	ubiquitin associate domain
WWE	Trp–Trp–Glu
WB	Western blot
WT	wild-type
XIAP	X-chromosome linked IAP

Chapter 1 Introduction

1.1 Apoptotic and necroptotic cell death

Programmed cell death (PCD) plays a crucial role in development and tissue homeostasis. The failure to undergo PCD results in a wide range of human diseases, including immunological disorders and cancer (Fuchs and Steller, 2011).

Apoptosis is the best understood form of PCD, which occurs under normal physiological conditions. It is driven by cysteine proteases which cleave after an aspartate residue and are therefore known as caspases (Thornberry and Lazebnik, 1998). The proteolytic activation of caspases in apoptotic cells causes cell shrinkage, membrane blebbing, aggregation of chromatin and formation of apoptotic bodies. Apoptosis is regulated by mainly two mechanisms: mitochondria dependent (intrinsic) pathway or death receptor dependent (extrinsic) pathway (Salvesen and Duckett, 2002). Intrinsic apoptosis is triggered by intracellular damage or stress signals such us DNA damage and oxidative stress. The extrinsic pathway occurs in response to extracellular stress signals such as damage or pathogen-associated molecular patterns (DAMPs or PAMPs) or cytokines that are detected by usually constitutively expressed receptors (Silke et al., 2015). The upstream signalling events induce dimerization and activation of intrinsic (caspase-9) or extrinsic pathway (caspase-8) initiator caspases which can cleave and activate executioner caspases (caspase-3, -6, and -7). Executioner caspases subsequently coordinate their activities to demolish key structural proteins and activate other enzymes for apoptosis to proceed (McIlwain et al., 2015).

When caspases-mediated extrinsic apoptosis is inhibited, usually by caspase inhibitors or knock-out of caspases, cells undergo a “back up” death pathway, termed necroptosis. Necroptosis is morphologically characterized by organelle swelling, plasma membrane rupture and the release of cellular contents. Unlike apoptosis, necroptosis sends "danger" signals to the immune system (Fuchs and Steller, 2011; Murphy and Silke, 2014). The necroptotic cell death pathway leads to phosphorylation and consequent activation of the kinase RIPK3 which in turn leads to the phosphorylation of MLKL, which is essential for the execution of necroptosis (Murphy et al., 2013; Sun et al., 2012; Wang et al., 2014) **(Figure 1.1)**.

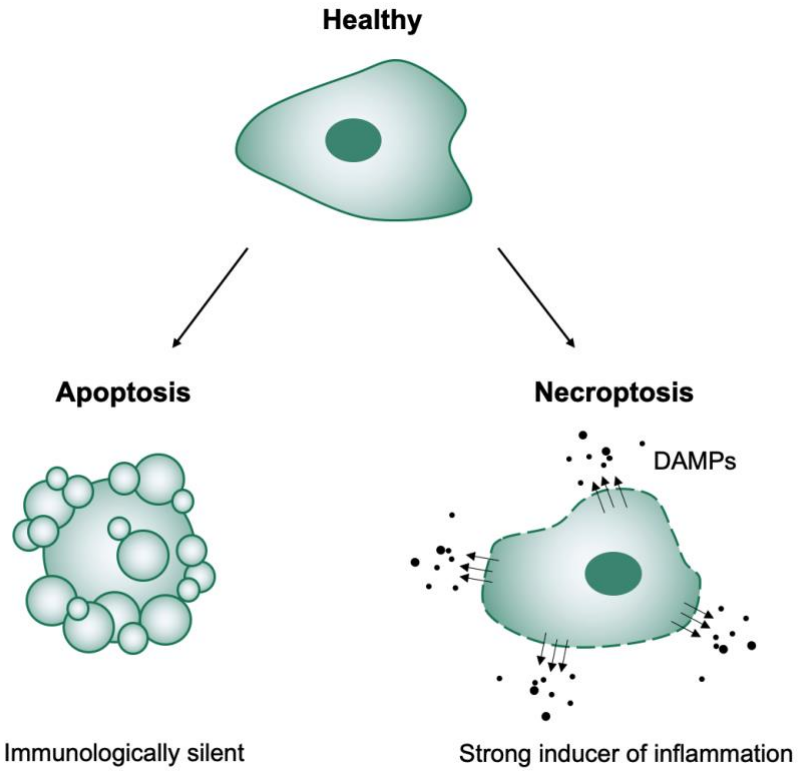

Figure 1.1. Schematic of apoptosis and necroptosis

Healthy cells can undergo programmed cell death to maintain homeostasis. One form of programmed cell death is called apoptosis which is characterized by "packaging" of a cell for rapid and safe disposal and entails cell shrinkage, membrane blebbing, aggregation of chromatin and formation of apoptotic bodies. Necroptosis is characterized by organelle swelling, plasma membrane rupture and the release of cellular contents such as damage-associated molecular patterns (DAMPs). While apoptosis, in many contexts, is immunologically silent, necroptosis acts as a strong inducer of inflammation.

1.2 Tumor necrosis factor (TNF)

Tumor necrosis factor (TNF) is a major pro-inflammatory cytokine with the capacity to induce caspase-dependent death (apoptosis) or caspase-independent death (necroptosis). It was identified in 1975 as a serum factor that caused tumors to necrose (Carswell et al., 1975). It is a 17 kDa soluble protein produced by a wide range of cell types, including monocytes/macrophages, T and B lymphocytes, neutrophils, natural killer cells, fibroblasts and osteoclasts (Grivennikov et al., 2005; Holbrook et al., 2019). It is a very potent cytokine and even though it is often only produced in small amounts in response to PAMPs and DAMPs, it can nevertheless have profound physiological effects (Silke et al., 2015). TNF belongs to a superfamily (TNFSF) which consists of 19 ligands and 29 receptors in human, such as CD95L/ Fas ligand (FasL), TNF-related apoptosis-inducing ligand (TRAIL), CD40L, Tumor necrosis factor (TNF)-like weak inducer of apoptosis (TWEAK) and receptor activator of NF-κB ligand (RANKL). The TNFSF members are involved in the modulation of multiple biological processes including cell proliferation, cell death, immune regulation and morphogenesis. Therefore, they are promising targets for treating diverse diseases like autoimmunity and cancer (Sonar and Lal, 2015; Vanamee and Faustman, 2018).

1.3 TNF-induced survival

Despite its name, it has been shown that in most human and mouse cells the predominant response to TNF is survival. TNF signalling triggers the activation of pro-survival and inflammatory NF-κB and MAPK signalling pathways which requires the formation of an intracellular signalling complex called complex-1.

In brief, binding of TNF to tumor necrosis factor receptor 1 (TNFR1) recruits intracellular adaptors to transmit the extracellular signal intracellularly. Two common adaptors are TRADD and receptor-interacting serine/threonine-protein kinase 1 (RIPK1) which can interact with the intracellular death domain (DD) of TNFR1, though they may not both be recruited in all cells (Chen et al., 2008; Ermolaeva et al., 2008; Pobezinskaya et al., 2008; Silke, 2011). Cellular inhibitor of apoptosis (cIAPs) bound to TRAF2 can be recruited either by TRADD or RIPK1. Within the complex, a cIAP RING dimer ubiquitylates several molecules including the kinase RIPK1 (Silke, 2011). cIAP-mediated ubiquitylation of complex-1 components allows the recruitment of TAK1-TAB2-TAB3, NEMO-IKK1-IKK2 and the E3 ligase linear ubiquitin chain assembly complex (LUBAC, comprising HOIL-1, HOIP and SHARPIN) (Haas et al., 2009). The LUBAC E3 ligase complex generates linear ubiquitin (Ub) chains which stabilize complex-1 and promote the phosphorylation of IKK2 and mitogen-activated protein kinases (MAPKs) by TAK1. Activation of IKK2 and MAPK kinases leads to the transcription of NF-κB-dependent and MAPK-dependent genes that induce inflammation, proliferation, and cell survival such as cFlip, A20 and cIAPs (Feltham et al., 2018; Lalaoui and Vaux, 2018; Micheau et al., 2001). TNF-induced NF-κB activation is terminated at early phases by the deubiquitylating enzyme USP21 and a ubiquitin-editing protein complex comprising A20, TAXBP1, Itch and RNF11 shuts down the later signalling phases (Vanden Berghe et al., 2015).

1.4 TNF-induced death

Within 2 hours of TNFR1 stimulation, the complex-1 matures into a large ~2MDa cytosolic death-inducing signalling complex (DISC) referred to as complex-2, which comprises TRADD, FADD, RIPK1, RIPK3, A20, caspase-8 and the catalytically-dead caspase-8 homolog, $cFlip_L$ (Cho et al., 2009; Micheau and Tschopp, 2003; Onizawa et al., 2015; Tenev et al., 2011). Caspase-8 is the major initiator caspase in the death receptor (extrinsic) pathway of apoptosis. Under normal situations, $cFlip_L$ forms heterodimers with caspase-8 and regulates caspase-8 substrate affinity. The $cFlip_L$:caspase-8 heterodimers cleave local substrates such as RIPK1, and distant substrates such as procaspase-3 and Bid cannot be cleaved so that apoptosis is blocked (Boatright et al., 2004; Hughes et al., 2016). The cleavage of RIPK1 induces the dissociation of complex-2 and prevents RIPK1 from activating RIPK3 and therefore inhibits necroptotic death (Kaiser et al., 2011; Lalaoui et al., 2020; Oberst et al., 2011).

Activated caspase-8 induces apoptosis by cleaving procaspase-3 or Bid. When caspase-8 activity is compromised, the accumulation of RIPK1 causes its autophosphorylation and binding to RIPK3 which promotes its phosphorylation. RIPK3 phosphorylates MLKL, causing MLKL oligomerization and translocation to the plasma membrane which rupture or permeabilize the plasma membrane, triggering necroptosis (Murphy et al., 2013; Silke and Vucic, 2014; Sun et al., 2012; Vandenabeele et al., 2010; Wang et al., 2014).

Whether TNF can lead to lethal levels of complex-2 is determined by multiple check points **(Figure 1.2)**.

1.4.1 Ubiquitylation-dependent checkpoint

The E3 ligases cIAPs and LUBAC generate ubiquitin chains of various linkage types on complex-1 components, which serve as scaffolds that allow the recruitment of kinase complexes. The recruitment and activation of kinases results in NF-κB- and MAPK-dependent production of cytokines and pro-survival proteins such as cFlip. In the absence of either cIAPs or LUBAC, TNF fails to activate canonical NF-κB signalling effectively, so that the levels of $cFlip_L$ are not sufficient to prevent caspase-8-induced apoptosis (Bertrand et al., 2008; Gerlach et al., 2011; Haas et al., 2009).

It is also believed that cIAPs-mediated RIPK1 ubiquitylation tethers RIPK1 in the complex-1. Deletion, a decrease in, or mutation of cIAPs results in a less ubiquitylated form of RIPK1 than

occurs during normal signalling, resulting in its accumulation in complex-2 and promoting cell death (Liu and Lalaoui, 2020). In some cell types, stimulations that inhibit cIAPs allow the formation and activation of a complex called the "ripoptosome". The composition of the ripoptosome is probably indistinguishable from complex-2 but it is formed in the absence of TNF or other death ligands (Estornes et al., 2012; Feoktistova et al., 2011; Tenev et al., 2011). Aberrant IAPs levels have been associated with human cancers and chemoresistance (Fulda and Vucic, 2012). Several small pharmacological molecules targeting IAPs, called Smac-mimetics (SM), have been developed for cancer therapy. SM binds to the BIR domains of the IAPs, preventing XIAPs from inhibiting caspases. SM treatment also triggers auto-ubiquitylation and proteasomal degradation of cIAPs (Silke and Meier, 2013), induces TNF secretion and sensitizes cells to cytotoxicity of TNF (Petersen et al., 2007; Varfolomeev et al., 2007; Vince et al., 2007).

RIPK1 is also ubiquitylated by other E3 ligases. For example, a recent study reported that the E3 ubiquitin ligase Mind Bomb-2 (MIB2) suppresses TNF-mediated death (Feltham et al., 2018). MIB2 causes RIPK1 ubiquitylation, prevents RIPK1 from oligomerization and interferes with the RIPK1-FADD association. In contrast, the ubiquitylation of RIPK1 by E3 ligase PELI-1 facilitates the interaction between activated RIPK1 and RIPK3, promoting the activation of RIPK3 and MLKL and necroptosis (Wang et al., 2017). The deubiquitylating enzyme (DUB) CYLD restricts RIPK1 ubiquitylation and facilitates RIPK1 to accumulate in complex-2, promoting cell death (Moquin et al., 2013).

1.4.2 Phosphorylation-dependent checkpoint

The ubiquitylation of complex-1 enables the recruitment and activation of kinases TAK1, IKK1/2/epsilon and TBK1.

In addition to driving the activation of the NF-κB and MAPK signalling pathway, these kinases directly phosphorylate RIPK1 to block its cytotoxic function by limiting its binding to complex -2 and its kinase activity (Liu and Lalaoui, 2020). MK2, a kinase of the MAPK signalling pathway that is not recruited to the complex-2, also phosphorylates RIPK1 at S321/S336 (mouse) and S320/S335 (human) in response to TNF stimulation. Similar to IKKs, TAK1 and TBK1, MK2 mediated phosphorylation on RIPK1 blocks its autophosphorylation and might interfere with the recruitment of RIPK1 to complex-2 (Liu and Lalaoui, 2020). MK2 also phosphorylates the cytosolic pool of RIPK1 (Dondelinger et al., 2017; Jaco et al., 2017).

1.4.3 Transcription-dependent checkpoint

While TNF simultaneously triggers the formation of the cell death platform complex-2, in most cells its cytotoxic activity is blocked by the production of pro-survival proteins such as cFlip, A20 and cIAPs (Micheau et al., 2001). However, if there is defective activation of NF-κB this incipient cell death platform is no longer held in check and the TNF response switches from survival to death. Cotreatment with the protein synthesis inhibitor cycloheximide sensitises cells to TNF induced cell death and is believed to do so by shutting down the synthesis of pro-survival proteins. In particular, cycloheximide can suppress the induction of endogenous caspase-8 inhibitor cFlip, which allows caspase-8 activation in the complex-2 and induces apoptosis (Hughes et al., 2016; Kreuz et al., 2001). Such inhibition can also be achieved by cFlip siRNA or activation of E3 ligases targeting cFlip, for example Itch (Chang et al., 2006).

1.4.4 Other mechanisms

The death outcome is also managed by the other mechanisms. The E3 ligase Pellino3 has been identified as a negative regulator of TNF-induced apoptosis since it interferes with the recruitment of RIPK1 to complex-2. Interestingly, Pellino3 prevents cell death through its phosphothreonine-binding domain, independently of its RING-like domain that is associated with E3 ubiquitin ligase activity (Yang et al., 2013b).The DUB A20 protects cells from necroptosis by restricting RIPK3 K5 ubiquitylation which supports the RIPK1-RIPK3 complex assembly (Onizawa et al., 2015).

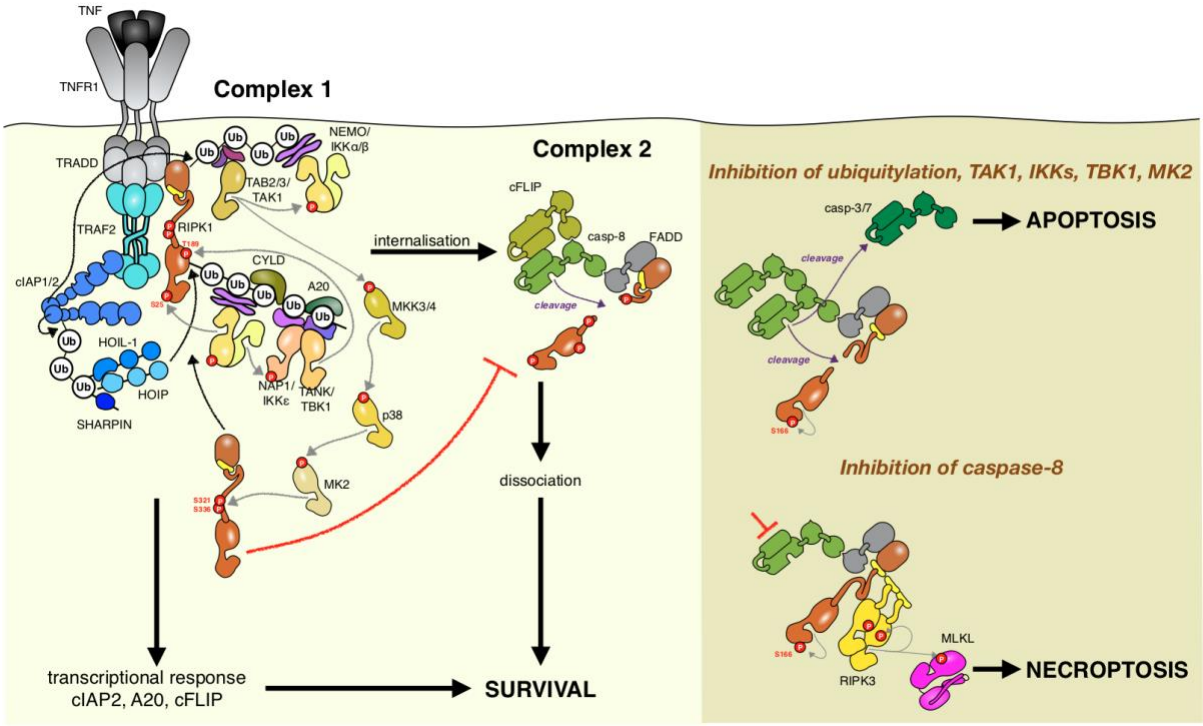

Figure 1.2. TNF induces two sequential complexes

TNF binding to TNFR1 triggers complex-1 formation, in which cIAP1/2 ubiquitylate themselves and RIPK1. The adaptors TAB2/3 and NEMO and the kinases TAK1 and IKK1/2 are recruited to the Ub chains attached to RIPK1, where TAK1 phosphorylates IKK2. The LUBAC complex, composed of HOIL-1, HOIP and SHARPIN, is recruited to the Ub chains attached to cIAPs. LUBAC linearly ubiquitylates RIPK1 and further recruitment of NEMO and IKK1/2 occurs. The adaptors NAP1 and TANK and the kinases IKKepsilon and TBK are recruited to the linear ubiquitin chains, where IKK1/2 phosphorylates IKKepsilon. Complex-1-containing RIPK1 is phosphorylated by IKKepsilon and TBK1. Cytosolic-containing RIPK1 is phosphorylated by MK2. Phosphorylation of RIPK1 inhibits its autophosphorylation and its incorporation to complex-2. Complex-1 formation leads to the induction of NF-κB- and MAPK-dependent genes including the ones encoding cFlip, A20 or cIAP2. Deubiquitylating enzymes A20 and CYLD hydrolyse ubiquitin chains to terminate the transcriptional response. Subsequently, complex-1 internalises to the cytosol to form complex-2 containing FADD, caspase-8, RIPK1 and cFlip. In this complex the heterodimers cFlip/caspase-8 cleave RIPK1 leading to the dissociation of complex-2. Inhibition of ubiquitylation or phosphorylation of RIPK1 accelerates the formation of complex-2 and impairs NF-κB activation reducing cFlip level. RIPK1 auto-phosphorylates inducing its conformation change and caspase-8 cleaves

caspase-3/7 to induce apoptosis. When caspase-8 activation is blocked, RIPK1 and RIPK3 oligomerise and auto-phosphorylate. RIPK3 phosphorylates MLKL and necroptosis is activated. Sourced from (Liu and Lalaoui, 2020).

1.5 TNF-mediated inflammatory diseases and treatment

The role of chronic TNF in mounting inflammatory responses has been observed in many inflammatory diseases such as rheumatoid arthritis (RA), inflammatory bowel disease (IBD), psoriasis (Annibaldi and Meier, 2018; Bradley, 2008).

Rheumatoid arthritis (RA) is a chronic autoimmune inflammatory disorder in which accumulation of inflammatory cells and production of a range of pro-inflammatory cytokines are associated with inflammation of synovial tissue, leading to progressive damage, erosion of adjacent cartilage and bone and chronic disability (Feldmann et al., 1996; Koch et al., 1994). TNF has been shown to play a dominant role in RA and *in vitro* and *in vivo* studies suggested that neutralizing TNF could provide benefits to RA patients (Brennan et al., 1989; Butler et al., 1995; Piguet et al., 1992; Thorbecke et al., 1992; Williams et al., 1992). The spectacular efficacy of anti-TNF therapies in RA has been demonstrated in randomized clinical trials (D'Souza et al., 2010).

TNF has likewise been implicated in causing the pathophysiology of bowel diseases such as Crohn's disease and ulcerative colitis (Breese et al., 1994; Murch et al., 1993). Increased TNF immunoreactivity is observed in intestinal specimens from these patients. Overexpressing TNF in mice drives a Crohn's disease-like inflammatory bowel disease (IBD) (Kontoyiannis et al., 1999). The success of anti-TNF treatments confirms that TNF is causative in Crohn's disease (Adegbola et al., 2018).

Similarly, psoriasis is an inflammatory skin disorder, characterized by inflammatory cell infiltration, leading to hyperkeratotic lesions and typical psoriatic plaques. The inflammation in the affected skin of patients with psoriasis is associated with upregulated TNF, TNFR1 and TNFR2 levels in dermal blood vessels (Ettehadi et al., 1994; Kristensen et al., 1993).

Current anti-TNF therapies fall into two classes: (i) soluble receptor (Etanercept): two extracellular domains of human TNFR2 fused to the Fc fragment of human IgG1; (ii) anti-TNF monoclonal antibodies (Infliximab and Adalimumab) (Wallis, 2011). While these anti-TNF treatments are extraordinarily effective in treating RA, psoriasis and IBD they are not without their limitations. For example, TNF blockade has been reported to cause serious, albeit uncommon adverse reactions. These events include serious bacterial infections, tuberculosis and certain opportunistic infections, demyelinating syndromes and systemic lupus erythaematosus-like reactions (Bradley, 2008). Therefore, patients receiving anti-TNF

treatments need to be monitored closely. It is also critical to have regular updates of analyses of observational databases for emerging problems.

For a long time, it was thought that anti-TNF treatments work solely by preventing TNF induced transcription of other inflammatory cytokines, but more recently it has been proposed that one of their major anti-inflammatory functions is to prevent TNF induced death. This viewpoint is supported by evidence that *Sharpin*-deficient mice (SHARPIN is a component of the LUBAC complex which is recruited to TNFR1 complex-1 upon TNF stimulation) develop dermatitis, multi-organ pathology and an immunological phenotype including disrupted lymphoid architecture, splenomegaly, liver inflammation and a loss of Peyer's patches in the gut (HogenEsch et al., 1993). While TNF-induced pro-survival signalling was compromised in cells from *Sharpin*-deficient mice, these cells were sensitive to TNF-induced death and the production of inflammatory cytokines was not greatly reduced (Gerlach et al., 2011). Furthermore, the TNF-driven systemic inflammation was rescued by the genetic ablation of cell death components, indicating that TNF-dependent cell death causes the inflammatory phenotype (Kumari et al., 2014; Rickard et al., 2014).

Overproduction of TNF has been identified as a key factor in systemic inflammatory response syndrome (SIRS), an uncontrolled inflammatory state that can lead to septic shock, organ dysfunction, and ultimately death (Jit et al., 2005). Injection of high doses of TNF is one mouse model of SIRS (Liu and Lalaoui, 2020). While inhibition of caspases sensitizes mice to TNF-induced septic shock, it was prevented in *Ripk3*$^{-/-}$ (Duprez et al., 2011) and RIPK1 kinase-dead (*Ripk1*^{D138N}) mice (Zelic et al., 2018). Inhibition of RIPK1 kinase activity protected against endothelial cell necroptosis, preventing intestinal breaks, activation of the clotting cascade and organ damage. Consistently, many septic patients show endothelial barrier dysfunction and coagulation defects and high level of RIPK3 has been observed in the plasma of non-survivors of sepsis, suggesting that endothelial necroptosis contribute to sepsis (Liu and Lalaoui, 2020). However, TNF-blocking reagents has shown limited efficacy in a number of clinical trials (Kox et al., 2000). A mathematical model has proposed that the low efficacy of anti-TNF treatments in SIRS may be due to a condition in which the production and inhibition of TNF are not in equilibrium. When free TNF drops to a low level in SIRS, the sequestered TNF-a can act as a slow-release reservoir, thereby sabotaging the effectiveness of TNF-blocking reagents (Jit et al., 2005).

Furthermore, recent studies from our lab and Zhou's lab have characterised a new autoinflammatory disease. We designated the cleavage-resistant RIPK1-induced auto-

inflammatory (CRIA) syndrome (Lalaoui et al., 2020; Tao et al., 2020). This disease is characterized by fevers and pronounced lymphadenopathy beginning in early childhood and continuing throughout adulthood. CRIA patients are heterozygous missense mutations in the D324 of *RIPK1* gene, a residue that is required for cleavage by caspase-8. Homozygous $Ripk1^{D325A/D325A}$ mice died during embryogenesis and the lethality could be completely rescued by the combined loss of caspase-8 and RIPK3 (Lalaoui et al., 2020; Newton et al., 2019; Zhang et al., 2019). Heterozygous $Ripk1^{D325A/+}$ mice were viable and grossly normal, but cells from these mice were hypersensitive to TNF-induced apoptosis and necroptosis, and showed increased levels of pro-inflammatory cytokines (Lalaoui et al., 2020; Newton et al., 2019; Tao et al., 2020; Zhang et al., 2019). Mechanistically, uncleaved RIPK1 stabilises complex-2, leading to apoptosis, necroptosis and cytokine production (Lalaoui et al., 2020).

1.6 Caspase-8

In death-receptor signalling, the assembly of death-inducing signalling complex (DISC) produces an environment conducive for the activation of the initiator caspase, caspase-8. Once activated, caspase-8 initiate the caspase cascade through cleavage of caspase-3 or Bid, ultimately inducing apoptosis. While rodents only contain caspase-8, other mammals also contain caspase-10. Human caspase-10 appears to be a homolog of caspase-8 which is recruited to the DISC upon death receptor engagement (Sprick et al., 2002), but its role in apoptosis is less clear.

1.6.1 Domains and activation

Caspase-8 is synthesized as an inactive proform (procaspase-8, FLICE/MACH/ Mch5), consisting of an N-terminal pro-domain that includes two death effector domains (DEDs), a large catalytic subunit p18, a short linker region and a small catalytic subunit p10 (Zamaraev et al., 2017) **(Figure 1.4A)**. In human, two procaspase-8 isoforms, caspase-8/a (p55) and caspase-8/b (p53) are predominantly expressed (Scaffidi et al., 1997), while murine caspase-8 has only one isoform (p55).

The current model for TRAIL DISC formation proposes that the ligation of ligands to a death receptor triggers the recruitment of an adapter molecule FADD through direct interaction between the death domains (DDs) present on both the death receptor and FADD. This exposes the FADD DED domain, promoting the recruitment of DED-only proteins (procaspase-8 or cFlip). Procaspase-8 interacts with DED of FADD through a pocket in its DED1 and subsequently this molecule of procaspase-8 can act as a scaffold and use its DED2 to recruit an additional molecule of procaspase-8 via its DED1 pocket. This in turn can recruit additional procaspase-8 molecules in a type of chain **(Figure 1.3A)**. Stoichiometric studies show that there are up to 9 procaspase-8 molecules bound to a single FADD protein (Dickens et al., 2012a) **(Figure 1.3A)**. The DED chain model has also been proposed for FasL DISC (Schleich et al., 2012).

A recent cryogenic electron microscopy (cryo-EM) study has suggested that DED chains represent only substructure of DISC platform. Instead, three linear DED chains assemble into oligomeric structures via three types of DED interactions: type I,II, and III. This results in a DED filament structure with a helical symmetry and a right-handed rotation which provides a

platform for procaspase-8 dimerization and activation (**Figure 1.3B**) (Fu et al., 2016; Seyrek et al., 2020).

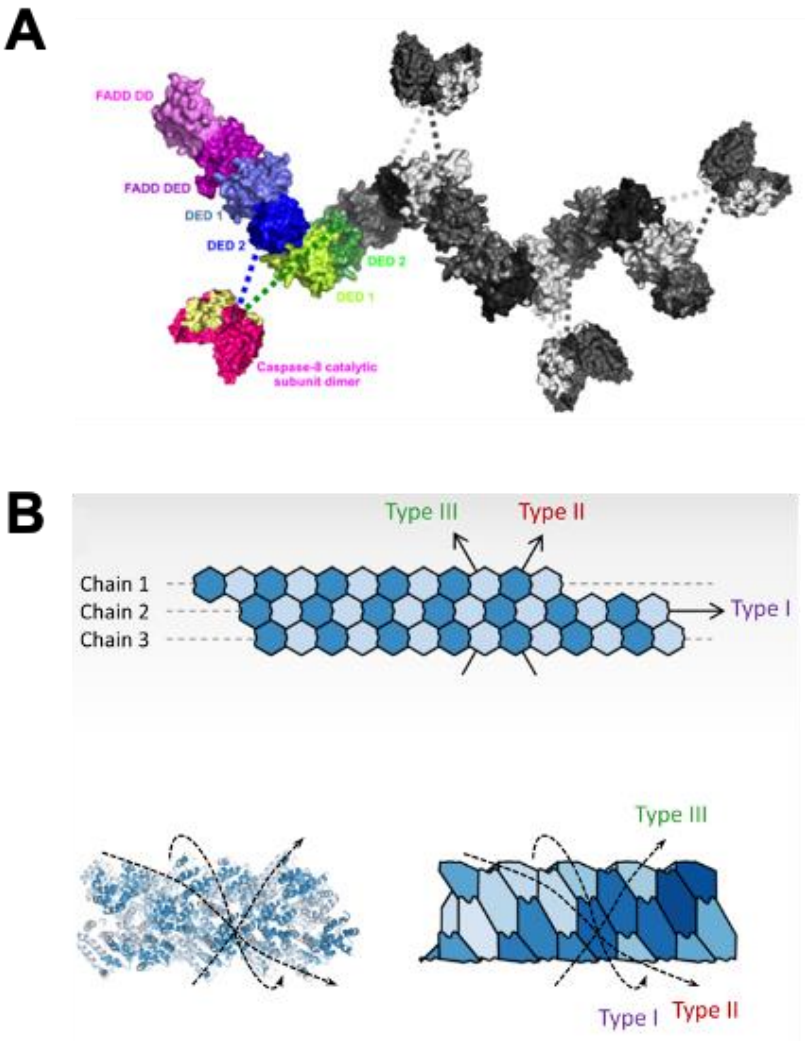

Figure 1.3. TRAIL DISC chain and DED filament

(A) Structural modelling of the interactions that may occur between the DEDs of FADD and procaspase-8 or between adjacent sets of procaspase-8 DEDs. The interaction between FADD DED and one dimer of procaspase-8 is shown in colour. The extended DISC chain is shown in grey. Sourced from (Dickens et al., 2012a).

(B) Scheme of DED filament in 2D and 3D presentation. Broken arrows indicate the directions of type I, II, and III interactions. Adapted from (Seyrek et al., 2020).

In case of FasL or TRAIL signalling, the DISC allows the homodimerization of the proteolytic domains of adjacent procaspase-8 at the plasma membrane. Unprocessed caspase-8 is catalytically active (Chang et al., 2003a; Yu and Shi, 2008). This is supported by the observation that non-cleavable *Casp8*$^{D387A/D387A}$ mutant mice are viable and the thymocytes from these mice are susceptible to CD95-induced apoptosis, which indicates that necroptosis is blocked *in vivo* (Kang et al., 2008; Tummers et al., 2020). However, uncleaved procaspase-8 exhibits a highly restricted substrate range limited to itself, cFlip$_L$ and possibly RIPK1 (Hughes et al., 2009).Within the procaspase-8 homodimer, autoproteolytic cleavage of an aspartate residue (D384 human, D387 mouse) connecting the linker and small subunit (p10) leads to the generation of caspase-8 p43 subunit. In an intradimer manner, the subsequent cleavage of an aspartate (D216 human, D218 mouse) in the region between the prodomain (p26) and the large subunit (p18) leads to fully matured caspase-8, which is released from the DISC to the cytosol as the enzymatically active heterotetramer $(p18)_2(p10)_2$ (Dickens et al., 2012b; Hughes et al., 2009; Kallenberger et al., 2014). Alternative caspase-8 cleavage has also been reported. For example, procaspase-8 can be processed into a prolonged prodomain termed CAP3, which is quickly processed to p26 (Golks et al., 2006). In addition, an 30kDa caspase-8 cleavage product has been observed upon FasL stimulation, which is catalytically active and is further converted to p18 and p10 (Hoffmann et al., 2009).

Release of caspase-8 from the plasma membrane location allows caspase-8 to cleave other substrates and initiate apoptosis **(Figure 1.4B)**. The possible explanation why caspase-8 fully activation requires two-step processing is that the processing of procaspase-8 may lock it into active conformation or help release from the membrane-bound DISC. This increases caspase-8 accessibility to substrates localized remotely from DISC, and also facilitates repetitive cycles of recruitment of new procaspase-8 molecules to the DISC where they are activated and processed (Kang et al., 2008). Caspase-8 induced apoptosis requires both dimerization and interdomain cleavage. *in vitro* studies have suggested that salt-induced dimerization of caspase-8 is sufficient to drive productive activation, and the interchain cleavage greatly enhances the stability of the catalytically active dimer (Pop et al., 2007). However, a following-up study using inducible dimerization and inducible cleavage system demonstrated that both dimerization and cleavage of caspase-8 zymogens are indispensable for efficient caspase-8 activation and apoptosis under physiological conditions (Oberst et al., 2010).

The C360 (human) or C362 (mouse) of procaspase-8 has been shown to be catalytic active site. The procaspase-8 mutant C360A can be recruited to DISC but is not cleaved and doesn't have proteolytic activity (Watt et al., 1999).

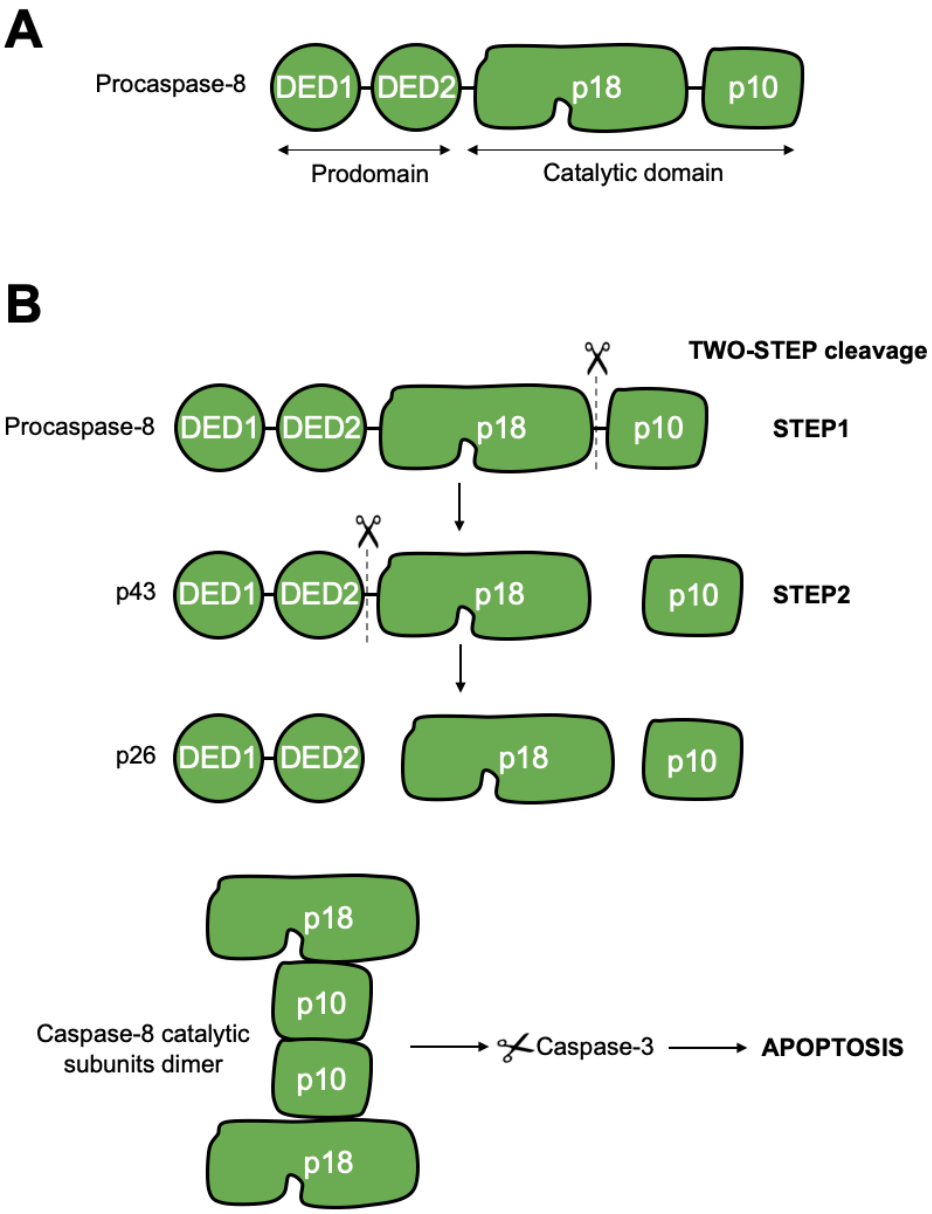

Figure 1.4. Domains of procaspase-8 and its activation

(A) Procaspase-8 consists of a N-terminal pro-domain that includes two death effector domains (DEDs), a large catalytic subunit p18, a short linker region and a small catalytic subunit p10 (Zamaraev et al., 2017).

(B) Full activation of caspase-8 requires two-step proteolytic cleavage: (i) separation of the larger subunits (p43) from the smaller subunits (p10); (ii) cleavage of the larger subunit (p18) from the prodomain (tandem DEDs). Alternative procaspase-8 processing has also been reported. The p18 and p10 subunits form enzymatically active heterotetramer $(p18)_2(p10)_2$ which is released from the DISC to the cytosol (Dickens et al., 2012b; Hughes et al., 2009;

Kallenberger et al., 2014). Release of caspase-8 from the plasma membrane allows caspase-8 to access other substrates and initiate apoptosis.

1.6.2 Regulation of caspase-8 activity

1.6.2.1 cFlip: a natural regulator of caspase-8

cFlip, encoded by gene *CFLAR*, is a natural regulator that determines the activity of caspase-8. *CFLAR* is located on human chromosome 2q33-34 which is 35 kb apart from the gene encoding caspase-8 (*FLICE*), suggesting that these two genes were generated as a result of ancient gene duplication (Tsuchiya et al., 2015). $cFlip_s$ and $cFlip_L$ are the major two isoforms. $cFlip_s$ contains tandem DEDs only, whereas $cFlip_L$ shares extensive homology with procaspase-8 but critically lacks the active site catalytic cysteine residue and therefore has no proteolytic activity. While $cFlip_s$ appears to act purely as an antagonist of caspase-8 activity, the role of $cFlip_L$ is more complex (Irmler et al., 1997; Krueger et al., 2001b; Scaffidi et al., 1999).

$cFlip_L$ was first described as anti-apoptotic due to its ability to block apoptosis at high levels of ectopic expression (Krueger et al., 2001a). At this time, it was assumed that $cFlip_s$ and $cFlip_L$, through DED interactions, compete with procaspase-8 for binding to FADD, therefore interfering with procaspase-8 recruitment and activation at the DISC. However, in many cell lines, the level of endogenous c-$Flip_L$ is merely 1% of that of endogenous procaspase-8 (Scaffidi et al., 1999). At physiological levels, $cFlip_L$ was observed to enhance procaspase-8 activation and apoptosis through heterodimerisation with the procaspase-8 proteolytic domain (Boatright et al., 2004; Chang et al., 2002; Fricker et al., 2010; Micheau et al., 2002). This is because caspase-8 needs to dimerise to become activated and as $cFlip_L$ is so similar to caspase-8 then even heterodimerisation is sufficient to allow the caspase-8 moiety to activate. Heterodimerisation of c-$Flip_L$ with procaspase-8 has been shown to cause rearrangement of the catalytic site of procaspase-8, producing an active conformation (Chang et al., 2002; Micheau et al., 2002; Yu et al., 2009).

A recent study on TRAIL DISC suggests that procaspase-8 binding to FADD is the primary event that initiates the recruitment of cFlip to the DISC in a co-operative and hierarchical manner. $cFlip_{L/S}$ and procaspase-8 form heterodimers and the different signalling outcomes (survival or death) are determined by the composition of the heterodimer. The procaspase-8: $cFlip_s$ heterodimer lacks enzymatic activity. Thus, high levels of $cFlip_S$ potently block procaspase-8 oligomerization and activation. However, $cFlip_L$ displays a biphasic effect. The procaspase-8: $cFlip_L$ heterodimer exhibits enzymatic activity at the DISC which can promote

DED-mediated procaspase-8 oligomer assembly. The alternate signalling outcome is dependent on $cFlip_L$:procaspase-8 ratio within the DISC. At low levels, c-$Flip_L$ act as an activator, promoting procaspase-8 oligomer assembly and apoptosis. In contrast, at high levels of ectopic expression, $cFlip_L$ blocks the DED-mediated recruitment of multiple procaspase-8 molecules to form active DISC. Therefore, this latest model explains how c-Flip isoforms differentially control cell fate and how $cFlip_L$ exhibits dual role in procaspase-8 activation and apoptosis (Hughes et al., 2016).

The proteolytically active procaspase-8:$cFlip_L$ heterodimer has been shown to mediate the survival activity of caspase-8 during embryonic development. Mice deficient in caspase-8 (Varfolomeev et al., 1998) , $cFlip_L$ (Yeh et al., 2000) or FADD (Yeh et al., 1998) present with E10.5 embryonic lethality. The development defects in caspase-8 deficient mice are rescued by RIPK3 ablation, suggesting the primary protective role of caspase-8 at this stage of development is to inhibit RIPK3-dependent necroptosis (Kaiser et al., 2011; Oberst et al., 2011). While non-cleavable $Casp8^{D387A/D387A}$ allows normal development (Kang et al., 2008; Tummers et al., 2020), knockdown of cFlip sensitizes cells expressing non-cleavable $Casp8^{D387A/D387A}$ to TNF-induced, RIPK3-dependent death (Oberst et al., 2011). This observation suggests that the proteolytically active procaspase-8:$cFlip_L$ heterodimer blocks RIPK3-dependent necroptosis. Moreover, the E10.5 embryonic lethality in cFlip deficient mice is not rescued by RIPK3 deficiency but the mice lacking FADD, cFlip, and RIPK3 are normal in embryonic development. This evidence further demonstrates the role of cFlip in preventing apoptosis mediated by the FADD-caspase-8 complex (Dillon et al., 2012).

1.6.2.2 Post-translational modifications

The activity of caspase-8 can be modulated by posttranslational modifications, especially phosphorylation. Phosphorylation of caspase-8 at Ser364 by p38 MAPK or at Thr263 by the RSK2 kinase protects cells from FasL-induced death (Alvarado-Kristensson et al., 2004; Peng et al., 2011). Interestingly, EGF-mediated Thr263 phosphorylation has been shown to cause caspase-8 ubiquitylation and degradation (Peng et al., 2011). EGF stimulation also leads to phosphorylation of caspase-8 at Y380, which is located in the linker region joining the large and small catalytic subunits, by kinases Src, Fyn and Lyn and this site could be regulated by phosphatase SHP1 (Jia et al., 2008; Kurokawa and Kornbluth, 2009). Y380 phosphorylation of caspase-8 does not impair its recruitment to the DISC but may cause the recruitment of other

proteins that hinder maturation in a steric way (Powley et al., 2016). Y380 phosphorylation of caspase-8 can also mediate its interaction with the p85a subunit of PI3K to promote endosome maturation and its translocation to the plasma membrane where it can promote cell migration (Senft et al., 2007; Torres et al., 2008). During mitosis, caspase-8 has been found to be a substrate of cdk1/cyclin B. Ser387 phosphorylation inhibits caspase-8 activation and Fas-induced apoptosis (Matthess et al., 2010). In contrast, during DISC formation, phosphorylation of caspase-8 at residue T273 by polo-like kinase 3 (PLK3) enhances its enzymatic activity (Helmke et al., 2016).

Caspase-8 activation also appears to be altered by ubiquitylation. A cullin3 (CUL3)-based E3 ligase has been shown to induce polyubiquitylation of caspase-8 after its recruitment to the DISC, allowing its binding to the poly-Ub binding protein, p62. The association between p62 and polyubiquitylated caspase-8 enhances caspase-8 aggregation and activation in the DISC, therefore promoting apoptosis. This modification has been found to be reversed by the DUB A20 (Jin et al., 2009).

Nitrosylation has been found to negatively regulate caspase-8 activity. S-nitroslyation of caspase-8 by nitric oxide (NO) inhibits caspase-8 activity and reduces the killing by TNF-a/ActD in hepatocytes (Kim et al., 2000).

1.6.2.3 Structural role of RIPK3 in caspase-8 activation?

While RIPK3 kinase activity is well known to be crucial for necroptosis, it may, also in some circumstances, contribute in a structural capacity to the activation of caspase-8 (Dondelinger et al., 2013; Lalaoui et al., 2020; Mandal et al., 2014; Newton et al., 2014). Initial studies indicated that overexpression of RIPK3 can cause apoptosis (Sun et al., 1999; Yu et al., 1999) In conditions of cIAP1/2 depletion or TAK1 kinase inhibition, RIPK3 has been suggested to promote caspase-8 activation, independently of its kinase activity or intact RHIM domain, through regulating ROS generation (Dondelinger et al., 2013). In contrast, another group suggested that RIPK3-induced apoptosis was not blocked by ROS inhibitor (Mandal et al., 2014). The apoptosis was induced via RHIM domain-driven assembly of ripoptosome-like RIPK1/caspase-8/FADD/cFlip complex (Mandal et al., 2014; Newton et al., 2014). However, a group has reported that in L929, loss of RIPK3 completely blocks necroptosis but induces a switch to RIPK1-dependent apoptosis, suggesting that RIPK3 was not needed for caspase-8 activation in these cells (Remijsen et al., 2014). Therefore, further studies are warranted to

address questions such as the exact role of RIPK3 in caspase-8 activation, the molecular mechanism and whether the effect is cell type dependent.

1.6.3 Caspase 8: roles beyond cell death

In addition to its roles in inducing apoptosis and inhibiting necroptosis, caspase-8 has been found to be involved in multiple non-death biological processes.

1.6.3.1 Molecular scaffold and inflammatory role

The TNFSF members, TRAIL and FasL, kill cells by generating a membrane-localized complex called DISC, where caspase-8 is activated (Kang et al., 2008; Varfolomeev et al., 2005). TRAIL and FasL can also promote cytokine production (Hartwig et al., 2017; Henry and Martin, 2017; Kreuz et al., 2004; Varfolomeev et al., 2005). TRAIL- and FasL -induced cytokine production is not caused by cell death because while cell death is prevented, cytokine production is not. On the other hand, both cell death and cytokine production were suppressed by the loss of caspase-8, suggesting that caspase-8 plays a structural rather than an enzymatic role in this process. Consistently, reconstitution of *CASP8* null HeLa cells with a catalytically inactive caspase-8 mutant rescued TRAIL-induced NF-κB activation and pro-inflammatory cytokine production, but not cell death. In response to TRAIL stimulation, caspase-8 acts as a protease to mediate apoptosis and as a scaffold for assembly of a caspase-8/FADD/RIPK1 containing ‘‘FADDosome’’ complex which induces NF-κB-dependent inflammation (Henry and Martin, 2017).

Caspase-8 also serves as a molecular scaffold during Toll-like receptor (TLR) signalling. It has been observed that upon TLR3 stimuli, caspase-8, independent of its enzymatic role, recruits a FADD/RIPK1/RIPK3 complex and triggers MLKL-dependent NLRP3 inflammasome activation (Kang et al., 2015).

The inflammatory role of caspase-8 has also been revealed by a most recent study using oligomerization-deficient $Casp8^{F122GL123G/F122GL123G}$ and non-cleavable $Casp8^{D387A/D387A}$ mutant mice. While abrogation of necroptosis in wild-type and $Casp8^{F122GL123G/F122GL123G}$ mice did not induce disease, necroptosis deficient $Casp8^{D387A/D387A}$ mice showed an exacerbated inflammatory phenotype. This observation suggests an inflammatory role of caspase-8, which is mediated by its oligomerization, and blocked by its autocleavage and necroptosis (Tummers et al., 2020).

1.6.3.2 Cell proliferation

While the major role of caspase-8 is to induce cell death, it is also essential for proliferation. This paradoxical role has been well established in lymphocytes. In mice, conditional depletion of caspase-8 in the T-cell lineage did not affect thymocyte development but significantly impaired activation-induced proliferation of peripheral T-cells (Salmena et al., 2003). In humans, the deficiency in caspase-8 leads to an immunodeficiency syndrome which is caused by a defect in the activation of T, B and natural killer lymphocytes (Chun et al., 2002).

The role of caspase-8 in B cells is more complex. Mice with B cell-specific caspase-8 deficiency displayed normal B-cell development, but the *in vivo* viral infection-mediated antibody production was attenuated. Furthermore, the B cell proliferation was impaired in response to certain stimuli. While the response to the TLR9 agonist CpG DNA was unaffected, B cell proliferation stimulated by dsRNA, LPS, TLR3 and TLR4 was attenuated (Beisner et al., 2005; Lemmers et al., 2007).

Mechanistically, caspase-8 may mediate proliferation in stimulated lymphocytes through inducing NF-κB activation and nuclear translocation. The caspase-8 deficient lymphocytes showed no NF-κB nuclear translocation after certain stimulations (Chun et al., 2002; Koenig et al., 2008). In T cells, it has been shown that caspase-8 is required for the formation of an active complex which consists of B cell lymphoma 10 (BCL10) and paracaspase MALT1. This complex is essential for the nuclear translocation of NF-κB (Su et al., 2005).

1.6.3.3 Hemopoietic progenitors functioning and macrophage differentiation

Caspase-8 is indispensable for the function of hemopoietic progenitors. Decreased *in vitro* myeloid or B lymphoid colonies formation or colony formation in the spleen of irradiated mice was observed for bone marrow cells with caspase-8 deficiency from pI-pC injected mice. In addition, M-CSF failed to induce differentiation in macrophage precursors that lack caspase-8. This was consistent with previous observations using caspase inhibitors (Kang et al., 2004; Kim et al., 2001; Sordet et al., 2002).

1.6.3.4 Cell cycle

Caspase-8 has been shown to facilitate the growth of human triple-negative breast cancer cell line MDA-MB-231. A delayed G0/G1- to S-phase transition was observed in caspase-8 knockdown MDA-MB-231 cells. Caspase-8 may keep cells permanently in cycle by increasing levels of the transcriptional factor KLF4 which is known to downregulate the cell cycle inhibitors p21 and p27, although this paper only reported a correlation between loss of caspase-8 and increases of KLF4 in these cells (De Blasio et al., 2016).

Caspase-8 is essential for maintaining chromosomal stability. Although mice that lack caspase-8 in the B-cell lineage develop normally and remain tumor free at young ages, these mice have been found to have a shorter lifespan compare with wild-type littermates. 42% of mutant mice bear tumors by 1 year of age with abnormal spindle pole formation and chromosomal segregation defects in *Casp8*$^{-/-}$ B cells. The failure of cytokinesis is associated with elevated genomic instability (Hakem et al., 2012). Mechanistically, it has been recently observed that during mitosis, caspase-8, RIPK1, FADD and cFlip form a ripoptosome which harbors sub-lethal levels of caspase activity. The polo-like kinase 1 (PLK1) is recruited to mitotic ripoptosome where it is cleaved by caspase-8. This can disrupt the interaction between PLK1 and its substrates, such as BUBR1. Defects in PLK1-mediated phosphorylation of BUBR1 can cause chromosomal congression and segregation defects (Liccardi et al., 2019).

1.6.3.5 Cell migration and metastasis

When apoptosis is compromised, caspase-8 can promote integrin-mediated cell motility and invasiveness through enhancing calpain activation (Barnhart et al., 2004; Helfer et al., 2006). During cell migration, caspase-8 was phosphorylated at Y380 which abolished its apoptotic function and facilitated its association with established cell migration components including p85 subunit of phosphatidylinositol 3-kinase and Src (Barbero et al., 2008; Senft et al., 2007). Furthermore, it has been observed that caspase-8 was recruited to a focal adhesion multiprotein complex consisting of focal adhesion kinase and calpain 2 and disrupted calpastatin-mediated inhibition of calpain 2 (Barbero et al., 2009).

1.6.3.6 Caspase-8 as tumor suppressor

The involvement of caspase-8 in cell proliferation, differentiation, and migration reveals a potential nonapoptotic role of caspase-8 in tumor progression. Caspase-8 deficient cells displayed a higher transformation rate compared with the cells expressing caspase-8, suggesting its tumor suppression function (Krelin et al., 2008). This is also supported by the evidence that mice lacking caspase-8 in the B-cell lineage develop B cell lymphoma and loss of caspase-8 contribute to the progression of human cancer such as neuroblastomas (Teitz et al., 2000). Moreover, mutations in caspase-8 has been observed in breast cancer, hepatocellular carcinomas and advanced gastric cancer (Soung et al., 2005a; Soung et al., 2005b; Stephens et al., 2012).

1.7 ADP-ribosylation

ADP-ribosylation is an abundant post-translational modification that happens by the transfer of a single or multiple ADP-ribose (ADPR) moieties from nicotinamide adenine dinucleotide (NAD^+) to substrates (termed mono or poly(ADP- ribosyl)ation, also called MARsylation or PARsylation, respectively). Proteins and other macromolecules such as DNA, or even small chemical groups can be ribosylated. ADP-ribosylation is catalysed by the diphtheria-toxin-like ADP-ribosyl transferase (ARTD) enzyme superfamily, which is alternatively referred to as the poly(ADP-ribose) polymerase (PARP) family (Riffell et al., 2012).

Surprisingly, the first ARTD enzymes identified were bacterial toxins, such as the Cholera and Diphtheria toxins. Once released from bacterial pathogens, bacterial toxins irreversibly modify host proteins to gain an advantage over the infected host (Palazzo et al., 2017). The PARP family of proteins has a highly conserved ADP-ribosyl transferase (ART) domain related to bacterial toxins. Within mammalian cells, several amino acids including lysine (K), arginine (R), aspartic acid (D), glutamic acid (E), cysteine (C), and serine (S) have been identified by proteomic studies as the main acceptor of ADP-ribosylation (Bonfiglio et al., 2017; Daniels et al., 2014; Hottiger, 2015; Leidecker et al., 2016; Martello et al., 2016; Rosenthal and Hottiger, 2014; Sharifi et al., 2013). K residues within a KS modification motif have been shown as substrates of PARP-1 in response to genotoxic stress (Altmeyer et al., 2009; Bilan et al., 2017; Martello et al., 2016). However, more evidence has suggested that serine residues, which usually follow immediately after these lysine residues, are actual modification sites (Bilan et al., 2017; Bonfiglio et al., 2017; Leidecker et al., 2016; Palazzo et al., 2018). The ADP-ribosylation of serine by PARP-1 and PARP-2 requires the coactivator HPF1/ C4orf27 (Bonfiglio et al., 2017; Gibbs-Seymour et al., 2016). Interestingly, serine ADPR has been observed to often overlap with phosphorylation sites on proteins, or compete with other PTMs through steric hindrance (Palazzo et al., 2019).

Like any other post-translational modification, ADP-ribosylation is tightly controlled in the cell, ensuring that suitable cellular responses happen in a timely manner. Such regulation is achieved not only by PARP family, but also by specialized ADP-ribose processing enzymes. Protein ADP-ribosylation can be reversed by several proteins including poly(ADP-ribose) glycohydrolase (PARG). While PARG has lower cellular abundance compared with PARPs, it efficiently cleaves the unique O-glycosidic ribose bonds in poly(ADP-ribose) chains and

allows for rapid turnover of poly(ADP-ribose) (Brochu et al., 1994; D'Amours et al., 1999; Lin et al., 1997; Slade et al., 2011).

Proteins that bind to ADP-ribose have one of three types of evolutionary conserved ADP-ribose binding module: the poly(ADP-ribose)-binding zinc finger (PBZ), WWE domains, and macrodomains. The PBZ module is found only in eukaryotic proteins. In humans, 11 WWE-domain-bearing proteins have been found, but their ability to bind ADP-ribose or PAR varies. Macrodomains are capable of binding PAR and different ADP-ribose metabolites. Some macrodomains have been shown to have evolved enzymatic activity and can process such ADP-ribose metabolites (Barkauskaite et al., 2015). While WWE domains recognize PAR and binds to iso-ADPR linkages joining ADPR monomers, macrodomains recognize MAR and the terminal ADPR moieties in PAR (Gibson et al., 2017; Wang et al., 2012).

1.8 PARPs family and PARP-1

1.8.1 PARP superfamily

In humans, a superfamily of 17 proteins that mediates ADP-ribosylation, termed PARP family, has been identified. These PARP family members share the ‘‘PARP signature motif’’ in the homologous catalytic domain and also possess variant domain structures outside the catalytic domain which may be reflective of their functions. Of these 17 structurally related PARPs, six have been shown to catalyse poly(ADP-ribosyl)ation (PARsylation), including PARP1, PARP2, PARP3, PARP4 (or vault PARP), tankyrase-1 (TNKS1or PARP5a) and tankyrase-2 (TNKS2 or PARP5b). The remaining members were found to mediate mono(ADP-ribosyl)ation (MARsylation): PARP6, PARP7 (or TIPARP), PARP8, PARP9 (or BAL1), PARP10, PARP11, PARP12, PARP13 (or ZC3HAV1), PARP14 (or BAL2), PARP15 (or BAL3) and PARP16 (Riffell et al., 2012) **(Figure 1.5)**.

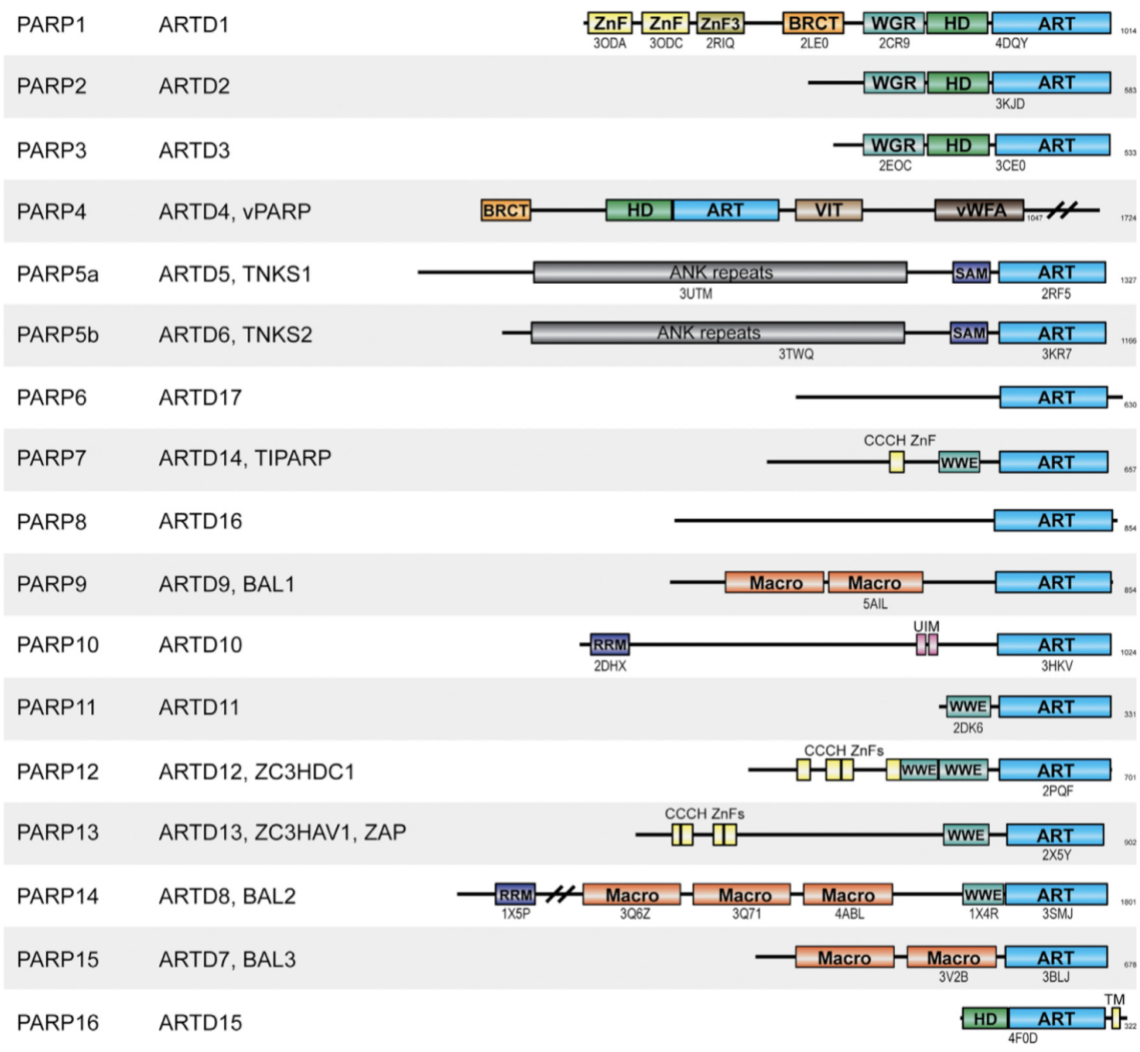

Figure 1.5. PARP superfamily

The PARP superfamily. The 17 human members of the PARP family share a homologous ADP-ribosyl transferase (ART) domain. Tankyrase-1 (TNKS/TNKS1/ARTD5/ PARP5a) and tankyrase-2 (TNKS2/ARTD6/PARP5b) are distinguished from the rest of the PARP superfamily, owing to the unique ankyrin repeat clusters (ARCs) and sterile α-motif (SAM). Sourced from (Barkauskaite et al., 2015).

1.8.2 The structure and function of PARP-1

PARP-1 (ARTD1) is the most well studied enzyme in PARP family. It has an N-terminal DNA binding domain (DBD), a central automodification domain (Rowlands et al.) and a C-terminal catalytic domain (Krishnakumar and Kraus, 2010). The DBD of PARP-1 contains three zinc finger motifs which facilitate its binding to single-strand breaks (SSBs) and double-strand breaks (DSBs) and are important for its catalytic activity. Specific glutamate, aspartate and lysine residues localised in the AMD serve as putative acceptors for PARP-1 auto ADP-ribosylation. The AMD domain also contains a BRCA1 carboxy-terminal (BRCT) motif which mediates protein-protein interaction and a tryptophan-/glycine-/arginine-rich (WGR) domain which is required for PARsylation chain synthesis. The C-terminal catalytic domain transfers the ADP-ribose (ADPR) moiety from nicotinamide adenine dinucleotide (NAD^+) to substrates (Virag et al., 2013).

As a DNA damage sensor, PARP-1 is responsible for the generation of nearly 90% of ribose chains in response to DNA damage (Faraoni and Graziani, 2018). PAR chains provide a docking platform for the recruitment of DNA repair factors (Liu et al., 2017). During apoptosis, activation of caspases causes cell death by cleaving several key proteins required for cellular functioning and survival. One of the first substrates identified, in 1994, was PARP-1 which is cleaved by caspase-3 to yield a 24 kDa and an 89 kDa PARP-1 fragments (Lazebnik et al., 1994). Although the exact consequences of PARP-1 cleavage by caspases are still not clear, two main effects have been observed: (i) decreased PARsylation in response to DNA damage (Soldani and Scovassi, 2002); (ii) the influence on NF-κB activity (Aguilar-Quesada et al., 2007; Castri et al., 2014; Chang and Alvarez-Gonzalez, 2001; Hassa et al., 2008; Lamkanfi et al., 2006; Oliver et al., 1999; Petrilli et al., 2004). Caspase-mediated PARP-1 cleavage can also prevent hyperactivation of PARP-1, which can cause high NAD^+ consumption and passive necroptosis (Chaitanya et al., 2010).

1.8.3 Olaparib: an FDA approved clinical PARP-1/2 inhibitor

The role of PARP-1-mediated PARsylation in DNA repair, and also the fact that cells with defects in DSBs repair such as BRCA-deficient cells are more dependent on PARP-1 and base-excision repair (BER) to maintain genomic integrity prompted the development of PARP-1 inhibitors (Saleh-Gohari et al., 2005). The striking activity of PARP inhibitors either as single-agent or in combination with DNA-damaging agents to treat cancer has been validated by many

in vitro and *in vivo* studies (Bryant et al., 2005; Durkacz et al., 1981; Farmer et al., 2005). To date, several PARP-1 inhibitors have entered clinical practice. For example, Olaparib (AZD2281, Ku-0059436, PARP-1/2 IC_{50} 5nM/1nM, AstraZeneca, London, UK) has shown encouraging single-agent activity in treating BRCA1- or BRCA2-mutant tumours in early clinical testing (Fong et al., 2009; Shen et al., 2015). Recently, more clinical trials have supported the approval of Olaparib tablets by Food and Drug Administration (FDA) for the maintenance treatment of recurrent epithelial ovarian, fallopian tube, or primary peritoneal cancer patients. In addition, Olaparib treatment has been shown to benefit the survival of human epidermal growth factor receptor-2 (Her-2) negative, metastatic breast cancer patients and germline BRCA1/2 mutated (gBRCAm) metastatic prostate cancer patients (Yi et al., 2019).

1.9 Tankyrases

Tankyrase-1 (TNKS/TNKS1/ARTD5/PARP5a) and tankyrase-2 (TNKS2/ARTD6/PARP5b) are distinguished from the rest of the PARP superfamily, owning to a unique domain containing several ankyrin repeats, so called ankyrin repeat clusters (ARCs), and sterile α-motif (SAM). Notably, TNKS1 and TNKS2 are two distinct proteins encoded by different genes, rather than splice variants (Hottiger et al., 2010). Murine TNKS1 and TNKS2 share 82% sequence identity but TNKS2 has a short seven-amino acid insertion between the ankyrin repeats and the SAM domain. In addition, TNKS1 contains an N-terminal histidine, proline and serine-rich (HPS) domain (Lehtio et al., 2013) **(Figure 1.6)**. While PARP-1 has been most studied and serine residues have been identified to be its major substrates during DNA damage, the acceptor amino acids for tankyrases have not been mapped in any of the acceptor proteins (Haikarainen et al., 2014).

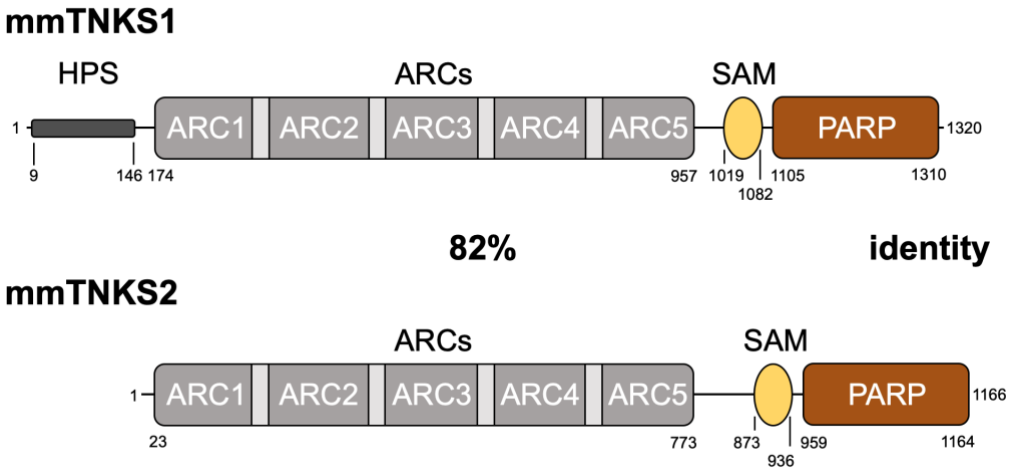

Figure 1.6. Schematic representation of the structures of murine TNKS1 and TNKS2

Murine TNKS1 and TNKS2 are very homologous and share 82% sequence identity. Domains are: HPS: histidine, proline and serine-rich domain; ARCs: ankyrin repeat clusters; SAM: sterile α-motif; PARP: poly(ADP-ribose) polymerases catalytic domain (Lehtio et al., 2013). ARCs provide binding sites for interaction between tankyrases and other proteins. The SAM domain mediates protein-protein interactions, form homo- and hetero-oligomers and also binds to DNA, RNA and lipids. SAM domain is also critical for optimal catalytic activity. The PARP domain (or ART domain) is responsible for the ADP-ribosyl transferase activity.

1.9.1 The structure of tankyrases

1.9.1.1 Ankyrin repeats

The ankyrin repeats of tankyrases can be clustered into five domains called ankyrin repeat clusters (ARCs), which provide multiple binding sites for interaction between tankyrases and other proteins. With the exception of ARC3, ARCs 1, 2, 4, and 5 have a highly conserved binding groove that can recognize a small "consensus" sequence (RXXPXG; X is any amino acid) in the TNKS-binding motif (TBM) of substrate proteins (Haikarainen et al., 2014). A recent study on TNKS-RNF146 interaction has reported an extended TBM: RXXXPXG. This could increase the number of predicted TNKS substrates and interacting partners (DaRosa et al., 2018).

1.9.1.2 SAM domain

Sterile α-motif (SAM) domains are found in many proteins. They are known to mediate protein-protein interactions, form homo- and hetero-oligomers and to bind DNA, RNA and lipids. TNKS1 has been reported to oligomerize through its SAM domain, forming a large protein complex. It is also capable of forming hetero-oligomers with TNKS2. The polymerization of tankyrases is reversible, and can be disrupted by auto-PARsylation (Haikarainen et al., 2014).

In addition to polymerization, the SAM domain is also critical for optimal catalytic activity of TNKS1. Two independent groups, using structural biology and mutagenesis, have revealed that SAM domain-mediated tankyrases polymerization is required for the efficient access of tankyrases to the cytoplasmic destruction complex in canonical WNT signalling (Mariotti et al., 2016; Riccio et al., 2016).

1.9.1.3 Catalytic domain

The C-terminal catalytic domain of TNKS1 and TNKS2 is responsible for their ADP- ribosyl transferase activity, with high (89%) sequence identity. In addition to the same α/β-fold as the other PARPs in their catalytic domain, tankyrases have a unique CHCC-type zinc-finger motif. Although the role of this motif is currently unclear, it may mediate the interaction with its own SAM domain or with other proteins or nucleotides (Lehtio et al., 2008).

The catalytic domain of PARPs contains a binding site for donor (NAD^+) which cleaves NAD^+ to nicotinamide and ADP-ribose, and a site for acceptor which mediates the modification of target proteins or the elongation of PAR chain. In the absence of donor NAD^+, the donor binding site of tankyrases displays a closed conformation due to the lining of a sequence called D-loop. The binding of tankyrases to NAD^+ requires the opening of the D-loop (Haikarainen et al., 2014; Lehtio et al., 2013).

Similar to PARP-1, tankyrases are capable of inducing auto ADP-ribosylation. Furthermore, their catalytic activity can be modulated by posttranslational modifications. For example, insulin or growth factor stimulation leads to phosphorylation of TNKS1 by MAPK in the Golgi (Chi and Lodish, 2000). During mitosis, Polo-like kinase-1 (PLK1), a TNKS1 interactor, phosphorylates TNKS1 and contributes to TNKS1 stability and PARsylation activity (Ha et al., 2012). TNKS1 can also be phosphorylated by GSK3β during mitosis (Yeh et al., 2006). Moreover, a mass spectrometry study has revealed that TNKS2 undergoes hypoxia-inducible factor asparagine hydroxylase (FIH)-induced hydroxylation (Cockman et al., 2009).

1.9.2 The function of tankyrases

1.9.2.1 Tankyrases knockout mice

The functions of tankyrases have been examined *in vivo* using knock-out mouse models. Mice deficient for either TNKS1 or TNKS2 are viable with mild phenotypes. TNKS1 knockout mice are hypermetabolic, with increased food intake and energy expenditure, as well as decreased adipose deposition and plasma leptin levels (Yeh et al., 2009). TNKS2-deficient mice show reduced body size, especially in males. Telomere length maintenance and cell cycle regulation are normal in TNKS1 or TNKS2 knockout mice (Chiang et al., 2008).

Intriguingly, genetic ablation of TNKS1 and TNKS2 results in embryonic lethality at embryonic day E10.5. Although the mechanism underlying the lethality remains to be clarified, the E10.5 *Tnks1*$^{-/-}$*Tnks2*$^{-/-}$ embryos, when compared with wildtype embryos, showed absence of umbilical vessels and abnormal placental development (Chiang et al., 2008). Taken together, these mouse studies have revealed that there is substantial redundancy between TNKS1 and TNKS2 and that tankyrases are essential for embryonic development.

1.9.2.2 WNT signalling

The most well-characterised function of tankyrases is to regulate WNT signalling. Activation of WNT signalling leads to nuclear translocation of the downstream effector β-catenin where it induces the transcription of target genes such as *MYC* and *CCND1* (Li et al., 2012a). In the absence of WNT ligand–receptor interactions, β-catenin undergoes proteolysis mediated by a destructive complex (DC) which contains APC, GSK3β and Axin. GSK3β in the DC phosphorylates β-catenin, resulting in its degradation via proteasome (Hart et al., 1998).

A high-throughput chemical inhibitor screen of the WNT–β-catenin pathway revealed that the tankyrases inhibitor XAV939 dramatically inhibited WNT signalling activity. XAV939 causes β-catenin degradation via stabilizing Axin. Mechanistically, tankyrases associate with Axin and cause its PARsylation. The E3 ubiquitin ligase ring finger protein 146 (RNF146; also known as iduna) recognises the PAR chain on Axin, via its Trp–Trp–Glu (WWE domain), then ubiquitylates Axin, targeting it for proteasomal degradation (Huang et al., 2009; Zhang et al., 2011).

Deregulation of WNT signalling has been observed in cancer progression. Constitutive β-catenin activation causes abnormal cell proliferation, which forms the initiating steps in tumorigenesis. Mutations in the WNT signalling pathway components are observed in 80% of colorectal cancers (Jin et al., 2003; Morin et al., 1997; Powell et al., 1992) and inactivation of tankyrases by XAV939 was found to suppress colony formation in the *APC*-mutant DLD1 colorectal cancer cells (Huang et al., 2009). Decreased cell proliferation after TNKS inhibition or siRNA-mediated abrogation of TNKS expression was also observed for multiple human lung cancer cell lines and human breast cancer cell line MDA-MB-231 (Bao et al., 2012; Busch et al., 2013). These studies suggest that targeting tankyrases by small molecular inhibitors may provide new avenues for treating WNT-related cancers and other diseases (Thorvaldsen, 2017).

1.9.2.3 Ubiquitylation

As with the canonical Axin example, tankyrases-dependent PARsylation can be coupled to ubiquitylation and degradation by the proteasome of other tankyrases substrates. For instance, it has been shown that tankyrases-mediated PARsylation results in ubiquitylation and proteasomal degradation of the telomeric-repeat-binding-factor 1 (TRF1) which then leads to

telomere elongation (Chang et al., 2003b), although the E3 ligase involved in the process remains to be identified.

The E3 ligase RNF146 is widely employed as the ubiquitin ligase that recognizes tankyrases-mediated PARsylation. RNF146 contains a RING domain which mediates its E3 ligase activity, and a Trp–Trp–Glu (WWE) domain which recognizes PAR and binds to iso-ADPR (Gibson et al., 2017; Wang et al., 2012; Zhang et al., 2011). Although the WWE domain containing proteins share low sequence identity, critical residues for iso-ADPR and PAR binding are conserved in most WWE domains, suggesting that a common function of WWE domain is to mediate PAR binding. Indeed, it has been shown that GST-tagged WWE domains from E3 ligases HUWE1, TRIP12, Deltex1, and the PARP superfamily member PARP11 are capable of interacting with PAR polymers (Wang et al., 2012).

Following tankyrases-induced PARsylation, RNF146 can tag the substrate, autoPARsylated tankyrases and even itself for proteasomal degradation (Callow et al., 2011; Zhang et al., 2011). The tankyrases-RNF146 axis has been implicated in regulating the stability of multiple proteins in addition to Axin, including, 3BP2, PTEN, LKB1 and AMOT (Levaot et al., 2011; Li et al., 2019; Li et al., 2015; Wang et al., 2015; Zhang et al., 2011). 3BP2 plays a role in bone formation, while Axin, PTEN, LKB1 and AMOT are associated with tumorigenesis. These studies provide insights into tankyrases-RNF146 axis-mediated diverse biological processes and also uncover tankyrases as drug targets for cancer therapy.

Tankyrases-mediated PARsylation can also cause degradation-independent ubiquitylation. In *Drosophila*, tankyrase has only one homolog and it has been observed to promote JNK signalling activation via triggering PARsylation and the subsequent K63-linked poly ubiquitylation on JNK kinase (Li et al., 2018).

1.9.2.4 Telomere

The Telomere is a structure that caps end of chromosomes. Telomere extension and elongation is specifically mediated by the telomerase enzyme. Telomeric repeat binding factor 1 (TRF1) prevents telomerase from accessing the telomere, therefore blocking extension (Palm and de Lange, 2008). TNKS1 was found to facilitate telomere extension by PARsylating TRF1, causing its degradation (Smith and de Lange, 2000) (Chang et al., 2003b). This process can be modulated by TRF1-interacting nuclear protein 2 (TIN2), which competes with TRF1 in

binding to TNKS1 and therefore prevents TRF1 PARsyaltion and proteasomal degradation (Ye and de Lange, 2004).

TNKS1 and TRF1 are also involved in resolution of telomere cohesion (Bisht et al., 2013; Bisht et al., 2012; Dynek and Smith, 2004; Smith et al., 1998). During cell cycle, the stability of TNKS1 at the telomere is controlled by ubiquitylation /deubiquitylation events. In late S/G2 phase, the E3 ligase RNF8 causes K63-linked polyubiquitylation of TNKS1 to increase its stabilization, association with telomeres, and resolution of cohesion. However, in G1 phase the K63-ubiquitin chains on TNKS1 are cleaved by the deubiquitylate complex BRISC to prevent premature loss of cohesion (Tripathi and Smith, 2017).

1.9.2.5 Mitosis

During mitosis, TNKS1 localizes to spindle poles where it PARsylates multiple proteins. TNKS1 interacts with and induces PARsylation of centrosomal P4.1-associated protein (CPAP), a protein regulates centriole elongation and multipolarity (Kim et al., 2012). During late G2 phase and prophase, Miki is PARsylated by TNKS1 and translocates from the Golgi to mitotic centrosomes, promoting prometaphase (Ozaki et al., 2012). TNKS1 also PARsylates the spindle pore protein NuMA and the PAR chains are believed to be required for bipolarity of spindle assembly (Chang et al., 2009; Chang et al., 2005b).

Phosphorylation events are involved in regulating the stability and PARsyaltion activity of TNKS1 during mitosis. For example, TNKS1 stability and activity is increased by Polo-like kinase-1 (PLK1)-mediated phosphorylation (Ha et al., 2012) . TNKS is also phosphorylated by GSK3β, which may facilitate the association of TNKS1 with NuMA or other spindle associated proteins (Yeh et al., 2006).

1.9.2.6 Insulin-mediated glucose uptake

Insulin-mediated glucose uptake is mediated by GLUT4 storage vesicles (GSVs) containing the glucose transporter GLUT4 and insulin-responsive aminopeptidase (IRAP), which undergo exocytosis and deliver GLUT4 and IRAP to the plasma membrane to facilitate glucose uptake. Tankyrases have been found to associate with IRAP and promote GSV translocation (Patki et al., 2001). Insulin stimulation leads phosphorylation of TNKS1 by MAPK, which enhances its PARP activity and glucose uptake (Chi and Lodish, 2000). TNKS2 also forms a complex with

kinesin-like protein KIF3A and Axin, where it PARsylates GLUT4 and causes GLUT4 degradation. This process can be inhibited by insulin stimulation (Guo et al., 2012).

1.9.2.7 Other functions

Tankyrases have been implicated in cherubism, which is characterized by symmetrical deformities of the facial bones. This syndrome is driven by inflammatory destructive bony lesions (Jones et al., 1950). A mouse model of cherubism has been established by introducing a P416R mutation into *Sh3bp2* locus, resulting in the accumulation of 3BP2 protein (Ueki et al., 2001). Mechanistically, the stability of 3BP2 is regulated by TNKS. TNKS-mediated PARsylation of 3BP2 results in its ubiquitylation by RNF146 and further proteasomal degradation. The P416R mutation is localised in the TNKS binding motif RSPPDG, which abolishes TNKS-RNF146-mediated degradation of 3BP2. This, in turn, causes hyperactivation of the SRC, SYK, and VAV signalling pathways, hyperactive bone-remodeling osteoclasts and elevated TNF secretion by macrophages, resulting in inflammation (Levaot et al., 2011). A follow-up study has suggested that 3BP2-mediated normal osteoclast development is regulated by RANKL, a TNFSF member, which negatively regulates transcription of RNF146 via NF-κB signalling (Matsumoto et al., 2017). These studies have indicated the possible relevance of tankyrases and E3 ligase RNF146 with TNFSF signalling and inflammatory cytokine production.

Following herpes simplex virus (HSV) infection, TNKS1 is phosphorylated by MAPK and is recruited to the nucleus where it colocalizes with HSV replication compartment. Knockdown of TNKS or TNKS inhibitor XAV939 treatment decreased viral growth, indicating that tankyrases are required for efficient HSV replication (Li et al., 2012b).

A recent study has revealed the potential of tankyrases as a target in treating neurodegenerative diseases such as amyotrophic lateral sclerosis (ALS) and frontotemporal degeneration (FTD). Tankyrases interact with TDP-43, an RNA/DNA- binding protein whose abnormal accumulation has been observed in ubiquitin-positive inclusions in the cytoplasm of affected neurons and glia. Instead of targeting TDP-43 for proteasomal degradation, tankyrases stabilize TDP-43 by sequestering it in the cytoplasm for accumulation. Inhibition of tankyrases activity protects primary rodent neurons from TDP-43-associated neurotoxicity (McGurk et al., 2020).

1.9.3 Tankyrases inhibitors

The roles of tankyrases in regulating diverse pathological processes suggest that tankyrases are promising drug targets. TNKS inhibitors could have broad utility, including treating WNT-related cancers and other diseases, targeting telomere dysfunction and mitosis dysregulation. Therefore, there has been increased interest in the development of small-molecule tankyrases inhibitors during the past few years. The tankyrases inhibitors can be divided into subgroups based on their binding mode: the nicotinamide subsite, the adenosine subsite and dual-site inhibitors.

1.9.3.1 The nicotinamide subsite

This group of TNKS inhibitors binds to the nicotinamide subsite in the tankyrases catalytic domain. For example, XAV939 was identified by a high-throughput screen as a small molecule inhibitor of the WNT signalling. XAV939 inhibits TNKS1 and TNKS2 at IC50 (half-maximal inhibitory concentration) of 11nM and 4nM, respectively, but was also shown to inhibit PARP-1 and PARP-2 at higher concentrations (2194 nM for PARP-1 and 114 nM for PARP-2) (Huang et al., 2009). However, this finding has been challenged by a recent study reporting that XAV939 is not a specific inhibitor of tankyrases. XAV939 shows very similar potency toward PARP-1 and PARP-2 as tankyrases (75nM for PARP-1 and 30nM for PARP-2; 95nM for TNKS1 and 5nM for TNKS2) (Thorsell et al., 2017). This could be explained by the fact that the donor NAD^+-binding site targeted by nicotinamide site inhibitors is conserved among PARP superfamily. Since the nicotinamide subsite in TNKS is more hydrophobic and restricted, increasing interest has been put into developing selective TNKS inhibitors by making use of the hydrophobic character of the binding site (Haikarainen et al., 2014).

1.9.3.2 The adenosine subsite

IWR-1 was also identified from a cell-based high-throughput screen for WNT signalling inhibitors (Chen et al., 2009). Instead of targeting the nicotinamide subsite, IWR-1 binds to the adenosine subsite of tankyrases and causes a conformational change that closes a loop within the pocket, preventing nicotinamide binding (Narwal et al., 2012). Since inhibitors binding exclusively to the adenosine subsite have not been described for other ARTDs, these compounds inhibit tankyrases with remarkable specificity. For example, IWR-1, AZ-6102 and

G007-LK have been shown to have high selectivity towards tankyrases over other PARP superfamily members (Thorsell et al., 2017) (**Table 1.1**).

Table 1.1. *In vitro* potency of selected PARP inhibitors

		IC_{50} (nM)			
	Refs	PARP-1	PARP-2	TNKS1	TNKS2
Olaparib	(Thorsell et al., 2017)	1.4	12.3	1230	2340
XAV939	(Huang et al., 2009)	2194	114	11	4
XAV939	(Thorsell et al., 2017)	71.4	26.9	94.6	5.2
IWR-1	(Huang et al., 2009)	>18750	>18750	131	56
AZ-6102	(Thorsell et al., 2017)	1600	990	100	0.6

1.9.3.3 Dual site

The small molecule CMP4b was identified to occupy both adenosine and nicotinamide subsites when binding with TNKS1 (Bregman et al., 2013). Another compound, NVP-TNKS656, was reported by Novartis to utilize both sub-sites (Shultz et al., 2013). Both of these dual site binders appeared to be highly potent tankyrases inhibitors. The PARP-1 inhibitor Olaparib, has also been characterized as a dual site binder. Although it shares similar hydrogen bonding pattern as CMP4b, it shows low potency towards tankyrases, which could be due to unfavorable interactions of this compound with the TNKS binding pocket (Narwal et al., 2012).

1.9.3.4 Challenges

There are some tankyrases inhibitors in preclinical trials that have shown encouraging anti-tumor effects in cultured human cancer cell lines and a subset of CRC xenograft models bearing APC-mutants (Huang et al., 2009; Lau et al., 2013; Okada-Iwasaki et al., 2016; Thorvaldsen, 2017; Waaler et al., 2012; Waaler et al., 2011). However, on-target toxicity in WNT-dependent tissues has been observed and TNKS inhibitors are only effective in a limited concentration range (Lau et al., 2013; Zhong et al., 2016). Therefore, it is necessary to examine whether TNKS inhibitors-induced tissue toxicity is reversible and manageable with an optimized administration regimen. These adverse effects could be potentially minimized by combining TNKS inhibitors with other therapeutic agents. For example, synergistic anti-tumour effects have been observed by using TNKS inhibitors with PI3K or AKT inhibitors (Arques et al.,

2016), tyrosine kinase (EGFR) inhibitors (Casas-Selves et al., 2012; Okada-Iwasaki et al., 2016) and chemotherapeutic agents (Wu et al., 2016) in multiple cancer types.

1.10 Hypothesis and aims

TNF is a master inflammatory cytokine that can, depending on the circumstances, promote survival and proliferation or induce cell death. Binding of TNF ligand to TNFR1 leads to the formation of two distinct signalling complexes (Micheau and Tschopp, 2003). The membrane bound, transcription activating, complex (complex-1) stimulates transcriptional responses and cell survival, and the cytosolic, caspase-8 containing, death inducing, complex (complex-2) can trigger cell death (Lalaoui and Vaux, 2018).

Over the past few years, most studies have focused on complex-1 and it has been revealed that TNF signalling is heavily regulated by a plethora of post-translational modifications (PTMs), including phosphorylation and diverse types of ubiquitin chains. These PTMs, together with TNF-mediated transcriptional responses, serve as checkpoints that control the formation and cytotoxic potential of complex-2 (Annibaldi and Meier, 2018; Liu and Lalaoui, 2020).

Since it was discovered in 2003 (Micheau and Tschopp, 2003), the composition and post-translational modifications in complex-2 remain far less well defined. This could be due to the lack of highly efficient and specific tools. In the past few years, our knowledge of its composition was limited to only a few components such as TRADD, FADD, caspase-8, cFlip, RIPK1, RIPK3 and A20. However, it has been shown that complex-2 is a large ~2MDa cell death-inducing platform (Micheau and Tschopp, 2003; Tenev et al., 2011). Therefore, **we hypothesized that** there are novel interactors/post-translational modifications (PTMs) in TNFR1 complex-2.

My PhD project has **three aims**:

(i) Characterize novel interactors in complex-2.

(ii) Identify new post-translational modifications in complex-2.

(iii) Understand the mechanism by which the novel regulator and post-translational modifications may regulate TNF-induced death.

Chapter 2 Materials and Methods

2.1 Cell culture

Mouse embryonic fibroblasts (MEFs), mouse dermal fibroblasts (MDFs), bone marrow derived macrophages (BMDMs), human colonic adenocarcinoma HT29 cell lines, human fibrosarcoma HT1080 cell lines, human embryonic kidney 293T (HEK293T) cells were cultured in Dulbecco's Modified Eagle's Medium (DMEM) supplemented with 8% (v/v) Fetal Calf Serum (FCS). Leukemic cells were cultured in Iscove's Modified Dulbecco's Media (IMDM) supplemented with 10% FCS (v/v) and 2.5 ng/mL IL-3. All cells were cultured at 37°C in a 10% CO2 humidified atmosphere. Cells were routinely screened for mycoplasma using the MycoAlert kit (Lonza, Switzerland) according to manufacturer's instructions.

2.1.1 Isolation of primary MEFs and immortalization

Primary mouse embryonic fibroblasts (MEFs) were generated from E13.5 embryos. After removing the placenta, yolk sac, head and the dark red organs, embryos were finely minced and crushed through a 100-micron cell strainer. Cells were resuspended in DMEM supplemented with 8% (v/v) FCS and then plated on to 6 well plates coated with 1% gelatin. SV40 large T antigen lentivirus were used to immortalize MEF cell lines.

2.1.2 Isolation of primary MDFs and immortalization

Mice tails were collected and wiped with 70% ethanol. Following a longitudinal incision down the tail, the skin was peeled off using suing tweezers and incubated with serum free DMEM + disphase II (Roche 10805300, 2.1 U/mL) at 37°C for 2 hours. The thin outer layer (epidermis) were then peeled off and incubated with serum free DMEM + collagenase (420 μg/mL, Sigma C5138) at 4°C for 24 hours. Collagenase treated dermis was mashed and crushed through a cell strainer (100-micron) by using plunger of syringe. The flowthrough was pelleted down by centrifugation (300 g, 5 min) and cells were re-suspended in DMEM supplemented with 8% (v/v) FCS. SV40 large T antigen lentivirus were used to immortalize MDF cell lines.

2.1.3 Generation of BMDMs

Bone marrow (BM) was flushed out from tibia and femur of mice in phosphate buffered saline (PBS) by using syringes. After pelleting down by centrifugation (300 g, 5 min), BM cells were resuspended and plated in non-coated petri dishes and cultured for 6 days in DMEM supplemented with 8% (v/v) FCS + 20% (v/v) L929 mouse fibroblast conditioned medium.

2.2 Genetic manipulation

2.2.1 Generation of constructs

All vectors are listed in Table 1 in Appendix 1. In brief, inserts were generated by mutagenesis polymerase chain reaction (PCR) fragments and sub-cloned into the pFTRE3G vector backbone. Fragments and vectors were ligated following BamH1/Nhe1 restriction digestion.

2.2.2 Generation of shRNAs

The Dox-inducible pF H1tUTG-GFP shRNA vector was kindly provided by A/Prof. Marco Herold. The sequences of shRNAs are listed as following:

shRNF146 sense: 5'-tcccATTTCTGCCCACGTAACATTATtcaagagaTAATGTTACGTGG GCAGAAATtttttc-3';

shRNF146 antisense: 5'- tcgagaaaaaATTTCTGCCCACGTAACATTAtctcttgaaTAATGTTA CGTGGGCAGAAAT-3';

shLuciferase sense: 5'-tcccTGCGTTGCTAGTACCAACTtcaagagaGTTGGTACTAGCAAC GCAttttttc-3';

shLuciferase antisense: 5'-tcgagaaaaaTGCGTTGCTAGTACCAACtctcttgaaGTTGGTACTA GCAACGCA-3'

shRNAs and pF H1tUTG-GFP vectors were ligated following XhoI/BsmBI restriction digrestion. Restriction enzymes, T4 DNA ligase and corresponding buffers were used as per manufacturer's instructions (New England Biolabs, MA). Ligation products were transformed into XL1-Blue competent cells (Agilent Technologies) and constructs were purified by miniprep kit (QIAGEN). Construct sequences were verified by Sanger sequencing performed by the Australian Genome Research Facility (AGRF).

2.3 Transfection and infection of mammalian cells with lentivirus

Constructs were first introduced into HEK293T cells by Effectene transfection reagent (QIAGEN), together with pCMV VSV-G and pCMV ðR8.2 plasmids non-replicating lentivirus assembly. 48 hours after transfection, lentivirus was harvested by filtering HEK293T medium supernatant and was used to infect target cells. Cells stably transduced with the pFTRE3G constructs were selected using puromycin (5 µg/mL, Thermo Fisher). shRNA expressing cell lines were sorted by fluorescence-activated cell sorting (FACS) for GFP fluorescent signal (excitation/emission= 488/509 nm).

2.4 Cell death assay

2.4.1 Flow cytometry

2 x 10^4 MEFs or MDFs were seeded in 96 well plates and 2 x 10^5 BMDMs were seeded in 48 well plates. 24 hours later cells were treated as indicated for the indicated times. Cells were then trypsinized and collected into 1.2 mL FACS tubes. Propidium iodide (PI, 1 mg/mL) were added and cells were spun down at 300 g for 5 min at 4°C. PI signal was excited by Blue laser (488 nM) and the emission was received through B660LP filter. 1x10^4 of MLL-AF9/NRas^{G12D} cells were seeded in 96 well plates and as indicated for the indicated times. Cell death was analysed by flow cytometry using a FACSCalibur (BD Biosciences).

2.4.2 Time-lapse imaging (IncuCyte)

Percentage cell death was assayed every 45 min to 1 hour by time-lapse imaging using the IncuCyte live cell analysis imaging (Essenbioscience) for 17-22 hours with 5% CO2 and 37 °C climate control. For the IncuCyte imaging, dead cells were identified by PI (0.25 µg/mL) staining. PI was added to the cells 2 hours before imaging and compounds were added 10 min before the start of imaging. Dead cells were counted using the in-built 'Basic' analysis software and PI positive cells were calculated based on the imaged area.

2.5 Immunoblotting

Cell lysates were prepared in DISC lysis buffer (150 mM sodium chloride, 2 mM EDTA, 1% Triton X-100, 10% glycerol, 20 mM Tris pH 7.5, 1 x final concentration of Protease Cocktain (Roche) and 1 x final concentration of PhosSTOP (Roche)). Lysate or pulldown samples were denatured by boiling at 100°C for 15min in sodium dodecyl sulphate (SDS)-loading buffer (1% SDS (w/v), 100 mM Tris-Cl pH=6.8, 15% glycerol (v/v), 9 µg/mL bromophenol blue, 25 mM dithiothreitol or β-mercaptoethanol). Lysates were then run on SDS-polyacrylamide gel electrophoresis (SDS-PAGE) gradient gels (Bio-Rad), transferred to polyvinylidene fluoride (PVDF, Millipore, MA) membrane and blotted with indicated antibodies. All antibodies are listed in Table 5 in Appendix 3. Bound antibodies were visualised by X-Ray Hyperfilm (Bio-Strategy) or Chemidoc Touch Imaging System (Bio-Rad) using enzyme-linked chemiluminescence (ECL; Immobilion Western, Millipore or Amersham ECL, GE Healthcare Life Sciences).

2.6 Immunoprecipitation

2.6.1 Complex-1 purification

MEFs were seeded in 15 cm dishes and treated as indicated with Fc-TNF (1 µg/mL). Media was removed and plates were washed with ice cold PBS. Cells were lysed on ice for 30min in DISC lysis buffer. Cell lysates were clarified at 4°C at 15,000 rpm for 15 min. Proteins were immunoprecipitated with protein A Sepharose (40 µL/sample, WEHI antibody facility) for 4 hours at 4°C. Beads were washed 4 times with DISC lysis buffer and samples were eluted by boiling in 1x SDS loading buffer at 100°C for 15min.

2.6.2 Complex-2 purification

Cells were seeded in 15 cm dishes and treated as indicated. Media was removed and plates were washed with ice cold PBS. Cells were lysed on ice as above and the lysates were clarified at 4°C at 15,000 rpm for 15 min. After blocking for 1 hour at 4°C with DISC lysis buffer containing 2% BSA, protein G or protein A Sepharose (20 µL/sample, WEHI antibody facility) were bound with indicated antibody (1.5 µg antibody/ sample) and incubated with protein lysates at 4 °C for overnight. Beads were washed 4 times with DISC lysis buffer and samples were eluted by boiling in 1x SDS loading buffer. For anti-FLAG immunoprecipitation, ANTI-

FLAG® M2 Affinity Gel (15 µL/sample, Sigma) were blocked with DISC lysis buffer containing 2% BSA for 1 hour at 4°C and incubated with protein lysates at 4 °C for overnight. After washing 4 times with DISC lysis buffer, samples were eluted with FLAG peptides (1mg/mL, Apex Bio) and denatured by boiling in 5 x SDS loading buffer at 100°C for 15min.

2.7 GST pulldown assay

2.7.1 Purification of recombinant protein and enrichment of PARsylated proteins

Plasmids pGEX 6P3 hs GST RNF146 WWE, pGEX 6P3 hs GST RNF146 WWE R163A, pGEX 6P3 hs HUWE1 WWE, pGEX 6P3 mm TRIP12 WWE, pGEX 6P3 AF1521 (Gibson et al., 2017; Wang et al., 2012; Zhang et al., 2011) were designed by Prof. John Silke (WEHI, Australia) and generated by Genscript (Nanjing, CN). Plasmids were transformed into BL21 *E. coli* (DE3) (Thermo Fisher) and grown at 37°C to an optical density (600 nm) of ~0.6-0.8 in Super Broth before protein expression was induced with 1 mM IPTG (Sigma) for overnight at 18°C. Recombinant protein was purified by Glutathione Xpure Agarose Resin (UBPBio) and size exclusion chromatography (SEC). BMDMs, MEFs or MDFs were treated as indicated and cells were lysed in DISC lysis buffer supplemented with 5 µM ADP-HPD (Enzo). Equal protein amounts were incubated with Glutathione Sepharose® 4B (GE Healthcare) charged with GST fusion proteins for overnight at 4°C. After washing 4 times with PBST buffer (PBS + 0.2% Tween-20 (Sigma)), samples were eluted by boiling at 100°C in 1x SDS loading buffer for 15min.

2.7.2 Enrichment of ubiquitylated proteins

GST-UBA1 fusion protein was produced by Aleksandra Bankovacki (WEHI, Australia). MEFs or MDFs were treated as indicated and cells were lysed in DISC lysis buffer supplemented with 10 mM NEM (Sigma) and incubated with Glutathione Sepharose® 4B (GE Healthcare) pre-coupled with GST-UBA1 fusion protein for overnight at 4°C. After washing 4 times with PBST buffer, samples were eluted by boiling in 1x SDS loading buffer at 100°C for 15min.

2.8 PARG treatment

Recombinant PARG was a gift from Prof. Michael O. Hottiger (University of Zurich). Immunoprecipitated TNFR1 complex-2 was eluted with FLAG peptides and the immunoprecipitants were diluted with 2x PARG reaction buffer (100 mM KH_2PO_4, 100 mM KCl, 0.2 mg/mL BSA, 0.2% Triton X-100). Recombinant PARG (7.2 µg/sample) was added and the reaction mixture was incubated at 37°C for 3 hours, followed by GST-WWE or GST-AF1521 pulldown for overnight at 4°C.

2.9 Mass spectrometry

After anti-FLAG immunoprecipitation, samples were eluted with FLAG peptide and then added to a filter-aided sample preparation (FASP) column (supplied by Dr Jarrod Sandow, WEHI, Australia) and spun (14,000 g) until volume hadpassed through the column. Protein material was reduced with tris(2-carboxyethyl) phosphine (TCEP; 10 mM final) and digested overnight with 2 µg sequence-grade modified trypsin Gold (Promega, V5280) in 50 mM ammonium bicarbonate (NH4HCO3) at 37°C. Peptides were collected into microvial tubes and acidified with formic acid (FA) to a final concentration of 1% (v/v). Samples were frozen at -80°C and subsequently lyophilised.

Peptides were resuspended in 2% (v/v) acetonitrile (ACN) and 1% (v/v) FA and injected and separated by reversed phase liquid chromatography on a M-class UHPLC system (Waters, USA) using a 250 mm x 75 mm column (1.7mm C18, packed emitter tip, Ion Opticks, Australia) with a linear 90 min gradient at a flow rate of 400 nl/min from 98% (v/v) solvent A (0.1% (v/v) FA in Milli-Q water) to 35% (v/v) solvent B (0.1% (v/v) FA, 99.9% (v/v) ACN). The nano-UHPLC was coupled on-line to a Q-Exactive Orbitrap mass spectrometer equipped with an EASY-spray ionization source (Thermo Fisher Scientific, Germany). The Q-Exactive was operated in a data-dependent mode, switching automatically between one full-scan and subsequent MS/MS scans of the ten most abundant peaks. The instrument was controlled using Exactive series version 2.8 build 2806 and Xcalibur 4.0. Full-scans (m/z 350–1,850) were acquired with a resolution of 70,000 at 200 m/z. The 10 most intense ions were sequentially isolated with a target value of 1e5 ions and an isolation width of 2 m/z and fragmented using higher-energy collisional dissociation with stepped normalised collision energy of 19.5, 26, 32. Maximum ion accumulation times were set to 80 ms for full MS scan and 200 ms for MS/MS.

All raw files were analyzed by MaxQuant v1.6.10.43 software using the integrated Andromeda search engine. Data was searched against the mouse Uniprot Reference Proteome with isoforms (downloaded March 2018) and a separate reverse decoy database using a strict trypsin specificity allowing up to 2 missed cleavages. The minimum required peptide length was set to 7 amino acids. Modifications: Carbamidomethylation of Cys was set as a fixed modification, while N-terminal acetylation of proteins and oxidation of Met were set as variable modifications. First search peptide tolerance was set at 20 ppm and main search set at 4.5 ppm (other settings left as default). Matching between runs and LFQ quantitation was turned on. Maximum peptide mass [Da] was set at 8000. All other settings in group or global parameters were left as default.

Further analysis was performed using a custom pipeline developed in R (3.6.1), which utilizes the LFQ intensity values in the MaxQuant output file proteinGroups.txt. Proteins not found in at least 50% of the replicates in one group were removed. Missing values were imputed using a random normal distribution of values with the mean set at mean of the real distribution of values minus 1.8 s.d., and a s.d. of 0.3 times the s.d. of the distribution of the measured intensities. The log2 fold changes and probability of differential expression between groups was calculated using the Limma R package (3.4.2). Probability values were corrected for multiple testing using Benjamini–Hochberg method.

2.10 Immunofluorescence staining (IF) and confocal imaging

5×10^3 to 1×10^4 of the respective cells were seeded per well in 8-well chamber slide chamber µ-slides (Ibidi). Following overnight incubation for adherence, cells were stimulated as indicated. Subsequently, cells were fixed with ice cold methanol for 20 min, washed with PBS, and incubated with anti-FLAG M2 antibody (Sigma F1804) at room temperature (RT) for 1 hour. Following washing in PBS, samples were probed with the specific secondary antibody (Thermo Fisher; goat anti-mouse AF488; 1:500) at RT for 50 min. On harvest, cells were stained with DAPI (Roche) for 10 min. All images were obtained by using a confocal laser scanning Leica TCS SP8 microscope, with z-stacks obtained using a 40x objective.

2.11 Preparation of Mouse Organs for Immunoblotting

Organs were harvested from euthanised mice and snap frozen using liquid nitrogen and stored at -80°C. Organs were homogenised in DISC lysis buffer with 1 x final concentration of Protease Cocktain (Roche) and 1 x final concentration of PhosSTOP (Roche) using a Dounce homogeniser. Lysates were clarified at 4°C at 15,000 rpm for 15 min. The concentration of protein in soluble supernatants was determined by bicinchoninic acid (BCA) assay (Thermo Fisher) according to manufacturer's instructions. Equal amounts of protein were loaded per well and SDS-PAGE was run as previously described.

2.12 Genotyping

Genomic DNA from mice tissue was obtained using DirectPCR Lysis Reagent (Viagen Biotech; Los Angeles, CA, USA) with proteinase K (Sigma) as per manufacturer instructions. In brief, sample tissue (ear clips or tails) from mice was resuspended in 130 µL of Direct PCR mix for 2 hours at 56°C with agitation and then proteinase K was inactivated by brief incubation of samples at 95°C for 15 min. 1 µL of sample mix was added to GoTaq Green Master Mix (Promega, WI) in a 10 µL final volume as per manufacturer's instructions with 300 nM of the appropriate primers. After PCR, products were run on 1.5-2% agarose gels and visualised using ethidium bromide staining. Primer are listed in Table 3 in Appendix 2.

2.13 Statistical analyses

The number of independent experiments for each dataset is stipulated in the respective figure legend. The employed statistical analyses are stipulated in the respective figure legend and performed using Prism v.8.2 (GraphPad).

Chapter 3 In vitro comparison of N-terminal or C-terminal end FLAG-tagged caspase-8 by using doxycycline-inducible lentiviral system

Introduction

Tumor necrosis factor (TNF) is a master inflammatory cytokine that can, depending on the circumstances, promote survival and proliferation or induce caspase-dependent death (apoptosis) or caspase-independent death (necroptosis). TNF stimulation induces the formation of at least two signalling complexes: the membrane-bound complex (complex-1) that promotes the production of pro-inflammatory cytokines, and a cytosolic complex (complex-2) that initiates cell death (Micheau and Tschopp, 2003).

In brief, binding of TNF to tumor necrosis factor receptor 1 (TNFR1) recruits intracellular adaptors TRADD and RIPK1 (Chen et al., 2008; Ermolaeva et al., 2008; Pobezinskaya et al., 2008; Silke, 2011). Cellular inhibitor of apoptosis (cIAPs) bound to TRAF2 can be recruited either by TRADD or RIPK1 where a cIAP RING dimer ubiquitylates several molecules including the kinase RIPK1 (Silke, 2011). cIAP-mediated ubiquitylation of complex-1 further leads to the assembly of TAK1-TAB2-TAB3, NEMO-IKK1-IKK2 and the E3 ligase linear ubiquitin chain assembly complex (LUBAC, comprising HOIL-1, HOIP and SHARPIN) (Haas et al., 2009). The LUBAC E3 ligase complex stabilizes complex-1 via generating linear ubiquitin (Ub) chains, promoting the phosphorylation of IKK2 and mitogen-activated protein kinases (MAPKs) by TAK1. Activation of IKK2 and MAPK kinases causes the transcription of NF- κB-dependent and MAPK-dependent genes that induce inflammation, proliferation, and cell survival such as cFlip, A20 and cIAPs (Feltham et al., 2018; Lalaoui and Vaux, 2018; Micheau et al., 2001).

Within 2 hours of TNFR1 stimulation, the complex-1 matures into a large ~2MDa cytosolic death-inducing signalling complex (DISC) referred to as complex-2, which comprises TRADD, FADD, RIPK1, RIPK3, A20, caspase-8 and the catalytically-dead caspase-8 homolog, $cFlip_L$ (Cho et al., 2009; Micheau and Tschopp, 2003; Onizawa et al., 2015; Tenev et al., 2011). In death-receptor signalling, the assembly of DISC produces an environment conducive for the activation of the major initiator caspase, caspase-8.

Caspase-8 is synthesized as an inactive proform (procaspase-8, FLICE/MACH/ Mch5), consisting of an N-terminal pro-domain that includes two death effector domains (DEDs), a

large catalytic subunit p18, a short linker region and a small catalytic subunit p10 (Zamaraev et al., 2017). It has been suggested that the DISC allows the homodimerization of the proteolytic domains of adjacent procaspase-8. Within the procaspase-8 homodimer, autoproteolytic cleavage of an aspartate residue (D384 human, D387 mouse) connecting the linker and small subunit (p10) leads to the generation of caspase-8 p43 subunit. In an intradimer manner, the subsequent cleavage of an aspartate (D216 human, D218 mouse) in the region between the prodomain (p26) and the large subunit (p18) leads to fully matured caspase-8, which is released from the DISC to the cytosol as the enzymatically active heterotetramer $(p18)_2(p10)_2$ (Dickens et al., 2012b; Hughes et al., 2009; Kallenberger et al., 2014). Release of caspase-8 from the plasma membrane location allows caspase-8 to cleave other substrates and initiate apoptosis. When caspase-8 activation is blocked, RIPK1 and RIPK3 oligomerise and auto-phosphorylate. RIPK3 phosphorylates MLKL and necroptosis is activated (Liu and Lalaoui, 2020).

Over the past few years, most studies have focused on complex-1 and it has been revealed that TNF signalling is heavily regulated by a plethora of post-translational modifications (PTMs), including phosphorylation and diverse types of ubiquitin chains. These PTMs, together with TNF-mediated transcriptional responses, serve as checkpoints that control the formation and cytotoxic potential of complex-2 (Annibaldi and Meier, 2018; Liu and Lalaoui, 2020).

Since it was discovered in 2003 (Micheau and Tschopp, 2003), the composition and post-translational modifications in complex-2 remain far less well defined. This could be due to the lack of highly efficient and specific tools. In the past few years our knowledge of its composition was limited to only a few components such as TRADD, FADD, caspase-8, cFlip, A20, RIPK1 and RIPK3. It has been reported that the TNFR1 complex-2 is a large ~2MDa cell death-inducing platform (Micheau and Tschopp, 2003; Tenev et al., 2011). Therefore, we hypothesized that not all components and posttranslational modifications of this signalling complex had been identified.

To test this hypothesis, we generated 3x FLAG tagged caspase-8 knock-in mouse strains to enable us to analyse the composition of endogenous, caspase-8 containing, TNFR1 complex-2. Before generating the mouse strains, in this chapter I tested *in vitro* whether an N or C-terminal 3x FLAG tag interfered with caspase-8 expression and function using doxycycline (Dox)-inducible lentiviral system.

3.1 An N- or C-terminal FLAG tag does not affect caspase-8 expression and function

3.1.1 Expression of caspase-8 is not affected by a single FLAG tag

N-terminally or C-terminally single FLAG tagged or, as a control, tagless mouse caspase-8 constructs were stably introduced into *Casp8*$^{-/-}$.*Mlkl*$^{-/-}$ mouse dermal fibroblasts (MDFs). It was necessary to reconstitute double knock-out cells because mice deficient in caspase-8 present with E10.5 embryonic lethality (Varfolomeev et al., 1998), therefore *Casp8*$^{-/-}$ MDFs are not obtainable. Mouse embryonic fibroblasts (MEFs) were not chosen because they intend to lose necroptotic pathway elements (Cook et al., 2014).

Cells were infected with a puromycin-selectable lentiviral vector, from which caspase-8 expression could be induced using Dox (**Figure 3.1A**). Cells were treated with a titration of Dox for 24 hours to induce the expression of FLAG tagged or tagless caspase-8. The expression of caspase-8 was tightly controlled by Dox as in the absence of Dox caspase-8 expression could not be detected (**Figure 3.1B**). While 2 ng/mL of Dox did not induce caspase-8 expression, 20 ng/mL of Dox caused readily detectable expression of caspase-8 which was slightly increased with 200 ng/mL of Dox treatment. The level of expression was comparable for N-terminally or C-terminally single FLAG tagged or tagless mouse caspase-8, indicating that expression of caspase-8 was not affected by a single FLAG tag. Wild-type (WT) and *Mlkl*$^{-/-}$ MDFs were used to compare the endogenous and Dox-induced caspase-8 levels. Dox treatment increased 5 to 10 folds the expression of caspase-8 in the *Casp8*$^{-/-}$.*Mlkl*$^{-/-}$ cells when compare to the endogenous expression in the WT and *Mlkl*$^{-/-}$ cells. In addition, induction of tagged or tagless caspase-8, caused auto-activation and cleavage of caspase-8, however this did not cause significant spontaneous cell death (**Figure 3.1B and C**).

3.1.2 The killing function of caspase-8 is not affected by a single FLAG tag

As previously described, TNF and Smac-mimetic (TNF/SM) induce apoptosis *via* activating caspase-8 (Li et al., 2004; Varfolomeev et al., 2007; Vince et al., 2007). To examine whether tagging caspase-8 with a single FLAG affects its ability to induce cell death, cells were stimulated with TNF/SM to induce apoptosis, in the presence or absence of Dox for 24 hours. Dox-induced expression of tagged or tagless caspase-8 led to comparable level of apoptotic

cell death and was in a dose-dependent manner (**Figure 3.1C**). This result suggested that a single FLAG tag did not affect the killing activity of caspase-8.

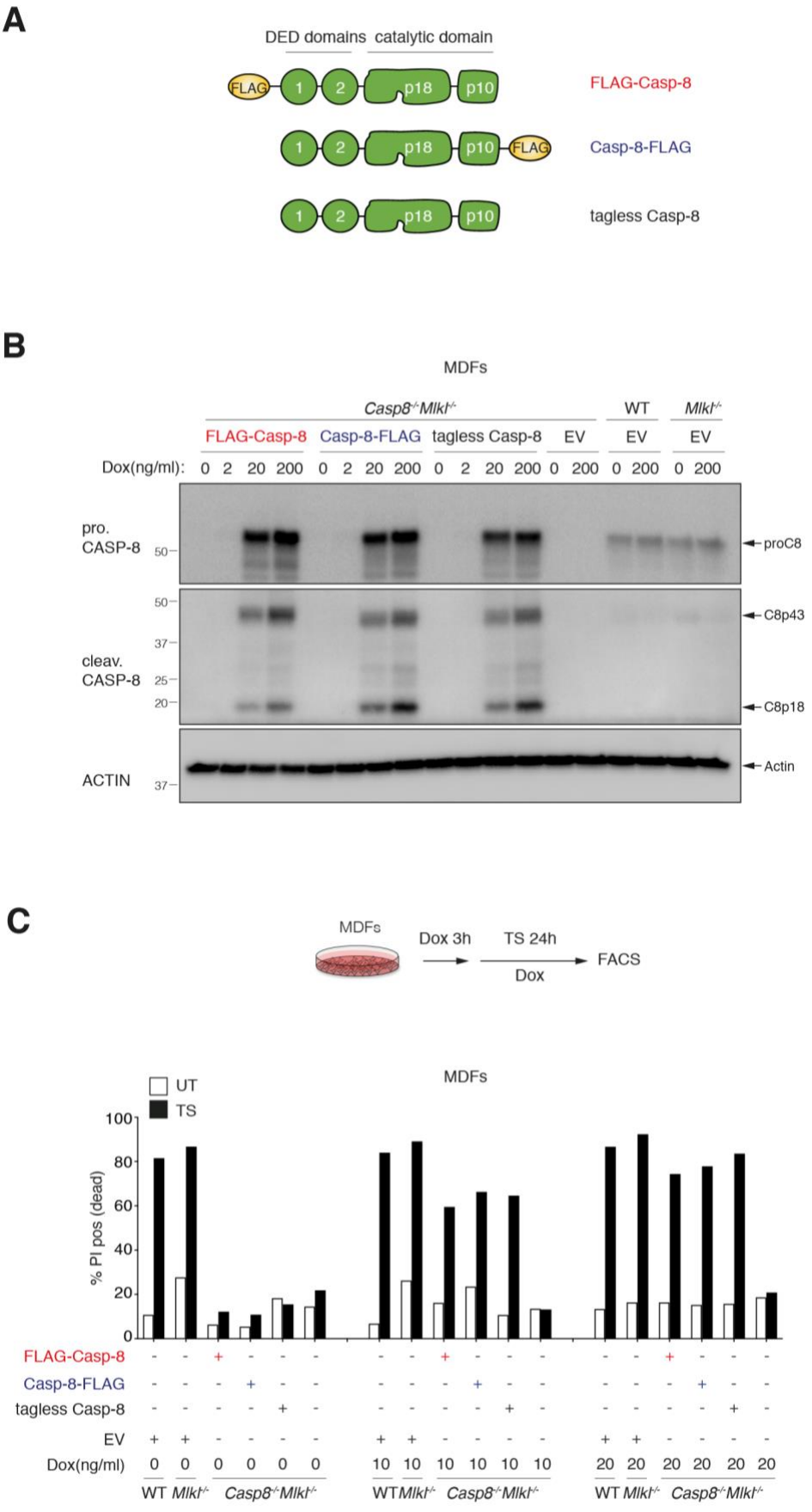
A
DED domains
catalytic domain
FLAG
1
2
p18
p10
FLAG-Casp-8
Casp-8-FLAG
tagless Casp-8
B
MDFs
Casp8-/-Mlkl-/-
WT
Mlkl-/-
FLAG-Casp-8
Casp-8-FLAG
tagless Casp-8
EV
Dox(ng/ml): 0 2 20 200 0 2 20 200 0 2 20 200 0 200 0 200 0 200
pro. CASP-8
cleav. CASP-8
ACTIN
50
37
25
20
proC8
C8p43
C8p18
Actin
C
MDFs
Dox 3h
TS 24h
Dox
FACS
MDFs
UT
TS
% PI pos (dead)
100
80
60
40
20
0
FLAG-Casp-8
Casp-8-FLAG
tagless Casp-8
EV
Dox(ng/ml)
0 0 0 0 0 0 10 10 10 10 10 10 20 20 20 20 20 20
WT Mlkl-/- Casp8-/-Mlkl-/-
WT Mlkl-/- Casp8-/-Mlkl-/-
WT Mlkl-/- Casp8-/-Mlkl-/-

Figure 3.1. A N-terminal or C-terminal single FLAG tag does not interfere with caspase-8 expression and function.

(A) Schematic representation of single FLAG tagged or tagless caspase-8. N-terminally or C-terminally single FLAG tagged caspase-8 is in red and blue, respectively. Tagless caspase-8 is in black.

(B) Western blot analysis of cell lysates from *Casp8*$^{-/-}$.*Mlkl*$^{-/-}$ MDFs expressing Dox-inducible N-terminally or C-terminally single FLAG tagged caspase-8 or tagless caspase-8 or empty vectors (EV). WT or *Mlkl*$^{-/-}$ MDFs expressing an EV were used as controls. Cells were treated with the indicated dose of Dox for 24 hours. The Western blot is representative of three independent experiments.

(C) Level of cell death assessed by propidium iodide (PI) positive cells. Cells were pre-treated with 10 ng/mL or 20 ng/mL Dox for 3 hours followed by stimulation with TNF (100 ng/mL) + SM CompA (500 nM) (TS) for 24 hours in the presence of 10 ng/mL or 20 ng/mL Dox. n=1 biological repeat.

3.2 The expression and function of caspase-8 are not affected by a N-terminal or C-terminal 3x FLAG tag

While I was performing these experiments, another single FLAG tag knock-in mouse strain had been developed in our lab and tests on this mouse indicated that a single FLAG tag was not optimal for detecting or working with an endogenously tagged protein *in vivo*. Since a 3x FLAG tag has been reported by Sigma and literatures to be ultrasensitive for detection *in vitro* and *in vivo* (Dai et al., 2014; Ferrando et al., 2015; LaCava et al., 2015), I tested whether a 3x FLAG tag was also compatible with caspase-8 expression and function.

3.2.1 Expression level of caspase-8 is unaffected by a 3x FLAG tag

Similar to **Figure 3.1A**, *Casp8*$^{-/-}$.*Mlkl*$^{-/-}$ MDFs containing Dox-inducible N- or C-terminally 3x FLAG tagged or tagless mouse caspase-8 (**Figure 3.2A**) stable lines were generated. WT and *Mlkl*$^{-/-}$ MDFs were used as controls to show endogenous level of caspase-8. As before, the expression of caspase-8 was tightly controlled by Dox. Dox induced the expression of 3x FLAG tagged or tagless caspase-8 in a time-dependent manner, and the levels of N-terminally or C-terminally 3x FLAG tagged or tagless mouse caspase-8 were comparable at all time points. Importantly, the expression levels of tagged or tagless caspase-8 after 3 hours Dox treatment were similar to endogenous level of caspase-8, however longer Dox treatment caused overexpression and auto-cleavage of caspase-8 (**Figure 3.2B**).

3.2.2 A 3x FLAG tag is compatible with caspase-8 activity

As before, cells were stimulated with TNF/SM to induce apoptosis in the presence or absence of Dox for 24 hours. Dox-induced expression of C-terminally 3x FLAG tagged or tagless caspase-8 caused similar levels of apoptotic cell death although slightly less death was observed in cells containing N-terminally 3x FLAG tagged caspase-8 (**Figure 3.2C**).

TNF/SM induces a caspase-8 dependent apoptosis, however if caspase-8 function is absent or inhibited, this leads to an accumulation of RIPK1 and its autoactivation which promotes the phosphorylation of RIPK3, which in turn activates MLKL to trigger necroptosis (Murphy et al., 2013; Silke and Vucic, 2014; Vandenabeele et al., 2010). Thus caspase-8 activity is required to prevent necroptosis and therefore its ability to prevent necroptosis serves as another

measure of caspase-8 activity. Consistent with this, neither *Mlkl*$^{-/-}$ MDFs nor *Casp8*$^{-/-}$.*Mlkl*$^{-/-}$ MDFs can die via the necroptotic pathway due to the absence of MLKL (**Figure 3.2C**).

To explore whether tagging caspase-8 with 3x FLAG might have more subtle effects on caspase-8 activity and affect complex-2 formation and the subsequent necroptotic cell death, *Mlkl*$^{-/-}$ MDFs or *Casp8*$^{-/-}$.*Mlkl*$^{-/-}$ MDFs containing Dox-inducible 3x FLAG tagged or tagless caspase-8 were reconstituted with Dox-inducible GFP-tagged mouse MLKL and stimulated with TNF/SM and TNF/SM plus the caspase inhibitor IDN-6556 (TNF/SM/IDN) in the presence or absence of Dox for 24 hours. The percentage of GFP positive cells indicated the levels of MLKL-GFP or GFP control in each cell line. The level of MLKL-GFP was similar across *Casp8*$^{-/-}$.*Mlkl*$^{-/-}$ MDFs containing Dox-inducible tagged or tagless caspase-8 and these cell lines showed comparable levels of necroptotic cell death. Slightly more death was observed in *Mlkl*$^{-/-}$ MDFs reconstituted with Dox-inducible MLKL-GFP, possibly due to higher MLKL-GFP expression (**Figure 3.2D**). Taken together, these data suggested that a 3x FLAG tag did not affect caspase-8 expression and function when expressed above endogenous levels.

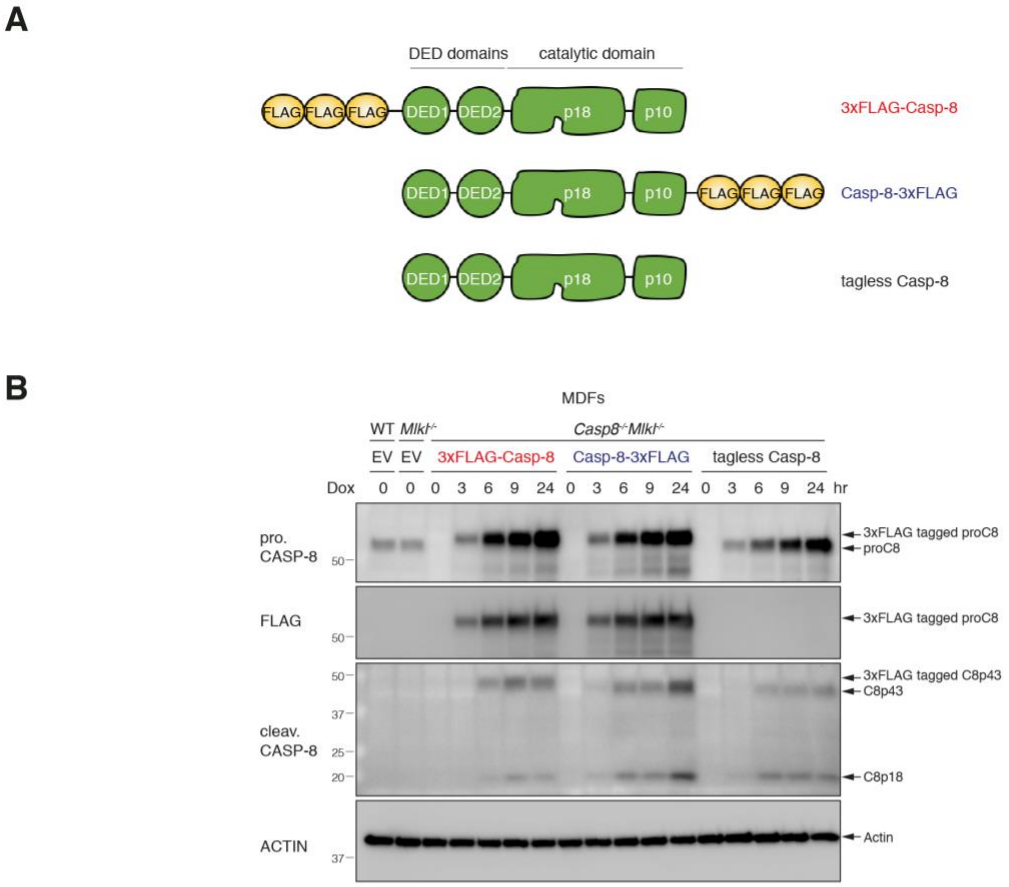
A
DED domains
catalytic domain
FLAG
DED1
DED2
p18
p10
3xFLAG-Casp-8
Casp-8-3xFLAG
tagless Casp-8
B
MDFs
WT
Mlkl-/-
Casp8-/-Mlkl-/-
EV
3xFLAG-Casp-8
Casp-8-3xFLAG
tagless Casp-8
Dox
0 3 6 9 24 hr
pro. CASP-8
FLAG
cleav. CASP-8
ACTIN
3xFLAG tagged proC8
proC8
3xFLAG tagged C8p43
C8p43
C8p18
Actin
C
MDFs
Dox 3h
TS/TSI 24h
Dox
FACS
UT
TS
TSI
% PI pos (dead)
3xFLAG-Casp-8
Casp-8-3xFLAG
tagless Casp-8
EV
Dox(ng/ml)
WT Mlkl-/- Casp8-/-Mlkl-/-
D
MDFs
Dox 3h
TS/TSI 24h
Dox
FACS
UT
TS
TSI
n.s.
% PI pos (dead)
% GFP pos
3xFLAG-Casp-8
Casp-8-3xFLAG
tagless Casp-8
MLKL-GFP
GFP
Dox(ng/ml)
WT Mlkl-/- Casp8-/-Mlkl-/-

Figure 3.2. The expression and function of caspase-8 are not affected by an N- or C-terminal 3x FLAG tag

(A) Schematic representation of 3x FLAG tagged or tagless caspase-8. N-terminally or C-terminally 3x FLAG tagged caspase-8 is in red and blue, respectively. Tagless caspase-8 is in black.

(B) Western blot analysis of cell lysates from *Casp8*$^{-/-}$.*Mlkl*$^{-/-}$ MDFs expressing Dox-inducible N-terminally or C-terminally 3x FLAG tagged caspase-8 or tagless caspase-8. WT or *Mlkl*$^{-/-}$ MDFs expressing an EV were used as controls. Cells were treated with 20 ng/mL Dox for the indicated times. The Western blot is representative of three independent experiments.

(C) and **(D)** Level of cell death assessed by PI positive cells. Cells were pre-treated with 20 ng/mL Dox for 3 hours followed by stimulation with TNF (100 ng/mL) + SM CompA (500 nM) (TS) or TNF (100 ng/mL) +SM CompA (500 nM) + IDN-6556 (5 μM) (TSI) for 24 hours in the presence of 20 ng/mL Dox. Graphs show mean ± SD, n=3 independent experiments. Comparisons were performed with a Student's t test whose values are denoted in the figures as *$p \leq 0.05$, ***$p \leq 0.001$, and n.s.= no significance

3.3 Caspase-8-3x FLAG functions like WT caspase-8 when expressed at endogenous levels

According to the previous results, 3 hours of 20 ng/mL of Dox was sufficient to achieve endogenous level of caspase-8. However, constant and longer treatment with Dox induced caspase-8 accumulation reaching levels above the endogenous one, and this led to its auto-cleavage (**Fig 3.2B**). In this sub-chapter, I optimised conditions to obtain constant endogenous level of caspase-8 and determined whether 3x FLAG tag affects the turnover of caspase-8 and response to death stimuli when expressed at endogenous level.

3.3.1 At physiological levels, turnover of caspase-8 is unaffected by a 3x FLAG tag

To avoid caspase-8 accumulation due to long term Dox treatment, *Casp8*$^{-/-}$*.Mlkl*$^{-/-}$ MDFs expressing Dox-inducible tagged or tagless caspase-8 were treated with 20 ng/mL Dox for 3 hours and then Dox was withdrawn. To examine caspase-8 turnover, samples were harvested 0 hour or 20 hours after Dox withdrawal for Western blot analysis. WT and *Mlkl*$^{-/-}$ MDFs were used as controls to show endogenous level of caspase-8. After 20 hours of Dox withdrawal, the expression of tagged and tagless caspase-8 were comparable to endogenous level as shown in controls (**Figure 3.3A**). This result suggested that: (i) 3 hours of 20 ng/mL of Dox is sufficient to induce a constant endogenous level of caspase-8 and (ii) 3x FLAG tag did not affect the turnover of caspase-8 when expressed at physiological levels.

3.3.2 At physiological levels, tagging caspase-8 with a C-terminal 3x FLAG tag does not affect the response to apoptotic stimuli

I next tested whether tagging caspase-8 with 3x FLAG would affect the response to apoptotic stimuli when expressed at endogenous level. Two distinct apoptotic stimulations were used: Smac-mimetic (TNF/SM) induces apoptosis by causing the auto-degradation of cIAPs while cycloheximide (TNF/CHX) promotes caspase-8 activation by reducing levels of the natural caspase-8 inhibitor, cFlip$_L$ (Wang et al., 2008). *Casp8*$^{-/-}$*.Mlkl*$^{-/-}$ MDFs containing Dox-inducible tagged or tagless caspase-8 were treated with 20 ng/mL Dox for 3 hours to achieve physiological levels of caspase-8 before Dox was withdrawn. Cells were then stimulated with TNF/SM, TNF/SM/IDN, TNF/CHX or TNF/CHX/IDN for 20 hours in the absence of Dox then cell death was quantified using PI staining and flow cytometry. When expressed at endogenous level, the C-terminally 3x FLAG tagged caspase-8 showed similar response to

TNF/SM or TNF/CHX compared to tagless caspase-8. However, less apoptotic death was observed in *Casp8*$^{-/-}$.*Mlkl*$^{-/-}$ MDFs expressing endogenous levels of N-terminally 3x FLAG tagged caspase-8. These cells did not respond to necroptotic stimuli TNF/SM/IDN and TNF/CHX/IDN due to the absence of MLKL (**Figure 3.3B**).

3.3.3 At physiological levels, the response to necroptotic stimuli is unaffected by tagging caspase-8 with a 3x FLAG tag

To explore whether endogenous levels of 3x FLAG tagged caspase-8 would affect complex-2 formation and the subsequent necroptotic cell death, I used cells described in **Figure 3.2D**. In brief, *Mlkl*$^{-/-}$ MDFs or *Casp8*$^{-/-}$.*Mlkl*$^{-/-}$ MDFs expressing Dox-inducible tagged or tagless caspase-8 were reconstituted with Dox-inducible GFP-tagged mouse MLKL and were treated with 20 ng/mL Dox for 3 hours to induce physiological levels of caspase-8. These cells were then stimulated with TNF/SM or TNF/SM/IDN for 20 hours in the absence of Dox before subjected to cell death analysis. Surprisingly, these cells showed very little necroptotic death upon TNF/SM/IDN. The percentage of GFP positive cells suggested that the levels of MLKL-GFP in these cells were low at the timepoint of cell death assay (**Figure 3.3C**), which could be due to the fast turnover of MLKL-GFP after Dox withdrawal. To test this hypothesis, cells were treated with 20 ng/mL Dox for 3 hours to induce physiological levels of caspase-8 and then with 3 hours TNF/SM/IDN in the absence of Dox before conducting cell death assay. As expected, increased levels of MLKL-GFP and necroptotic death were observed at the earlier time point. The response to TNF/SM/IDN stimulation was very comparable across *Casp8*$^{-/-}$.*Mlkl*$^{-/-}$ MDFs expressing endogenous levels of 3x FLAG tagged or tagless caspase-8 (**Figure 3.3D**). Together, this result suggested that when expressed at endogenous levels, the ability of caspase-8 in inhibiting necroptosis was unaffected by a 3x FLAG tag.

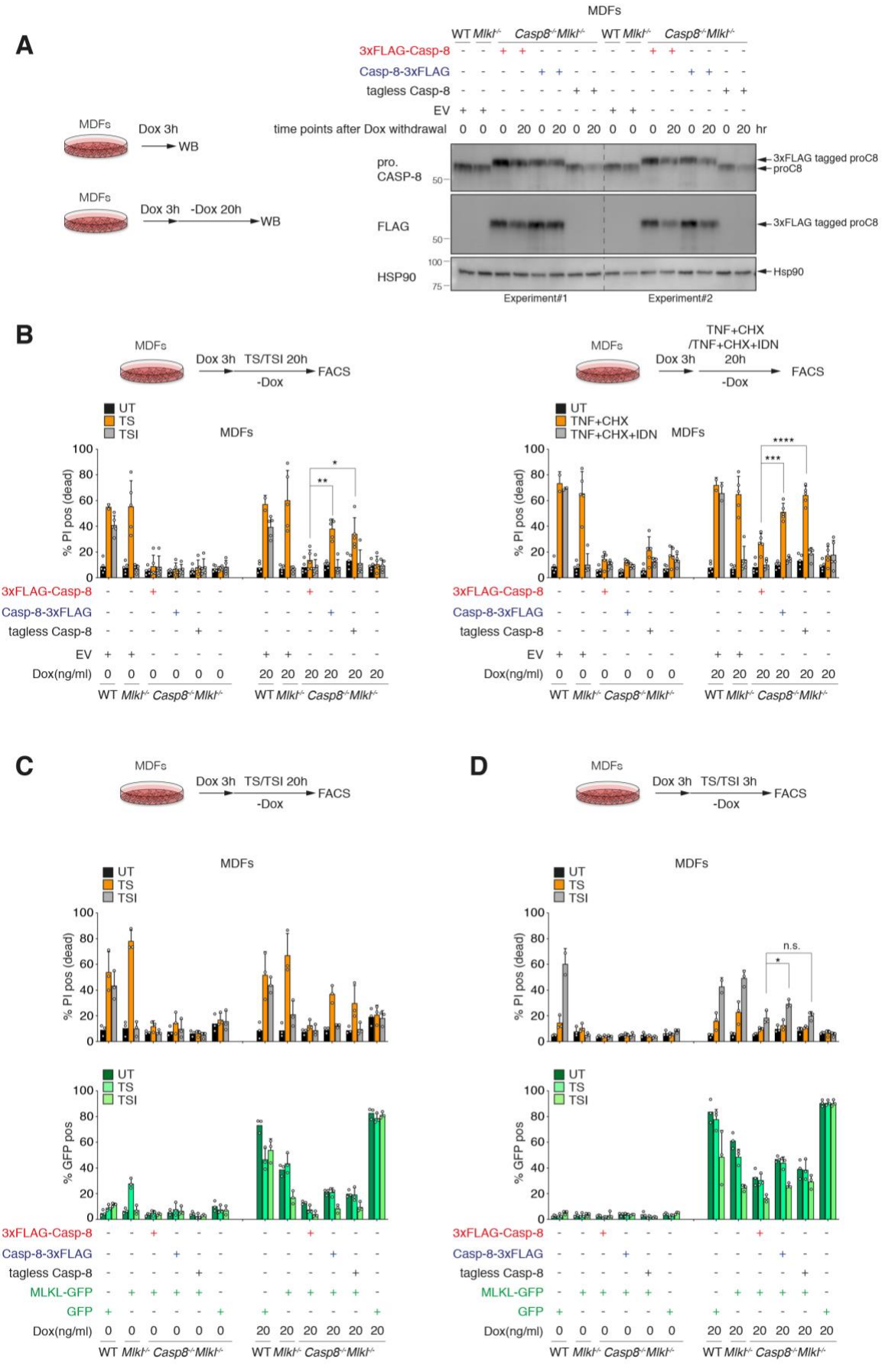
A
MDFs
Dox 3h
WB
MDFs
Dox 3h -Dox 20h
WB
MDFs
WT Mlkl-/- Casp8-/-Mlkl-/- WT Mlkl-/- Casp8-/-Mlkl-/-
3xFLAG-Casp-8
Casp-8-3xFLAG
tagless Casp-8
EV
time points after Dox withdrawal 0 0 0 20 0 20 0 20 0 0 0 20 0 20 0 20 hr
pro. CASP-8
FLAG
HSP90
3xFLAG tagged proC8
proC8
3xFLAG tagged proC8
Hsp90
Experiment#1
Experiment#2
B
MDFs
Dox 3h TS/TSI 20h
-Dox
FACS
UT
TS
TSI
MDFs
% PI pos (dead)
MDFs
TNF+CHX
/TNF+CHX+IDN
Dox 3h 20h
-Dox
FACS
UT
TNF+CHX
TNF+CHX+IDN
MDFs
% PI pos (dead)
3xFLAG-Casp-8
Casp-8-3xFLAG
tagless Casp-8
EV
Dox(ng/ml) 0 0 0 0 0 0 20 20 20 20 20 20
WT Mlkl-/- Casp8-/-Mlkl-/- WT Mlkl-/- Casp8-/-Mlkl-/-
C
MDFs
Dox 3h TS/TSI 20h
-Dox
FACS
MDFs
UT
TS
TSI
% PI pos (dead)
% GFP pos
3xFLAG-Casp-8
Casp-8-3xFLAG
tagless Casp-8
MLKL-GFP
GFP
Dox(ng/ml) 0 0 0 0 0 0 20 20 20 20 20 20
WT Mlkl-/- Casp8-/-Mlkl-/- WT Mlkl-/- Casp8-/-Mlkl-/-
D
MDFs
Dox 3h TS/TSI 3h
-Dox
FACS
MDFs
UT
TS
TSI
% PI pos (dead)
n.s.
% GFP pos
3xFLAG-Casp-8
Casp-8-3xFLAG
tagless Casp-8
MLKL-GFP
GFP
Dox(ng/ml) 0 0 0 0 0 0 20 20 20 20 20 20
WT Mlkl-/- Casp8-/-Mlkl-/- WT Mlkl-/- Casp8-/-Mlkl-/-

Figure 3.3. C-terminally 3x FLAG tagged caspase-8 functions like WT caspase-8 when expressed at endogenous levels

(A) Western blot analysis of cell lysates from *Casp8*$^{-/-}$.*Mlkl*$^{-/-}$ MDFs expressing Dox-inducible N-terminally or C-terminally 3x FLAG tagged caspase-8 or tagless caspase-8. WT or *Mlkl*$^{-/-}$ MDFs expressing an EV were used as controls. Cells were treated with 20 ng/mL Dox for 3 hours and then Dox was withdrawn. Samples were harvested 0 hour or 20 hours after Dox withdrawal for Western blot analysis. The Western blot is representative of two independent experiments.

(B) Level of cell death assessed by PI positive cells. Cells were pre-treated with 20 ng/mL Dox for 3 hours followed by stimulation with TNF (100 ng/mL) + SM CompA (500 nM) (TS) or TNF (100 ng/mL) +SM CompA (500 nM) + IDN-6556 (5 μM) (TSI) **(Left panel)** or TNF (100 ng/mL) +cycloheximide (1 μg/mL) (TNF+CHX) or TNF (100 ng/mL) + cycloheximide (1μg/mL) + IDN-6556 (5 μM) (TNF+CHX+IDN) **(Right panel)** for 20 hours in the absence of Dox. Graphs show mean ± SD, n=3 independent experiments. Comparisons were performed with a Student's t test whose values are denoted in the figures as *$p \leq 0.05$, **$p \leq 0.01$, ***$p \leq 0.001$ and ****$p \leq 0.0001$.

(C) and **(D)** Level of cell death assessed by PI positive cells. Cells were pre-treated with 20ng/mL Dox for 3 hours followed by stimulation with TNF (100 ng/mL) + SM CompA (500 nM) (TS) or TNF (100 ng/mL) +SM CompA (500 nM) + IDN-6556 (5 μM) (TSI) for 20 hours **(C)** or 3 hours **(D)** in the absence of Dox. Graphs show mean ± SD, n=3 independent experiments. Comparisons were performed with a Student's t test whose values are denoted in the figures as *$p \leq 0.05$ and n.s.= no significance.

3.4 3x FLAG tagged caspase-8 expressed at endogenous levels has a diffuse cytoplasmic distribution

Next I examined the subcellular localization of 3x FLAG tagged caspase-8 when expressed at physiological levels by performing immunofluorescence staining (IF) with an anti-FLAG M2 antibody (Sigma F1804). *Casp8*$^{-/-}$.*Mlkl*$^{-/-}$ MDFs expressing Dox-inducible N- or C-terminally 3x FLAG tagged caspase-8 were treated with 20 ng/ml Dox for 3 hours to induce physiological levels of caspase-8 and then were subjected to IF. As in the Western blot analysis, the expression of 3x FLAG tagged caspase-8 was tightly controlled by Dox, and FLAG staining was only observed upon Dox treatment. When expressed at endogenous levels, both N- and C-terminally 3x FLAG tagged caspase-8 displayed a diffuse pattern throughout the cytoplasm (**Figure 3.4**), which was consistent with previous reports (MacFarlane et al., 2000). Notably, effective commercial anti-procaspase-8 antibodies for detecting mouse endogenous procaspase-8 are currently not available. Therefore, the Dox-inducible lentiviral system which could achieve physiological levels of 3x FLAG tagged caspase-8 will provide insight into the subcellular distribution and activation mechanism of caspase-8. A 3x FLAG tagged caspase-8 knock-in mouse will allow to determine the localise endogenous caspase-8 *in vivo*.

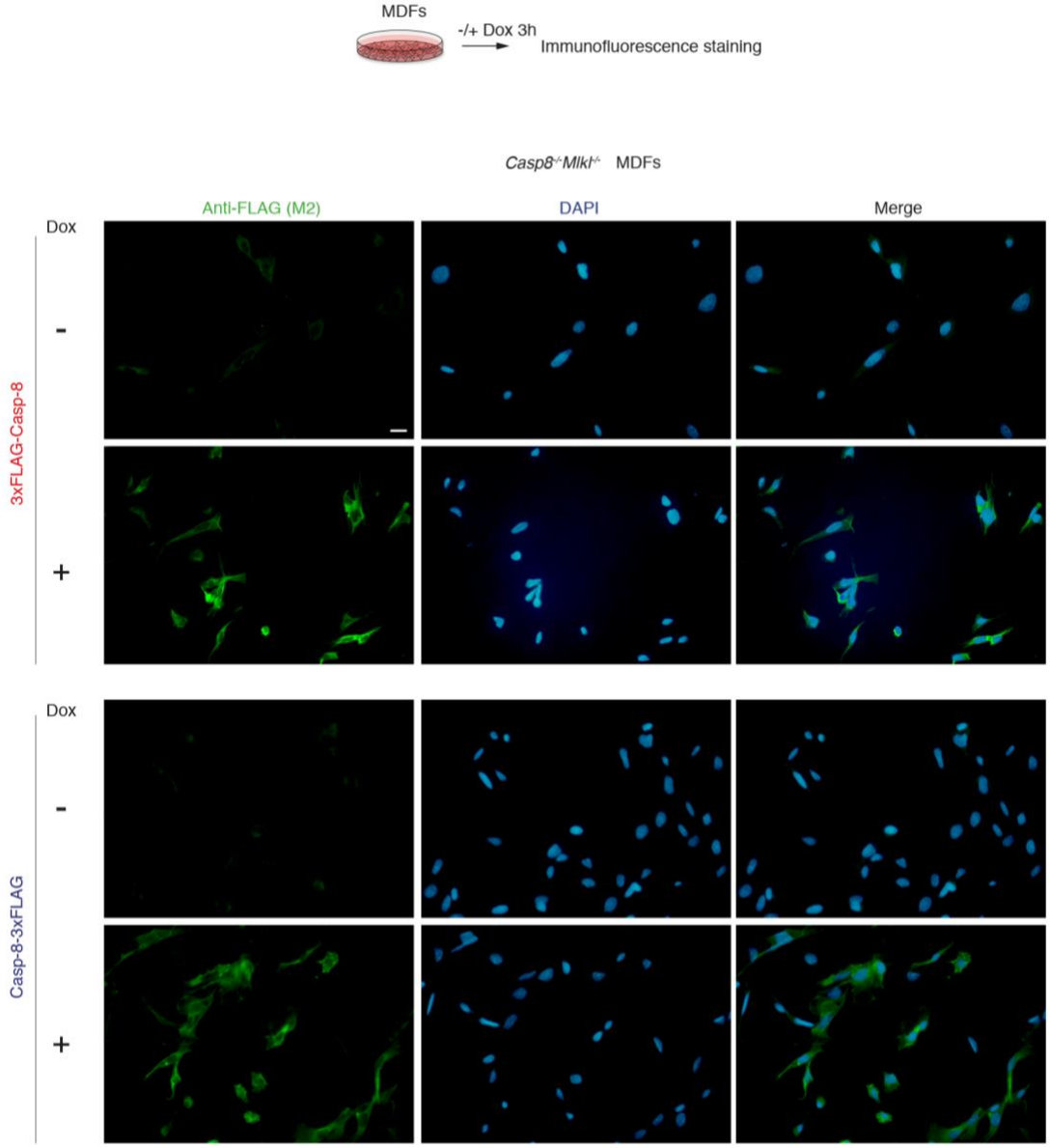

Figure 3.4. At physiological levels, the 3x FLAG tagged caspase-8 showed a diffuse cytoplasmic distribution

Immunofluorescence staining of *Casp8*$^{-/-}$*.Mlkl*$^{-/-}$ MDFs expressing Dox-inducible N-terminally or C-terminally 3x FLAG tagged caspase-8 using anti-FLAG M2 antibody (1:1000 for N-terminally and 1:500 for C-terminally 3x FLAG tagged caspase-8). Cells were pre-treated with 20 ng/mL Dox for 3 hours before harvested for IF. Magnification, 40 x. Scale bar, 10 μm.

3.5 Immunoprecipitation and mass spectrometry analysis of TNFR1 complex-2 in cells expressing endogenous 3x FLAG tagged caspase-8

3.5.1 Immunoprecipitation of TNFR1 complex-2

Since caspase-8 is a crucial component in TNFR1 complex-2, I therefore examined complex-2 formation in *Casp8*$^{-/-}$*.Mlkl*$^{-/-}$ MDFs containing Dox-inducible 3x FLAG tagged or tagless caspase-8 by anti-FLAG immunoprecipitation. Cells were treated with 20 ng/mL Dox for 3 hours to induce physiological levels of tagged or tagless caspase-8. After Dox withdrawal, cells were further stimulated with TNF/SM/IDN for 1.5 hours before subjected to anti-FLAG immunoprecipitation (**Figure 3.5A**).

The anti-FLAG immunoprecipitation was very specific as the association of complex-2 was not detectable in *Casp8*$^{-/-}$*.Mlkl*$^{-/-}$ expressing tagless caspase-8. TNF/SM/IDN stimulation induced the formation of complex-2 in *Casp8*$^{-/-}$*.Mlkl*$^{-/-}$ MDFs expressing endogenous level of C-terminally 3x FLAG tagged caspase-8, as indicated by significant enrichment of complex-2 components RIPK1 and cleaved caspase-8. Intriguingly, the cleavage product of procaspase-8 p10 was clearly detectable in anti-FLAG immunoprecipitation sample upon TNF/SM/IDN stimulation. The formation of complex-2 was also observed in *Casp8*$^{-/-}$*.Mlkl*$^{-/-}$ MDFs expressing endogenous level of N-terminally 3x FLAG tagged caspase-8, although there was less enrichment of RIPK1 compared with the C-terminally 3x FLAG tagged caspase-8 expressing cells (**Figure 3.5B**). This was consistent with less cell death as shown in **Figure 3.3B**.

3.5.2 TNFR1 complex-2 characterization by mass spectrometry

To analyse the composition of TNFR1 complex-2, complex-2 was eluted from anti-FLAG M2 affinity beads using 3x FLAG peptides before subjected to mass spectrometry (MS). Multiple controls were designed for rigorous MS data analysis (**Figure 3.5C**). Notably, FLAG spiking sample which consisted in adding high concentration of 3x FLAG peptides to compete with 3x FLAG tagged caspase-8 containing complex-2 in binding with FLAG M2 affinity beads so that the purification of complex-2 was interrupted. This ensured the elimination of nonspecific binders to 3x FLAG tag. Complex-2 components were expected to be observed only in TNF/SM/IDN-treated samples without FLAG peptide spiking (as indicated by greens arrows).

A list of 39 proteins which were significantly enriched (P.Value<0.05) in either the 3x FLAG tagged caspase-8 untreated or TNF/SM/IDN stimulated samples relative to negative controls were selected (**Table 3.1 and 3.2**). Log2 fold change volcano plots of protein enrichment upon TNF/SM/IDN stimulation compared to the untreated control were generated from 5 independent experiments (**Figure 3.5D**). For both N- and C- terminally 3x FLAG tagged caspase-8, caspase-8 showed no fold change upon TNF/SM/IDN stimulation. This was as expected because (i) anti-FLAG immunoprecipitation should enrich 3x FLAG tagged caspase-8; (ii) a previous study has suggested that upon death stimulation, only a small proportion of cytosolic procaspase-8 is recruited into complex-2 where they are cleaved (Tenev et al., 2011). Known constituents of the native TNFR1 complex-2, such as RIPK1, RIPK3, FADD and A20 (encoded by gene *TNFAIP3*) (He et al., 2009; Micheau and Tschopp, 2003; Onizawa et al., 2015) were identified upon TNF/SM/IDN stimulation with high confidence, multiple peptide matches, and good coverage of the protein sequences (**Figure 3.5D, Table 3.1 and 3.2**). Consistent with the observation in **Figure 3.5B**, RIPK1 and RIPK3 displayed increased fold of enrichment upon TNF/SM/IDN stimulation from cells expressing C-terminally 3x FLAG tagged caspase-8, indicating an increased complex-2 assembly in these cells. Interestingly, TRADD, a known complex-2 component (Micheau and Tschopp, 2003), was enriched upon TNF/SM/IDN stimulation from cells expressing C-terminally 3x FLAG tagged caspase-8 whereas showed an opposite trend in cells expressing N-terminally 3x FLAG tagged caspase-8.

Several novel proteins also appeared to be enriched or decreased upon TNF/SM/IDN stimulation. For example, the MS raw data (**Table 3.1 and 3.2**) suggested that Vps52 and Fgps were enriched while Hacd3 and Cwc22 were decreased in respond to TNF/SM/IDN in both N- and C-terminally 3x FLAG tagged caspase-8 expressing cells. However, the peptide information (data not shown) indicated that they might not to be real interactors. HUWE1, an E3 ligase, did not show fold change upon TNF/SM/IDN whereas the peptide information suggested that it appeared to be a constitutive caspase-8 interactor. However, HUWE1 knockout MDFs or MEFs didn't show any effect on TNF-induced death (data not shown). Therefore, it was not followed up.

Finally, based on Log2 fold change values, -Log 10 P.Values and peptide information, we focused on tankyrase-1 (TNKS1/TNKS/ARTD5/PARP5a), a member of the poly(ADP-ribose) polymerase superfamily. Interestingly, TNKS1 was significantly enriched upon TNF/SM/IDN in cells expressing C-terminally 3x FLAG tagged caspase-8 and was also present in cells

expressing N-terminally 3x FLAG tagged caspase-8 (**Figure 3.5D**). This could be due to the less efficient formation of complex-2 in these cells as indicated in **Figure 3.5B**. Together, this data suggested that TNKS1 might represent a novel interactor of the TNFR1 complex-2.

Before characterising this novel interactor, in **Chapter 4** we generated knock-in mouse strains which have the physiological levels of 3x FLAG tagged caspase-8. By using primary cells from these knock-in mice, the association between TNKS1 and caspase-8-containing TNFR1 complex-2 was validated and the biological relevance was established in **Chapter 5**.

Table 3.1. MS raw data for N-terminally 3x FLAG tagged caspase-8 IP

Name	Unique peptides	Unique sequence coverage	Log2 FC TSI - Untreated	-Log10 P Value
Cth	3	10.3	-1.55231904	0.001866237
Hacd3	5	16.9	-1.499195615	0.011280391
Tradd	6	26.8	-1.03833574	0.116404011
Rragc	5	13.1	-0.568945419	0.254654794
Fam45a	7	22.4	-0.405700389	0.463850605
TNKS	9	11.1	-0.269265919	0.632340202
Copg2	12	21	-0.183491536	0.670683851
Slc1a5	5	13.2	-0.163404165	0.773214949
Rint1	4	8.7	-0.151692285	0.718217062
Fbxo38	11	12.8	-0.138370184	0.744381249
Armc10	3	21.8	-0.123003677	0.770514879
Dnajc13	36	21.4	-0.114298319	0.808295198
Ncbp1	9	14.2	-0.100755268	0.867001535
Rraga	1	22.4	-0.093543823	0.843067521
Ilk	16	40.7	-0.090974148	0.785006133
Prmt3	5	11.7	-0.078655014	0.891238397
Apaf1	8	7.9	-0.061645065	0.903192199
Cwc22	5	7.7	-0.059609561	0.927202694
Dars	31	65.5	-0.056939914	0.828417635
Hsdl1	6	25.8	-0.048899679	0.943522086
Immt	1	44	-0.043133425	0.934643932
Huwe1	37	13	-0.041242933	0.941315053
Urod	7	30.8	-0.037466571	0.939456719
Fam129a	16	21.3	-0.008216098	0.988758854
Tab1	10	33.3	0.00188904	0.997432895
Nab1	3	11.9	0.011306415	0.980658744
Carkd	1	27.9	0.084852306	0.855798398
Casp8	45	82.9	0.106346793	0.917734973
Akap12	30	30.6	0.117023141	0.853871689
Kti12	7	33.9	0.220429037	0.643556759
Tmem173	8	31.5	0.256955734	0.658104186
Mbnl1	6	23.6	0.261824575	0.641866737
Vps52	5	8.2	0.544437981	0.44046754
FADD	7	50.2	0.582160173	0.418133381
Tu52	5	10.8	0.771912196	0.195505436
RIPK3	15	46.7	0.882962781	0.179296368
Tnfaip3	4	8	0.987221992	0.057068387
Fpgs	6	18.3	1.308096496	0.036023404
RIPK1	24	50.2	2.504504819	0.00221978

Table 3.2. MS raw data for C-terminally 3x FLAG tagged caspase-8 IP

Name	Unique peptides	Unique sequence coverage	Log2 FC TSI - Untreated	-Log10 P Value
Cwc22	5	7.7	-1.35464667	0.041064744
Hacd3	4	14.6	-1.130565453	0.053465734
Hsdl1	5	21.5	-0.850644077	0.220485339
Rint1	5	9.9	-0.774115304	0.068939932
Cth	3	10.3	-0.744953041	0.124432073
Tmem173	8	31.5	-0.384831123	0.507883214
Rragc	5	13.1	-0.374816222	0.451705868
Armc10	3	21.8	-0.259452622	0.538825218
Prmt3	6	13.6	-0.207968112	0.717812253
Copg2	11	20.9	-0.173267603	0.688016766
Kti12	6	30.5	-0.157597437	0.740668893
Fbxo38	11	12.8	-0.12138871	0.774825437
Urod	7	30.8	-0.068842159	0.889015317
Slc1a5	4	11.5	-0.068131908	0.904335578
Apaf1	8	7.9	-0.028387618	0.955331299
Rraga	1	22.4	-0.023222948	0.960795894
Fam45a	7	22.4	0.001850216	0.997328962
Fam129a	16	21.3	0.022212704	0.969615388
Nab1	3	11.9	0.058952891	0.899416604
Akap12	30	30.6	0.121361613	0.848520058
Casp8	45	82.9	0.143835601	0.888902737
Dars	32	67.5	0.168725747	0.521316515
Ilk	16	40.7	0.262911338	0.431445802
Carkd	1	27.9	0.295202121	0.527825761
Ncbp1	10	15.1	0.354189041	0.556543279
Huwe1	40	14.4	0.365433613	0.514899654
FADD	7	50.2	0.444853954	0.535684027
Tu52	5	10.8	0.458070466	0.44047155
Mbnl1	6	23.6	0.504436655	0.371306866
Dnajc13	35	20.6	0.546987562	0.247936394
Tradd	6	26.8	0.553553731	0.399366699
Immt	1	47.2	0.781157408	0.140837608
Tab1	9	31.3	0.785481623	0.183952657
Tnfaip3	7	10.3	1.235722032	0.018104917
Vps52	6	9.1	1.341662819	0.060196607
RIPK3	14	42.4	1.441788767	0.030145634
Fpgs	6	18.3	1.575974192	0.01216456
TNKS	11	12.6	1.7166617	0.0031725
RIPK1	26	54.9	3.144171099	0.000165174

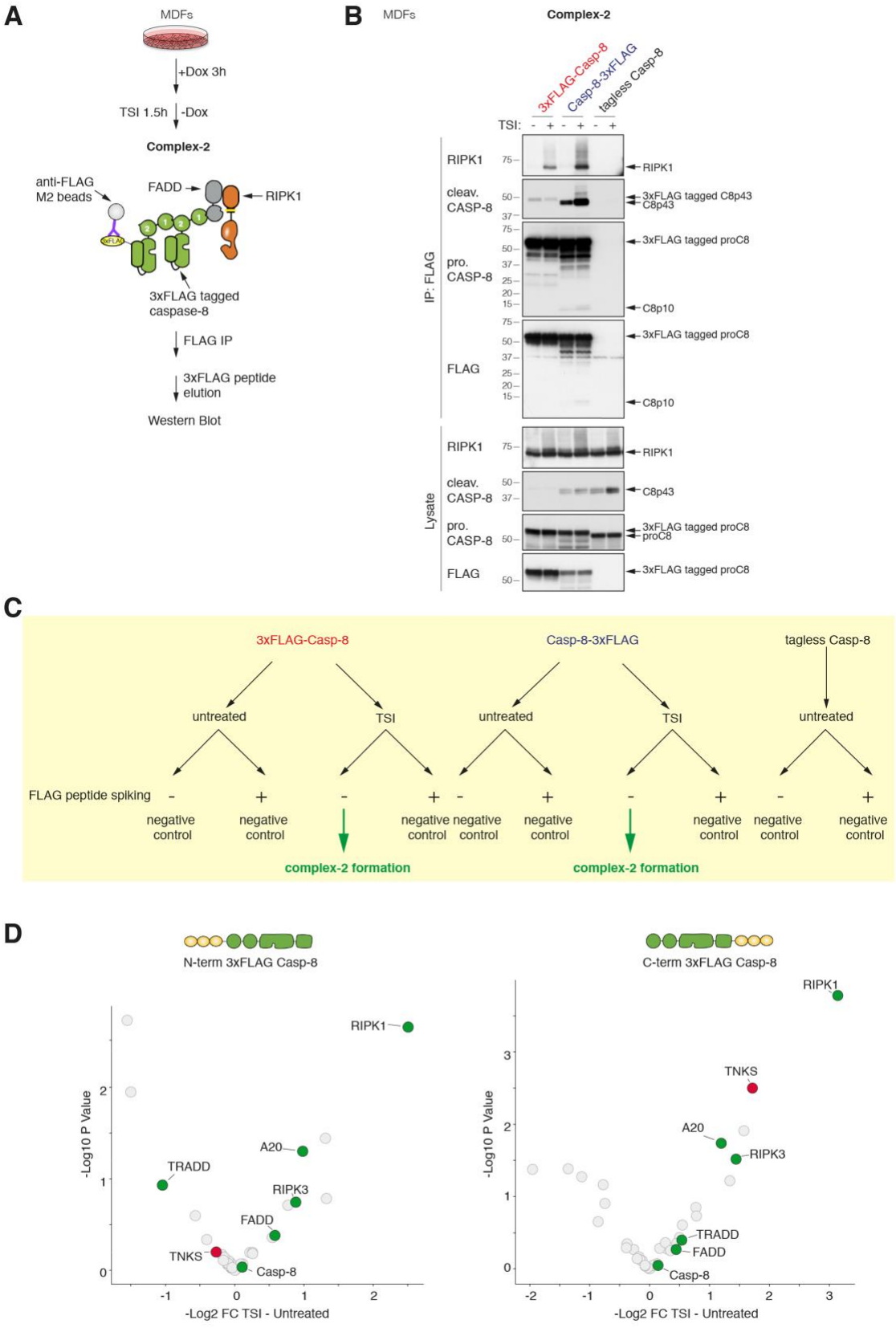
A
MDFs
+Dox 3h
TSI 1.5h
-Dox
Complex-2
anti-FLAG M2 beads
FADD
RIPK1
3xFLAG tagged caspase-8
FLAG IP
3xFLAG peptide elution
Western Blot
B
MDFs
Complex-2
3xFLAG-Casp-8
Casp-8-3xFLAG
tagless Casp-8
TSI:
IP: FLAG
RIPK1
cleav. CASP-8
pro. CASP-8
FLAG
3xFLAG tagged C8p43
C8p43
3xFLAG tagged proC8
C8p10
Lysate
proC8
C
3xFLAG-Casp-8
Casp-8-3xFLAG
tagless Casp-8
untreated
TSI
FLAG peptide spiking
negative control
complex-2 formation
D
N-term 3xFLAG Casp-8
C-term 3xFLAG Casp-8
-Log10 P Value
-Log2 FC TSI - Untreated
RIPK1
TNKS
A20
RIPK3
TRADD
FADD
Casp-8

Figure 3.5. Immunoprecipitation and mass spectrometry analysis of TNFR1 complex-2 in cells expressing endogenous 3x FLAG tagged caspase-8

(A) Schematic depicting the anti-FLAG immunoprecipitation.

(B) TNF-induced complex-2 immunoprecipitation using anti-FLAG M2 affinity beads. Western blot analysis of TNFR1 complex-2 from *Casp8*$^{-/-}$.*Mlkl*$^{-/-}$ MDFs expressing Dox-inducible N-terminally or C-terminally 3x FLAG tagged caspase-8 or tagless caspase-8 using the indicated antibodies. Cells were treated with 20 ng/mL Dox for 3 hours followed by stimulation with TNF (100 ng/mL) +SM CompA (500 nM) + IDN-6556 (5 μM) (TSI) for 1.5 hours in the absence of Dox before subjected to anti-FLAG immunoprecipitation. IDN-6556 was used to stabilize complex-2. The Western blot is representative of five independent experiments.

(C) Schematic representation of experimental design for mass spectrometry.

(D) Log2 fold change volcano plots of protein enrichment upon TSI stimulation in cells expressing either N-terminally (**Left panel**) or C-terminally 3x FLAG tagged caspase-8 (**Right panel**) compared to the untreated control. Proteins were first filtered by requiring a P Value<0.05 in a pairwise comparison between the unexpressed negative controls in either the untreated or TSI treated samples. Known constituents of the native TNFR1 complex-2 (RIPK1, RIPK3, FADD, TRADD and A20) are labelled and highlighted in green while TNKS1 (or TNKS) is highlighted in red. P.Values calculated using Limma (n = 5).

3.6 Discussion

Caspase-8 is an essential initiator of the extrinsic apoptotic pathway and repressor of necroptosis. Mice deficient in caspase-8 show embryonic lethality at E10.5 (Varfolomeev et al., 1998), and the developments defects can be rescue by RIPK3 or MLKL ablation (Alvarez-Diaz et al., 2016; Kaiser et al., 2011). Caspase-8 is synthesized as inactive proform (procaspase-8), consisting of a N-terminal tandem death effector domains (DEDs), a large catalytic subunit p18, a short linker region and a small catalytic subunit p10 (Zamaraev et al., 2017). Upon death ligands stimulation, procaspase-8 are integrated into a large cytoplasmic cell death-inducing platform where they are fully activated. The FasL and TRAIL-induced platform, referred to as death-inducing signalling complex (DISC), have been extensively characterized. The current model for DISC formation proposes that upon TRAIL stimulation, the adaptor molecule FADD, which also harbors an N-terminal DED domain, recruits procaspase-8 *via* direct DED domain interactions. Multiple procaspase-8 molecules then interact through their DED domains, forming a caspase-activating chain. In the DISC, procaspase-8 molecules undergo proximity-induced dimerization and proteolytic cleavage. The proteolytic cleavage happens in two steps: (i) separation of the subunits (p43) from the smaller subunits (p10); (ii) cleavage of the larger subunit (p18) from the DED domains. The p18 and p10 subunits then form caspase-8 catalytic subunit dimers, which are able to cleave a wide range of cellular substrates and therefore drive apoptotic cell death. In the DISC, procaspase-8 also interacts with its catalytically inactive homolog, c-Flip (Dickens et al., 2012a; Hughes et al., 2016; Powley et al., 2016; Yao et al., 2007). In brief, the N-terminal domain of procaspase-8 mediates its self-association and its interaction with FADD or cFlip, while the C-terminal domain possesses catalytic activity.

In TNFR1 signaling, the internalization of membrane-bound complex-1 results in the assembly of a cytosolic complex called complex-2 (Micheau and Tschopp, 2003). Complex-2 contains the core components RIPK1, FADD, caspase-8 and cFlip, and has the potential to trigger apoptosis or to mediate necroptosis. There are extensive research on complex-1 and it-mediated prosurvial signaling. It has been revealed that TNF signalling is heavily regulated by a plethora of post-translational modifications (PTMs), including phosphorylation and diverse types of ubiquitin chains. These PTMs, together with TNF-mediated transcriptional responses, serve as checkpoints that control the formation and cytotoxic potential of complex-2 (Annibaldi and Meier, 2018; Liu and Lalaoui, 2020). However, the composition and PTMs in the cytosolic,

death-inducing complex-2 remain far less well defined. Considering the fact that complex-2 is a large ~2MDa cell death-inducing platform (Micheau and Tschopp, 2003; Tenev et al., 2011), we hypothesized that not all components and posttranslational modifications of this signalling complex had been identified. By generating a FLAG tagged caspase-8 knock-in mice strain, we aimed to analyse the composition of endogenous, caspase-8 containing, complex-2. Before generating the mouse strain, in this chapter I tested *in vitro* whether an N- or C-terminal FLAG tag would affect the ability of caspase-8 in binding with complex-2 components and thereby interfere with its killing activity.

By using Dox-inducible stably integrated lentiviral system, I found that a single FLAG tag was compatible with caspase-8 expression and killing activity. In addition, I've shown that when expressed above physiological levels, the expression and activity of caspase-8 was unaffected by a 3x FLAG tag. Furthermore, after optimisation of Dox treatment we managed to express 3x FLAG tagged caspase-8 at physiological levels and found that neither N- nor C- terminal 3x FLAG significantly perturbed its death function, although C-terminally 3x FLAG tagged caspase-8 appeared to be marginally more efficient in mediating complex-2 formation and cell death. Finally, I purified complex-2 from cells expressing endogenous levels of 3x FLAG tagged caspase-8 and did mass spectrometry (MS) analysis. The MS identified tankyrase-1 (TNKS1/TNKS/ARTD5/PARP5a) as a potential complex-2 interactor and it was characterized in **Chapter 5**.

Overexpression of caspase-8 causes its spontaneous autocleavage which can lead to apoptosis in the absence of death ligand stimulation (Chang et al., 2003a). In addition, overexpression can cause artefacts including ectopic subcellular localization or erroneous protein complexes formation. Lentiviruses, in contrast to retroviruses, typically integrate only once into the host genome and therefore expression levels are usually reproducible between independently generated cell lines and at levels that are not dramatically above endogenous levels (Tanzer et al., 2016; Vince et al., 2007). By using Dox-inducible lentiviral system and titrating the concentration of Dox, we were able to achieve physiological levels of tagged caspase-8 and to analyse the composition of endogenous, caspase-8 containing complex-2 by MS. Therefore, autocleavage-induced spontaneous cell death and non-specific protein interactome could be avoided.

3x FLAG tag has been reported by Sigma and literatures to be ultrasensitive for detection *in vitro* and *in vivo* (Dai et al., 2014; Ferrando et al., 2015; LaCava et al., 2015). Indeed, an anti-

FLAG M2 antibody enabled us to successfully observe the localization of 3x FLAG tagged caspase-8 at physiological levels by immunofluorescence staining. This could also benefit us in exploring the subcellular localization of endogenous, caspase-8-containing protein complexes in Dox-inducible 3x FLAG tagged caspase-8 cell line or primary cells and tissues from knock-in mice, given the fact that effective commercial antibodies against murine procaspase-8 for immunofluorescence staining are currently not available. Furthermore, our approach of tagging caspase-8 with 3x FLAG allowed us to successfully isolate complex-2 for MS analysis because: (i) the anti-FLAG immunoprecipitation is highly efficient; (ii) the immunoprecipitants was eluted by 3x FLAG peptides therefore offered higher specificity without loss of sensitivity; (iii) a FLAG spiking sample ensured the elimination of non-specific interactors of 3x FLAG tag. Since caspase-8 is known to be recruited to the other non-death inducing signalling complexes, for example the ripoptosome, FADDosome and the BCL10 and MALT1 containing signalling platform in the T cells, the Dox-inducible 3xFLAG tagged caspase-8 cell lines and knock-in mice would be great tools to study endogenous protein interactomes in these signalling complexes (Hartwig et al., 2017; Henry and Martin, 2017; Kreuz et al., 2004; Su et al., 2005; Varfolomeev et al., 2005).

When expressed at physiological levels, C-terminally 3x FLAG tagged caspase-8 appeared to be marginally more efficient in mediating complex-2 formation and TNF-induced death compared with N-terminally 3x FLAG tagged caspase-8. Since N-terminal DEDs domain of procaspase-8 is believed to mediate its integration into the cytosolic death-inducing platform upon TRAIL stimulation (Dickens et al., 2012a; Hughes et al., 2016), it is possible that a N-terminal 3x FLAG tag interferes with the assembly of caspase-8 in complex-2 and therefore affects its killing activity.

Formation of DISC chain facilitates the proteolytic domains of adjacent procaspase-8 molecules to homodimerize (Chang et al., 2003a). Within the homodimer, procaspase-8 undergoes autoproteolytic cleavage leads to separation of the subunits (p43) from the smaller subunits (p10). A subsequent cleavage separating DED domains and p18 subunits allows fully activation of caspase-8 and release of the enzymatically active heterotetramer $(p18)_2(p10)_2$ into cytosol (Dickens et al., 2012b; Hughes et al., 2009; Kallenberger et al., 2014). It has been clearly shown that the p43 is retained in TNFR1 complex-2 (Bertrand et al., 2008; Jaco et al., 2017; Lalaoui et al., 2020). The question is whether the smaller subunit p10 are released from complex-2 upon the first cleavage and form heterotetramer with p18 in the cytosol, or retained in the complex-2 until forming heterotetramer with p18 and then released from complex-2.

A previous study on CD95 DISC has suggested that both p18 and p10 were presented in the DISC, which reached a maximum level 1-5 min after stimulation and started to remarkably decrease after 20 min. Consistently, maximum cytosolic p18 and p10 were observed after 20 min CD95 stimulation (Lavrik et al., 2003). This discovery is supported by another *in vitro* study. This study reported that the procaspase-8 and all its cleavage products were detectable in the CD95 DISC, although the p18 subunit was believed to be rapidly released from the complex (Hughes et al., 2009).

The anti-FLAG immunoprecipitation performed in cells expressing C-terminally 3x FLAG tagged caspase-8 indicated that more p10 subunit was detectable upon TNF/SM/IDN stimuli. However, this couldn't help to answer the question. For C-terminally 3x FLAG tagged caspase-8, the p10 subunit which is generated upon death stimulation and has a 3x FLAG tag, was supposed to be enriched by anti-FLAG immunoprecipitation upon TNF/SM/IDN stimulation. However, in **Chapter 4 Figure 4.5B**, the p10 subunit was also detectable upon TNF/SM/IDN by anti-FLAG immunoprecipitation in cells expressing N-terminally 3x FLAG tagged caspase-8 (whose p10 subunit doesn't have a 3x FLAG tag so that it cannot be captured directly by anti-FLAG M2 beads), indicating that a least a small proportion of p10 subunit is retained in TNFR1 complex-2. Our data, together with the previous studies on CD95 DISC, indicate that the death-inducing signalling complex not only facilitates caspase-8 oligomerization but also places them in a spatial orientation favourable for their activation.

Chapter 4 Characterization of 3xFLAG tagged caspase-8 knock-in mice

In **Chapter 3**, I showed that a 3x FLAG tag was compatible with caspase-8 expression and function when expressed above endogenous levels using a Dox-inducible lentiviral system. Interestingly, cells expressing physiological levels of N-terminally 3x FLAG tagged caspase-8 were less sensitive to apoptotic stimuli, probably due to less TNFR1 complex-2 assembly. To understand how a 3x FLAG tag at N-terminal or C-terminal end of caspase-8 may affect its expression and activity *in vivo,* and to study caspase-8 in endogenous complexes, we decided to generate both N-terminally or C-terminally 3x FLAG tagged caspase-8 knock-in mice and I characterized these mice in this chapter.

4.1 CRIPSR/Cas9 knock-in strategy

CRISPR/Cas9 genome editing has been adapted to knock-in epitope tags and fluorophores to accurately track and assay proteins *in vivo* and to analyse protein interactomes at the endogenous level (Yang et al., 2013a). N-terminally or C-terminally 3x FLAG tagged caspase-8 knock-in mice were generated by microinjection of single guide RNAs (sgRNAs), recombinant Cas9, as well as homology-direct repair (HDR) templates into wild-type C57BL/6 embryos. As a result of this sgRNA-dependent Cas9 endonuclease activity, double-strand breaks (DSBs) were introduced into the genomic DNA, allowing for homologous recombination with the HDR templates, generating stable, genetically inheritable 3x FLAG tagged *Casp8* alleles. Deletion mutations could also be generated from this process, resulting in knock-out *Casp8* alleles. However, a full *Casp8* knock-out strain was not obtained because complete loss of caspase-8 causes embryonic lethality (Varfolomeev et al., 1998).

For N-terminally 3x FLAG tagged caspase-8 knock-in mice, a sgRNA targeting the start codon of *Casp8* gene was designed. A double-stranded DNA (dsDNA) encoding 5' region of the *Casp8* gene with an additional N-terminal 3x FLAG tag as well as homologous arms upstream and downstream of the sgRNA targeted region acted as efficient HDR template. An Asn Spacer was introduced into the HDR template to ensure successful gene translation (**Figure 4.1A; Appendix 2 Table 2**).

Generating a C-terminally 3x FLAG tagged caspase-8 knock-in mouse was more challenging because: (i) there was no usable PAM site at the last exon (exon 9) of *Casp*8 gene; (ii) a *Casp8* pseudogene known as *Gm20257* showed ~133 bp of sequence identity to *Casp*8 exon 9, and

was nearby on the same chromosome (chromosome 1). Thus, Cas9 would cut both the *Casp*8 exon 9 and also the pseudogene, resulting in deletions and inefficient gene targeting. Given these challenges, a sgRNA recognizing PAM site at *Casp8* exon 8 was designed. The dsDNA HDR template was composed of protein coding region of exon 9 with an additional C-terminal 3x FLAG tag, followed by two stop codons that were designed to efficiently terminate protein translation. This dsDNA also contained flanking DNA upstream and downstream of sgRNA targeted region to facilitate homologous recombination. After splicing, transcripts contained two exon 9 sequences with a 3x FLAG tag in between which was followed by two translation stops were generated. Therefore, caspase-8 protein with a C-terminal 3x FLAG tag was expected to be produced (**Figure 4.1B; Appendix 2 Table 2**).

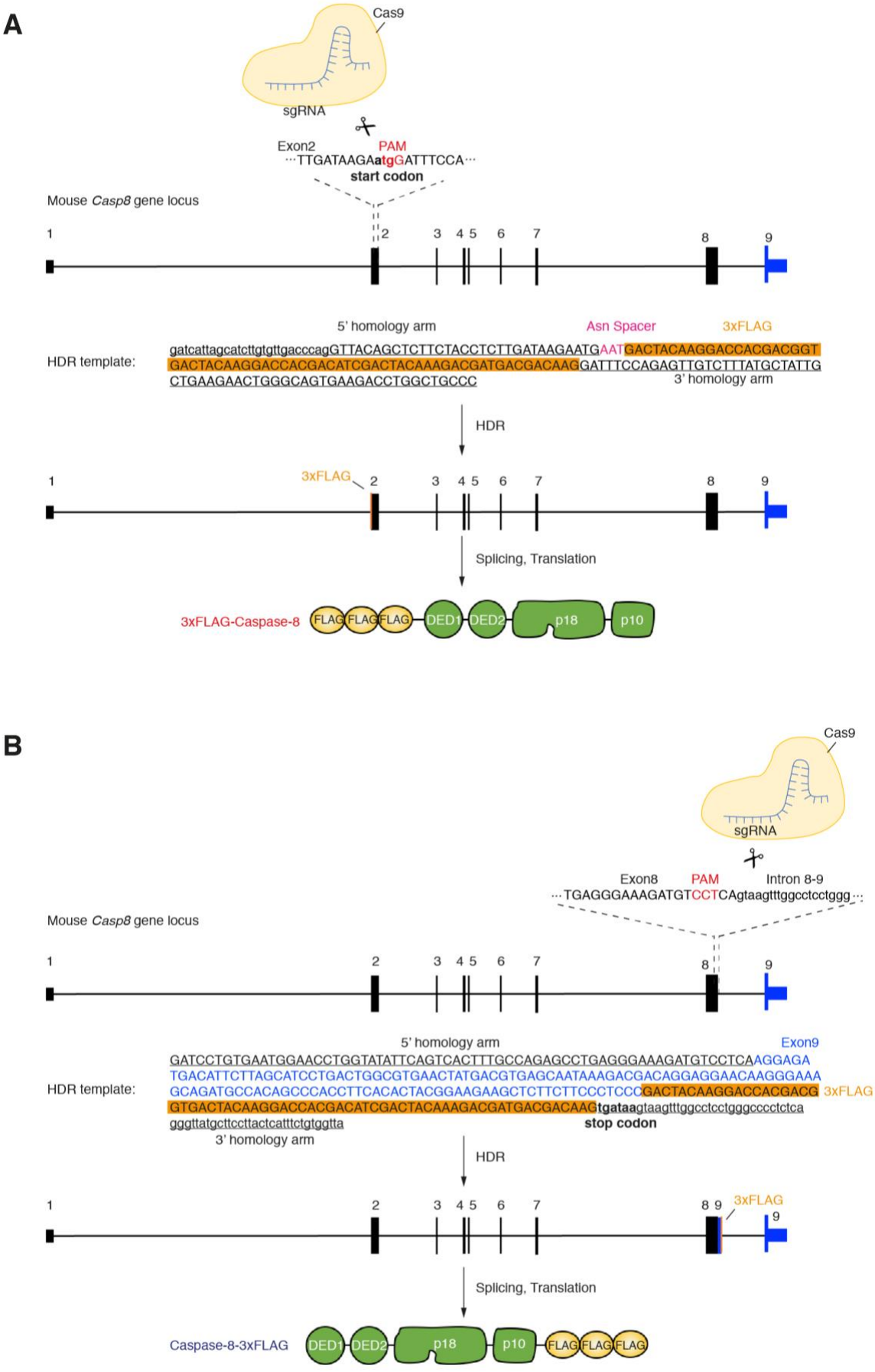
A
Cas9
sgRNA
Exon2
PAM
···TTGATAAGAatgGATTTCCA···
start codon
Mouse Casp8 gene locus
1
2
3
4 5
6
7
8
9
5' homology arm
Asn Spacer
3xFLAG
HDR template:
gatcattagcatcttgtgttgacccagGTTACAGCTCTTCTACCTCTTGATAAGAATGAATGACTACAAGGACCACGACGGT
GACTACAAGGACCACGACATCGACTACAAAGACGATGACGACAAGGATTTCCAGAGTTGTCTTTATGCTATTG
CTGAAGAACTGGGCAGTGAAGACCTGGCTGCCC
3' homology arm
HDR
3xFLAG
Splicing, Translation
3xFLAG-Caspase-8
FLAG
FLAG
FLAG
DED1
DED2
p18
p10
B
Cas9
sgRNA
Exon8
PAM
Intron 8-9
···TGAGGGAAAGATGTCCTCAgtaagtttggcctcctggg···
Mouse Casp8 gene locus
1
2
3
4 5
6
7
8
9
5' homology arm
Exon9
HDR template:
GATCCTGTGAATGGAACCTGGTATATTCAGTCACTTTGCCAGAGCCTGAGGGAAAGATGTCCTCAAGGAGA
TGACATTCTTAGCATCCTGACTGGCGTGAACTATGACGTGAGCAATAAAGACGACAGGAGGAACAAGGGAAA
GCAGATGCCACAGCCCACCTTCACACTACGGAAGAAGCTCTTCTTCCCTCCCGACTACAAGGACCACGACG 3xFLAG
GTGACTACAAGGACCACGACATCGACTACAAAGACGATGACGACAAGtgataagtaagtttggcctcctgggcccctctca
gggttatgcttccttactcatttctgtggtta
stop codon
3' homology arm
HDR
1
2
3
4 5
6
7
8 9
3xFLAG
9
Splicing, Translation
Caspase-8-3xFLAG
DED1
DED2
p18
p10
FLAG
FLAG
FLAG

Figure 4.1. CRIPSR/Cas9 knock-in strategy

Schematic representation of the generation of N-terminally **(A)** or C-terminally **(B)** 3x FLAG tagged caspase-8 knock-in mice using CRIPSR/Cas9 technology.

4.2 Tissue expression of 3x FLAG tagged caspase-8

The 3x FLAG tagged caspase-8 knock-in mice were generated using CRISPR/Cas9 technology. After at least two backcrosses with C57BL/6 mice, heterozygous and homozygous N-terminally or C-terminally 3x FLAG tagged caspase-8 knock-in mice were obtained. Complete caspase-8 deficiency causes embryonic lethality in mice at ~E10.5 due to defects in vascular development while *Casp8*$^{+/-}$ mice appear to be phenotypically normal (Varfolomeev et al., 1998). The homozygous 3x FLAG tagged caspase-8 knock-in mice are viable, fertile and developed normally, indicating that N-terminally or C-terminally 3x FLAG tagged caspase-8 were expressed and active *in vivo*, at least to heterozygous caspase-8 levels.

To explore the expression and tissue distribution of tagged caspase-8, homogenates from organs of heterozygous and homozygous N-terminally or C-terminally 3x FLAG tagged caspase-8 knock-in mice were tested for the expression of caspase-8 by Western blot. The organs from *Casp8*$^{+/+}$ and *Casp8*$^{-/-}$*.Ripk3*$^{-/-}$ mice were used as controls. As indicated in **Figure 4.2**, N-terminally (**Figure 4.2A**) or C-terminally (**Figure 4.2B**) 3x FLAG tagged caspase-8 displayed similar tissue distribution. While caspase-8 was undetectable in the brain, it was readily expressed in the colon, small intestine, heart, kidney, liver, lung, spleen, thymus and skin. The spleen and thymus showed relatively high expression of caspase-8, which was consistent with previous reports (Alvarez-Diaz et al., 2016), highlighting its important role in lymphocytes (Beisner et al., 2005; Salmena et al., 2003).

A clear detection of tagged and tagless caspase-8 from wild-type and knock-in mice but not *Casp8*$^{-/-}$*.Ripk3*$^{-/-}$ mice was obtained using an anti-procaspase-8 antibody. A shift in the molecular weight of caspase-8 was observed for heterozygous and homozygous knock-in mice, suggesting the detection of 3x FLAG tagged caspase-8 knock-in alleles. Probing with an anti-FLAG antibody showed that both N- and C-terminally tagged caspase-8 were expressed and no signal was detected in wild-type mice. Furthermore, the signal intensity was doubled in tissues from homozygous knock-in mice compared with heterozygous knock-in mice, indicating the specificity of the antibody and the fact that the antibody was used within its linear range. However, a strong signal was observed at a smaller size (between 37 kDa and 50 kDa) in *Casp8*$^{-/-}$*.Ripk3*$^{-/-}$ mice. The relevant mouse strains were described in (Kaiser et al., 2011; Oberst et al., 2011) and no mention of a FLAG tagged construct was made, however the strong specific band in these mice is strongly suggestive that they might contain a FLAG-tagged protein.

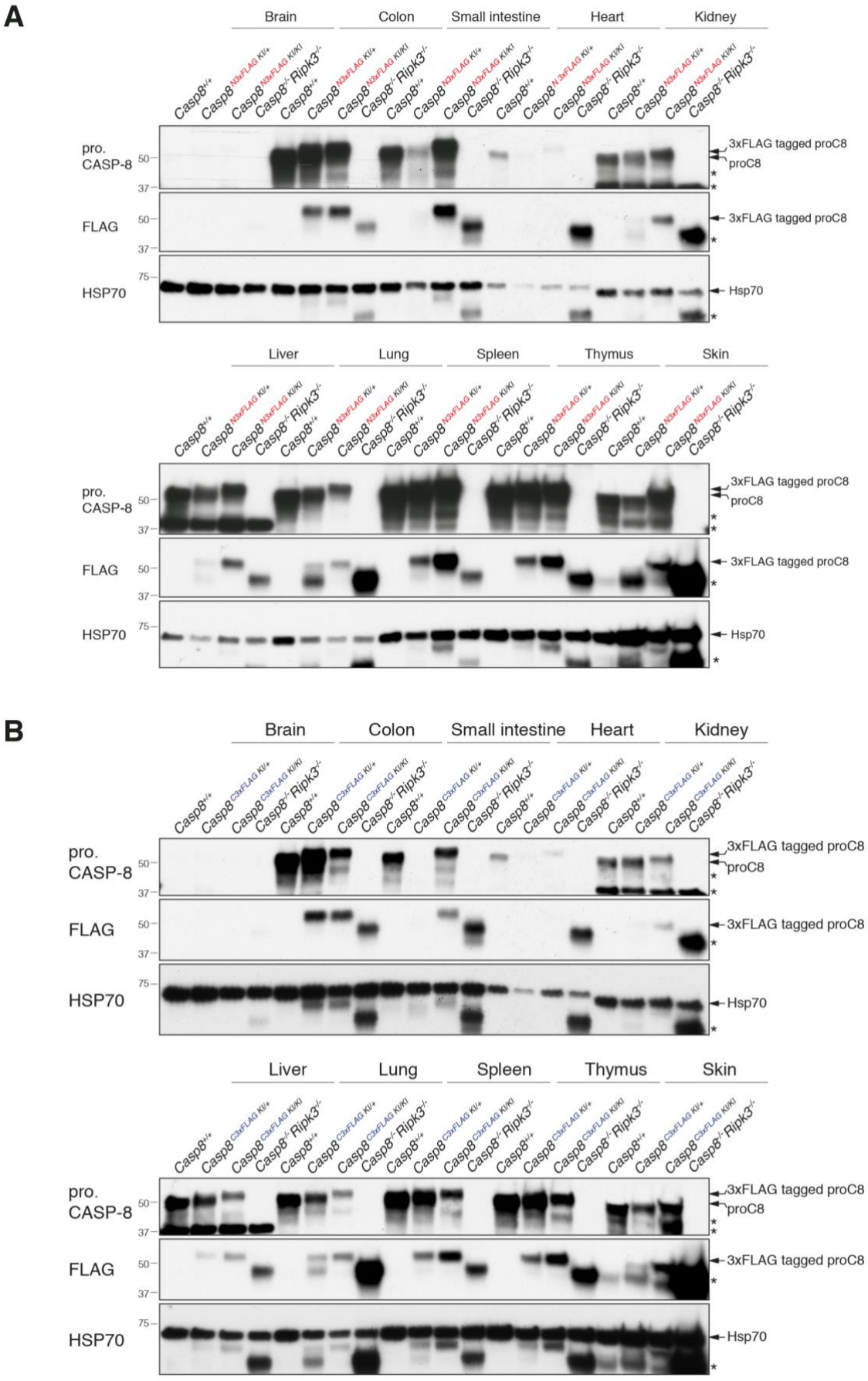
A
Brain
Colon
Small intestine
Heart
Kidney
Liver
Lung
Spleen
Thymus
Skin
pro. CASP-8
FLAG
HSP70
3xFLAG tagged proC8
proC8
Hsp70
B
Brain
Colon
Small intestine
Heart
Kidney
Liver
Lung
Spleen
Thymus
Skin
pro. CASP-8
FLAG
HSP70
3xFLAG tagged proC8
proC8
Hsp70

Figure 4.2. The tissue expression of 3x FLAG tagged caspase-8

Western blot analysis of solid organs and lymphoid tissues from (**A**) N-terminally or (**B**) C-terminally 3x FLAG tagged caspase-8 mice using the indicated antibodies. The organs from *Casp8*$^{+/+}$ and *Casp8*$^{-/-}$.*Ripk3*$^{-/-}$ mice were used as controls. HSP70 was used as loading control.

4.3 Subcellular localization of 3x FLAG tagged caspase-8

Although the localization of procaspase-8 has been shown by an overexpression study (MacFarlane et al., 2000), the distribution of caspase-8 protein *in vivo* is unknown due to the lack of effective commercial anti-procaspase-8 antibodies. I therefore tried to visualize the localization of endogenous caspase-8 by immunofluorescence stain using an anti-FLAG antibody.

MDFs from heterozygous N- or C-terminally 3x FLAG tagged caspase-8 knock-in mice (*Casp8*$^{N3xFLAG\ KI/+}$ and *Casp8*$^{C3xFLAG\ KI/+}$) were generated. MDFs derived from wild-type mice (*Casp8*$^{+/+}$) and *Casp8*$^{-/-}$.*Mlkl*$^{-/-}$ MDFs containing Dox-inducible C-terminally 3x FLAG tagged caspase-8 were used as controls. The reason why *Casp8*$^{-/-}$.*Mlkl*$^{-/-}$ MDFs were chosen had been mentioned in **Chapter 3**. In addition, as shown in **Figure 4.2**, a strong specific band was picked up by anti-FLAG antibody in the tissues from *Casp8*$^{-/-}$.*Ripk3*$^{-/-}$ mice. Therefore, *Casp8*$^{-/-}$.*Mlkl*$^{-/-}$ MDFs appeared to be a better choice compared with *Casp8*$^{-/-}$.*Ripk3*$^{-/-}$ MDFs for anti-FLAG immunofluorescence staining as *Casp8*$^{-/-}$.*Ripk3*$^{-/-}$ MDFs might have a non-specific staining.

The anti-FLAG fluorescent signal was specifically observed in MDFs derived from knock-in mice and also *Casp8*$^{-/-}$.*Mlkl*$^{-/-}$ MDFs containing Dox-inducible C-terminally 3x FLAG tagged caspase-8, but not wild-type MDFs. In MDFs derived from knock-in mice, both N-terminally and C-terminally 3x FLAG tagged caspase-8 displayed a diffuse pattern throughout the cytoplasm, which was consistent with earlier overexpression studies and my observation using the Dox-inducible lentiviral system (**Figure 3.4B**). The expression level of tagged caspase-8 in MDFs from knock-in mice was homogenous while, unsurprisingly, polyclonal *Casp8*$^{-/-}$.*Mlkl*$^{-/-}$ MDFs containing Dox-inducible C-terminally 3x FLAG tagged caspase-8 showed differential expression between cells (**Figure 4.3A**).

A death effector domain chain DISC model has been proposed in which caspase-8 molecules are believed to form an activating chain *via* their DED domains upon TRAIL stimulation and filament formation has been observed during transient overexpression of caspase-8 DED domains (Dickens et al., 2012a). To test this model at endogenous level and with TNF treatment, I treated *Casp8*$^{C3xFLAG\ KI/+}$ MDFs over a TNF/SM time course and performed an anti-FLAG immunofluorescence staining. The caspase-8 DED filament was not observed during the TNF/SM stimuli, however punctate staining (as indicated by white arrows) was observed after 8 hours of TNF/SM treatment (**Figure 4.3B**). Similar punctate staining had been observed

after 3 hours TNF/SM treatment using an *in situ* proximity ligation assay (Jaco et al., 2017). Although on my hand this punctate staining was detected after 8 hours of TNF/SM treatment, this pattern might represent the formation of caspase-8-containing TNFR1 complex-2.

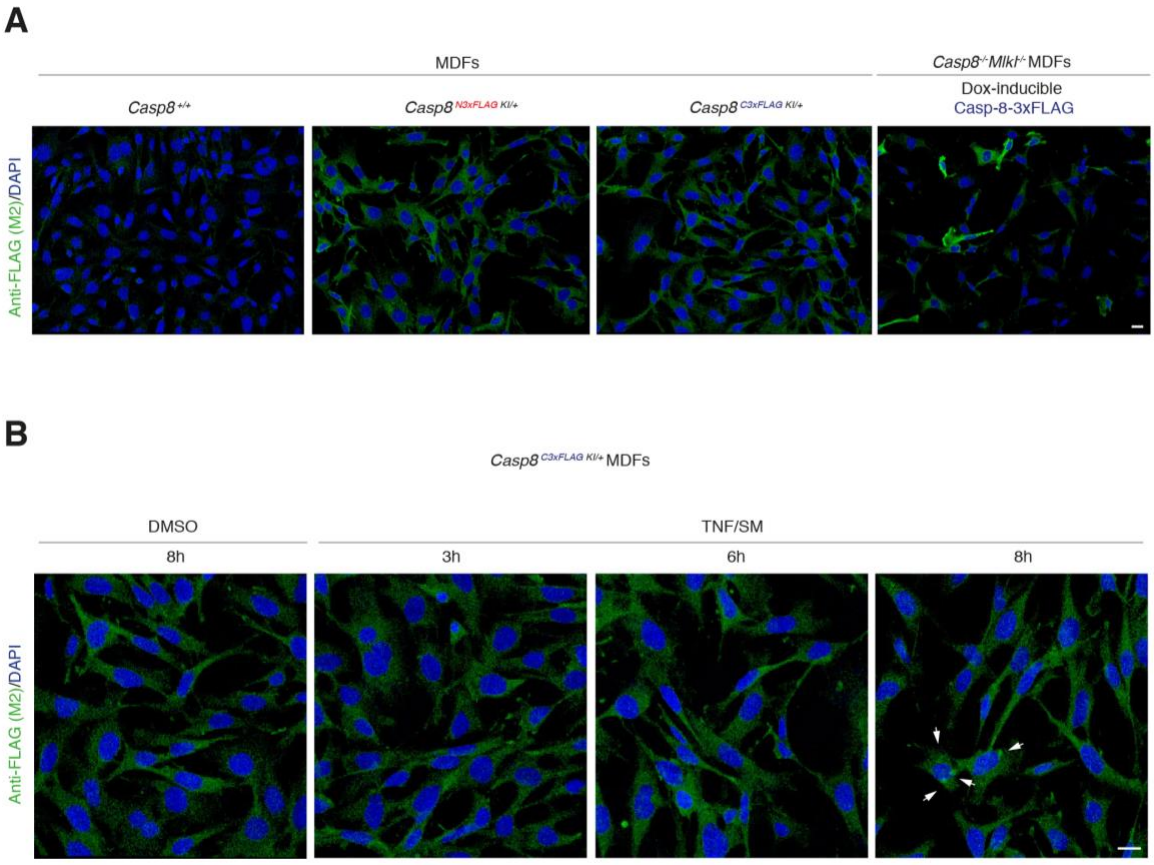

Figure 4.3. The subcellular localization of 3x FLAG tagged caspase-8

(A) Immunofluorescence staining of *Casp8*$^{+/+}$, *Casp8*$^{N3xFLAG\ KI/+}$ and *Casp8*$^{C3xFLAG\ KI/+}$ MDFs or *Casp8*$^{-/-}$.*Mlkl*$^{-/-}$ MDFs expressing Dox-inducible C-terminally 3x FLAG tagged caspase-8 using anti-FLAG M2 antibody (1:500). *Casp8*$^{-/-}$.*Mlkl*$^{-/-}$ MDFs expressing Dox-inducible C-terminally 3x FLAG tagged caspase-8 were pre-treated with 20 ng/mL Dox for 3 hours before harvested for anti-FLAG immunofluorescence staining. Scale bar, 10 μm.

(B) Immunofluorescence staining of *Casp8*$^{C3xFLAG\ KI/+}$ MDFs during TNF/SM stimulation using anti-FLAG M2 antibody (1:500). Cells were stimulated with TNF (100 ng/mL) + SM CompA (500 nM) for the indicated times before harvested for anti-FLAG immunofluorescence staining. White arrows show punctate staining. Scale bar, 10 μm.

4.4 Cells derived from knock-in mice respond similarly to wild-type upon death stimulation

To determine whether tagged caspase-8 behaves similarly to tagless caspase-8 at physiological levels, *Casp8*$^{N3xFLAG\ KI/+}$ and *Casp8*$^{C3xFLAG\ KI/+}$ MDFs were first stimulated with apoptotic stimuli (TNF/SM or TNF/CHX) and necroptotic stimuli (TNF/SM/IDN or TNF/CHX/IDN). Wild-type MDFs (*Casp8*$^{+/+}$) were used as controls. Both *Casp8*$^{N3xFLAG\ KI/+}$ and *Casp8*$^{C3xFLAG\ KI/+}$ MDFs displayed similar extent of apoptotic and necroptotic death when compared to wild-type MDFs (**Figure 4.4A**).

Bone marrow-derived macrophages (BMDMs) were also generated from homozygous N-terminally or C-terminally 3x FLAG tagged caspase-8 knock-in mice (*Casp8*$^{N3xFLAG\ KI/KI}$ and *Casp8*$^{C3xFLAG\ KI/KI}$), and from wild-type mice (*Casp8*$^{+/+}$) (**Figure 4.4B**). As expected, the apoptotic death induced by TNF/SM and necroptotic death induced by TNF/SM/IDN was comparable between BMDMs from homozygous knock-in mice and wild-type mice. These results suggested that a 3x FLAG tag was compatible with caspase-8 cell death function.

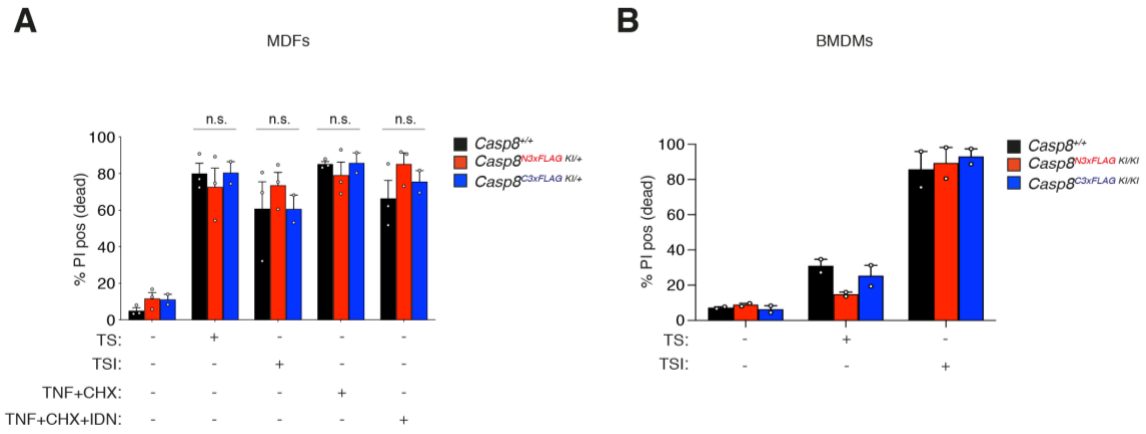

Figure 4.4. The response of cells derived from knock-in mice to death stimulation

(A) Level of cell death assessed by propidium iodide (PI) positive cells. MDFs from *Casp8*$^{+/+}$, *Casp8*$^{N3xFLAG\ KI/+}$ and *Casp8*$^{C3xFLAG\ KI/+}$ mice were stimulated with TNF (100 ng/mL) + SM CompA (500 nM) or TNF (100 ng/mL) +SM CompA (500 nM) + IDN-6556 (5 µM) or TNF (100 ng/mL) + cycloheximide (1µg/mL) or TNF (100 ng/mL) + cycloheximide (1 µg/mL) + IDN-6556 (5 µM) for 20 hours before subjected to FACS analysis. Graphs show mean ± SEM, n=2-3 biological replicates. Comparisons were performed with a Student's t test whose values are denoted in the figures as n.s.= no significance.

(B) Level of cell death assessed by PI positive cells. BMDMs from *Casp8*$^{+/+}$, *Casp8*$^{N3xFLAG\ KI/KI}$ and *Casp8*$^{C3xFLAG\ KI/KI}$ mice were stimulated with TNF (100 ng/mL) +SM CompA (500 nM) or TNF (10 ng/mL) +SM CompA (50 nM) + IDN-6556 (5 µM) for 20 hours before subjected to FACS analysis. Graphs show mean ± SEM, n=2 biological replicates.

4.5 TNFR1 complex-2 formation in cells derived from knock-in mice

To determine whether complex-2 could be efficiently isolated from cells expressing endogenous levels of 3x FLAG tagged caspase-8, anti-FLAG immunoprecipitation was performed in wild-type (*Casp8*$^{+/+}$), *Casp8*$^{N3xFLAG\ KI/+}$ and *Casp8*$^{C3xFLAG\ KI/+}$ MDFs after 1.5 hours TNF/SM or TNF/SM/IDN stimulation. As shown in **Figure 4.5A**, complex-2 components could be detected upon TNF/SM/IDN, and not TNF/SM treatment only in 3x FLAG tagged caspase-8 expressing MDFs. This observation demonstrated the specificity of anti-FLAG immunoprecipitation and was consistent with complex-2 stabilisation induced by caspase inhibitors as previously described (Micheau and Tschopp, 2003). While complex-2 was only captured in 3x FLAG tagged caspase-8 expressing MDFs, cleavage of caspase-8 and cFlip$_L$ were detected in the whole lysate of all cell types and genotypes. Formation of complex-2 was less efficient in *Casp8*$^{N3xFLAG\ KI/+}$ MDFs when compared to *Casp8*$^{C3xFLAG\ KI/}$ MDFs, as indicated by the decreased levels of RIPK1, cleaved caspase-8, cFlip$_L$, FADD and RIPK3 in complex-2.

Complex-2 assembly was also assessed in wild-type, *Casp8*$^{N3xFLAG\ KI/+}$ and *Casp8*$^{C3xFLAG\ KI/+}$ BMDMs (**Figure 4.5B**). Similar to MDFs, the complex-2 was only captured in BMDMs from knock-in mice but not those from wild-type mice. Intriguingly, while cleaved caspase-8 (p43 and p10) and FADD recruitment were reduced in the *Casp8*$^{N3xFLAG\ KI/+}$ BMDMs when compared to the ones in the *Casp8*$^{C3xFLAG\ KI/+}$ BMDMs, comparable level of RIPK1, cFlip$_L$ and RIPK3 were immunoprecipitated in both *Casp8*$^{N3xFLAG\ KI/+}$ and *Casp8*$^{C3xFLAG\ KI/+}$ BMDMs. Less cleaved caspase-8 was detected in the *Casp8*$^{N3xFLAG\ KI/+}$ BMDM lysates that might account for the reduced cleaved caspase-8 levels in the *Casp8*$^{N3xFLAG\ KI/+}$ BMDMs complex-2, and also suggest that an N-terminal 3xFLAG tag might affect caspase-8 activity at early time points. That said, the extent of caspase-8 activation in *Casp8*$^{N3xFLAG\ KI/+}$ BMDMs was sufficient to drive the same level of cell death at later time point in these cells (**Figure 4.4B**).

Taken together, the expression of one allele of 3x FLAG tagged caspase-8 is sufficient to isolate complex-2 demonstrating that these mice are ideal tools to characterize caspase-8-containing complex-2 at endogenous levels and to study caspase-8 functions *in vivo*.

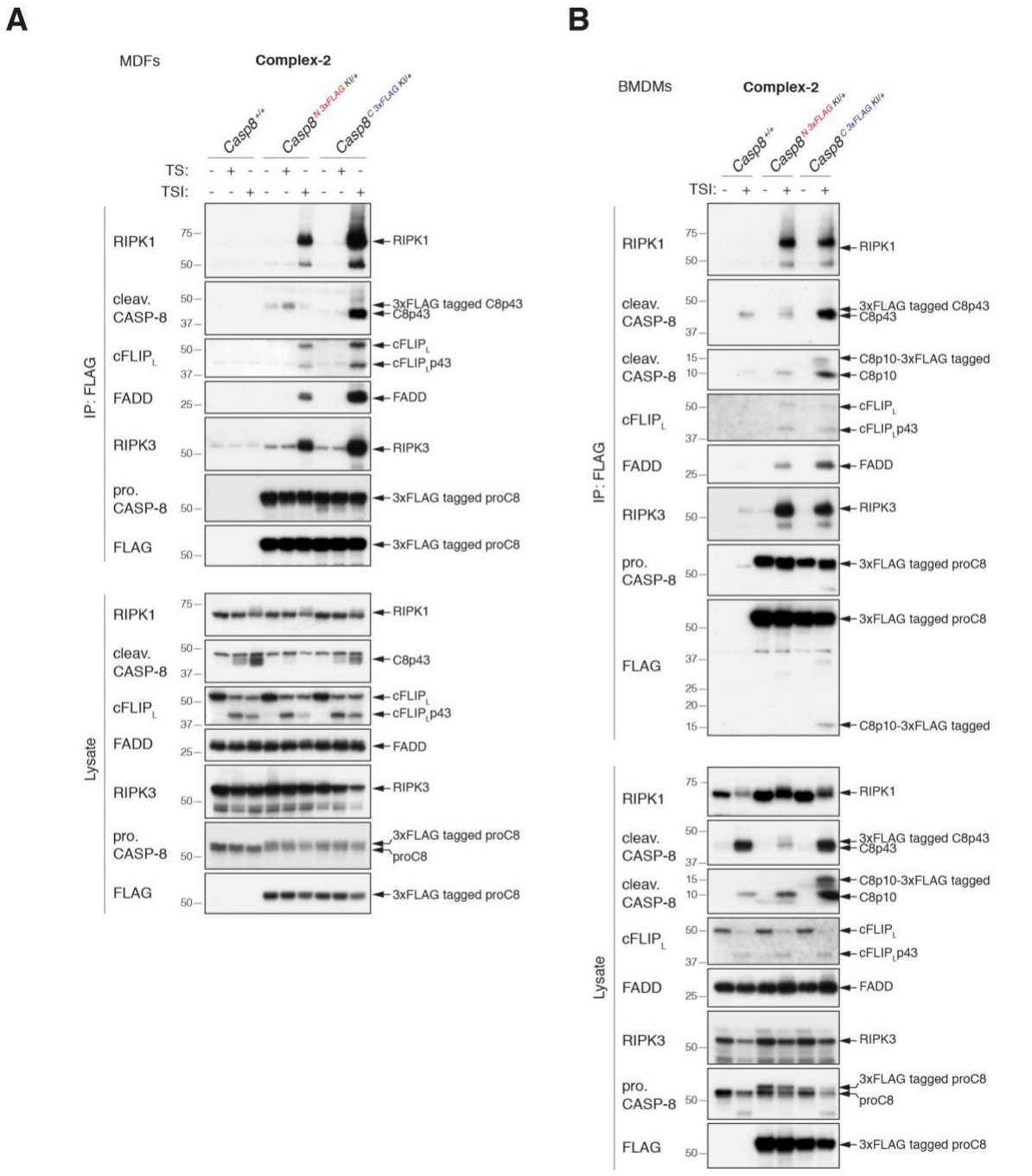

Figure 4.5. TNFR1 complex-2 formation in cells from knock-in mice

TNF-induced complex-2 immunoprecipitation using anti-FLAG M2 affinity beads. Western blot analysis of complex-2 from *Casp8*$^{+/+}$, *Casp8*$^{N3xFLAG\ KI/+}$ and *Casp8*$^{C3xFLAG\ KI/+}$ MDFs **(A)** or BMDMs **(B)** using the indicated antibodies. Cells were stimulated with TNF (100 ng/mL) + SM CompA (500 nM) stimulation for 1.5 hours. IDN-6556 (5 μM) was used to stabilize complex-2.

Discussion

Our *in vitro* data (**Chapter 3**) suggested that while neither tag affected caspase-8 activity greatly, the C-terminally 3x FLAG tagged caspase-8 was slightly closer in activity to wild-type caspase-8 than N-terminally 3x FLAG tagged caspase-8. Unfortunately, generating a C-terminally 3x FLAG tag caspase-8 in mice required an innovative but unproven strategy. To ensure that we had tagged mice to work with, we generated both N-terminally or C-terminally 3x FLAG tagged caspase-8 knock-in mice and these mice were characterized *in vitro* in this chapter.

By using CRIPSR/Cas9 technology, we created knock-in mice strains which express 3x FLAG tagged caspase-8 from the endogenous *Casp8* locus. This unique tool provides three main advantages. First, it allows for sensitive detection of endogenous interacting partners. The knock-in mice ensure that the 3x FLAG tagged caspase-8 protein is expressed at the physiological level, so that non-specific protein-protein interactions caused by the overexpression of tagged caspase-8 is minimized. Second, it facilitates the purification of caspase-8 or caspase-8 containing protein complexes using the highly efficient anti-FLAG immunoprecipitation. The immunoprecipitants are eluted by 3x FLAG peptide with high efficiency and specificity, which helps focus the mass spectrometry analysis by limiting background and non-specific interactors. Furthermore, it allows the visualisation of endogenous caspase-8 protein by anti-FLAG immunofluorescence staining. The endogenous subcellular localization of caspase-8 is currently unknown due to the lack of effective commercial anti-procaspase-8 antibodies. The knock-in mice will provide insight into the distribution and activation of caspase-8 *in vivo*.

Although a tagged caspase-8 knock-in mouse has not been reported yet, the caspase-8 knockout mice are well studied. While heterozygous mice lacking one allele of caspase-8 ($Casp8^{+/-}$) appear grossly normal, homozygous $Casp8^{-/-}$ mice are embryonically lethal at day 10.5 (~E10.5) due to defects in vascular development (Varfolomeev et al., 1998). Loss of RIPK3 or MLKL overcomes the embryonic lethality by preventing abnormal necroptosis caused by loss of caspase-8 (Alvarez-Diaz et al., 2016; Kaiser et al., 2011; Oberst et al., 2011). The observation that homozygous N-terminally or C-terminally 3x FLAG tagged caspase-8 knock-in mice were viable, fertile and developed normally indicated that N-terminally or C-terminally 3x FLAG tagged caspase-8 were expressed and active *in vivo*, at least to heterozygous caspase-8 levels.

The anti-procaspase-8 blot of mice tissues suggested that the expression of 3x FLAG tagged caspase-8 was comparable to physiological levels. The spleen and thymus showed relatively higher expression of caspase-8 compared with the other organs, implying its important role in lymphocyte homeostasis (Beisner et al., 2005; Kang et al., 2004; Salmena et al., 2003). The anti-FLAG blot specifically showed the expression of 3x FLAG tagged caspase-8, with doubled signal intensity observed in homozygous knock-in mice compared with heterozygous knock-in mice. Interestingly, a band between 37 kDa and 50 kDa was detected by anti-FLAG M2 antibody in *Casp8*$^{-/-}$*.Ripk3*$^{-/-}$ mice. These mice have been previously described (Kaiser et al., 2011; Oberst et al., 2011), however no mention of a FLAG tagged construct was made when generating these mice. Therefore, there are several possibilities that could help explain the detection of this band: (i) Deletion of caspase-8 and RIPK3 causes elevated levels of a cellular protein that has a F-L-A-G sequence in it, which could be detected by commercial anti-FLAG M2 antibody. To test this possibility, homogenates from organs of *Ripk3*$^{-/-}$ mice and *Casp8*$^{-/-}$*.Mlkl*$^{-/-}$ mice could be probed using other anti-FLAG antibody clones. (ii) Since *Casp8*$^{-/-}$*.Ripk3*$^{-/-}$ mice mice have autoimmune pathology with excess IgG and other antibodies, this band could be IgG light or heavy chain that is abnormally increased in tissues from these mice. This could be avoided by using biotinylated anti-FLAG M2 antibody and then streptavidin-HRP for Western blotting.

Immunofluorescence staining of 3x FLAG tagged caspase-8 revealed a diffused endogenous caspase-8 expression throughout the cytoplasm. This was consistent with a previous overexpression study (MacFarlane et al., 2000) and my data using the Dox-inducible lentiviral system. According to the death effector domain chain DISC model, caspase-8 molecules form an activating chain *via* their DED domains upon TRAIL stimulation. This model was supported by the observation that transient overexpression of caspase-8 DED domains induced filament formation (Dickens et al., 2012a). However, on my hand upon TNF/SM treatment, filaments were not detected but instead punctate staining was observed at later time point (8 hours). This could be explained by several possibilities: (i) upon death stimulation, only a small proportion of cytosolic procaspase-8 is recruited into complex-2 (Tenev et al., 2011); (ii) DED interactions are different between the FasL/TRAIL-induced DISC and the TNFR1-induced complex-2. The punctuate pattern upon TNF/SM stimulation was nevertheless similar to previous observations using *in situ* proximity ligation assay (Jaco et al., 2017). To test this hypothesis, a comparison between FasL, TRAIL and TNF/SM treatments should be performed in the 3x FLAG tagged caspase-8 expressing cells.

In contrast to the Dox-inducible system, *Casp8*$^{N3xFLAG\ KI/+}$ and *Casp8*$^{C3xFLAG\ KI/+}$MDFs showed similar response to apoptotic or necroptotic stimulations compared with wild-type MDFs. Although, and like the Dox-inducible system, *Casp8*$^{N3xFLAG\ KI/+}$ MDFs were less efficient in forming complex-2. Since the N-terminal domain of procaspase-8 mediates its interaction with FADD or cFlip, it is possible that an N-terminal 3x FLAG tag in caspase-8 interfered with self-association as well as the interaction with the other complex-2 components, resulting in decreased complex-2 assembly. However, contrary to this interpretation, similar levels of RIPK1, RIPK3 and cFlip$_L$ were recruited to caspase-8 in *Casp8*$^{N3xFLAG\ KI/+}$ and *Casp8*$^{C3xFLAG\ KI/+}$ BMDMs. Furthermore, these BMDMs also displayed comparable sensitivity to death stimulation. This suggested that complex-2 size/formation might differ from a cell type to another and once caspase-8 activation reached the point of no return cells die. This could be tested in TNF titration experiment.

To summarise, in this chapter I found that an N-terminal or C-terminal 3x FLAG tag did not affect caspase-8 steady-state, as both knock-in mice were viable, fertile and developed normally. These mice offered the possibility of visualising endogenous caspase-8 protein as well as purifying caspase-8-containing protein complexes. Both Dox-inducible system and knock-in mice revealed that an N-terminal 3x FLAG tag slightly affect caspase-8 integration into complex-2, which should be taken into consideration for caspase-8 function readouts in (patho) physiological settings.

Chapter 5 Identification of tankyrases as novel regulators of TNF-induced death

Abstract

Tumor necrosis factor (TNF) is an inflammatory cytokine that, upon binding to its receptor TNFR1, can drive cytokine production, cell survival, or cell death. It is known that TNF stimulation leads to the formation of two distinct signalling complexes. While most previous studies have focused on the membrane bound complex (complex-1), the composition and post-translational modifications of the cytosolic death inducing complex (complex-2) remain poorly defined. Here we identify the poly(ADP-ribose) polymerase (PARP) family members, tankyrase -1 and -2 as novel native complex-2 interactors using a mass spectrometry approach. We find that tankyrases are recruited to complex-2 when cIAPs are depleted after Smac-mimetic (SM) treatment, resulting in complex-2 poly(ADP-ribosyl)ation (PARsylation). Tankyrases-specific inhibitor treatment sensitizes cells to TNF-induced death, which is correlated with increased complex-2 assembly. Mechanistically, tankyrases may decrease the stability of complex-2 via a tankyrases-RNF146 axis. Moreover, inactivation of tankyrases dramatically increases the killing of the clinical SM birinapant in a primary acute myeloid leukemia (AML) model. Thus, tankyrases-mediated PARsylation of complex-2 can serve as a checkpoint within the TNF signalling pathway and can be explored further for cancer treatment.

Introduction

Tumor necrosis factor (TNF) is a pleiotropic cytokine that maintains homeostasis by regulating inflammation, cell proliferation, cell survival, differentiation and cell death (Annibaldi and Meier, 2018). TNFR1-mediated excessive or chronic production of inflammatory cytokines and aberrant TNFR1-induced cell death have been implicated in the pathology of cancer, sepsis, diabetes, and autoimmune diseases (Pasparakis and Vandenabeele, 2015; Silke et al., 2015).

Binding of TNF ligand to TNFR1 leads to the formation of two distinct signalling complexes (Micheau and Tschopp, 2003). TNFR1 rapidly assembles complex-1 at the plasma membrane by recruiting the adaptors TRADD and TRAF2 and the kinase RIPK1. TRAF2 then recruits

the E3 ubiquitin ligases cellular Inhibitor of APoptosis 1 (cIAP1) and cIAP2. cIAPs ubiquitylate several molecules within this membrane complex including RIPK1 (Silke, 2011). Ubiquitylation of complex-1 components allows the recruitment of TAK1-TAB1-TAB2, NEMO-IKK1-IKK2 and the E3 ligase Linear UBiquitin chain Assembly Complex (LUBAC) (Haas et al., 2009). The LUBAC E3 ligase complex generates linear ubiquitin chains which stabilize complex-1 and promote the phosphorylation of IKK2 and mitogen-activated protein kinases (MAPKs) by TAK1. Activation of IKK2 and MAPK kinases lead to the transcription of NF-κB-dependent and MAPK-dependent genes that induce inflammation, proliferation, and cell survival such as cFlip (Lalaoui and Vaux, 2018; Micheau et al., 2001).

Internalization of complex-1 leads to the formation of a cytosolic death inducing complex referred to as complex-2 which comprises TRADD, FADD, caspase-8, cFlip, RIPK1, RIPK3 and A20 (Cho et al., 2009; Micheau and Tschopp, 2003; Onizawa et al., 2015). Whether complex-2 is lethal to cells is determined by multiple checkpoints. The most studied post-translational modifications are ubiquitylation by cIAPs and LUBAC and phosphorylation by TAK1, IKKs, MK2 or TBK1 of RIPK1. Defects in RIPK1 ubiquitylation or phosphorylation accelerate the formation and increase activation of complex-2 (Bertrand et al., 2008; Dondelinger et al., 2013; Dondelinger et al., 2015; Jaco et al., 2017; Lafont et al., 2018; Lalaoui et al., 2016; Liu and Lalaoui, 2020; Moquin et al., 2013; Onizawa et al., 2015). In addition, the absence of cIAPs or TAK1/IKKs reduces canonical NF-κB signalling, which results in a reduction in the levels of $cFlip_L$ and thereby increases caspase-8 activation. Under such perturbed conditions, if caspase-8 activity is sufficient, caspase-3 and RIPK1 are cleaved and cells die by apoptosis. However, if caspase-8 function is absent or inhibited, the accumulation of full length RIPK1 causes its auto-activation which promotes the phosphorylation of RIPK3 and the activation of MLKL, triggering necroptosis (Murphy et al., 2013; Silke and Vucic, 2014; Sun et al., 2012; Vandenabeele et al., 2010). Aberrant IAPs levels have been associated with human cancers and chemoresistance (Fulda and Vucic, 2012). Several small pharmacological molecules targeting IAPs, called Smac-mimetics (SM), have been developed for cancer therapy. SM binds to the BIR domains of the IAPs, preventing XIAPs from inhibiting caspases. SM treatment also triggers auto-ubiquitylation and proteasomal degradation of cIAPs (Silke and Meier, 2013), inducing TNF secretion and sensitizing cells to TNF induced cytotoxicity (Petersen et al., 2007; Varfolomeev et al., 2007; Vince et al., 2007).

How post translational modifications on RIPK1 affects complex-2 activity post TNF stimulation has been extensively studied, however those occurring on the other complex-2

components have not been as well characterised. More work has been done on the cytosolic complex induced following TRAIL and FasL stimulation, where complex-2 is known as the Death Inducing Signalling Complex (DISC), and where post translational modifications on caspase-8 have been shown to regulate its activity. For example, upon FasL stimulation, Src kinase-mediated phosphorylation of caspase-8 at Y380 blocks its autoproteolytic activity and attenuates DISC activity (Powley et al., 2016). In TRAIL signalling, polyubiquitylation of caspase-8 by a cullin3 (CUL3)-based E3 ligase has been found to cause caspase-8 aggregation, and thereby increasing DISC activity (Jin et al., 2009). Furthermore, pathogens try and interfere with signalling by post-translational modification of DISC components. For example, Enteropathogenic *Escherichia coli* (EPEC) encodes an N-acetylglucosamine transferase enzyme, NleB1, that modifies Arg117 in the Death Domain of FADD which inhibits FasL induced death in response to EPEC infection (Li et al., 2013; Pearson et al., 2013).

Complex-2 is a large ~2MDa cell death-inducing platform, and so far the known components are TRADD, TRAF2, cIAP1 FADD, caspase-8, cFlip, RIPK1, RIPK3 and A20 (He et al., 2009; Micheau and Tschopp, 2003; Onizawa et al., 2015). Given its size, we hypothesized that there may be other components and different post translational modifications that regulate this signalling complex. Using a mass spectrometry approach, we identified tankyrase-1 as a novel interactor in TNFR1 complex-2 and biochemically and functionally analyse the role of tankyrase-1 and -2 in TNF-mediated death.

Tankyrase-1 (TNKS1/TNKS/ARTD5/PARP5a) and tankyrase-2 (TNKS2/ARTD6/PARP5b) belong to the poly(ADP-ribose) polymerase (PARP) family of proteins, which use NAD^+ to synthesize ADP-ribose polymers on protein acceptors (Hsiao and Smith, 2008). Notably, TNKS1 and TNKS2 are two distinct proteins encoded by different genes, rather than splice variants (Hottiger et al., 2010). Tankyrases have been shown to modulate processes as diverse as telomere maintenance, WNT signalling pathway, mitosis and insulin-stimulated glucose uptake (Riffell et al., 2012). The most studied role of tankyrases-induced poly (ADP-ribosyl)ation (PARsylation) is to promote poly-ubiquitylation and proteasomal degradation of their substrates. The E3 ligase RNF146 is widely employed as the ubiquitin ligase that recognizes tankyrases-mediated PARsylation. Following tankyrases-induced PARsylation, RNF146 tags the substrate, auto-PARsylated tankyrases and itself for proteasomal degradation (Callow et al., 2011; Zhang et al., 2011). The tankyrases-RNF146 axis has been implicated in regulating the stability of multiple proteins including Axin, 3BP2, PTEN, LKB1 and AMOT (Levaot et al., 2011; Li et al., 2019; Li et al., 2015; Wang et al., 2015; Zhang et al., 2011).

3BP2 plays a role in bone formation, while Axin, PTEN, LKB1 and AMOT are associated with tumorigenesis signalling pathways. These studies provide insights into a range of tankyrases-RNF146 axis-mediated diverse biological processes and also uncover tankyrases as drug targets for cancer therapy. Tankyrases-mediated PARsylation can also induce degradation-independent ubiquitylation. A recent study has demonstrated that tankyrases enhance JNK signalling by inducing K63-linked ubiquitylation of JNK kinase in *Drosophila* (Li et al., 2018).

A previous study has shown that inhibition of tankyrases in macrophages leads to increased TNF secretion. Mechanistically, tankyrases-mediated PARsylation of 3BP2 results in its ubiquitylation by RNF146 and that in turn leads to 3BP2 proteasomal degradation. Inactivation of tankyrases stabilizes 3BP2, which causes hyperactivation of the SRC, SYK, and VAV signalling pathways. This in turn leads to hyperactive bone-remodelling osteoclasts and elevated TNF secretion by macrophages, resulting in inflammation (Levaot et al., 2011). A follow-up study has suggested that RANKL, a TNF superfamily (TNFSF) member, facilitates 3BP2-mediated normal osteoclast development via negatively regulating the transcription of RNF146 through NF-κB signalling (Matsumoto et al., 2017). These studies have indicated the possible relevance of tankyrases and E3 ligase RNF146 with TNFSF signalling and inflammatory cytokine production.

In this study we demonstrate that tankyrases are novel TNFR1 complex-2 components. We find that during TNF signalling, complex-2 becomes PARsylated in a tankyrases-dependent manner. Furthermore, tankyrases-specific inhibitors sensitize cells to TNF-induced cell death, which correlates with increased levels of complex-2. This suggests that normally tankyrases help limit TNF induced death. Mechanistically, tankyrases may modulate the stability of complex-2 by recruiting the E3 ligase RNF146, that in turn promotes ubiquitylation and degradation of complex-2. Moreover, inactivation of tankyrases dramatically increases the killing of the clinical SM birinapant in a primary acute myeloid leukemia (AML) model. Thus, tankyrases-mediated PARsylation of complex-2 can serve as a checkpoint within the TNF signalling pathway and can be explored further for cancer treatment.

5.1 Identification of tankyrases as components of the native TNFR1 complex-2

5.1.1 Validation of MS result by Western blot

To analyse TNFR1 complex-2 composition, we undertook an unbiased proteomic-based approach using 3x FLAG tagged caspase-8. This allowed the purification of caspase-8 or caspase-8 containing protein complexes using anti-FLAG immunoprecipitation. To generate proof of principle data, while the 3x FLAG tagged caspase-8 CRISPR knock-in mice were generated, *Casp8*$^{-/-}$.*Mlkl*$^{-/-}$ MDFs expressing doxycycline (Dox)-inducible N- or C-terminally 3x FLAG tagged caspase-8, characterised in **Chapter 3**, were used for the mass spectrometry analysis.

As described in **Chapter 3**, mass spectrometry analysis of native TNFR1 complex-2 purified from cells expressing N- or C-terminally 3x FLAG tagged caspase-8 revealed that known complex-2 constituents, such as RIPK1, RIPK3, A20 and FADD, were enriched upon TNF/Smac-mimetic (SM)/IDN stimulation with high confidence, multiple peptide matches, and good coverage of the protein sequences (**Table 3.1 and 3.2**). This observation indicated successful purification of native TNFR1 complex-2 by anti-FLAG immunoprecipitation and detection by mass spectrometry. Based on Log2 fold change values, -Log 10 P Values and peptide information, we focused on tankyrase-1 (TNKS1/TNKS/ARTD5/PARP5a), a member of the poly(ADP-ribose) polymerase superfamily, because it was significantly enriched upon TNF/SM/IDN treatment compared to untreated control in cells expressing C-terminally 3x FLAG tagged caspase-8 and was also present in cells expressing N-terminally 3x FLAG tagged caspase-8 (**Figure 5.1A**; **Table 3.1 and 3.2**).

Once the CRISPR knock-in mouse strains were established and characterized (**Chapter 4**), we verified the interaction of TNKS1 with complex-2 in primary BMDMs from *Casp8*$^{N3xFLAG\ KI/+}$ and *Casp8*$^{C3xFLAG\ KI/+}$ mice by Western blot (**Figure 5.1B**). Anti-FLAG immunoprecipitation of TNF/SM/IDN treated *Casp8*$^{N3xFLAG\ KI/+}$ and *Casp8*$^{C3xFLAG\ KI/+}$ BMDMs revealed a strong signal at ~150kDa corresponding to TNKS1. Considering the fact that mouse TNKS1 and TNKS2 share 82% sequence identity and the anti-tankyrases antibody recognizes both TNKS1 and TNKS2 (ARTD6/PARP5b), a slight band at ~130kDa might correspond to TNKS2. TNKS1 was more abundant in the lysate compared with the putative TNKS2, which may explain the observation that TNKS1 was more prominent in complex-2. As already shown in

Chapter 4, the levels of complex-2 were more pronounced in the *Casp8*$^{C3xFLAG\ KI/+}$ BMDMs than in the *Casp8*$^{N3xFLAG\ KI/+}$ BMDMs (**Figure 4.5B**). Similarly, more TNKS1&2 were recruited to the complex-2 formed in *Casp8*$^{C3xFLAG\ KI/+}$ BMDMs (**Figure 5.1B**). Notably, TNKS1 and TNKS2 were not co-purified in the 3x FLAG peptide spiked sample (in which a high concentration of 3x FLAG peptide competed with 3x FLAG tagged caspase-8 and 3x FLAG tagged caspase-8 containing complexes in binding to anti-FLAG M2 affinity beads), implying that the precipitation of tankyrases was not due to nonspecific interaction with 3x FLAG tag .

Similar results were obtained in the *Casp8*$^{N3xFLAG\ KI/+}$ and *Casp8*$^{C3xFLAG\ KI/+}$ MDFs. Although only TNKS1 was clearly detectable in the *Casp8*$^{C3xFLAG\ KI/+}$ MDFs, both TNKS1/2 were undetectable in *Casp8*$^{N3xFLAG\ KI/+}$ MDFs, probably due to decreased complex-2 formation in these cells (**Supplementary Figure 5.1A**). Together, these data reflected our mass spectrometry analysis that tankyrases are recruited to complex-2 upon TNF/SM/IDN stimulation with a predominance for TNKS1 isoform.

5.1.2 Verification of interaction by endogenous immunoprecipitations

To determine whether tankyrases are bona fide complex-2 interactors, we analysed complex-2 composition after immunoprecipitation of endogenous complex-2 components (RIPK1 or cleaved caspase-8 or FADD) and performed reciprocal immunoprecipitation of endogenous tankyrases. Immunoprecipitation of endogenous RIPK1, cleaved caspase-8 or FADD co-purified tankyrases along with the other components of complex-2 in BMDM, MDFs and MEFs (**Figure 5.1C, D** and **Supplementary Figure 5.1B, C**). Similarly, immunoprecipitation of tankyrases also co-purified RIPK1, caspase-8 and FADD in a TNF/SM/IDN-dependent manner (**Figure 5.1D** and **Supplementary Figure 5.1C**). Importantly, the association of tankyrases with complex-2 was not specific to mouse cells as tankyrases were also present in TNF/SM/IDN-induced complex-2 in two human cell lines (**Figure 5.1E, F**). Interestingly, the association of tankyrases with complex-2 was transient which suggests a dynamic function of tankyrases within complex-2.

PARP-1 is the most widely studied poly (ADP-ribose) polymerase member and its function is negatively regulated during apoptosis. Thus, PARP-1 is cleaved upon caspase activation, preventing DNA break repair induced by the caspase activated DNase, CAD (Diamantopoulos et al., 2014; Soldani and Scovassi, 2002). PARP-1 has also been proposed to activate RIPK1

which in turn activates JNK1 and induces necroptosis in a mitochondrial permeability transition (MPT)-dependent manner (Douglas and Baines, 2014). We therefore tested whether PARP-1 was also recruited to TNFR1 complex-2 upon TNF/SM/IDN stimulation. However, no such interaction was observed, suggesting that the association of tankyrases with complex-2 was specific (**Supplementary Figure 5.1D**).

Since binding of TNF to TNFR1 results in the formation of two sequential signalling complexes (Micheau and Tschopp, 2003), we also examined whether tankyrases are part of TNFR1 complex-1. While complex-1 was readily formed following TNF treatment, we found no evidence for the presence of tankyrases in complex-1 (**Supplementary Figure 5.1E**). Together, these data support the idea that tankyrases are novel and specific constituents of native TNFR1 complex-2.

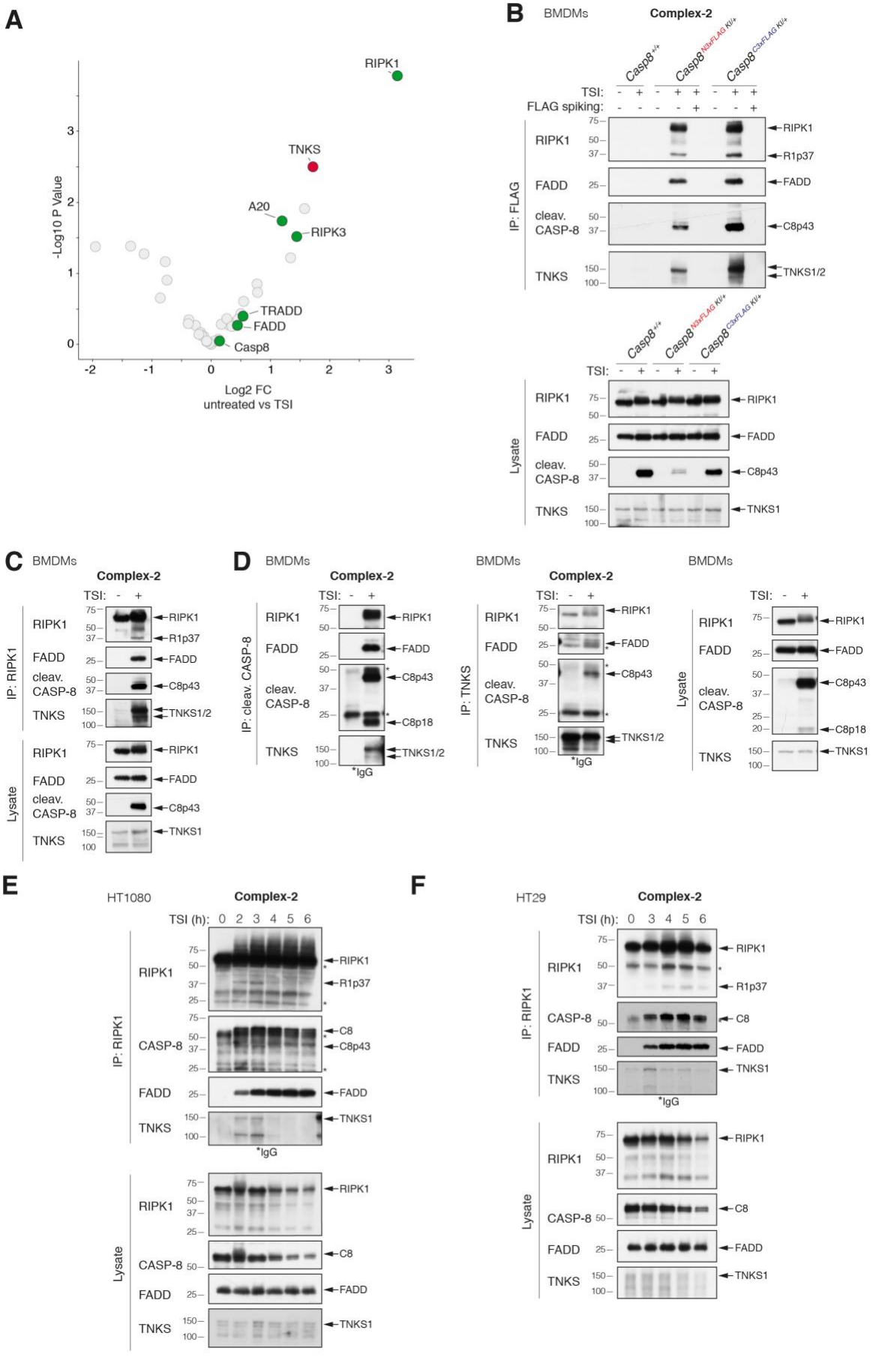
A
RIPK1
TNKS
A20
RIPK3
TRADD
FADD
Casp8
-Log10 P Value
Log2 FC
untreated vs TSI
B
BMDMs
Complex-2
Casp8+/+
Casp8 N3xFLAG KI/+
Casp8 C3xFLAG KI/+
TSI:
FLAG spiking:
IP: FLAG
RIPK1
R1p37
FADD
cleav. CASP-8
C8p43
TNKS
TNKS1/2
Lysate
TNKS1
C
BMDMs
Complex-2
IP: RIPK1
Lysate
D
BMDMs
Complex-2
IP: cleav. CASP-8
C8p18
*IgG
BMDMs
Complex-2
IP: TNKS
BMDMs
Lysate
E
HT1080
Complex-2
TSI (h): 0 2 3 4 5 6
IP: RIPK1
CASP-8
C8
Lysate
F
HT29
Complex-2
TSI (h): 0 3 4 5 6
IP: RIPK1
Lysate

Figure 5.1. Identification of tankyrases as components of the native TNFR1 complex-2

(A) Log2 fold change volcano plots of protein enrichment upon TNF/Smac-mimetic (SM)/IDN (TSI) stimulation in *Casp8*$^{-/-}$.*Mlkl*$^{-/-}$ MDFs cells expressing C-terminally 3x FLAG tagged caspase-8 compared to the untreated control. Known constituents of the native TNFR1 complex-2 (RIPK1, RIPK3, FADD, TRADD and A20) are labelled and highlighted in green while tankyrase-1 (TNKS1 or TNKS) is highlighted in red. P.Values calculated using Limma (n = 5). This figure is identical to **Figure 3.5D**.

(B) TNF-induced complex-2 immunoprecipitation using anti-FLAG M2 affinity beads. Western blot analysis of complex-2 and lysates from *Casp8*$^{+/+}$, *Casp8*$^{N3xFLAG\ KI/+}$ and *Casp8*$^{C3xFLAG\ KI/+}$ BMDMs using the indicated antibodies is shown. Cells were treated with TNF (100 ng/mL) +SM CompA (500 nM) + IDN-6556 (5 μM) (TSI) for 1.5 hours before being subjected to anti-FLAG immunoprecipitation. IDN-6556 was used to stabilize complex-2. 3x FLAG peptides were added to a final concentration of 50 μg/mL in FLAG spiked controls.

(C-D) TNF-induced complex-2 immunoprecipitation. Wild-type BMDMs were treated with TSI (as in **B**) to induce complex-2 assembly. The lysates were immunoprecipitated with anti-RIPK1 **(C)** or anti-cleaved caspase-8 or anti-tankyrases **(D)** antibodies. Western blot analysis using the indicated antibodies is shown.

(Schuster et al.) TNF-induced complex-2 immunoprecipitation using anti-RIPK1 antibody. Western blot analysis of complex-2 and lysates from HT1080 **(E)** and HT29 **(F)** using the indicated antibodies is shown. Cells were treated with TSI (as in **B**) for indicated time points.

Western blots are representative of three independent experiments.

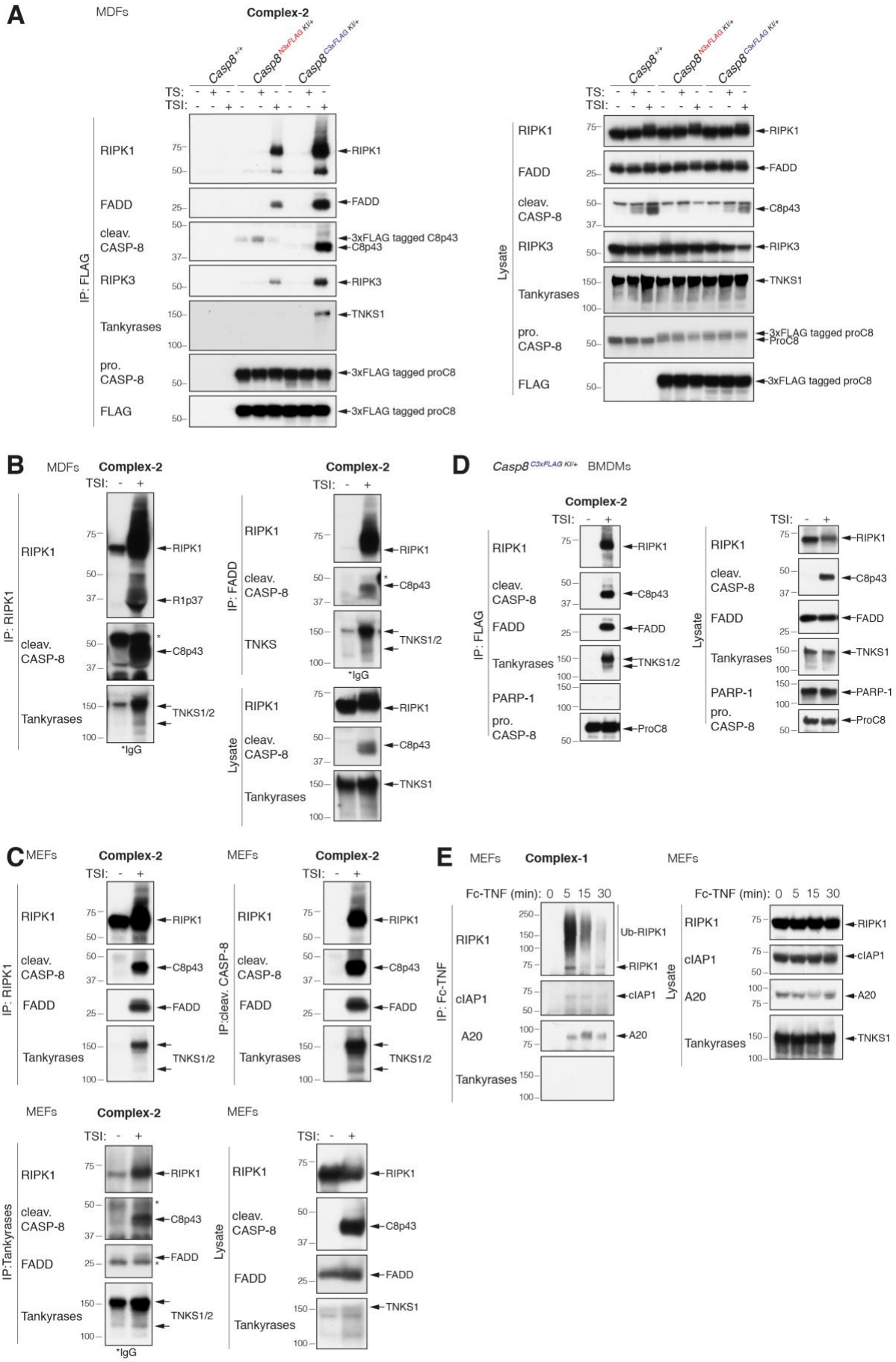
A
MDFs
Complex-2
Casp8+/+
Casp8 N3xFLAG KI/+
Casp8 C3xFLAG KI/+
TS:
TSI:
IP: FLAG
RIPK1
FADD
cleav. CASP-8
RIPK3
Tankyrases
pro. CASP-8
FLAG
3xFLAG tagged C8p43
C8p43
3xFLAG tagged proC8
Lysate
TNKS1
ProC8
B
MDFs
Complex-2
IP: RIPK1
R1p37
C8p43
TNKS1/2
*IgG
IP: FADD
TNKS
Lysate
TNKS1
C
MEFs
IP: cleav. CASP-8
D
Casp8 C3xFLAG KI/+ BMDMs
E
MEFs
Complex-1
Fc-TNF (min): 0 5 15 30
IP: Fc-TNF
Ub-RIPK1
cIAP1
A20
IP:Tankyrases

Figure S5.1. related to Figure 5.1. | Identification of tankyrases as components of the native TNFR1 complex-2

(A) TNF-induced complex-2 immunoprecipitation using anti-FLAG M2 affinity beads. Western blot analysis of complex-2 and lysates from *Casp8*$^{+/+}$, *Casp8*$^{N3xFLAG\ KI/+}$ and *Casp8*$^{C3xFLAG\ KI/+}$ MDFs using the indicated antibodies is shown. Cells were treated with TNF (100 ng/mL) +SM CompA (500 nM) in the absence or presence of IDN-6556 (5 μM) for 1.5 hours before being subjected to anti-FLAG immunoprecipitation. IDN-6556 was used to stabilize complex-2.

(B-C) TNF-induced complex-2 immunoprecipitation. Wild-type MDFs (B) or MEFs (C) were treated with TSI (as in **A**) to induce complex-2 assembly. The lysates were immunoprecipitated with anti-RIPK1 or anti-cleaved caspase-8 or anti-FADD or anti-tankyrases antibodies. Western blot analysis using the indicated antibodies is shown.

(D) TNF-induced complex-2 immunoprecipitation using anti-FLAG M2 affinity beads. Western blot analysis of complex-2 and lysates from *Casp8*$^{C3xFLAG\ KI/+}$ BMDMs using the indicated antibodies is shown. Cells were treated with TSI (as in **A**).

(E) TNF-induced complex-1 immunoprecipitation. Wild-type MEFs were treated with Fc-TNF (1 μg/mL) for the indicated time points, followed by immunoprecipitation with protein A Sepharose and Western blot analysis.

Blots are representative of three independent experiments.

5.2 TNFR1 complex-2 is PARsylated by tankyrases

Since tankyrases are known to catalyse PARsylation on their substrates (Hsiao and Smith, 2008), we speculated that they may also induce PARsylation of complex-2 components. To determine whether complex-2 components were PARsylated or associated with PARsylated proteins, an anti-poly(ADP-ribose) (PAR) immunoprecipitation was performed in lysates from TNF/SM/IDN-treated BMDMs. Cleaved caspase-8 was immunoprecipitated with an anti-PAR antibody upon TNF/SM/IDN treatment and this interaction was abolished by the tankyrases specific inhibitor IWR-1 (Levaot et al., 2011). This indicates that either caspase-8 itself is PARsylated or associates with PARsylated proteins upon TNF/SM/IDN treatment (**Figure 5.2A**).

Tankyrases-induced ribosylation can serve as a docking sites for the recruitment of the E3 ubiquitin ligase RNF146/Iduna via the Trp–Trp–Glu (WWE) domain and therefore the purified RNF146 WWE domain has been developed as a tool to isolate PARsylated proteins from cells (Zhang et al., 2011). To confirm our observation in **Figure 5.2A**, we coupled the human RNF146 WWE domain to glutathione S-transferase (GST) and performed GST-WWE pull downs. As a negative control, we used a GST-WWE^{R163A} construct - a mutant in which an arginine to alanine substitution in the RNF146 WWE domain abolishes the interaction with PAR (Zhang et al., 2011). As shown in **Figure 5.2B,** GST-WWE, but not GST-WWE^{R163A}, was able to pulldown complex-2 components upon TNF/SM/IDN stimulation. The levels of complex-2 components pulled down with GST-WWE was significantly decreased upon treatment with the tankyrases inhibitor IWR-1 (**Figure 5.2B**), while the PARP-1/2 inhibitor, olaparib, had no effect. This decreased complex-2 PARsylation upon IWR-1 treatment was accompanied by an increase in the levels of cleaved caspase-8 in cell lysates, suggesting that PARsylation inhibits the activation of caspase-8 (**Figure 5.2B** and **Supplementary Figure 5.2A**).

Conversely, overexpression of the tankyrases enhanced the PARsylation of complex-2 (**Supplementary Figure 5.2B**). Importantly, complex-2 PARsylation was caspase-8-dependent, because complex-2 components were not co-purified with GST-WWE in the absence of caspase-8 (**Figure 5.2C**). There are a number of possible interpretations of this result: either caspase-8 is the PARsylated component in complex-2, or caspase-8 must be present for another component to become PARsylated because it binds tankyrases directly or

lastly that complex-2 fails to form properly in the absence of caspase-8 and therefore tankyrases fail to be recruited.

WWE domains have been found in many E3 ubiquitin ligases (Aravind, 2001), for example HUWE1 and TRIP12. The critical residues for PAR binding are conserved in most WWE domains and these WWE domains were also capable of specifically interacting with PAR chains (Wang et al., 2012). Therefore, we performed a PAR pulldown assay using GST-HUWE1 WWE and GST-TRIP12 WWE fusion proteins (**Supplementary Figure 5.2C**). With the TRIP12 WWE domain, complex-2 components were barely pulled down, possibly due to its poor affinity to PAR as indicated by total PARsylation blot. Complex-2 components were successfully co-purified with GST-RNF146 WWE and GST-HUWE1 WWE, although there were less complex-2 components pulled down with HUWE1 WWE domain when compared with RNF146 WWE domain.

Poly(ADP-ribose) glycohydrolase (PARG) cleaves conjugated ADP-ribose (ADPR) polymers to generate ADPR monomers (Hatakeyama et al., 1986). The WWE domain recognizes PAR and binds to iso-ADPR linkages joining ADPR monomers, but not with mono-ADPR (Wang et al., 2012) (Gibson et al., 2017). To further confirm that complex-2 was PARsylated, we eluted complex-2 from anti-FLAG immunoprecipitation, treated the immunoprecipitants with PARG to cleave PAR polymer and performed a GST-WWE pulldown. As shown in **Figure 5.2D**, exposing complex-2 to PARG abolished the interaction between complex-2 and GST-WWE.

It has been revealed that the macrodomains from *A. fulgidus* Af1521 binds mono-ADPR and the terminal ADPR moieties in PAR (Gibson et al., 2017). We therefore fused Af1521 macrodomain with GST tag and performed sequential pulldown assay. Similar to WWE domains, PARsylated complex-2 was successfully enriched by Af1521 macrodomain (**Figure 5.2E**). Taken together, these observations strongly support the hypothesis that TNFR1 complex-2 is PARsylated in a tankyrases-dependent manner.

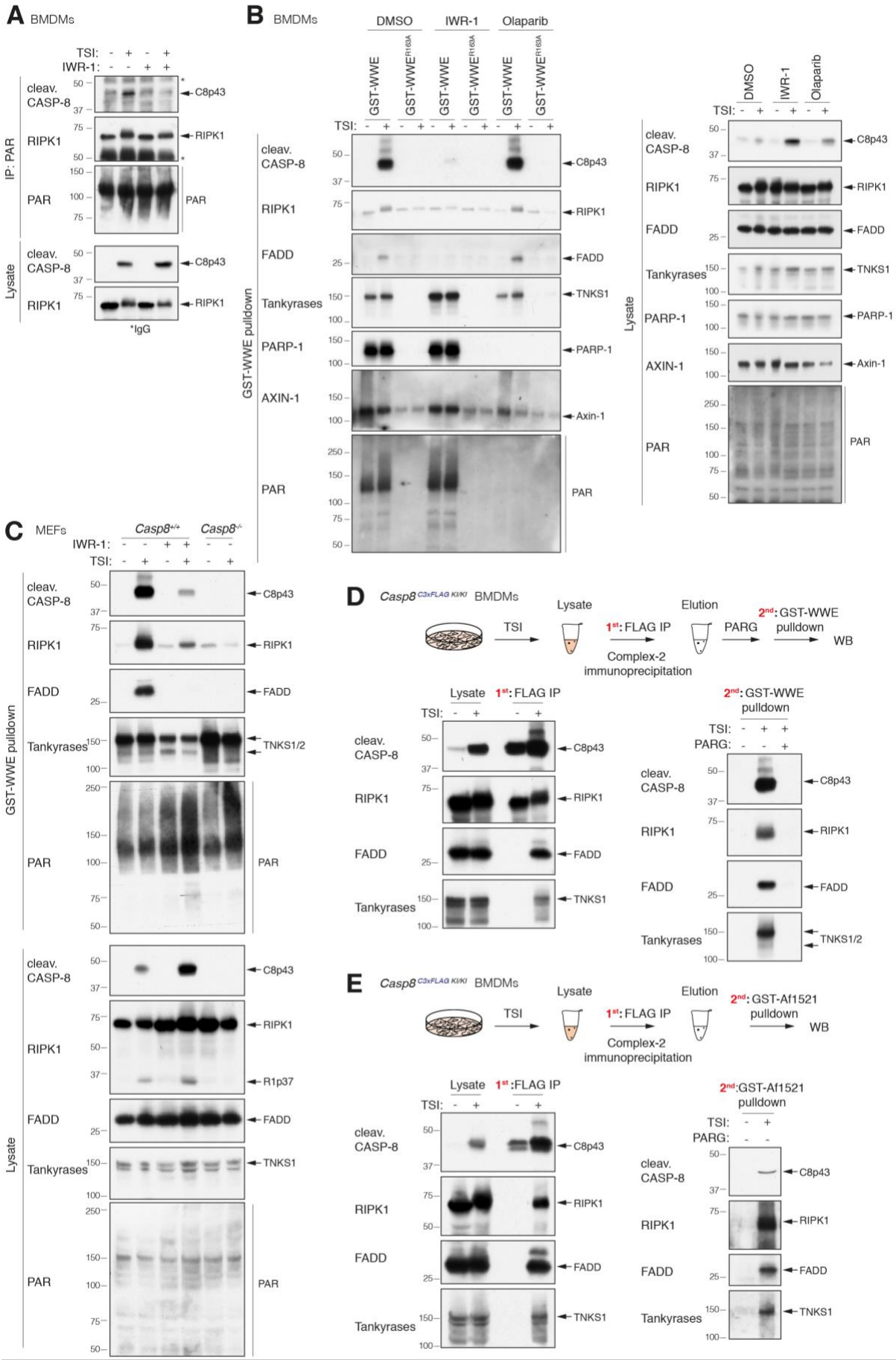
A BMDMs
TSI:
IWR-1:
IP: PAR
cleav. CASP-8
RIPK1
PAR
Lysate
C8p43
RIPK1
PAR
*IgG
B BMDMs
DMSO
IWR-1
Olaparib
GST-WWE
GST-WWE^R163A
GST-WWE pulldown
cleav. CASP-8
RIPK1
FADD
Tankyrases
PARP-1
AXIN-1
PAR
C8p43
FADD
TNKS1
Axin-1
Lysate
C MEFs
Casp8+/+
Casp8-/-
GST-WWE pulldown
TNKS1/2
R1p37
Lysate
D Casp8 C3xFLAG KI/KI BMDMs
TSI
Lysate
Elution
1st: FLAG IP
Complex-2 immunoprecipitation
PARG
2nd: GST-WWE pulldown
WB
E Casp8 C3xFLAG KI/KI BMDMs
2nd: GST-Af1521 pulldown

Figure 5.2. Tankyrases induce PARsylation of TNFR1 complex-2

(A) TNF-induced complex-2 immunoprecipitation using anti-PAR antibody. Western blot analysis of complex-2 and lysates from wild-type BMDMs using the indicated antibodies is shown. Cells were treated with TNF (100 ng/mL) + SM CompA (500 nM) + IDN-6556 (5 μM) (TSI) ± tankyrases inhibitor, IWR-1 (5 μM) for 1.5 hours before being subjected to anti-PAR immunoprecipitation. IDN-6556 was used to stabilize complex-2.

(B) GST-WWE and GST-WWE^{R163A} pulldown of TNF-induced complex-2 from wild-type BMDMs lysates. Cells were treated with TNF (10 ng/mL) + SM CompA (250 nM) + IDN-6556 (5 μM) (TSI) ± tankyrases inhibitor, IWR-1 (5 μM) or PARP-1/2 inhibitor, olaparib (1μM) for 1.5 hours. IDN-6556 was used to stabilize complex-2. Western blot analysis of complex-2 and lysates using the indicated antibodies is shown.

(C) GST-WWE pulldown of TNF-induced complex-2 from *Casp8*$^{+/+}$ or *Casp8*$^{-/-}$ MEFs lysates. Cells were treated with TSI (as in **A**) ± tankyrases inhibitor, IWR-1 (10 μM). Western blot analysis of complex-2 and lysates using the indicated antibodies is shown.

(D) Enrichment of PARsylated complex-2 using GST–WWE in a sequential pulldown analysis. *Casp8*$^{C3xFLAG\ KI/KI}$ BMDMs were treated with TSI (as in **A**) and complex-2 was immunoprecipitated using anti-FLAG M2 affinity beads. Immunoprecipitants were eluted using 3xFLAG peptides followed by PARG treatment at 37°C for 3hr before being subjected to GST-WWE pulldown. Western blot analysis of lysates and sequential pulldown using the indicated antibodies is shown.

(E) Enrichment of PARsylated complex-2 using GST–Af1521 in a sequential pulldown analysis. *Casp8*$^{C3xFLAG\ KI/KI}$ BMDMs were treated with TSI (as in **A**) and complex-2 was immunoprecipitated using anti-FLAG M2 affinity beads. Immunoprecipitants were eluted using 3xFLAG peptides followed by GST-Af1521 pulldown. Western blot analysis of lysates and sequential pulldown using the indicated antibodies is shown.

Blots are representative of three independent experiments.

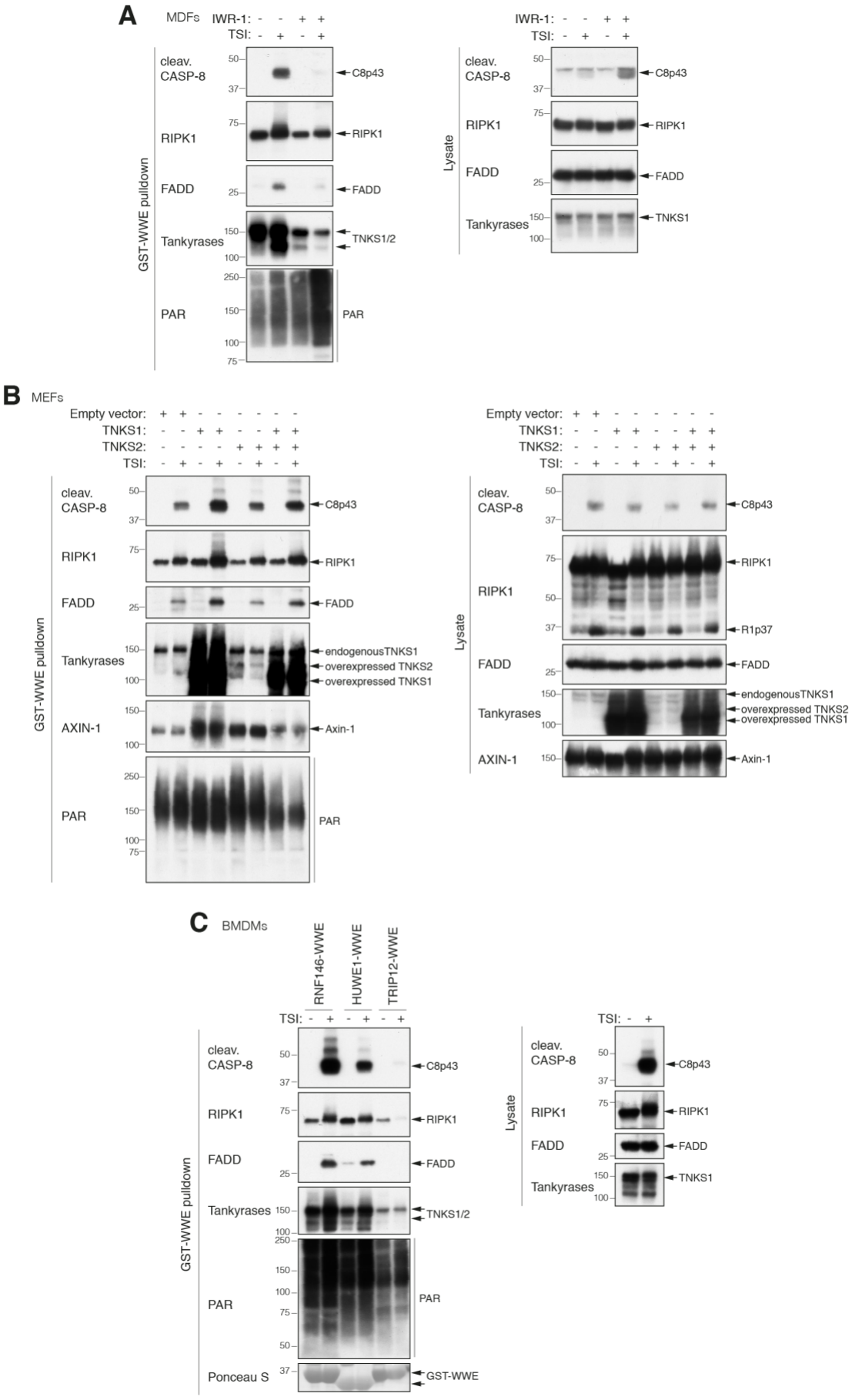
A
MDFs
IWR-1: - - + +
TSI: - + - +
cleav. CASP-8
C8p43
RIPK1
FADD
Tankyrases
TNKS1/2
PAR
GST-WWE pulldown
Lysate
TNKS1
B
MEFs
Empty vector: + + - - - - - -
TNKS1: - - + + - - + +
TNKS2: - - - - + + + +
endogenousTNKS1
overexpressed TNKS2
overexpressed TNKS1
AXIN-1
Axin-1
R1p37
C
BMDMs
RNF146-WWE
HUWE1-WWE
TRIP12-WWE
Ponceau S
GST-WWE

Figure S5.2. related to Figure 5.2. | Tankyrases induce PARsylation of TNFR1 complex-2

(A) GST-WWE pulldown of TNF-induced complex-2 from wild-type MDF lysates. Cells were treated with TNF (100 ng/mL) + SM CompA (500 nM) + IDN-6556 (5 μM) (TSI) for 1.5 hours ± tankyrases inhibitor, IWR-1 (10 μM). IDN-6556 was used to stabilize complex-2. Western blot analysis of complex-2 and lysates using the indicated antibodies is shown.

(B) GST-WWE pulldown of TNF-induced complex-2. Wild-type MEFs expressing doxycycline-inducible mouse TNKS1 (isoform 2) or/and mouse TNKS2 or empty vector were pre-treated with 20 ng/mL doxycycline overnight before being stimulated with TNF (100 ng/mL) + SM CompA (500 nM) + IDN-6556 (5 μM) (TSI) for 1.5 hours. IDN-6556 was used to stabilize complex-2. Cell lysates were subjected to GST-WWE pulldown. Western blot analysis of complex-2 and lysates using the indicated antibodies is shown.

(C) GST-RNF146 WWE, GST-HUWE1 WWE and GST-TRIP12 WWE pulldown of TNF-induced complex-2 from wild-type BMDMs. Cells were treated with TSI (as in **B**) and lysates were subjected to GST pulldown assays. Western blot analysis of complex-2 and lysates using the indicated antibodies is shown. Ponceau S staining of the purified proteins and their quantities used in the pulldown assay is shown.

Blots are representative of three independent experiments.

5.3 Tankyrases regulate TNF-induced cell death

Our data showed that tankyrases are recruited to complex-2, causing its PARsylation. We next investigated whether complex-2 PARsylation affected TNF-induced cell death.

We found that while the PARP-1/2 inhibitor olaparib had no effect on TNF-induced death, two tankyrases inhibitors, IWR-1 and Az6102, sensitized BMDMs to TNF/SM and TNF/SM/IDN-induced cell death in a dose-dependent manner (**Figure 5.3A, B** and **Supplementary Figure 5.3A**). Inhibition of RIPK1 kinase activity with necrostatin-1s reversed this sensitization (**Figure 5.3A, B**). This suggested that tankyrases inhibitors sensitised cells to TNF-induced cell death in RIPK1 kinase-dependent manner. The tankyrases inhibitor IWR-1 increased TNF/SM-induced caspase-8 and caspase-3 cleavage in a dose-dependent manner (**Figure 5.3C**). Surprisingly and despite the presence of the caspase inhibitor IDN-6556, IWR-1 also increased caspase-8 cleavage upon TNF/SM/IDN (**Figure 5.3D**). In addition, the increase in necroptotic cell death induced by IWR-1 was accompanied with increased phosphorylation of RIPK3 and MLKL (**Figure 5.3D**). Inhibition of tankyrases also sensitized MDFs and human HT29 cells to TNF-induced cell death (**Supplementary Figure 5.3B, C**). This increase in cell death induced by IWR-1 correlated with increased formation of RIPK1-caspase-8-containing complex-2 (**Figure 5.3E** and **Supplementary Figure 5.3D**). Together, these data demonstrate that tankyrases control TNF-induced cell death by limiting complex-2 formation.

Given that Smac-mimetic can kill cancer cells in a TNF-dependent manner (Petersen et al., 2007; Varfolomeev et al., 2007; Vince et al., 2007). we next determined whether a tankyrases inhibitor could increase the efficacy of the clinical Smac-mimetic, birinapant. We used the AML mouse model MLL-AF9/Nras^{G12D} and found that inhibition of tankyrases activity dramatically increased apoptotic cell death of MLL-AF9/Nras^{G12D} leukemic cells induced by birinapant alone (**Figure 5.3F**). Tankyrases have been shown to regulate Axin abundance (Huang et al., 2009). As indicated in **Figure 3.5F**, the level of Axin-1 was stabilized after tankyrases inhibitor IWR-1 treatment at nanomolar concentrations in MLL-AF9/Nras^{G12D} leukemic cells, indicating an on-target effect. Treatment with IWR-1 plus birinapant induced a strong activation of caspase-8 and caspase-3, whereas phosphorylation of RIPK3 and MLKL were undetectable (**Figure 5.3G**). This observation suggested that the tankyrases inhibitor functioned by enhancing birinapant-induced apoptotic death, and not by switching apoptosis to necroptosis. Blockade of tankyrases activity by IWR-1 also potentiated MLL-AF9/Nras^{G12D} leukemic cells to low nanomolar dose of birinapant in the presence of caspases inhibitor IDN-

6556 (**Figure 5.3F**). These observations suggest the combination of tankyrases inhibitor/birinapant has potential for treating leukemia.

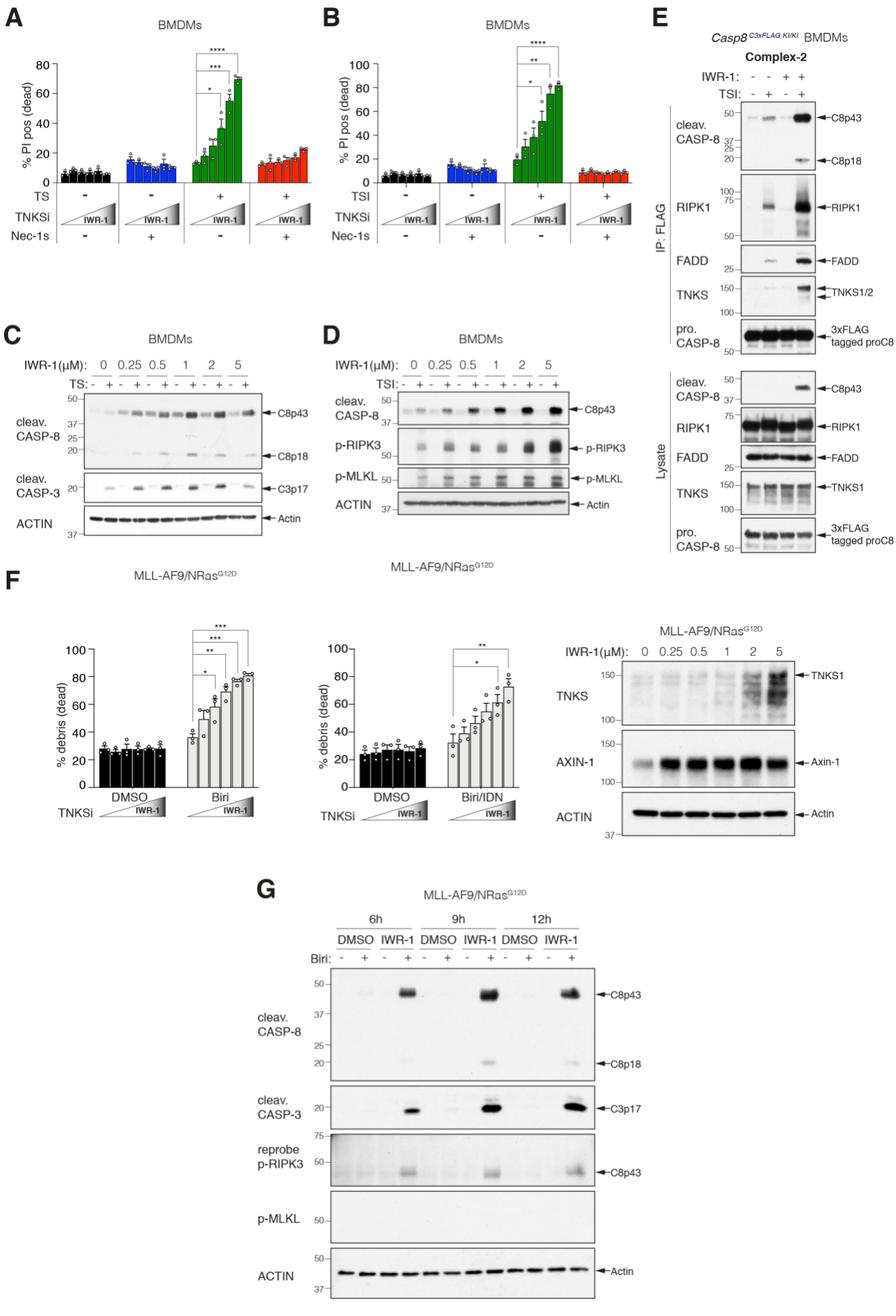
A
BMDMs
% PI pos (dead)
TS
TNKSi
Nec-1s
IWR-1
B
BMDMs
% PI pos (dead)
TSI
TNKSi
Nec-1s
IWR-1
C
BMDMs
IWR-1(μM): 0 0.25 0.5 1 2 5
TS:
cleav. CASP-8
C8p43
C8p18
cleav. CASP-3
C3p17
ACTIN
Actin
D
BMDMs
IWR-1(μM): 0 0.25 0.5 1 2 5
TSI:
cleav. CASP-8
C8p43
p-RIPK3
p-MLKL
ACTIN
Actin
E
Casp8 C3xFLAG KI/KI BMDMs
Complex-2
IWR-1:
TSI:
IP: FLAG
cleav. CASP-8
C8p43
C8p18
RIPK1
FADD
TNKS
TNKS1/2
pro. CASP-8
3xFLAG tagged proC8
Lysate
cleav. CASP-8
C8p43
RIPK1
FADD
TNKS
TNKS1
pro. CASP-8
3xFLAG tagged proC8
F
MLL-AF9/NRasG12D
% debris (dead)
DMSO
Biri
TNKSi
IWR-1
MLL-AF9/NRasG12D
% debris (dead)
DMSO
Biri/IDN
TNKSi
IWR-1
MLL-AF9/NRasG12D
IWR-1(μM): 0 0.25 0.5 1 2 5
TNKS
TNKS1
AXIN-1
Axin-1
ACTIN
Actin
G
MLL-AF9/NRasG12D
6h
9h
12h
DMSO
IWR-1
Biri:
cleav. CASP-8
C8p43
C8p18
cleav. CASP-3
C3p17
reprobe p-RIPK3
C8p43
p-MLKL
ACTIN
Actin

Figure 5.3. Tankyrases inhibition sensitizes SM-mediated killing

(A) Level of cell death assessed by propidium iodide (PI) positive cells. Wild-type BMDMs were treated with TNF (10 ng/mL) + SM CompA (500 nM) (TS) ± IWR-1 (250nM, 500nM, 1 μM, 2 μM, 5 μM) ± Nec-1s (10 μM) for 24 hours. Graphs show mean ± SEM, n=3 independent experiments. Comparisons were performed with a Student's t test whose values are denoted in the figures as *p ≤ 0.05, ***p ≤ 0.001 and ****p ≤ 0.0001.

(B) Level of cell death assessed by PI positive cells. Wild-type BMDMs were treated with TNF (10 ng/mL) + CompA (10 nM) + IDN-6556 (5 μM) (TSI) ± IWR-1 (250nM, 500nM, 1 μM, 2 μM, 5 μM) ± Nec-1s (10 μM) for 16 hours. Graphs show mean ± SEM, n=3 independent experiments. Comparisons were performed with a Student's t test whose values are denoted in the figures as *p ≤ 0.05, **p ≤ 0.01 and ****p ≤ 0.0001.

(C) Western blot analysis of cell lysates from wild-type BMDMs using indicated antibodies is shown. Cells were treated with TNF (10 ng/mL) + SM CompA (500 nM) ± IWR-1 (250nM, 500nM, 1 μM, 2 μM, 5 μM) for 8 hours.

(D) Western blot analysis of cell lysates from wild-type BMDMs using indicated antibodies is shown. Cells were treated with TNF (10 ng/mL) + SM CompA (20 nM) + IDN-6556 (5 μM) ± IWR-1 (250nM, 500nM, 1 μM, 2 μM, 5 μM) for 8 hours.

(E) TNF-induced complex-2 immunoprecipitation using anti-FLAG M2 affinity beads. Western blot analysis of complex-2 and lysates from *Casp8*$^{C3xFLAG\ KI/KI}$ BMDMs using the indicated antibodies is shown. Cells were treated with TNF (10 ng/mL) + SM CompA (50 nM) + IDN-6556 (5 μM) (TSI) ± IWR-1 (5 μM) for 1.5 hours before being subjected to anti-FLAG immunoprecipitation. IDN-6556 was used to stabilize complex-2.

(F) Level of cell death assessed by percentage of cell debris. MLL-AF9/Nras^{G12D} leukemic cells were treated with SM birinapant (500 nM) ± IWR-1 (250nM, 500nM, 1 μM, 2 μM, 5 μM) for 15 hours or SM birinapant (20 nM) + IDN-6556 (5 μM) ± IWR-1 (250nM, 500nM, 1 μM, 2 μM, 5 μM) for 7 hours. Graphs show mean ± SEM, n=3 independent experiments. Comparisons were performed with a Student's t test whose values are denoted in the figures as *p ≤ 0.05, **p ≤ 0.01 and ***p ≤ 0.001.

Western blot analysis of lysates from MLL-AF9/Nras^{G12D} leukemic cells treated with IWR-1 (250nM, 500nM, 1 μM, 2 μM, 5 μM) for 7 hours using indicated antibodies is shown.

(G) WB analysis of lysates from MLL-AF9/Nras^{G12D} leukemic cells using indicated antibodies is shown. Cell were treated with SM birinapant (500 nM) ± IWR-1 (5 μM) for indicated time points.

Blots are representative of three independent experiments.

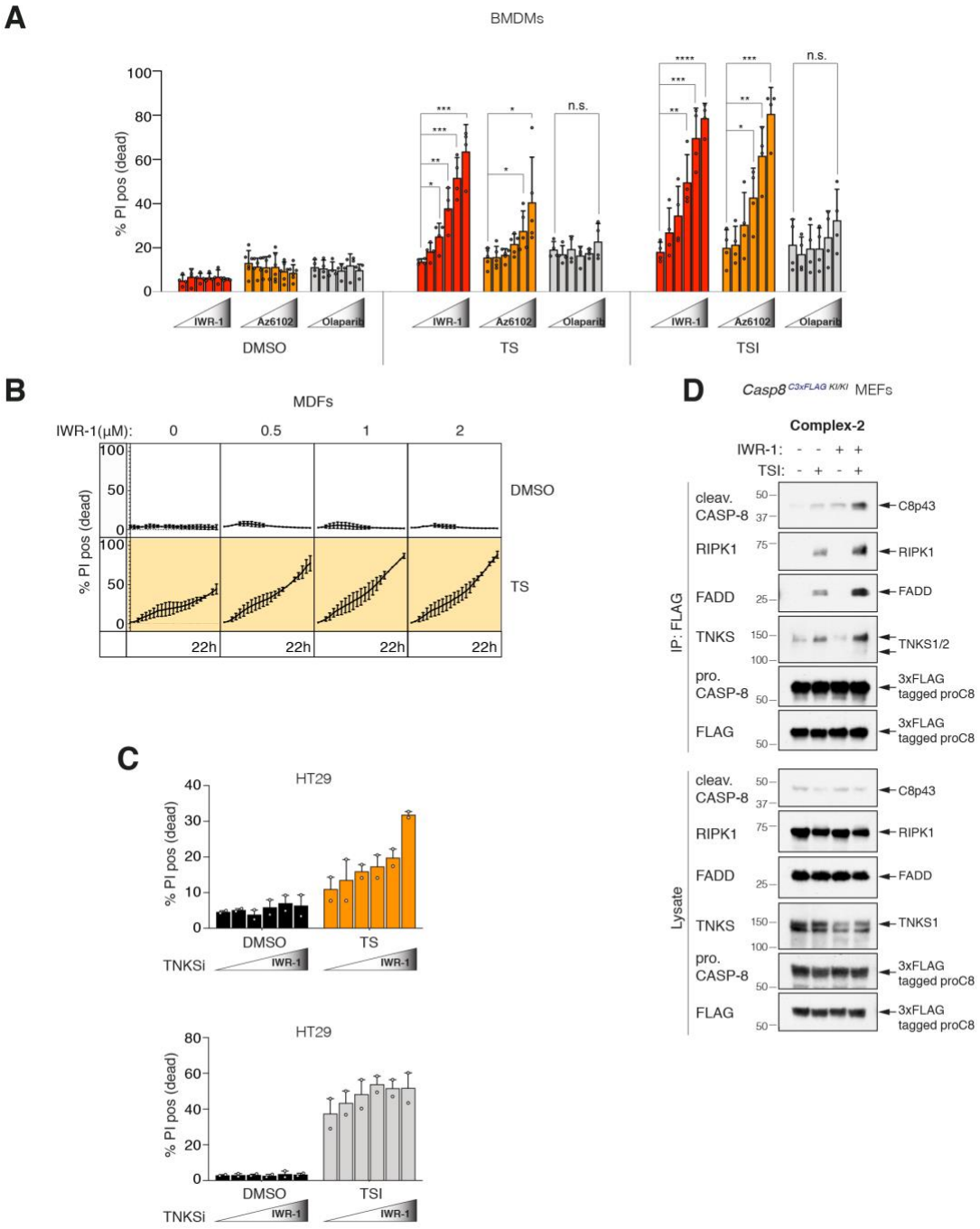
A
BMDMs
% PI pos (dead)
IWR-1
Az6102
Olaparib
DMSO
TS
TSI
n.s.
B
MDFs
IWR-1(μM): 0 0.5 1 2
% PI pos (dead)
DMSO
TS
22h
C
HT29
% PI pos (dead)
DMSO
TS
TSI
TNKSi
IWR-1
D
Casp8 C3xFLAG KI/KI MEFs
Complex-2
IWR-1:
TSI:
IP: FLAG
cleav. CASP-8
RIPK1
FADD
TNKS
pro. CASP-8
FLAG
C8p43
TNKS1/2
3xFLAG tagged proC8
Lysate
TNKS1

Figure S5.3. related to Figure 5.3. | Tankyrases inhibition sensitizes SM-mediated killing

(A) Level of cell death assessed by PI positive cells. Wild-type BMDMs were treated with TNF (10 ng/mL) + SM CompA (500 nM) (TS) or TNF (10 ng/mL) + SM CompA (10 nM) + IDN-6556 (5 μM) (TSI) ± IWR-1 or ± Az6102 or ± olaparib for 16 hours. IWR-1: 250nM, 500nM, 1 μM, 2 μM, 5 μM. Az6102: 125nM, 250nM, 500nM, 1 μM, 2 μM. Olaparib: 62.5nM, 125nM, 250nM, 500nM, 1 μM. Graphs show mean ± SEM, n = 4-5 independent biological repeats. Comparisons were performed with a Student's t test whose values are denoted in the figures as *p ≤ 0.05, **p ≤ 0.01 , ***p ≤ 0.001, ****p ≤ 0.0001and n.s.= no significance.

(B) Cell death of wild-type MDFs monitored by time-lapse imaging of PI staining over 22 hours. Cells were treated with TNF (100 ng/mL) + SM CompA (100 nM) ± IWR-1 (500nM, 1 μM, 2 μM). Graphs are performed with 2 independent biological repeats.

(C) Level of cell death assessed by PI positive cells. Human HT29 cells were treated with TNF (50 ng/mL) + SM CompA (500 nM) (TS) or TNF (100 ng/mL) + SM CompA (50nM) + IDN-6556 (5 μM) (TSI) ± IWR-1 (500nM, 1 μM, 2 μM, 5 μM, 10 μM) for 48 hours and 18 hours, respectively. Graphs show mean ± SD, n = 2 independent experiments.

(D) TNF-induced complex-2 immunoprecipitation using anti-FLAG M2 affinity beads. Western blot analysis of complex-2 and lysates from *Casp8*$^{C3xFLAG\ KI/KI}$ MEFs using the indicated antibodies is shown. Cells were treated with TNF (100 ng/mL) + SM CompA (50 nM) + IDN-6556 (5 μM) (TSI) ± IWR-1 (5 μM) for 2 hours before being subjected to anti-FLAG immunoprecipitation. IDN-6556 was used to stabilize complex-2. Blots are representative of three independent experiments.

5.4 RNF146 may be required for PARsylation-dependent regulation of TNF-induced death

I have shown that tankyrases reduce the ability of TNF to induce cell death by limiting complex-2 formation. Since the most apparent role of tankyrases-induced PARsylation is to promote poly-ubiquitylation and proteasomal degradation of their substrates (Huang et al., 2009; Kim et al., 2012; Levaot et al., 2011), we next tested whether tankyrases-mediated PARsylation would affect complex-2 stability by targeting it for ubiquitylation and degradation.

To interrogate ubiquitylation events on complex-2 components upon tankyrases inhibition, we isolated ubiquitylated proteins from wild-type BMDMs using a GST-UBA pulldown (Lin et al., 2010). Ubiquitylation of complex-2 components RIPK1, FADD and cleaved caspase-8 occurred upon TNF/SM/IDN stimulation, as indicated by successful precipitation of these proteins by GST-UBA in the presence and not the absence of this stimulus (**Figure 5.4A**). Furthermore, precipitation of these proteins was greatly reduced when tankyrases activity was inhibited (**Figure 5.4A**). This indicates that tankyrases-mediated PARsylation contributed to ubiquitylation of complex-2 components. Ubiquitylated complex-2 was probably targeted for proteasomal degradation, because the proteasome inhibitor MG132 induced accumulation of polyubiquitylated complex-2 (**Figure 5.4B**).

The E3 ligase RNF146 is frequently used as the ubiquitin ligase that recognizes tankyrases-mediated PARsylation. Following tankyrases-induced PARsylation, RNF146 tags the substrate, autoPARsylated tankyrases and itself for proteasomal degradation (Callow et al., 2011; Zhang et al., 2011). The tankyrases-RNF146 axis has been implicated in regulating the stability of multiple proteins including Axin, 3BP2, PTEN, LKB1 and AMOT (Levaot et al., 2011; Li et al., 2019; Li et al., 2015; Wang et al., 2015; Zhang et al., 2011). Therefore, we examined whether RNF146 also played a role in tankyrases-mediated regulation of complex-2. We purified complex-2 from *Casp8*$^{C3xFLAG\ KI/+}$ MEFs using anti-FLAG immunoprecipitation. As shown in **Figure 5.4C**, RNF146 co-purified with the other complex-2 components in a TNF/SM/IDN stimulation-dependent manner.

We next reasoned that if the E3 ligase RNF146 was responsible for targeting PARsylated complex-2 for ubiquitylation and proteasomal degradation, complex-2 should accumulate in the absence of RNF146. Consistent with this hypothesis, conditional depletion of RNF146

using a Dox-inducible RNF146 short hairpin RNA (shRNA) markedly enhanced TNF-induced complex-2 formation (**Figure 5.4D**), and dramatically sensitized MDFs and MEFs to TNF-induced cell death (**Figure 5.4E** and **Supplementary Figure 5.4**). Taken together, these results suggest that tankyrases-mediated PARsylation may limit TNFR1 complex-2 formation and TNF-induced cell death through the tankyrases-RNF146 axis.

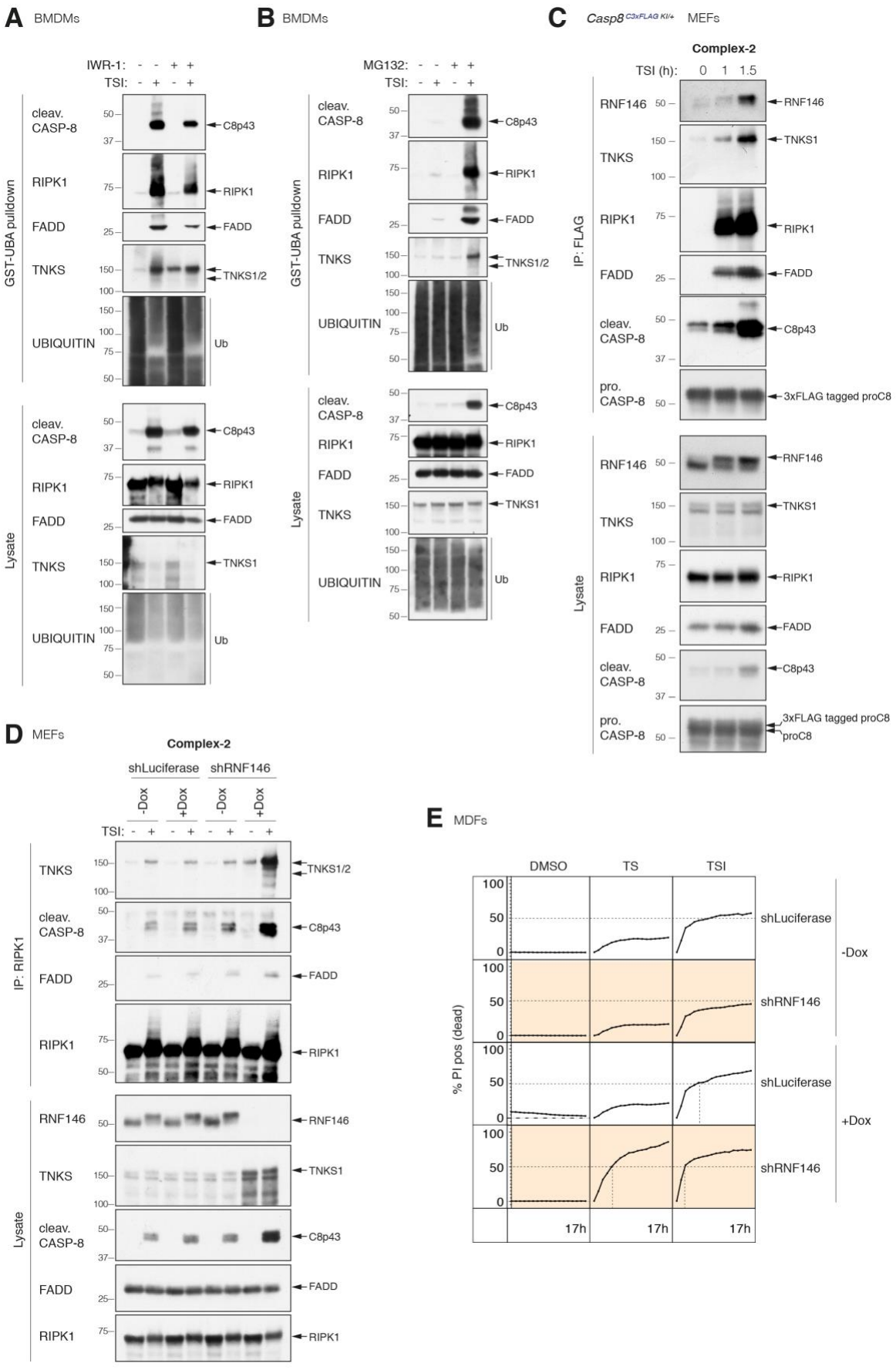
A BMDMs
IWR-1: - - + +
TSI: - + - +
GST-UBA pulldown
cleav. CASP-8
C8p43
RIPK1
RIPK1
FADD
FADD
TNKS
TNKS1/2
UBIQUITIN
Ub
Lysate
cleav. CASP-8
C8p43
RIPK1
RIPK1
FADD
FADD
TNKS
TNKS1
UBIQUITIN
Ub
B BMDMs
MG132: - - + +
TSI: - + - +
GST-UBA pulldown
cleav. CASP-8
C8p43
RIPK1
RIPK1
FADD
FADD
TNKS
TNKS1/2
UBIQUITIN
Ub
Lysate
cleav. CASP-8
C8p43
RIPK1
RIPK1
FADD
FADD
TNKS
TNKS1
UBIQUITIN
Ub
C Casp8 C3xFLAG KI/+ MEFs
Complex-2
TSI (h): 0 1 1.5
IP: FLAG
RNF146
RNF146
TNKS
TNKS1
RIPK1
RIPK1
FADD
FADD
cleav. CASP-8
C8p43
pro. CASP-8
3xFLAG tagged proC8
Lysate
RNF146
RNF146
TNKS
TNKS1
RIPK1
RIPK1
FADD
FADD
cleav. CASP-8
C8p43
pro. CASP-8
3xFLAG tagged proC8
proC8
D MEFs
Complex-2
shLuciferase
shRNF146
-Dox
+Dox
-Dox
+Dox
TSI: - + - + - + - +
IP: RIPK1
TNKS
TNKS1/2
cleav. CASP-8
C8p43
FADD
FADD
RIPK1
RIPK1
Lysate
RNF146
RNF146
TNKS
TNKS1
cleav. CASP-8
C8p43
FADD
FADD
RIPK1
RIPK1
E MDFs
DMSO
TS
TSI
% PI pos (dead)
shLuciferase
shRNF146
shLuciferase
shRNF146
-Dox
+Dox
17h
17h
17h

Figure 5.4. RNF146 may be involved in PARsylation-mediated complex-2 regulation

(A) GST-UBA pulldown of TNF-induced complex-2 from wild-type BMDM lysates. Cells were treated with TNF (100 ng/mL) + SM CompA (500 nM) + IDN-6556 (5 μM) (TSI) for 1.5 hours ± tankyrases inhibitor, IWR-1 (5 μM). IDN-6556 was used to stabilize complex-2. Western blot analysis of complex-2 and lysates using the indicated antibodies is shown.

(B) GST-UBA pulldown of TNF-induced complex-2 from wild-type BMDMs lysates. Cells were pre-treated with ± proteasome inhibitor MG132 (10 μM) for 2 hours, followed by TNF (10 ng/mL) + SM CompA (50 nM) + IDN-6556 (5 μM) (TSI) stimulation for another 2 hours. IDN-6556 was used to stabilize complex-2. Western blot analysis of complex-2 and lysates using the indicated antibodies is shown.

(C) TNF-induced complex-2 immunoprecipitation using anti-FLAG M2 affinity beads. Western blot analysis of complex-2 and lysates from *Casp8*$^{C3xFLAG\ KI/+}$ MEFs using the indicated antibodies is shown. Cells were treated with TNF (100 ng/mL) + SM CompA (500 nM) + IDN-6556 (5 μM) (TSI) for indicated timepoints before being subjected to anti-FLAG immunoprecipitation. IDN-6556 was used to stabilize complex-2.

(D) TNF-induced complex-2 immunoprecipitation using anti-RIPK1 antibody. Wild-type MEFs expressing Dox-inducible shLuciferase or shRNF146 were pre-treated with ± Dox (1μg/mL) for 48 hours. Cells were then treated with TNF (100 ng/mL) + SM CompA (500 nM) + IDN-6556 (5 μM) (TSI) ± Dox (1μg/mL) for another 2 hours. IDN-6556 was used to stabilize complex-2. Western blot analysis of complex-2 and lysates using the indicated antibodies is shown.

(E) Cell death monitored by time-lapse imaging of PI staining over 17 hours. Wild-type MDFs expressing Dox-inducible shLuciferase or shRNF146 were pre-treated with ± Dox (1μg/mL) for 48 hours, followed by TNF (100 ng/mL) + SM CompA (50 nM) (TS) ± Dox (1μg/mL) or TNF (100 ng/mL) + SM CompA (50nM) + IDN-6556 (5 μM) (TSI) ± Dox (1μg/mL) for another 17 hours. n=1 biological repeat.

Blots are representative of two to three independent experiments.

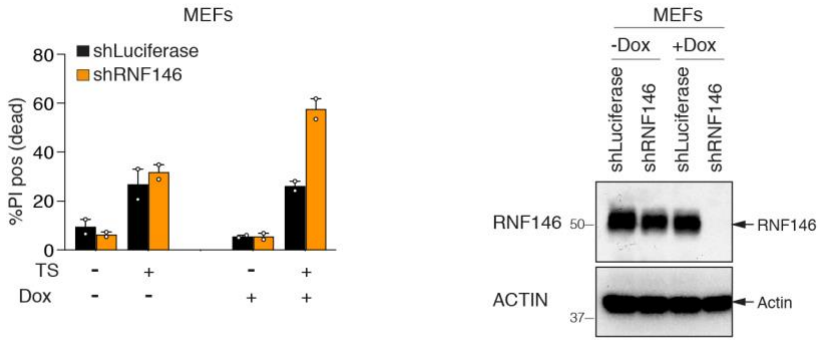

Figure S5.4. related to Figure 5.4. | RNF146 may be involved in PARsylation-mediated complex-2 regulation

Level of cell death assessed by PI positive cells. Wild-type MEFs expressing Dox-inducible shLuciferase or shRNF146 were pre-treated with ± Dox (1 μg/mL) for 48 hours. Cells were then subjected to Western blot analysis or treated with TNF (100 ng/mL) + SM CompA (25 nM) (TS) ± Dox (1μg/mL) for another 12 hours.

Blots are representative of two independent experiments.

Graphs show mean ± SD throughout, n = 2 independent biological repeats.

5.5 Discussion

TNF is a major inflammatory cytokine. TNF stimulation induces the formation of at least two signalling complexes: the membrane-bound complex (complex-1) that promotes the production of pro-inflammatory cytokines, and a cytosolic complex (complex-2) that initiates cell death (Micheau and Tschopp, 2003).

Whether TNF can induce lethal levels of complex-2 is dependent on multiple checkpoints: (i) Ubiquitylation events on complex-1 mediated by E3 ligases such as cIAPs and LUBAC and deubiquitylating enzymes (DUBs) (Bertrand et al., 2008; Gerlach et al., 2011; Haas et al., 2009; Moquin et al., 2013); (ii) Phosphorylation of RIPK1 by kinases TAK1, IKKs, MK2 or TBK1 (Dondelinger et al., 2013; Dondelinger et al., 2015; Jaco et al., 2017; Lafont et al., 2018; Lalaoui et al., 2016); (iii) Transcription-dependent checkpoint which is based on NF-κB and MAPK signalling-induced production of prosurvival proteins such as the natural caspase-8 inhibitor $cFlip_L$ (Kreuz et al., 2001; Micheau et al., 2001); (iv) Caspase-8-mediated cleavage of RIPK1 (Lalaoui et al., 2020; Lin et al., 1999; Liu and Lalaoui, 2020).

In this study, we found that the poly (ADP-ribose) polymerase family members, TNKS1 and TNKS2, associated with complex-2 and caused complex-2 PARsylation. Inactivation of tankyrases significantly sensitized cells to TNF-induced death by increasing complex-2 formation. Although further supporting evidence is required, our data indicated that tankyrases-induced PARsylation may cause ubiquitylation-mediated proteolysis of complex-2 via the E3 ligase RNF146. Therefore, despite the known cell death checkpoints, PARsylation-mediated ubiquitylation of complex-2 may serve as a novel mechanism to limit TNF-induced death by dissociating complex-2.

The anti-tankyrases antibody used in this thesis (Santa Cruz Biotechnology, sc-365897) is expected to detect TNKS1 and TNKS2 of human, mouse and rat origin. The predicted molecular weight of murine TNKS1, TNKS1 isoform 2 and TNKS2 are 140kDa, 106kDa and 127kDa, respectively. In literatures, TNKS1 has always been detected as a 150kDa protein (Koirala et al., 2020; Li et al., 2019; Li et al., 2015), possibly due to its autoPARsylation. Across all the cells lines used in this thesis (BMDMs, MEFs and MDFs), a strong signal at ~150kDa corresponding to TNKS1 and a slight band at ~130kDa which might correspond to have been observed in all the complex-2 immunoprecipitation and pulldown samples. In the lysate samples, TNKS1 was more abundant in the lysate compared with the putative TNKS2,

which may explain the observation that TNKS1 was more prominent in complex-2. In addition, a signal at ~110kDa, is often observed in the lysate. Especially in BMDMs and human cell lines, it showed similar intensity as TNKS1. Considering its molecular weight, this band might represent TNKS1 isoform2. Moreover, in MEFs, TNKS1 often appeared as a double band. However, only the 150kDa band was prominent in complex-2 immunoprecipitation and pulldowns (**Figure 5.2C** and **Figure 5.4C**). This could be due to several possibilities: (i) the lower band (<150kDa) might indicate an inactive form of TNKS1, which is expressed in a cell type independent manner. Therefore, it is not proportionally incorporated into complex-2 as the 150kDa TNKS1. (ii) It is a nonspecific band picked up by the anti-tankyrases antibody. Considering that the protein ladder used in these blots doesn't clearly show molecular weights between 100kDa and 150kDa, and the fact that these bands were detected in a cell type dependent manner, they were not indicated in the figures in this thesis. However, which tankyrase these bands are corresponding to could be addressed later by overexpressing TNKS1, TNKS2 and TNKS1 isoform 2. Finally, tankyrases have been reported to undergo autoPARsylation . In this thesis, with longer exposure, a smeared pattern but not a shift was observed for TNKS1 band (**Figure 5.1B** and **C**; **Supplementary Figure 5.2B**). This is consistent with previous reports that PARsylated TNKS migrated as a trailing smear (Chang et al., 2005a; Yeh et al., 2005; Zhong et al., 2015).

The recruitment of tankyrases to complex-2 has been validated in mouse and human cell lines. Interestingly, **Figure 5.1E** and **F** suggested that in human cell lines, TNKS1 bound to complex-2 at earlier timepoint, and it was disassociated from complex-2 at later timepoint. It will be interesting to explore whether in mouse cell lines tankyrases are recruited to complex-2 in a similar manner. Also, it will be worthwhile performing time-dependent analysis of complex-2 PARsyaltion by using the anti-PAR antibody. However, this could be challenging as the PARsylation on a protein complex could be difficult to detect, due to the extremely low level.

Given the highly complex regulation of TNF induced death, the reason for yet another level of regulation is not immediately clear. One explanation might be that PARsylation-mediated ubiquitylation of complex-2 is yet another evolutionary response to help fight certain pathogens. For instance, pathogens such as *Yersinia* and *Shigella* can both trigger RIPK1 kinase-dependent cell death and inflammation by inhibition of TAK1 and the IKKs or the cIAP1/2 functions (Andree et al., 2014; Dondelinger et al., 2019; Sun et al., 2012; Suzuki et al., 2018).

While knockout of TNK1 or TNKS2 in mice revealed only minor phenotypes (Chiang et al., 2006; Hsiao et al., 2006), genetic ablation of TNKS1 and TNKS2 results in embryonic lethality at embryonic day E10.5 with defective vasculature (Chiang et al., 2008). This phenotype is reminiscent of several strains of knockout mice with defects in TNF signalling, including *Casp8*$^{-/-}$ mice (Kaiser et al., 2011; Moulin et al., 2012; Oberst et al., 2011; Peltzer et al., 2018; Peltzer et al., 2014; Varfolomeev et al., 1998; Yeh et al., 1998; Yeh et al., 2000). The E10.5 lethality of *Casp8*$^{-/-}$ mice is TNFR1-dependent, and can be prevented by loss of either *Ripk3* or *Mlkl* (Alvarez-Diaz et al., 2016; Kaiser et al., 2011; Oberst et al., 2011). It will be interesting to explore whether TNKS1/2 double-knockout mice die in the TNFR1-dependent manner.

Tankyrases are overexpressed in multiple cancers (Lehtio et al., 2013; Riffell et al., 2012). While most the of previous studies showed that tankyrases act through down-regulating tumor suppressors (Li et al., 2019; Li et al., 2015; Wang et al., 2015; Zhang et al., 2011), our data suggested that tankyrases may contribute to cancer progression also via helping evade cell death. A range of potent and highly selective small molecule inhibitors of tankyrases have recently been developed. However, they are limited to preclinical trials due to a narrow efficacious concentration range as single agents (Thorvaldsen, 2017). Using a primary AML model, we showed that tankyrases-specific inhibitors could increase the efficacy of birinapant, a clinical Smac-mimetic that has limited effectiveness as monotherapy (Brumatti et al., 2016; Lalaoui et al., 2016). Our data suggested that the combination of birinapant and tankyrases inhibitors is a new therapeutic avenue for AML. To further explore the potential of the tankyrases inhibitor plus birinapant co-therapy, it will be important to test whether tankyrases inhibition could increase birinapant killing of other types of cancers, not just AML.

Although the precise mechanistic details remain unclear, we showed that tankyrases may regulate the assembly of complex-2 via PARsylation-induced ubiquitylation by E3 ligase RNF146. A recent study comparing the proteome of human tankyrases double knockout cells vs WT cells has reported a list of proteins that are targets of tankyrases-mediated degradation. This study identified novel tankyrases substrates such as NKD1, NKD2, HectD1 and Notch 1, 2, 3 (Bhardwaj et al., 2017). While the TNFR1 complex-2 components FADD, TRADD, RIPK1, caspase-10 isoform 7 and caspase-8 isoform C were detected in this proteomic study, they didn't show any significant changes in the abundance in the DKO cells, suggesting that they are not substrates of tankyrases-dependent degradation in unstimulated cells. This is consistent with our observation that tankyrases are recruited to complex-2 components and cause complex-2 PARsyaltion only upon TNF/SM/IDN stimulation. It is possible that

complex-2 components undergo conformational change or posttranslational modifications during complex-2 assembly, providing docking sites for tankyrases binding.

The tankyrases-RNF146 axis has been implicated in multiple signalling pathways, including WNT signalling. Tankyrases interact with Axin, cause its PARsylation and then stimulate its degradation through RNF146-mediated ubiquitin-proteasome pathway, therefore promoting WNT/β-catenin signalling (Huang et al., 2009; Zhang et al., 2011). Despite its crucial role in development and tissue regeneration, WNT/β-catenin signalling has been revealed to possess anti-inflammatory functions. This is supported by the evidence that WNT/β-catenin signalling downregulates the production of proinflammatory cytokines, including TNF, in multiple cell types with various stimulations. On the other hand, TNF released from macrophages contributes to WNT signalling activation and tumor cell proliferation through GSK3β and Akt signalling (Ma and Hottiger, 2016). Given the role of tankyrases and RNF146 in both TNF signalling and WNT signalling, it will be interesting to examine whether tankyrases-RNF146 axis is involved in the crosstalk between these two signalling pathways.

In summary, we have shown that tankyrases are novel interactors of TNFR1 complex-2. Tankyrases-mediated PARsylation suppressed complex-2 formation, possibly via tankyrases-RNF146 axis. Inactivation of tankyrases using specific inhibitors sensitized cells to TNF-induced cell death. Tankyrases inhibitor increased the killing of the clinical SM birinapant in primary AML model, suggesting the therapeutic potential of this combination treatment for cancer therapy.

Chapter 6 Summary and future directions

This thesis aimed to develop and characterise 3x FLAG tagged caspase-8 knock-in mice to study caspase-8-containing protein complexes at physiological levels. This new tool allowed to discover tankyrases (TNKS1 and TNKS2) as novel interactors in TNFR1 complex-2 and tankyrases-mediated poly(ADP-ribosyl)ation (PARsylation) as a new checkpoint of TNF-induced cell death. This study expands our understanding of how TNF signalling pathway is regulated and given the availability of tankyrases inhibitors may have clinical applications.

6.1 Summary

In **Chapter 3** I performed extensive *in vitro* comparison of N-terminally or C-terminally 3x FLAG-tagged caspase-8 by using doxycycline (Dox)-inducible stably integrated lentiviral system. I have shown that the expression of caspase-8 was unaffected by a 3x FLAG tag. When expressed above physiological levels, a 3x FLAG tag was compatible with the killing activity of caspase-8. Interestingly, when expressed at endogenous levels, C-terminally 3x FLAG tagged caspase-8 appeared to be equivalent to untagged caspase-8 and marginally marginally more efficient in mediating TNF-induced death and complex-2 formation compared to N-terminally 3x FLAG tagged caspase-8. Since N-terminal domain of procaspase-8 (DEDs) is believed to mediate the assembly of Death Inducing Signalling Complex (DISC) chain in TRAIL signalling (Dickens et al., 2012a; Hughes et al., 2016), it is possible that an N-terminal 3x FLAG tag may interfere with caspase-8 in assembling TNFR1 complex-2 via their DEDs and therefore affect cell death. Additionally, I purified TNFR1 complex-2 from cells expressing endogenous levels of 3x FLAG tagged caspase-8 and did mass spectrometry (MS) analysis. The MS analysis identified tankyrase-1 (TNKS1/TNKS/PARP5a/ARTD5), a member of the poly(ADP-ribose) (PARP) superfamily, was enriched upon TNF/Smac-mimetic (SM)/IDN stimulation which induces complex-2 formation.

According to the *in vitro* data shown in Chapter 3, we generated N-terminally or C-terminally 3x FLAG tagged caspase-8 knock-in mice using CRIPSR/Cas9 technology and I characterized these mice in **Chapter 4**. I have shown by Western blot and immunofluorescence stain that 3x FLAG tagged caspase-8 was detectable in tissue and cells from knock-in mice. Consistent with *in vitro* data, the primary cells and transformed cells from 3x FLAG tagged caspase-8 knock-in mice responded similarly as wild-type cells to apoptotic and necroptotic stimulations.

Furthermore, I successfully purified endogenous TNFR1 complex-2 from knock-in mice derived cells by performing anti-FLAG immunoprecipitation. These data suggested that 3x FLAG tagged caspase-8 knock-in mice are useful tools to study caspase-8-containing protein complexes at physiological levels.

The data presented in **Chapter 5** illuminated a role for tankyrases-mediated poly(ADP-ribosyl)ation (PARsylation) in TNF signalling. Using primary cells from the 3x FLAG tagged caspase-8 knock-in mice described in Chapter 4, I identified that the enzyme tankyrase-1 (TNKS1/TNKS/PAR5a/ARTD5), which was identified by mass spectrometry in Chapter 3, was recruited to endogenous TNFR1 complex-2. Western blot data indicates that tankyrase-2 (TNKS2/PARP5b/ARTD6) may also be recruited. During TNF signalling, tankyrases caused complex-2 PARsylation, limiting its assembly and cytotoxic activity. Furthermore, I have generated some preliminary data which suggested that tankyrases may modulate the stability of complex-2 via tankyrases-RNF146 axis.

6.2 Knock-in mice: a great tool to study caspase-8-containing complexes

6.2.1 Structure and localization of complex-2?

The ligation of TRAIL to its death receptor TRAILR1 (DR4) and TRAILR2 (DR5) induced a caspase-8-containing cell death signalling complex called death-inducing signalling complex (DISC). Many researchers have determined the localisation and the composition of DISC. A death effector domain chain DISC model has been proposed in which caspase-8 molecules are believed to form an activating chain via their DED domains upon death stimulation. This model is supported by the observation that transient overexpression of caspase-8 DED domains induced filament formation (Dickens et al., 2012a). However, the exact localization and pattern of DISC could not be addressed by simply overexpressing full length caspase-8 because it can kill cells (Chang et al., 2003a). In addition, effective commercial antibodies against murine procaspase-8 which allow the observation of endogenous caspase-8 are currently not available.

Therefore, these facts raise the importance of generating and utilizing 3x FLAG tagged caspase-8 knock-in mice because: (i) 3x FLAG tag has been reported by Sigma-Aldrich and literatures to be ultrasensitive for detection *in vitro* and *in vivo* (Dai et al., 2014; Ferrando et al., 2015; LaCava et al., 2015); (ii) antibodies against FLAG tag are very specific with little batch to batch variability and their specificity can be confirmed readily using 3x FLAG peptides; (iii) tissue or cells from knock-in mice allow the observation of caspase-8 at endogenous levels. Indeed, by using MDFs from knock-in mice, I showed via anti-FLAG immunofluorescence stain that endogenous caspase-8 displayed a diffuse pattern throughout the cytoplasm. Importantly, DISC-like filaments were not observed for complex-2, although I observed punctate staining at later time point of TNF/SM treatment. This could be due to (i) the low-resolution microscopy used or because caspase-8 does not form filament in the complex-2. To fully address the structure of complex-2, images will need to be taken at higher resolution and magnification, with proper controls. (ii) DED interactions are different between the FasL/TRAIL-induced DISC and the TNFR1-induced complex-2. To test this hypothesis, a comparison between FasL, TRAIL and TNF/SM treatments should be performed in the 3x FLAG tagged caspase-8 expressing cells.

Within 2 hours of TNFR1 stimulation, the membrane bound complex-1 matures into cytosolic, death-inducing complex-2. Perturbed ubiquitylation by cIAPs and phosphorylation by TAK1, IKKs, MK2 or TBK1 of RIPK1 accelerate the internalization of complex-1 and the assembly

of complex-2, leading to RIPK1-dependent apoptosis (RDA) (Liu and Lalaoui, 2020). It has been observed that a detergent-insoluble, highly ubiquitinated, and activated RIPK1 pool, termed "iuRIPK1", was a critical intermediate between complex-1 and the caspase-8 activation platform complex-2 (Amin et al., 2018). It remains unknown whether caspase-8 is readily recruited to RIPK1 in this insoluble fraction before complex-2 is assembled, and when it is recruited. This is due to the fact that examination of the components in insoluble fraction requires harsh lysis buffer, which can cause disassociation of protein complexes. Therefore, 3x FLAG tagged caspase-8 knock-in mice could act as a great tool. Performing immunofluorescence stain on 3x FLAG tagged caspase-8 knock-in mice-derived cells would allow us to observe the distribution and subcellular localization of caspase-8 and caspase-8-containing complex-2 in a time- and stimulation-dependent manner.

6.2.2 Composition of complex-2?

It has been shown that TNF can induce, depending on the stimulations, distinct caspase-8-containing platforms. Inhibition of translation with cycloheximide (CHX) sensitise cells to TNF by reducing levels of the natural caspase-8 inhibitor, cFlip. This type of apoptosis is induced by a molecular platform widely called complex-2a. So far, the known components are TRADD, FADD and caspase-8. Importantly, the TNF plus CHX-induced cell death is independent on RIPK1 kinase activity (Dondelinger et al., 2013; Wang et al., 2008). On the other hand, TNF induces a RIPK1 kinase-dependent apoptosis (RDA) when RIPK1 ubiquitylation by cIAPs and LUBAC or RIPK1 phosphorylation by TAK1, IKK1/2/ε, TBK1 or MK2 are inhibited (Dondelinger et al., 2013; Dondelinger et al., 2015; Lafont et al., 2018; Liu and Lalaoui, 2020; Wang et al., 2008). This type of apoptosis is mediated by a signalling complex contains TRADD, FADD, caspase-8, RIPK1 and RIPK3 and is known as complex-2b. Therefore, it would be interesting to know the differences in the composition of these caspase-8-containing complexes that mediate either RIPK1-independent or RIPK1-dependent apoptosis.

These caspase-8-containing complexes remain far less well defined, possibly due to technical limitations. Immunoprecipitation and elution of a protein complex is required before it is subjected to mass spectrometry analysis. However, the traditional Glycine elution or SDS elution method is either of low efficiency or low specificity, which is not ideal for mass spectrometry identification of protein interactome.

In this thesis, I purified TNFR1 complex-2 (complex-2b) from cells expressing endogenous levels of 3x FLAG tagged caspase-8 and successfully identified novel TNFR1 complex-2 interactors, tankyrases. The endogenous expression of 3x FLAG tagged caspase-8 minimized artefacts. A 3x FLAG tag facilitated the purification of caspase-8 or caspase-8-containing protein complexes using the highly efficient anti-FLAG immunoprecipitation. The immunoprecipitants could be eluted by 3x FLAG peptides, offering higher specificity without loss of sensitivity. Also, a FLAG spiking sample (in which high concentration of 3x FLAG peptides competed with 3x FLAG tagged caspase-8-containing complex-2 in binding with FLAG M2 affinity beads so that the purification of complex-2 was interrupted) was included, which enabled the elimination of non-specific interactors of 3x FLAG tag.

Considering the high specificity and efficiency of anti-FLAG immunoprecipitation, and also the fact that 3x FLAG tagged caspase-8 knock-in mice contain physiological levels of caspase-8, the cells from knock-in mice would be ideal for purification of various caspase-8-containing complexes and the follow-up characterization of interactome by mass spectrometry.

6.2.3 Localization and composition of other caspase-8-containing protein complexes?

Many studies have suggested that caspase-8 are involved in multiple biological processes via forming various non-death inducing protein complexes. For example, during mitosis, caspase-8, RIPK1, FADD and cFlip form ripoptosome which harbors sub-lethal levels of caspase activity (Liccardi et al., 2019). PLK1, a key kinase that regulates chromosomal congression and segregation, is recruited to mitotic ripoptosome where it is cleaved by caspase-8. Therefore, PLK1 is not able to phosphorylate its substrate BUBR1, resulting in mitotic defects (Liccardi et al., 2019). Caspase-8-containing cytosolic complexes have been identified to mediate TRAIL- and FasL -induced cytokine production, in which caspase-8 plays a structural rather than enzymatic role (Hartwig et al., 2017; Henry and Martin, 2017; Kreuz et al., 2004; Varfolomeev et al., 2005). In addition, caspase-8 has been found to mediate proliferation in stimulated lymphocytes through inducing NF-κB activation and nuclear translocation. In T cells, caspase-8 is required for the formation of an active complex which consists of B cell lymphoma 10 (BCL10) and paracaspase MALT1. This complex is essential for the nuclear translocation of NF-κB (Su et al., 2005).

Cells from 3x FLAG tagged caspase-8 knock-in mice will also allow to examine the structure and subcellular localization of these non-death inducing, caspase-8-containing protein platforms, and to characterize their compositions at physiological levels.

6.3 Tankyrases: more implications in TNF signalling and caspase-8?

6.3.1 Tankyrases substrate(s) in TNFR1 complex-2?

Our data suggested that TNFR1 complex-2 is PARsylated in a tankyrases-dependent manner. However, it remains unknown which component directly interacts with tankyrases, and what is/are the substrate(s) of tankyrases in complex-2.

A "consensus" sequence (RXXPXG; X is any amino acid) has been found in the tankyrases-binding motif (TBM) of their substrate proteins. This sequence has recently been extended to RXXXPXG (DaRosa et al., 2018). However, such canonical consensus sequences didn't appear in complex-2 components that we examined such as caspase-8, RIPK1 and FADD. Anti-FLAG immunoprecipitation of 3x FLAG tagged caspase-8 and immunoprecipitation of endogenous complex-2 components (RIPK1 or cleaved caspase-8 or FADD) showed that tankyrases were recruited to complex-2 only upon TNF/SM/IDN stimulation, but not in unstimulated control. These data indicated that tankyrases are not constitutive interactors of any of these components. It is possible that complex-2 components undergo conformational change or posttranslational modifications during complex-2 assembly, providing docking sites for tankyrases binding.

Intriguingly, complex-2 PARsylation requires the presence of caspase-8, because complex-2 components were not co-purified with GST-WWE in the *Casp8*$^{-/-}$ MEFs. There are a number of possible interpretations of this result: (i) caspase-8 is the tankyrases substrate in complex-2; (ii) caspase-8 binds to tankyrases directly, and it is required for another component to become PARsylated; (iii) in the absence of caspase-8, complex-2 fails to form properly and therefore tankyrases fail to be recruited.

To explore which complex-2 component(s) is/are PARsylated by tankyrases upon TNF/SM/IDN stimulation, we are currently in collaboration with Prof. Michael O. Hottiger and Dr. Deena Leslie Pedrioli from the University of Zurich, performing ribosylation mass spectrometry which would help address this question.

6.3.2 The relevance of tankyrases in the TNF signalling?

A previous study has observed that inhibition of tankyrases increases TNF secretion by macrophages (Levaot et al., 2011). Mechanistically, this study suggested that tankyrases

regulated the stability of 3BP2 via inducing its PARsylation and RNF146-mediated proteasomal degradation. Accumulation of 3BP2 caused hyperactivation of the SRC, SYK, and VAV signalling pathways, hyperactive bone-remodeling osteoclasts and elevated TNF secretion by macrophages, resulting in inflammation. A follow-up study has found that RANKL, a TNFSF member, negatively regulates transcription of RNF146 via NF-κB signalling (Matsumoto et al., 2017).

TNKS1/2 double-knockout mice show embryonic lethality at E10.5 (Chiang et al., 2008) with defective vasculature, which is reminiscent of several strains of knockout mice with defects in TNF signalling, including *Casp8*$^{-/-}$ mice (Kaiser et al., 2011; Moulin et al., 2012; Oberst et al., 2011; Peltzer et al., 2018; Peltzer et al., 2014; Varfolomeev et al., 1998; Yeh et al., 1998; Yeh et al., 2000). The E10.5 lethality of *Casp8*$^{-/-}$ mice is TNFR1-dependent, and can be prevented by loss of either *Ripk3* or *Mlkl* (Alvarez-Diaz et al., 2016; Kaiser et al., 2011; Oberst et al., 2011).

All these previous observations, together with my finding that tankyrases-mediated PARsylation acts as a new checkpoint that limits TNF-induced cytotoxicity, suggest that the significance of tankyrases in regulating TNF signalling has been underestimated. The relevance between tankyrases and TNF signalling should be addressed in future studies. For example, it will be interesting to explore whether TNKS1/2 double-knockout mice die in the TNFR1-dependent manner. This question could be addressed by crossing *Tnks1*$^{-/-}$*Tnks2*$^{-/-}$mice with *Tnfr1*$^{-/-}$mice and examining whether the E10.5 lethality could be rescued.

6.3.3 Tankyrases: a general regulator of the caspase-8-containing complexes?

As described in 6.2.2, caspase-8 participates in a wide range of biological processes via forming non-death inducing signalling platforms (Hartwig et al., 2017; Henry and Martin, 2017; Kreuz et al., 2004; Liccardi et al., 2019; Su et al., 2005; Varfolomeev et al., 2005). In these protein complexes, caspase-8 was found to either play a non-enzymatic role as a scaffold for the recruitment of other components, or harbour sublethal activity. My study has revealed a role of tankyrases as negative regulators of caspase-8 activation platform. Therefore, tankyrases might be more important for non-death inducing, caspase-8-containing protein complexes due to the fact that they can limit the activation of caspase-8.

6.3.4 Tankyrases: good therapeutic targets?

Although tankyrases inhibitors have shown encouraging anti-tumor effects in cultured human cancer cell lines and a subset of CRC xenograft models bearing APC-mutants (Huang et al., 2009; Lau et al., 2013; Okada-Iwasaki et al., 2016; Thorvaldsen, 2017; Waaler et al., 2012; Waaler et al., 2011), on-target toxicity has been observed in preclinical trials. Another challenge is that tankyrases inhibitors are only effective in a limited concentration range (Lau et al., 2013; Zhong et al., 2016). It has been suggested that combination of tankyrases inhibitors with other therapeutic agents could help minimize these adverse effects. Indeed, synergistic anti-tumour effects have been observed by using tankyrases inhibitors with PI3K or AKT inhibitors (Arques et al., 2016), tyrosine kinase (EGFR) inhibitors (Casas-Selves et al., 2012; Okada-Iwasaki et al., 2016) and chemotherapeutic agents (Wu et al., 2016) in multiple cancer types.

Birinapant is a Smac-mimetic that is currently in clinical trials for a range of cancers, including AML. Although it has shown promising anti-cancer effects, the limited effectiveness as monotherapy remains one of the major challenges (Brumatti et al., 2016; Lalaoui et al., 2016). In this thesis I found that the combination of tankyrases specific inhibitor IWR-1 and SM birinapant at low doses dramatically decreased the viability of MLL-AF9/Nras^{G12D} AML cells, which is an aggressive AML mouse model with high resistance to birinapant treatment alone. This observation suggested that tankyrases drugs may have clinical applications in treating cancer. To further explore the potential of the tankyrases inhibitors plus birinapant co-therapy, the future studies should focus on testing whether tankyrases inhibition could increase birinapant killing of the other types of cancer *in vitro* and the efficacy and tolerability of this combination *in vivo*.

Appendices

Appendix 1 Construct Details

Table 1 Vectors for Mammalian and Bacterial Expression

Construct	Selection	Source	Purpose
pCMV VSV-G	-	Silke lab stock	Lentivirus assembly
pCMV ðR8.2	-	Silke lab stock	Lentivirus assembly
pFTRE3G N-terminus FLAG mm caspase-8	Puromycin	Generated by Lin Liu	Mammalian expression
pFTRE3G mm caspase-8 C terminus FLAG	Puromycin	Generated by Lin Liu	Mammalian expression
pFTRE3G N-terminus 3x FLAG mm caspase-8	Puromycin	Generated by Lin Liu	Mammalian expression
pFTRE3G mm caspase-8 C-terminus 3x FLAG	Puromycin	Generated by Lin Liu	Mammalian expression
pFTRE3G tagless mm caspase-8	Puromycin	Generated by Lin Liu	Mammalian expression
pFTRE3G rtTAAd PGK Puro	Puromycin	Gift from Toru	Mammalian expression
pFTRE3G mm MLKL GFP	GFP	Gift from James Murphy	Mammalian expression
pFTRE3G eGFP	GFP	Gift from Guy Salvesen	Mammalian expression
pFTRE3G mm TNKS1 isoform2 rtTAAd puro	Puromycin	Designed by John Silke and cloned by Tracy Willson	Mammalian expression
pF TRE3G mm TNKS2 HpaI XhoI BstBI rtTAAd puro	Puromycin	Purchased from Genscript	Mammalian expression
pGEX 6P3 hs GST RNF146 WWE	-	Purchased from Genscript	Bacterial expression
pGEX 6P3 hs GST RNF146 WWE R163A	-	Purchased from Genscript	Bacterial expression
pGEX 6P3 AF1521	-	Generated by Natasha Silke	Bacterial expression
pGEX 6P3 hs HUWE1 WWE	-	Purchased from Genscript	Bacterial expression
pGEX 6P3 mm TRIP12 WWE	-	Purchased from Genscript	Bacterial expression
pF H1t UTG-GFP*	GFP	Gift from Marco Herold	Mammalian expression

** See Appendix 2 for shRNA sequences*

Appendix 2 Oligo Details

Table 2 sgRNAs and HDR templates for generating knock-in mice

Target gene	Species	Sequences	Purpose
Casp8	Mouse	CTTCTACCTCTTGATAAGAA	sgRNA sequence for generating N-terminally 3xFLAG tagged caspase-8 knock-in mice
Casp8	Mouse	GATCATTAGCATCTTGTGTT GACCCAGGTTACAGCTCTTC TACCTCTTGATAAGAATGAA TGACTACAAGGACCACGAC GGTGACTACAAGGACCACG ACATCGACTACAAAGACGAT GACGACAAGGATTTCCAGA GTTGTCTTTATGCTATTGCTG AAGAACTGGGCAGTGAAGA CCTGGCTGCCC	HDR template sequence for generating N-terminally 3xFLAG tagged caspase-8 knock-in mice
Casp8	Mouse	CCAGGAGGCCAAACTTACTG	sgRNA sequence for generating C-terminally 3xFLAG tagged caspase-8 knock-in mice
Casp8	Mouse	GATCCTGTGAATGGAACCTG GTATATTCAGTCACTTTGCC AGAGCCTGAGGGAAAGATG TCCTCAAGGAGATGACATTC TTAGCATCCTGACTGGCGTG AACTATGACGTGAGCAATAA AGACGACAGGAGGAACAAG GGAAAGCAGATGCCACAGC CCACCTTCACACTACGGAAG AAGCTCTTCTTCCCTCCCGA CTACAAGGACCACGACGGT GACTACAAGGACCACGACA TCGACTACAAAGACGATGAC GACAAGTAATGAAGGTAAG TTTGGCCTCCTGGGCCCCTC TCAGGGTTATGCTTCCTTAC TCATTTCTGTGGTTA	HDR template sequence for generating C-terminally 3xFLAG tagged caspase-8 knock-in mice

Table 3 Primers for genotyping knock-in mice

Purpose	sequences
Primers for genotyping N-terminally 3x FLAG tagged caspase-8 knock-in mice	Forward: AGCTGACACTTAACTTCCTCAC Reverse: ATCTCCTCTCGGTTGCAGTC
Primers for genotyping C-terminally 3x FLAG tagged caspase-8 knock-in mice	Forward: CTCGGCCATAAAGCACCTTC Reverse: CGGTGAAGAACTGCGTTTCC

Table 4 shRNA sequences

Target gene	Species	Sequences	Purpose
Luciferase	-	sense: TCCCTGCGTTGCTAGTACCAACTTCAAGAGAGTTGGTACTAGCAACGCATTTTTC antisense: TCGAGAAAAATGCGTTGCTAGTACCAACTCTCTTGAAGTTGGTACTAGCAACGCA	Control shRNA
RNF146	Mouse	sense: TCCCATTTCTGCCCACGTAACATTATTCAAGAGATAATGTTACGTGGGCAGAAATTTTTTC antisense: TCGAGAAAAAATTTCTGCCCACGTAACATTATCTCTTGAATAATGTTACGTGGGCAGAAAT	shRNA targeting mouse RNF146

Appendix 3 Antibody Details

Table 5 Antibody details for immunoblotting, immunofluorescence staining and immunoprecipitation

Reagent	Source	Identifier
Anti-β-actin (AC-15) mAb for WB	Sigma	A1978
Anti-HSP90 (16F1) mAb for WB	Enzo	ADI-SPA-835
Anti-HSP70 (3A3) mAb for WB	Thermo Fisher	MA3-006
Anti-FLAG® M2 mAb for IF and WB	Sigma	F1804
Anti-caspase-8 (D35G2) mAb for WB (full length and p10 subunit)	Cell Signalling technology	4790
Anti-caspase-8 pAb for mouse WB	Cell Signalling technology	4927
Anti-caspase-8 (5D3) mAb for human WB	MBL Life Science	M058-3
Anti-cleaved caspase-8 (Asp387) (D5B2) XP® mAb for mouse WB and IP	Cell Signalling technology	8592
Anti-Flip (Dave-2) mAb for WB	Adipogen	AG-20B-0005
Anti-RIPK1 (D94C12) XP® mAb for WB and IP	Cell Signalling technology	3493
Anti-RIPK3 mAb for WB	WEHI	33/16-8G7-1-1
Anti-phospho-RIPK3 for WB	Gift from Genentech	N/A
Anti-phosphor-MLKL (S345) [EPR9515(2)] mAb for mouse WB	Abcam	ab196436
Anti-FADD (1F7) mAb for WB	Enzo	ADI-AAM-212-E
Anti-cleaved caspase-3 (Asp175) pAb for WB	Cell Signalling technology	9661
Anti-tankyrase-1/2 (E-10) mAb for WB and IP	Santa Cruz Biotechnology	sc-365897
Anti-Poly ADP-ribose (10H) mAb for WB	Sigma	MABC547
Anti-Poly ADP-ribose mAb for IP	Trevigen	4335-MC-100
Anti- Ubiquitin (P4D1) mAb for WB	Cell Signalling technology	3936
Anti-Axin1(C76H11) mAb for WB	Cell Signalling technology	2087
Anti-PARP (46D11) mAb for WB	Cell Signalling technology	9532
Anti-Iduna/RNF146 (N201/35) mAb for mouse WB	NeuroMab	73-233
Anti-cIAP1 (1E1-1-12) mAb for WB	In house (by John Silke and Diep Chau)	N/A
Anti- A20/TNFAIP3 (D13H3) mAb for WB	Cell Signalling technology	5630
Anti-Mouse IgG, HRP-conjugated pAb for WB	Southern Biotech	#1010-05
Anti-Rabbit IgG, HRP-conjugated pAb for WB	Southern Biotech	#4010-05

Anti-Rat IgG, HRP-conjugated pAb for WB	Southern Biotech	#3010-05
Anti-Mouse IgG, HRP-conjugated pAb for WB (light chain specific)	Jackson Immuno Research	115-035-174
Anti-Rabbit IgG, HRP-conjugated pAb for WB (light chain specific)	Jackson Immuno Research	211-032-171
Anti-Mouse IgG, HRP-conjugated pAb for WB (heavy chain specific)	Jackson Immuno Research	115-035-071
Anti-Rabbit IgG, HRP-conjugated pAb for WB (heavy chain specific)	Jackson Immuno Research	111-035-046
Goat anti-Mouse AF488 pAb for IF	Thermo Fisher	A32723
DAPI	Roche	10236276001

Appendix 4 Reagent Details

Table 6 Chemicals and reagents

Reagents	Source	Identifier
CompA	Gift from TetraLogic Pharmaceuticals	N/A
Birinapant	Gift from TetraLogic Pharmaceuticals	N/A
Cycloheximide	Sigma	C4859
Necrostatin-1s	Gift from TetraLogic Pharmaceuticals	N/A
IDN-6556	Gift from TetraLogic Pharmaceuticals	N/A
Fc-TNF	In house	N/A
Lyophilised human TNF	Gift from Daniela N. Männel	N/A
Puromycin	Thermo Fisher	A1113802
Doxycycline	Sigma	D9891
3xFLAG Peptide	Apex Bio	A6001
IWR-1	Sigma	I0161
AZ6102	Selleckchem	S7767
Olaparib	Selleckchem	S1060
PARG	Gift from Michael O. Hottiger	N/A
ADP-HPD	Enzo	ALX-480-094-C060
MG132	Sigma	M7449
ANTI-FLAG® M2 Affinity Gel	Sigma	A2220
Protein A Sepharose	WEHI antibody facillity	N/A
Protein G Sepharose	WEHI antibody facillity	N/A
Glutathione Sepharose® 4B	GE Healthcare	GE17-0756-01
Glutathione Xpure Agarose Resin	UBPBio	P3060-10

Appendix 5 Experimental Models: cell lines

Table 7 Cell lines

Cell lines	Source	Identifier
HEK293T	In house	N/A
HT1080	Gift from John Mariadason	N/A
HT29	In house	N/A
MEFs	In house	N/A
MDFs	In house	N/A
Casp8$^{-/-}$.*Mlkl*$^{-/-}$MDFs	In house (Generated by Maria Tanzer)	N/A
Mlkl$^{-/-}$MDFs	In house (Generated by Maria Tanzer)	N/A
MLL-AF9/NRas^{G12D}	In house (Generated by Gabriela Brumatti)	N/A

Bibliography

Adegbola, S.O., Sahnan, K., Warusavitarne, J., Hart, A., and Tozer, P. (2018). Anti-TNF Therapy in Crohn's Disease. Int J Mol Sci *19*.

Aguilar-Quesada, R., Munoz-Gamez, J.A., Martin-Oliva, D., Peralta-Leal, A., Quiles-Perez, R., Rodriguez-Vargas, J.M., Ruiz de Almodovar, M., Conde, C., Ruiz-Extremera, A., and Oliver, F.J. (2007). Modulation of transcription by PARP-1: consequences in carcinogenesis and inflammation. Curr Med Chem *14*, 1179-1187.

Altmeyer, M., Messner, S., Hassa, P.O., Fey, M., and Hottiger, M.O. (2009). Molecular mechanism of poly(ADP-ribosyl)ation by PARP1 and identification of lysine residues as ADP-ribose acceptor sites. Nucleic Acids Res *37*, 3723-3738.

Alvarado-Kristensson, M., Melander, F., Leandersson, K., Ronnstrand, L., Wernstedt, C., and Andersson, T. (2004). p38-MAPK signals survival by phosphorylation of caspase-8 and caspase-3 in human neutrophils. J Exp Med *199*, 449-458.

Alvarez-Diaz, S., Dillon, C.P., Lalaoui, N., Tanzer, M.C., Rodriguez, D.A., Lin, A., Lebois, M., Hakem, R., Josefsson, E.C., O'Reilly, L.A., *et al.* (2016). The Pseudokinase MLKL and the Kinase RIPK3 Have Distinct Roles in Autoimmune Disease Caused by Loss of Death-Receptor-Induced Apoptosis. Immunity *45*, 513-526.

Amin, P., Florez, M., Najafov, A., Pan, H., Geng, J., Ofengeim, D., Dziedzic, S.A., Wang, H., Barrett, V.J., Ito, Y., *et al.* (2018). Regulation of a distinct activated RIPK1 intermediate bridging complex I and complex II in TNFalpha-mediated apoptosis. Proc Natl Acad Sci U S A *115*, E5944-E5953.

Andree, M., Seeger, J.M., Schull, S., Coutelle, O., Wagner-Stippich, D., Wiegmann, K., Wunderlich, C.M., Brinkmann, K., Broxtermann, P., Witt, A., *et al.* (2014). BID-dependent release of mitochondrial SMAC dampens XIAP-mediated immunity against Shigella. EMBO J *33*, 2171-2187.

Annibaldi, A., and Meier, P. (2018). Checkpoints in TNF-Induced Cell Death: Implications in Inflammation and Cancer. Trends Mol Med *24*, 49-65.

Aravind, L. (2001). The WWE domain: a common interaction module in protein ubiquitination and ADP ribosylation. Trends Biochem Sci *26*, 273-275.

Arques, O., Chicote, I., Puig, I., Tenbaum, S.P., Argiles, G., Dienstmann, R., Fernandez, N., Caratu, G., Matito, J., Silberschmidt, D., *et al.* (2016). Tankyrase Inhibition Blocks Wnt/beta-Catenin Pathway and Reverts Resistance to PI3K and AKT Inhibitors in the Treatment of Colorectal Cancer. Clin Cancer Res *22*, 644-656.

Bao, R., Christova, T., Song, S., Angers, S., Yan, X., and Attisano, L. (2012). Inhibition of tankyrases induces Axin stabilization and blocks Wnt signalling in breast cancer cells. PLoS One *7*, e48670.

Barbero, S., Barila, D., Mielgo, A., Stagni, V., Clair, K., and Stupack, D. (2008). Identification of a critical tyrosine residue in caspase 8 that promotes cell migration. J Biol Chem *283*, 13031-13034.

Barbero, S., Mielgo, A., Torres, V., Teitz, T., Shields, D.J., Mikolon, D., Bogyo, M., Barila, D., Lahti, J.M., Schlaepfer, D., *et al.* (2009). Caspase-8 association with the focal adhesion complex promotes tumor cell migration and metastasis. Cancer Res *69*, 3755-3763.

Barkauskaite, E., Jankevicius, G., and Ahel, I. (2015). Structures and Mechanisms of Enzymes Employed in the Synthesis and Degradation of PARP-Dependent Protein ADP-Ribosylation. Mol Cell *58*, 935-946.

Barnhart, B.C., Legembre, P., Pietras, E., Bubici, C., Franzoso, G., and Peter, M.E. (2004). CD95 ligand induces motility and invasiveness of apoptosis-resistant tumor cells. EMBO J *23*, 3175-3185.

Beisner, D.R., Ch'en, I.L., Kolla, R.V., Hoffmann, A., and Hedrick, S.M. (2005). Cutting edge: innate immunity conferred by B cells is regulated by caspase-8. J Immunol *175*, 3469-3473.
Bertrand, M.J., Milutinovic, S., Dickson, K.M., Ho, W.C., Boudreault, A., Durkin, J., Gillard, J.W., Jaquith, J.B., Morris, S.J., and Barker, P.A. (2008). cIAP1 and cIAP2 facilitate cancer cell survival by functioning as E3 ligases that promote RIP1 ubiquitination. Mol Cell *30*, 689-700.
Bhardwaj, A., Yang, Y., Ueberheide, B., and Smith, S. (2017). Whole proteome analysis of human tankyrase knockout cells reveals targets of tankyrase-mediated degradation. Nat Commun *8*, 2214.
Bilan, V., Leutert, M., Nanni, P., Panse, C., and Hottiger, M.O. (2017). Combining Higher-Energy Collision Dissociation and Electron-Transfer/Higher-Energy Collision Dissociation Fragmentation in a Product-Dependent Manner Confidently Assigns Proteomewide ADP-Ribose Acceptor Sites. Anal Chem *89*, 1523-1530.
Bisht, K.K., Daniloski, Z., and Smith, S. (2013). SA1 binds directly to DNA through its unique AT-hook to promote sister chromatid cohesion at telomeres. J Cell Sci *126*, 3493-3503.
Bisht, K.K., Dudognon, C., Chang, W.G., Sokol, E.S., Ramirez, A., and Smith, S. (2012). GDP-mannose-4,6-dehydratase is a cytosolic partner of tankyrase 1 that inhibits its poly(ADP-ribose) polymerase activity. Mol Cell Biol *32*, 3044-3053.
Boatright, K.M., Deis, C., Denault, J.B., Sutherlin, D.P., and Salvesen, G.S. (2004). Activation of caspases-8 and -10 by FLIP(L). Biochem J *382*, 651-657.
Bonfiglio, J.J., Fontana, P., Zhang, Q., Colby, T., Gibbs-Seymour, I., Atanassov, I., Bartlett, E., Zaja, R., Ahel, I., and Matic, I. (2017). Serine ADP-Ribosylation Depends on HPF1. Mol Cell *65*, 932-940 e936.
Bradley, J.R. (2008). TNF-mediated inflammatory disease. J Pathol *214*, 149-160.
Breese, E.J., Michie, C.A., Nicholls, S.W., Murch, S.H., Williams, C.B., Domizio, P., Walker-Smith, J.A., and MacDonald, T.T. (1994). Tumor necrosis factor alpha-producing cells in the intestinal mucosa of children with inflammatory bowel disease. Gastroenterology *106*, 1455-1466.
Bregman, H., Gunaydin, H., Gu, Y., Schneider, S., Wilson, C., DiMauro, E.F., and Huang, X. (2013). Discovery of a class of novel tankyrase inhibitors that bind to both the nicotinamide pocket and the induced pocket. J Med Chem *56*, 1341-1345.
Brennan, F.M., Chantry, D., Jackson, A., Maini, R., and Feldmann, M. (1989). Inhibitory effect of TNF alpha antibodies on synovial cell interleukin-1 production in rheumatoid arthritis. Lancet *2*, 244-247.
Brochu, G., Duchaine, C., Thibeault, L., Lagueux, J., Shah, G.M., and Poirier, G.G. (1994). Mode of action of poly(ADP-ribose) glycohydrolase. Biochim Biophys Acta *1219*, 342-350.
Brumatti, G., Ma, C., Lalaoui, N., Nguyen, N.Y., Navarro, M., Tanzer, M.C., Richmond, J., Ghisi, M., Salmon, J.M., Silke, N., *et al.* (2016). The caspase-8 inhibitor emricasan combines with the SMAC mimetic birinapant to induce necroptosis and treat acute myeloid leukemia. Sci Transl Med *8*, 339ra369.
Bryant, H.E., Schultz, N., Thomas, H.D., Parker, K.M., Flower, D., Lopez, E., Kyle, S., Meuth, M., Curtin, N.J., and Helleday, T. (2005). Specific killing of BRCA2-deficient tumours with inhibitors of poly(ADP-ribose) polymerase. Nature *434*, 913-917.
Busch, A.M., Johnson, K.C., Stan, R.V., Sanglikar, A., Ahmed, Y., Dmitrovsky, E., and Freemantle, S.J. (2013). Evidence for tankyrases as antineoplastic targets in lung cancer. BMC Cancer *13*, 211.
Butler, D.M., Maini, R.N., Feldmann, M., and Brennan, F.M. (1995). Modulation of proinflammatory cytokine release in rheumatoid synovial membrane cell cultures. Comparison of monoclonal anti TNF-alpha antibody with the interleukin-1 receptor antagonist. Eur Cytokine Netw *6*, 225-230.

Callow, M.G., Tran, H., Phu, L., Lau, T., Lee, J., Sandoval, W.N., Liu, P.S., Bheddah, S., Tao, J., Lill, J.R., *et al.* (2011). Ubiquitin ligase RNF146 regulates tankyrase and Axin to promote Wnt signaling. PLoS One *6*, e22595.
Carswell, E.A., Old, L.J., Kassel, R.L., Green, S., Fiore, N., and Williamson, B. (1975). An endotoxin-induced serum factor that causes necrosis of tumors. Proc Natl Acad Sci U S A *72*, 3666-3670.
Casas-Selves, M., Kim, J., Zhang, Z., Helfrich, B.A., Gao, D., Porter, C.C., Scarborough, H.A., Bunn, P.A., Jr., Chan, D.C., Tan, A.C., *et al.* (2012). Tankyrase and the canonical Wnt pathway protect lung cancer cells from EGFR inhibition. Cancer Res *72*, 4154-4164.
Castri, P., Lee, Y.J., Ponzio, T., Maric, D., Spatz, M., Bembry, J., and Hallenbeck, J. (2014). Poly(ADP-ribose) polymerase-1 and its cleavage products differentially modulate cellular protection through NF-kappaB-dependent signaling. Biochim Biophys Acta *1843*, 640-651.
Chaitanya, G.V., Steven, A.J., and Babu, P.P. (2010). PARP-1 cleavage fragments: signatures of cell-death proteases in neurodegeneration. Cell Commun Signal *8*, 31.
Chang, D.W., Xing, Z., Capacio, V.L., Peter, M.E., and Yang, X. (2003a). Interdimer processing mechanism of procaspase-8 activation. EMBO J *22*, 4132-4142.
Chang, D.W., Xing, Z., Pan, Y., Algeciras-Schimnich, A., Barnhart, B.C., Yaish-Ohad, S., Peter, M.E., and Yang, X. (2002). c-FLIP(L) is a dual function regulator for caspase-8 activation and CD95-mediated apoptosis. EMBO J *21*, 3704-3714.
Chang, L., Kamata, H., Solinas, G., Luo, J.L., Maeda, S., Venuprasad, K., Liu, Y.C., and Karin, M. (2006). The E3 ubiquitin ligase itch couples JNK activation to TNFalpha-induced cell death by inducing c-FLIP(L) turnover. Cell *124*, 601-613.
Chang, P., Coughlin, M., and Mitchison, T.J. (2005a). Tankyrase-1 polymerization of poly(ADP-ribose) is required for spindle structure and function. Nat Cell Biol *7*, 1133-1139.
Chang, P., Coughlin, M., and Mitchison, T.J. (2009). Interaction between Poly(ADP-ribose) and NuMA contributes to mitotic spindle pole assembly. Mol Biol Cell *20*, 4575-4585.
Chang, W., Dynek, J.N., and Smith, S. (2003b). TRF1 is degraded by ubiquitin-mediated proteolysis after release from telomeres. Genes Dev *17*, 1328-1333.
Chang, W., Dynek, J.N., and Smith, S. (2005b). NuMA is a major acceptor of poly(ADP-ribosyl)ation by tankyrase 1 in mitosis. Biochem J *391*, 177-184.
Chang, W.J., and Alvarez-Gonzalez, R. (2001). The sequence-specific DNA binding of NF-kappa B is reversibly regulated by the automodification reaction of poly (ADP-ribose) polymerase 1. J Biol Chem *276*, 47664-47670.
Chen, B., Dodge, M.E., Tang, W., Lu, J., Ma, Z., Fan, C.W., Wei, S., Hao, W., Kilgore, J., Williams, N.S., *et al.* (2009). Small molecule-mediated disruption of Wnt-dependent signaling in tissue regeneration and cancer. Nat Chem Biol *5*, 100-107.
Chen, N.J., Chio, II, Lin, W.J., Duncan, G., Chau, H., Katz, D., Huang, H.L., Pike, K.A., Hao, Z., Su, Y.W., *et al.* (2008). Beyond tumor necrosis factor receptor: TRADD signaling in toll-like receptors. Proc Natl Acad Sci U S A *105*, 12429-12434.
Chi, N.W., and Lodish, H.F. (2000). Tankyrase is a golgi-associated mitogen-activated protein kinase substrate that interacts with IRAP in GLUT4 vesicles. J Biol Chem *275*, 38437-38444.
Chiang, Y.J., Hsiao, S.J., Yver, D., Cushman, S.W., Tessarollo, L., Smith, S., and Hodes, R.J. (2008). Tankyrase 1 and tankyrase 2 are essential but redundant for mouse embryonic development. PLoS One *3*, e2639.
Chiang, Y.J., Nguyen, M.L., Gurunathan, S., Kaminker, P., Tessarollo, L., Campisi, J., and Hodes, R.J. (2006). Generation and characterization of telomere length maintenance in tankyrase 2-deficient mice. Mol Cell Biol *26*, 2037-2043.
Cho, Y.S., Challa, S., Moquin, D., Genga, R., Ray, T.D., Guildford, M., and Chan, F.K. (2009). Phosphorylation-driven assembly of the RIP1-RIP3 complex regulates programmed necrosis and virus-induced inflammation. Cell *137*, 1112-1123.

Chun, H.J., Zheng, L., Ahmad, M., Wang, J., Speirs, C.K., Siegel, R.M., Dale, J.K., Puck, J., Davis, J., Hall, C.G., *et al.* (2002). Pleiotropic defects in lymphocyte activation caused by caspase-8 mutations lead to human immunodeficiency. Nature *419*, 395-399.
Cockman, M.E., Webb, J.D., Kramer, H.B., Kessler, B.M., and Ratcliffe, P.J. (2009). Proteomics-based identification of novel factor inhibiting hypoxia-inducible factor (FIH) substrates indicates widespread asparaginyl hydroxylation of ankyrin repeat domain-containing proteins. Mol Cell Proteomics *8*, 535-546.
Cook, W.D., Moujalled, D.M., Ralph, T.J., Lock, P., Young, S.N., Murphy, J.M., and Vaux, D.L. (2014). RIPK1- and RIPK3-induced cell death mode is determined by target availability. Cell Death Differ *21*, 1600-1612.
D'Amours, D., Desnoyers, S., D'Silva, I., and Poirier, G.G. (1999). Poly(ADP-ribosyl)ation reactions in the regulation of nuclear functions. Biochem J *342 (Pt 2)*, 249-268.
D'Souza, A., Meissner, B.L., Tang, B., McKenzie, R.S., and Piech, C.T. (2010). Effectiveness of anti-tumor necrosis factor agents in the treatment of rheumatoid arthritis: observational study. Am Health Drug Benefits *3*, 266-273.
Dai, L., LaCava, J., Taylor, M.S., and Boeke, J.D. (2014). Expression and detection of LINE-1 ORF-encoded proteins. Mob Genet Elements *4*, e29319.
Daniels, C.M., Ong, S.E., and Leung, A.K. (2014). Phosphoproteomic approach to characterize protein mono- and poly(ADP-ribosyl)ation sites from cells. J Proteome Res *13*, 3510-3522.
DaRosa, P.A., Klevit, R.E., and Xu, W. (2018). Structural basis for tankyrase-RNF146 interaction reveals noncanonical tankyrase-binding motifs. Protein Sci *27*, 1057-1067.
De Blasio, A., Di Fiore, R., Morreale, M., Carlisi, D., Drago-Ferrante, R., Montalbano, M., Scerri, C., Tesoriere, G., and Vento, R. (2016). Unusual roles of caspase-8 in triple-negative breast cancer cell line MDA-MB-231. Int J Oncol *48*, 2339-2348.
Diamantopoulos, P.T., Sofotasiou, M., Papadopoulou, V., Polonyfi, K., Iliakis, T., and Viniou, N.A. (2014). PARP1-driven apoptosis in chronic lymphocytic leukemia. Biomed Res Int *2014*, 106713.
Dickens, L.S., Boyd, R.S., Jukes-Jones, R., Hughes, M.A., Robinson, G.L., Fairall, L., Schwabe, J.W., Cain, K., and Macfarlane, M. (2012a). A death effector domain chain DISC model reveals a crucial role for caspase-8 chain assembly in mediating apoptotic cell death. Mol Cell *47*, 291-305.
Dickens, L.S., Powley, I.R., Hughes, M.A., and MacFarlane, M. (2012b). The 'complexities' of life and death: death receptor signalling platforms. Exp Cell Res *318*, 1269-1277.
Dillon, C.P., Oberst, A., Weinlich, R., Janke, L.J., Kang, T.B., Ben-Moshe, T., Mak, T.W., Wallach, D., and Green, D.R. (2012). Survival function of the FADD-CASPASE-8-cFLIP(L) complex. Cell Rep *1*, 401-407.
Dondelinger, Y., Aguileta, M.A., Goossens, V., Dubuisson, C., Grootjans, S., Dejardin, E., Vandenabeele, P., and Bertrand, M.J. (2013). RIPK3 contributes to TNFR1-mediated RIPK1 kinase-dependent apoptosis in conditions of cIAP1/2 depletion or TAK1 kinase inhibition. Cell Death Differ *20*, 1381-1392.
Dondelinger, Y., Delanghe, T., Priem, D., Wynosky-Dolfi, M.A., Sorobetea, D., Rojas-Rivera, D., Giansanti, P., Roelandt, R., Gropengiesser, J., Ruckdeschel, K., *et al.* (2019). Serine 25 phosphorylation inhibits RIPK1 kinase-dependent cell death in models of infection and inflammation. Nat Commun *10*, 1729.
Dondelinger, Y., Delanghe, T., Rojas-Rivera, D., Priem, D., Delvaeye, T., Bruggeman, I., Van Herreweghe, F., Vandenabeele, P., and Bertrand, M.J.M. (2017). MK2 phosphorylation of RIPK1 regulates TNF-mediated cell death. Nat Cell Biol *19*, 1237-1247.
Dondelinger, Y., Jouan-Lanhouet, S., Divert, T., Theatre, E., Bertin, J., Gough, P.J., Giansanti, P., Heck, A.J., Dejardin, E., Vandenabeele, P., *et al.* (2015). NF-kappaB-Independent Role of

IKKalpha/IKKbeta in Preventing RIPK1 Kinase-Dependent Apoptotic and Necroptotic Cell Death during TNF Signaling. Mol Cell *60*, 63-76.
Douglas, D.L., and Baines, C.P. (2014). PARP1-mediated necrosis is dependent on parallel JNK and Ca(2)(+)/calpain pathways. J Cell Sci *127*, 4134-4145.
Duprez, L., Takahashi, N., Van Hauwermeiren, F., Vandendriessche, B., Goossens, V., Vanden Berghe, T., Declercq, W., Libert, C., Cauwels, A., and Vandenabeele, P. (2011). RIP kinase-dependent necrosis drives lethal systemic inflammatory response syndrome. Immunity *35*, 908-918.
Durkacz, B.W., Irwin, J., and Shall, S. (1981). Inhibition of (ADP-ribose)n biosynthesis retards DNA repair but does not inhibit DNA repair synthesis. Biochem Biophys Res Commun *101*, 1433-1441.
Dynek, J.N., and Smith, S. (2004). Resolution of sister telomere association is required for progression through mitosis. Science *304*, 97-100.
Ermolaeva, M.A., Michallet, M.C., Papadopoulou, N., Utermohlen, O., Kranidioti, K., Kollias, G., Tschopp, J., and Pasparakis, M. (2008). Function of TRADD in tumor necrosis factor receptor 1 signaling and in TRIF-dependent inflammatory responses. Nat Immunol *9*, 1037-1046.
Estornes, Y., Toscano, F., Virard, F., Jacquemin, G., Pierrot, A., Vanbervliet, B., Bonnin, M., Lalaoui, N., Mercier-Gouy, P., Pacheco, Y., *et al.* (2012). dsRNA induces apoptosis through an atypical death complex associating TLR3 to caspase-8. Cell Death Differ *19*, 1482-1494.
Ettehadi, P., Greaves, M.W., Wallach, D., Aderka, D., and Camp, R.D. (1994). Elevated tumour necrosis factor-alpha (TNF-alpha) biological activity in psoriatic skin lesions. Clin Exp Immunol *96*, 146-151.
Faraoni, I., and Graziani, G. (2018). Role of BRCA Mutations in Cancer Treatment with Poly(ADP-ribose) Polymerase (PARP) Inhibitors. Cancers (Basel) *10*.
Farmer, H., McCabe, N., Lord, C.J., Tutt, A.N., Johnson, D.A., Richardson, T.B., Santarosa, M., Dillon, K.J., Hickson, I., Knights, C., *et al.* (2005). Targeting the DNA repair defect in BRCA mutant cells as a therapeutic strategy. Nature *434*, 917-921.
Feldmann, M., Brennan, F.M., and Maini, R.N. (1996). Role of cytokines in rheumatoid arthritis. Annu Rev Immunol *14*, 397-440.
Feltham, R., Jamal, K., Tenev, T., Liccardi, G., Jaco, I., Domingues, C.M., Morris, O., John, S.W., Annibaldi, A., Widya, M., *et al.* (2018). Mind Bomb Regulates Cell Death during TNF Signaling by Suppressing RIPK1's Cytotoxic Potential. Cell Rep *23*, 470-484.
Feoktistova, M., Geserick, P., Kellert, B., Dimitrova, D.P., Langlais, C., Hupe, M., Cain, K., MacFarlane, M., Hacker, G., and Leverkus, M. (2011). cIAPs block Ripoptosome formation, a RIP1/caspase-8 containing intracellular cell death complex differentially regulated by cFLIP isoforms. Mol Cell *43*, 449-463.
Ferrando, R.E., Newton, K., Chu, F., Webster, J.D., and French, D.M. (2015). Immunohistochemical detection of FLAG-tagged endogenous proteins in knock-in mice. J Histochem Cytochem *63*, 244-255.
Fong, P.C., Boss, D.S., Yap, T.A., Tutt, A., Wu, P., Mergui-Roelvink, M., Mortimer, P., Swaisland, H., Lau, A., O'Connor, M.J., *et al.* (2009). Inhibition of poly(ADP-ribose) polymerase in tumors from BRCA mutation carriers. N Engl J Med *361*, 123-134.
Fricker, N., Beaudouin, J., Richter, P., Eils, R., Krammer, P.H., and Lavrik, I.N. (2010). Model-based dissection of CD95 signaling dynamics reveals both a pro- and antiapoptotic role of c-FLIPL. J Cell Biol *190*, 377-389.
Fu, T.M., Li, Y., Lu, A., Li, Z., Vajjhala, P.R., Cruz, A.C., Srivastava, D.B., DiMaio, F., Penczek, P.A., Siegel, R.M., *et al.* (2016). Cryo-EM Structure of Caspase-8 Tandem DED Filament Reveals Assembly and Regulation Mechanisms of the Death-Inducing Signaling Complex. Mol Cell *64*, 236-250.

Fuchs, Y., and Steller, H. (2011). Programmed cell death in animal development and disease. Cell *147*, 742-758.
Fulda, S., and Vucic, D. (2012). Targeting IAP proteins for therapeutic intervention in cancer. Nat Rev Drug Discov *11*, 109-124.
Gerlach, B., Cordier, S.M., Schmukle, A.C., Emmerich, C.H., Rieser, E., Haas, T.L., Webb, A.I., Rickard, J.A., Anderton, H., Wong, W.W., *et al.* (2011). Linear ubiquitination prevents inflammation and regulates immune signalling. Nature *471*, 591-596.
Gibbs-Seymour, I., Fontana, P., Rack, J.G.M., and Ahel, I. (2016). HPF1/C4orf27 Is a PARP-1-Interacting Protein that Regulates PARP-1 ADP-Ribosylation Activity. Mol Cell *62*, 432-442.
Gibson, B.A., Conrad, L.B., Huang, D., and Kraus, W.L. (2017). Generation and Characterization of Recombinant Antibody-like ADP-Ribose Binding Proteins. Biochemistry *56*, 6305-6316.
Golks, A., Brenner, D., Schmitz, I., Watzl, C., Krueger, A., Krammer, P.H., and Lavrik, I.N. (2006). The role of CAP3 in CD95 signaling: new insights into the mechanism of procaspase-8 activation. Cell Death Differ *13*, 489-498.
Grivennikov, S.I., Tumanov, A.V., Liepinsh, D.J., Kruglov, A.A., Marakusha, B.I., Shakhov, A.N., Murakami, T., Drutskaya, L.N., Forster, I., Clausen, B.E., *et al.* (2005). Distinct and nonredundant in vivo functions of TNF produced by t cells and macrophages/neutrophils: protective and deleterious effects. Immunity *22*, 93-104.
Guo, H.L., Zhang, C., Liu, Q., Li, Q., Lian, G., Wu, D., Li, X., Zhang, W., Shen, Y., Ye, Z., *et al.* (2012). The Axin/TNKS complex interacts with KIF3A and is required for insulin-stimulated GLUT4 translocation. Cell Res *22*, 1246-1257.
Ha, G.H., Kim, H.S., Go, H., Lee, H., Seimiya, H., Chung, D.H., and Lee, C.W. (2012). Tankyrase-1 function at telomeres and during mitosis is regulated by Polo-like kinase-1-mediated phosphorylation. Cell Death Differ *19*, 321-332.
Haas, T.L., Emmerich, C.H., Gerlach, B., Schmukle, A.C., Cordier, S.M., Rieser, E., Feltham, R., Vince, J., Warnken, U., Wenger, T., *et al.* (2009). Recruitment of the linear ubiquitin chain assembly complex stabilizes the TNF-R1 signaling complex and is required for TNF-mediated gene induction. Mol Cell *36*, 831-844.
Haikarainen, T., Krauss, S., and Lehtio, L. (2014). Tankyrases: structure, function and therapeutic implications in cancer. Curr Pharm Des *20*, 6472-6488.
Hakem, A., El Ghamrasni, S., Maire, G., Lemmers, B., Karaskova, J., Jurisicova, A., Sanchez, O., Squire, J., and Hakem, R. (2012). Caspase-8 is essential for maintaining chromosomal stability and suppressing B-cell lymphomagenesis. Blood *119*, 3495-3502.
Hart, M.J., de los Santos, R., Albert, I.N., Rubinfeld, B., and Polakis, P. (1998). Downregulation of beta-catenin by human Axin and its association with the APC tumor suppressor, beta-catenin and GSK3 beta. Curr Biol *8*, 573-581.
Hartwig, T., Montinaro, A., von Karstedt, S., Sevko, A., Surinova, S., Chakravarthy, A., Taraborrelli, L., Draber, P., Lafont, E., Arce Vargas, F., *et al.* (2017). The TRAIL-Induced Cancer Secretome Promotes a Tumor-Supportive Immune Microenvironment via CCR2. Mol Cell *65*, 730-742 e735.
Hassa, P.O., Covic, M., Bedford, M.T., and Hottiger, M.O. (2008). Protein arginine methyltransferase 1 coactivates NF-kappaB-dependent gene expression synergistically with CARM1 and PARP1. J Mol Biol *377*, 668-678.
Hatakeyama, K., Nemoto, Y., Ueda, K., and Hayaishi, O. (1986). Purification and characterization of poly(ADP-ribose) glycohydrolase. Different modes of action on large and small poly(ADP-ribose). J Biol Chem *261*, 14902-14911.

He, S., Wang, L., Miao, L., Wang, T., Du, F., Zhao, L., and Wang, X. (2009). Receptor interacting protein kinase-3 determines cellular necrotic response to TNF-alpha. Cell *137*, 1100-1111.
Helfer, B., Boswell, B.C., Finlay, D., Cipres, A., Vuori, K., Bong Kang, T., Wallach, D., Dorfleutner, A., Lahti, J.M., Flynn, D.C., *et al.* (2006). Caspase-8 promotes cell motility and calpain activity under nonapoptotic conditions. Cancer Res *66*, 4273-4278.
Helmke, C., Raab, M., Rodel, F., Matthess, Y., Oellerich, T., Mandal, R., Sanhaji, M., Urlaub, H., Rodel, C., Becker, S., *et al.* (2016). Ligand stimulation of CD95 induces activation of Plk3 followed by phosphorylation of caspase-8. Cell Res *26*, 914-934.
Henry, C.M., and Martin, S.J. (2017). Caspase-8 Acts in a Non-enzymatic Role as a Scaffold for Assembly of a Pro-inflammatory "FADDosome" Complex upon TRAIL Stimulation. Mol Cell *65*, 715-729 e715.
Hoffmann, J.C., Pappa, A., Krammer, P.H., and Lavrik, I.N. (2009). A new C-terminal cleavage product of procaspase-8, p30, defines an alternative pathway of procaspase-8 activation. Mol Cell Biol *29*, 4431-4440.
HogenEsch, H., Gijbels, M.J., Offerman, E., van Hooft, J., van Bekkum, D.W., and Zurcher, C. (1993). A spontaneous mutation characterized by chronic proliferative dermatitis in C57BL mice. Am J Pathol *143*, 972-982.
Holbrook, J., Lara-Reyna, S., Jarosz-Griffiths, H., and McDermott, M. (2019). Tumour necrosis factor signalling in health and disease. F1000Res *8*.
Hottiger, M.O. (2015). Nuclear ADP-Ribosylation and Its Role in Chromatin Plasticity, Cell Differentiation, and Epigenetics. Annu Rev Biochem *84*, 227-263.
Hottiger, M.O., Hassa, P.O., Luscher, B., Schuler, H., and Koch-Nolte, F. (2010). Toward a unified nomenclature for mammalian ADP-ribosyltransferases. Trends Biochem Sci *35*, 208-219.
Hsiao, S.J., Poitras, M.F., Cook, B.D., Liu, Y., and Smith, S. (2006). Tankyrase 2 poly(ADP-ribose) polymerase domain-deleted mice exhibit growth defects but have normal telomere length and capping. Mol Cell Biol *26*, 2044-2054.
Hsiao, S.J., and Smith, S. (2008). Tankyrase function at telomeres, spindle poles, and beyond. Biochimie *90*, 83-92.
Huang, S.M., Mishina, Y.M., Liu, S., Cheung, A., Stegmeier, F., Michaud, G.A., Charlat, O., Wiellette, E., Zhang, Y., Wiessner, S., *et al.* (2009). Tankyrase inhibition stabilizes axin and antagonizes Wnt signalling. Nature *461*, 614-620.
Hughes, M.A., Harper, N., Butterworth, M., Cain, K., Cohen, G.M., and MacFarlane, M. (2009). Reconstitution of the death-inducing signaling complex reveals a substrate switch that determines CD95-mediated death or survival. Mol Cell *35*, 265-279.
Hughes, M.A., Powley, I.R., Jukes-Jones, R., Horn, S., Feoktistova, M., Fairall, L., Schwabe, J.W., Leverkus, M., Cain, K., and MacFarlane, M. (2016). Co-operative and Hierarchical Binding of c-FLIP and Caspase-8: A Unified Model Defines How c-FLIP Isoforms Differentially Control Cell Fate. Mol Cell *61*, 834-849.
Irmler, M., Thome, M., Hahne, M., Schneider, P., Hofmann, K., Steiner, V., Bodmer, J.L., Schroter, M., Burns, K., Mattmann, C., *et al.* (1997). Inhibition of death receptor signals by cellular FLIP. Nature *388*, 190-195.
Jaco, I., Annibaldi, A., Lalaoui, N., Wilson, R., Tenev, T., Laurien, L., Kim, C., Jamal, K., Wicky John, S., Liccardi, G., *et al.* (2017). MK2 Phosphorylates RIPK1 to Prevent TNF-Induced Cell Death. Mol Cell *66*, 698-710 e695.
Jia, S.H., Parodo, J., Kapus, A., Rotstein, O.D., and Marshall, J.C. (2008). Dynamic regulation of neutrophil survival through tyrosine phosphorylation or dephosphorylation of caspase-8. J Biol Chem *283*, 5402-5413.

Jin, L.H., Shao, Q.J., Luo, W., Ye, Z.Y., Li, Q., and Lin, S.C. (2003). Detection of point mutations of the Axin1 gene in colorectal cancers. Int J Cancer *107*, 696-699.
Jin, Z., Li, Y., Pitti, R., Lawrence, D., Pham, V.C., Lill, J.R., and Ashkenazi, A. (2009). Cullin3-based polyubiquitination and p62-dependent aggregation of caspase-8 mediate extrinsic apoptosis signaling. Cell *137*, 721-735.
Jit, M., Henderson, B., Stevens, M., and Seymour, R.M. (2005). TNF-alpha neutralization in cytokine-driven diseases: a mathematical model to account for therapeutic success in rheumatoid arthritis but therapeutic failure in systemic inflammatory response syndrome. Rheumatology (Oxford) *44*, 323-331.
Jones, W.A., Gerrie, J., and Pritchard, J. (1950). Cherubism--familial fibrous dysplasia of the jaws. J Bone Joint Surg Br *32-B*, 334-347.
Kaiser, W.J., Upton, J.W., Long, A.B., Livingston-Rosanoff, D., Daley-Bauer, L.P., Hakem, R., Caspary, T., and Mocarski, E.S. (2011). RIP3 mediates the embryonic lethality of caspase-8-deficient mice. Nature *471*, 368-372.
Kallenberger, S.M., Beaudouin, J., Claus, J., Fischer, C., Sorger, P.K., Legewie, S., and Eils, R. (2014). Intra- and interdimeric caspase-8 self-cleavage controls strength and timing of CD95-induced apoptosis. Sci Signal *7*, ra23.
Kang, S., Fernandes-Alnemri, T., Rogers, C., Mayes, L., Wang, Y., Dillon, C., Roback, L., Kaiser, W., Oberst, A., Sagara, J., *et al.* (2015). Caspase-8 scaffolding function and MLKL regulate NLRP3 inflammasome activation downstream of TLR3. Nat Commun *6*, 7515.
Kang, T.B., Ben-Moshe, T., Varfolomeev, E.E., Pewzner-Jung, Y., Yogev, N., Jurewicz, A., Waisman, A., Brenner, O., Haffner, R., Gustafsson, E., *et al.* (2004). Caspase-8 serves both apoptotic and nonapoptotic roles. J Immunol *173*, 2976-2984.
Kang, T.B., Oh, G.S., Scandella, E., Bolinger, B., Ludewig, B., Kovalenko, A., and Wallach, D. (2008). Mutation of a self-processing site in caspase-8 compromises its apoptotic but not its nonapoptotic functions in bacterial artificial chromosome-transgenic mice. J Immunol *181*, 2522-2532.
Kim, M.K., Dudognon, C., and Smith, S. (2012). Tankyrase 1 regulates centrosome function by controlling CPAP stability. EMBO Rep *13*, 724-732.
Kim, S.O., Ono, K., and Han, J. (2001). Apoptosis by pan-caspase inhibitors in lipopolysaccharide-activated macrophages. Am J Physiol Lung Cell Mol Physiol *281*, L1095-1105.
Kim, Y.M., Kim, T.H., Chung, H.T., Talanian, R.V., Yin, X.M., and Billiar, T.R. (2000). Nitric oxide prevents tumor necrosis factor alpha-induced rat hepatocyte apoptosis by the interruption of mitochondrial apoptotic signaling through S-nitrosylation of caspase-8. Hepatology *32*, 770-778.
Koch, A.E., Harlow, L.A., Haines, G.K., Amento, E.P., Unemori, E.N., Wong, W.L., Pope, R.M., and Ferrara, N. (1994). Vascular endothelial growth factor. A cytokine modulating endothelial function in rheumatoid arthritis. J Immunol *152*, 4149-4156.
Koenig, A., Russell, J.Q., Rodgers, W.A., and Budd, R.C. (2008). Spatial differences in active caspase-8 defines its role in T-cell activation versus cell death. Cell Death Differ *15*, 1701-1711.
Koirala, S., Klein, J., Zheng, Y., Glenn, N.O., Eisemann, T., Fon Tacer, K., Miller, D.J., Kulak, O., Lu, M., Finkelstein, D.B., *et al.* (2020). Tissue-Specific Regulation of the Wnt/beta-Catenin Pathway by PAGE4 Inhibition of Tankyrase. Cell Rep *32*, 107922.
Kontoyiannis, D., Pasparakis, M., Pizarro, T.T., Cominelli, F., and Kollias, G. (1999). Impaired on/off regulation of TNF biosynthesis in mice lacking TNF AU-rich elements: implications for joint and gut-associated immunopathologies. Immunity *10*, 387-398.
Kox, W.J., Volk, T., Kox, S.N., and Volk, H.D. (2000). Immunomodulatory therapies in sepsis. Intensive Care Med *26 Suppl 1*, S124-128.

Krelin, Y., Zhang, L., Kang, T.B., Appel, E., Kovalenko, A., and Wallach, D. (2008). Caspase-8 deficiency facilitates cellular transformation in vitro. Cell Death Differ *15*, 1350-1355.
Kreuz, S., Siegmund, D., Rumpf, J.J., Samel, D., Leverkus, M., Janssen, O., Hacker, G., Dittrich-Breiholz, O., Kracht, M., Scheurich, P., *et al.* (2004). NFkappaB activation by Fas is mediated through FADD, caspase-8, and RIP and is inhibited by FLIP. J Cell Biol *166*, 369-380.
Kreuz, S., Siegmund, D., Scheurich, P., and Wajant, H. (2001). NF-kappaB inducers upregulate cFLIP, a cycloheximide-sensitive inhibitor of death receptor signaling. Mol Cell Biol *21*, 3964-3973.
Krishnakumar, R., and Kraus, W.L. (2010). The PARP side of the nucleus: molecular actions, physiological outcomes, and clinical targets. Mol Cell *39*, 8-24.
Kristensen, M., Chu, C.Q., Eedy, D.J., Feldmann, M., Brennan, F.M., and Breathnach, S.M. (1993). Localization of tumour necrosis factor-alpha (TNF-alpha) and its receptors in normal and psoriatic skin: epidermal cells express the 55-kD but not the 75-kD TNF receptor. Clin Exp Immunol *94*, 354-362.
Krueger, A., Baumann, S., Krammer, P.H., and Kirchhoff, S. (2001a). FLICE-inhibitory proteins: regulators of death receptor-mediated apoptosis. Mol Cell Biol *21*, 8247-8254.
Krueger, A., Schmitz, I., Baumann, S., Krammer, P.H., and Kirchhoff, S. (2001b). Cellular FLICE-inhibitory protein splice variants inhibit different steps of caspase-8 activation at the CD95 death-inducing signaling complex. J Biol Chem *276*, 20633-20640.
Kumari, S., Redouane, Y., Lopez-Mosqueda, J., Shiraishi, R., Romanowska, M., Lutzmayer, S., Kuiper, J., Martinez, C., Dikic, I., Pasparakis, M., *et al.* (2014). Sharpin prevents skin inflammation by inhibiting TNFR1-induced keratinocyte apoptosis. Elife *3*.
Kurokawa, M., and Kornbluth, S. (2009). Caspases and kinases in a death grip. Cell *138*, 838-854.
LaCava, J., Molloy, K.R., Taylor, M.S., Domanski, M., Chait, B.T., and Rout, M.P. (2015). Affinity proteomics to study endogenous protein complexes: pointers, pitfalls, preferences and perspectives. Biotechniques *58*, 103-119.
Lafont, E., Draber, P., Rieser, E., Reichert, M., Kupka, S., de Miguel, D., Draberova, H., von Massenhausen, A., Bhamra, A., Henderson, S., *et al.* (2018). TBK1 and IKKepsilon prevent TNF-induced cell death by RIPK1 phosphorylation. Nat Cell Biol *20*, 1389-1399.
Lalaoui, N., Boyden, S.E., Oda, H., Wood, G.M., Stone, D.L., Chau, D., Liu, L., Stoffels, M., Kratina, T., Lawlor, K.E., *et al.* (2020). Mutations that prevent caspase cleavage of RIPK1 cause autoinflammatory disease. Nature *577*, 103-108.
Lalaoui, N., Hanggi, K., Brumatti, G., Chau, D., Nguyen, N.Y., Vasilikos, L., Spilgies, L.M., Heckmann, D.A., Ma, C., Ghisi, M., *et al.* (2016). Targeting p38 or MK2 Enhances the Anti-Leukemic Activity of Smac-Mimetics. Cancer Cell *29*, 145-158.
Lalaoui, N., and Vaux, D.L. (2018). Recent advances in understanding inhibitor of apoptosis proteins. F1000Res *7*.
Lamkanfi, M., Declercq, W., Vanden Berghe, T., and Vandenabeele, P. (2006). Caspases leave the beaten track: caspase-mediated activation of NF-kappaB. J Cell Biol *173*, 165-171.
Lau, T., Chan, E., Callow, M., Waaler, J., Boggs, J., Blake, R.A., Magnuson, S., Sambrone, A., Schutten, M., Firestein, R., *et al.* (2013). A novel tankyrase small-molecule inhibitor suppresses APC mutation-driven colorectal tumor growth. Cancer Res *73*, 3132-3144.
Lavrik, I., Krueger, A., Schmitz, I., Baumann, S., Weyd, H., Krammer, P.H., and Kirchhoff, S. (2003). The active caspase-8 heterotetramer is formed at the CD95 DISC. Cell Death Differ *10*, 144-145.
Lazebnik, Y.A., Kaufmann, S.H., Desnoyers, S., Poirier, G.G., and Earnshaw, W.C. (1994). Cleavage of poly(ADP-ribose) polymerase by a proteinase with properties like ICE. Nature *371*, 346-347.

Lehtio, L., Chi, N.W., and Krauss, S. (2013). Tankyrases as drug targets. FEBS J *280*, 3576-3593.
Lehtio, L., Collins, R., van den Berg, S., Johansson, A., Dahlgren, L.G., Hammarstrom, M., Helleday, T., Holmberg-Schiavone, L., Karlberg, T., and Weigelt, J. (2008). Zinc binding catalytic domain of human tankyrase 1. J Mol Biol *379*, 136-145.
Leidecker, O., Bonfiglio, J.J., Colby, T., Zhang, Q., Atanassov, I., Zaja, R., Palazzo, L., Stockum, A., Ahel, I., and Matic, I. (2016). Serine is a new target residue for endogenous ADP-ribosylation on histones. Nat Chem Biol *12*, 998-1000.
Lemmers, B., Salmena, L., Bidere, N., Su, H., Matysiak-Zablocki, E., Murakami, K., Ohashi, P.S., Jurisicova, A., Lenardo, M., Hakem, R., *et al.* (2007). Essential role for caspase-8 in Toll-like receptors and NFkappaB signaling. J Biol Chem *282*, 7416-7423.
Levaot, N., Voytyuk, O., Dimitriou, I., Sircoulomb, F., Chandrakumar, A., Deckert, M., Krzyzanowski, P.M., Scotter, A., Gu, S., Janmohamed, S., *et al.* (2011). Loss of Tankyrase-mediated destruction of 3BP2 is the underlying pathogenic mechanism of cherubism. Cell *147*, 1324-1339.
Li, L., Thomas, R.M., Suzuki, H., De Brabander, J.K., Wang, X., and Harran, P.G. (2004). A small molecule Smac mimic potentiates TRAIL- and TNFalpha-mediated cell death. Science *305*, 1471-1474.
Li, N., Wang, Y., Neri, S., Zhen, Y., Fong, L.W.R., Qiao, Y., Li, X., Chen, Z., Stephan, C., Deng, W., *et al.* (2019). Tankyrase disrupts metabolic homeostasis and promotes tumorigenesis by inhibiting LKB1-AMPK signalling. Nat Commun *10*, 4363.
Li, N., Zhang, Y., Han, X., Liang, K., Wang, J., Feng, L., Wang, W., Songyang, Z., Lin, C., Yang, L., *et al.* (2015). Poly-ADP ribosylation of PTEN by tankyrases promotes PTEN degradation and tumor growth. Genes Dev *29*, 157-170.
Li, P., Huang, P., Li, X., Yin, D., Ma, Z., Wang, H., and Song, H. (2018). Tankyrase Mediates K63-Linked Ubiquitination of JNK to Confer Stress Tolerance and Influence Lifespan in Drosophila. Cell Rep *25*, 437-448.
Li, S., Zhang, L., Yao, Q., Li, L., Dong, N., Rong, J., Gao, W., Ding, X., Sun, L., Chen, X., *et al.* (2013). Pathogen blocks host death receptor signalling by arginine GlcNAcylation of death domains. Nature *501*, 242-246.
Li, V.S., Ng, S.S., Boersema, P.J., Low, T.Y., Karthaus, W.R., Gerlach, J.P., Mohammed, S., Heck, A.J., Maurice, M.M., Mahmoudi, T., *et al.* (2012a). Wnt signaling through inhibition of beta-catenin degradation in an intact Axin1 complex. Cell *149*, 1245-1256.
Li, Z., Yamauchi, Y., Kamakura, M., Murayama, T., Goshima, F., Kimura, H., and Nishiyama, Y. (2012b). Herpes simplex virus requires poly(ADP-ribose) polymerase activity for efficient replication and induces extracellular signal-related kinase-dependent phosphorylation and ICP0-dependent nuclear localization of tankyrase 1. J Virol *86*, 492-503.
Liccardi, G., Ramos Garcia, L., Tenev, T., Annibaldi, A., Legrand, A.J., Robertson, D., Feltham, R., Anderton, H., Darding, M., Peltzer, N., *et al.* (2019). RIPK1 and Caspase-8 Ensure Chromosome Stability Independently of Their Role in Cell Death and Inflammation. Mol Cell *73*, 413-428 e417.
Lin, Q., Wang, J., Childress, C., Sudol, M., Carey, D.J., and Yang, W. (2010). HECT E3 ubiquitin ligase Nedd4-1 ubiquitinates ACK and regulates epidermal growth factor (EGF)-induced degradation of EGF receptor and ACK. Mol Cell Biol *30*, 1541-1554.
Lin, W., Ame, J.C., Aboul-Ela, N., Jacobson, E.L., and Jacobson, M.K. (1997). Isolation and characterization of the cDNA encoding bovine poly(ADP-ribose) glycohydrolase. J Biol Chem *272*, 11895-11901.
Lin, Y., Devin, A., Rodriguez, Y., and Liu, Z.G. (1999). Cleavage of the death domain kinase RIP by caspase-8 prompts TNF-induced apoptosis. Genes Dev *13*, 2514-2526.

Liu, C., Vyas, A., Kassab, M.A., Singh, A.K., and Yu, X. (2017). The role of poly ADP-ribosylation in the first wave of DNA damage response. Nucleic Acids Res *45*, 8129-8141.
Liu, L., and Lalaoui, N. (2020). 25 years of research put RIPK1 in the clinic. Seminars in Cell and Developmental Biology *In press*, In press.
Ma, B., and Hottiger, M.O. (2016). Crosstalk between Wnt/beta-Catenin and NF-kappaB Signaling Pathway during Inflammation. Front Immunol *7*, 378.
MacFarlane, M., Merrison, W., Dinsdale, D., and Cohen, G.M. (2000). Active caspases and cleaved cytokeratins are sequestered into cytoplasmic inclusions in TRAIL-induced apoptosis. J Cell Biol *148*, 1239-1254.
Mandal, P., Berger, S.B., Pillay, S., Moriwaki, K., Huang, C., Guo, H., Lich, J.D., Finger, J., Kasparcova, V., Votta, B., *et al.* (2014). RIP3 induces apoptosis independent of pronecrotic kinase activity. Mol Cell *56*, 481-495.
Mariotti, L., Templeton, C.M., Ranes, M., Paracuellos, P., Cronin, N., Beuron, F., Morris, E., and Guettler, S. (2016). Tankyrase Requires SAM Domain-Dependent Polymerization to Support Wnt-beta-Catenin Signaling. Mol Cell *63*, 498-513.
Martello, R., Leutert, M., Jungmichel, S., Bilan, V., Larsen, S.C., Young, C., Hottiger, M.O., and Nielsen, M.L. (2016). Proteome-wide identification of the endogenous ADP-ribosylome of mammalian cells and tissue. Nat Commun *7*, 12917.
Matsumoto, Y., Larose, J., Kent, O.A., Lim, M., Changoor, A., Zhang, L., Storozhuk, Y., Mao, X., Grynpas, M.D., Cong, F., *et al.* (2017). RANKL coordinates multiple osteoclastogenic pathways by regulating expression of ubiquitin ligase RNF146. J Clin Invest *127*, 1303-1315.
Matthess, Y., Raab, M., Sanhaji, M., Lavrik, I.N., and Strebhardt, K. (2010). Cdk1/cyclin B1 controls Fas-mediated apoptosis by regulating caspase-8 activity. Mol Cell Biol *30*, 5726-5740.
McGurk, L., Rifai, O.M., and Bonini, N.M. (2020). TDP-43, a protein central to amyotrophic lateral sclerosis, is destabilized by tankyrase-1 and -2. J Cell Sci *133*.
McIlwain, D.R., Berger, T., and Mak, T.W. (2015). Caspase functions in cell death and disease. Cold Spring Harb Perspect Biol *7*.
Micheau, O., Lens, S., Gaide, O., Alevizopoulos, K., and Tschopp, J. (2001). NF-kappaB signals induce the expression of c-FLIP. Mol Cell Biol *21*, 5299-5305.
Micheau, O., Thome, M., Schneider, P., Holler, N., Tschopp, J., Nicholson, D.W., Briand, C., and Grutter, M.G. (2002). The long form of FLIP is an activator of caspase-8 at the Fas death-inducing signaling complex. J Biol Chem *277*, 45162-45171.
Micheau, O., and Tschopp, J. (2003). Induction of TNF receptor I-mediated apoptosis via two sequential signaling complexes. Cell *114*, 181-190.
Moquin, D.M., McQuade, T., and Chan, F.K. (2013). CYLD deubiquitinates RIP1 in the TNFalpha-induced necrosome to facilitate kinase activation and programmed necrosis. PLoS One *8*, e76841.
Morin, P.J., Sparks, A.B., Korinek, V., Barker, N., Clevers, H., Vogelstein, B., and Kinzler, K.W. (1997). Activation of beta-catenin-Tcf signaling in colon cancer by mutations in beta-catenin or APC. Science *275*, 1787-1790.
Moulin, M., Anderton, H., Voss, A.K., Thomas, T., Wong, W.W., Bankovacki, A., Feltham, R., Chau, D., Cook, W.D., Silke, J., *et al.* (2012). IAPs limit activation of RIP kinases by TNF receptor 1 during development. The EMBO journal *31*, 1679-1691.
Murch, S.H., Braegger, C.P., Walker-Smith, J.A., and MacDonald, T.T. (1993). Location of tumour necrosis factor alpha by immunohistochemistry in chronic inflammatory bowel disease. Gut *34*, 1705-1709.
Murphy, J.M., Czabotar, P.E., Hildebrand, J.M., Lucet, I.S., Zhang, J.G., Alvarez-Diaz, S., Lewis, R., Lalaoui, N., Metcalf, D., Webb, A.I., *et al.* (2013). The pseudokinase MLKL mediates necroptosis via a molecular switch mechanism. Immunity *39*, 443-453.

Murphy, J.M., and Silke, J. (2014). Ars Moriendi; the art of dying well - new insights into the molecular pathways of necroptotic cell death. EMBO Rep *15*, 155-164.
Narwal, M., Venkannagari, H., and Lehtio, L. (2012). Structural basis of selective inhibition of human tankyrases. J Med Chem *55*, 1360-1367.
Newton, K., Dugger, D.L., Wickliffe, K.E., Kapoor, N., de Almagro, M.C., Vucic, D., Komuves, L., Ferrando, R.E., French, D.M., Webster, J., *et al.* (2014). Activity of protein kinase RIPK3 determines whether cells die by necroptosis or apoptosis. Science *343*, 1357-1360.
Newton, K., Wickliffe, K.E., Dugger, D.L., Maltzman, A., Roose-Girma, M., Dohse, M., Komuves, L., Webster, J.D., and Dixit, V.M. (2019). Cleavage of RIPK1 by caspase-8 is crucial for limiting apoptosis and necroptosis. Nature *574*, 428-431.
Oberst, A., Dillon, C.P., Weinlich, R., McCormick, L.L., Fitzgerald, P., Pop, C., Hakem, R., Salvesen, G.S., and Green, D.R. (2011). Catalytic activity of the caspase-8-FLIP(L) complex inhibits RIPK3-dependent necrosis. Nature *471*, 363-367.
Oberst, A., Pop, C., Tremblay, A.G., Blais, V., Denault, J.B., Salvesen, G.S., and Green, D.R. (2010). Inducible dimerization and inducible cleavage reveal a requirement for both processes in caspase-8 activation. J Biol Chem *285*, 16632-16642.
Okada-Iwasaki, R., Takahashi, Y., Watanabe, Y., Ishida, H., Saito, J., Nakai, R., and Asai, A. (2016). The Discovery and Characterization of K-756, a Novel Wnt/beta-Catenin Pathway Inhibitor Targeting Tankyrase. Mol Cancer Ther *15*, 1525-1534.
Oliver, F.J., Menissier-de Murcia, J., Nacci, C., Decker, P., Andriantsitohaina, R., Muller, S., de la Rubia, G., Stoclet, J.C., and de Murcia, G. (1999). Resistance to endotoxic shock as a consequence of defective NF-kappaB activation in poly (ADP-ribose) polymerase-1 deficient mice. EMBO J *18*, 4446-4454.
Onizawa, M., Oshima, S., Schulze-Topphoff, U., Oses-Prieto, J.A., Lu, T., Tavares, R., Prodhomme, T., Duong, B., Whang, M.I., Advincula, R., *et al.* (2015). The ubiquitin-modifying enzyme A20 restricts ubiquitination of the kinase RIPK3 and protects cells from necroptosis. Nat Immunol *16*, 618-627.
Ozaki, Y., Matsui, H., Asou, H., Nagamachi, A., Aki, D., Honda, H., Yasunaga, S., Takihara, Y., Yamamoto, T., Izumi, S., *et al.* (2012). Poly-ADP ribosylation of Miki by tankyrase-1 promotes centrosome maturation. Mol Cell *47*, 694-706.
Palazzo, L., Leidecker, O., Prokhorova, E., Dauben, H., Matic, I., and Ahel, I. (2018). Serine is the major residue for ADP-ribosylation upon DNA damage. Elife *7*.
Palazzo, L., Mikoc, A., and Ahel, I. (2017). ADP-ribosylation: new facets of an ancient modification. FEBS J *284*, 2932-2946.
Palazzo, L., Mikolcevic, P., Mikoc, A., and Ahel, I. (2019). ADP-ribosylation signalling and human disease. Open Biol *9*, 190041.
Palm, W., and de Lange, T. (2008). How shelterin protects mammalian telomeres. Annu Rev Genet *42*, 301-334.
Pasparakis, M., and Vandenabeele, P. (2015). Necroptosis and its role in inflammation. Nature *517*, 311-320.
Patki, V., Buxton, J., Chawla, A., Lifshitz, L., Fogarty, K., Carrington, W., Tuft, R., and Corvera, S. (2001). Insulin action on GLUT4 traffic visualized in single 3T3-l1 adipocytes by using ultra-fast microscopy. Mol Biol Cell *12*, 129-141.
Pearson, J.S., Giogha, C., Ong, S.Y., Kennedy, C.L., Kelly, M., Robinson, K.S., Lung, T.W., Mansell, A., Riedmaier, P., Oates, C.V., *et al.* (2013). A type III effector antagonizes death receptor signalling during bacterial gut infection. Nature *501*, 247-251.
Peltzer, N., Darding, M., Montinaro, A., Draber, P., Draberova, H., Kupka, S., Rieser, E., Fisher, A., Hutchinson, C., Taraborrelli, L., *et al.* (2018). LUBAC is essential for embryogenesis by preventing cell death and enabling haematopoiesis. Nature *557*, 112-117.

Peltzer, N., Rieser, E., Taraborrelli, L., Draber, P., Darding, M., Pernaute, B., Shimizu, Y., Sarr, A., Draberova, H., Montinaro, A., *et al.* (2014). HOIP deficiency causes embryonic lethality by aberrant TNFR1-mediated endothelial cell death. Cell Rep *9*, 153-165.
Peng, C., Cho, Y.Y., Zhu, F., Zhang, J., Wen, W., Xu, Y., Yao, K., Ma, W.Y., Bode, A.M., and Dong, Z. (2011). Phosphorylation of caspase-8 (Thr-263) by ribosomal S6 kinase 2 (RSK2) mediates caspase-8 ubiquitination and stability. J Biol Chem *286*, 6946-6954.
Petersen, S.L., Wang, L., Yalcin-Chin, A., Li, L., Peyton, M., Minna, J., Harran, P., and Wang, X. (2007). Autocrine TNFalpha signaling renders human cancer cells susceptible to Smac-mimetic-induced apoptosis. Cancer Cell *12*, 445-456.
Petrilli, V., Herceg, Z., Hassa, P.O., Patel, N.S., Di Paola, R., Cortes, U., Dugo, L., Filipe, H.M., Thiemermann, C., Hottiger, M.O., *et al.* (2004). Noncleavable poly(ADP-ribose) polymerase-1 regulates the inflammation response in mice. J Clin Invest *114*, 1072-1081.
Piguet, P.F., Grau, G.E., Vesin, C., Loetscher, H., Gentz, R., and Lesslauer, W. (1992). Evolution of collagen arthritis in mice is arrested by treatment with anti-tumour necrosis factor (TNF) antibody or a recombinant soluble TNF receptor. Immunology *77*, 510-514.
Pobezinskaya, Y.L., Kim, Y.S., Choksi, S., Morgan, M.J., Li, T., Liu, C., and Liu, Z. (2008). The function of TRADD in signaling through tumor necrosis factor receptor 1 and TRIF-dependent Toll-like receptors. Nat Immunol *9*, 1047-1054.
Pop, C., Fitzgerald, P., Green, D.R., and Salvesen, G.S. (2007). Role of proteolysis in caspase-8 activation and stabilization. Biochemistry *46*, 4398-4407.
Powell, S.M., Zilz, N., Beazer-Barclay, Y., Bryan, T.M., Hamilton, S.R., Thibodeau, S.N., Vogelstein, B., and Kinzler, K.W. (1992). APC mutations occur early during colorectal tumorigenesis. Nature *359*, 235-237.
Powley, I.R., Hughes, M.A., Cain, K., and MacFarlane, M. (2016). Caspase-8 tyrosine-380 phosphorylation inhibits CD95 DISC function by preventing procaspase-8 maturation and cycling within the complex. Oncogene *35*, 5629-5640.
Remijsen, Q., Goossens, V., Grootjans, S., Van den Haute, C., Vanlangenakker, N., Dondelinger, Y., Roelandt, R., Bruggeman, I., Goncalves, A., Bertrand, M.J., *et al.* (2014). Depletion of RIPK3 or MLKL blocks TNF-driven necroptosis and switches towards a delayed RIPK1 kinase-dependent apoptosis. Cell Death Dis *5*, e1004.
Riccio, A.A., McCauley, M., Langelier, M.F., and Pascal, J.M. (2016). Tankyrase Sterile alpha Motif Domain Polymerization Is Required for Its Role in Wnt Signaling. Structure *24*, 1573-1581.
Rickard, J.A., Anderton, H., Etemadi, N., Nachbur, U., Darding, M., Peltzer, N., Lalaoui, N., Lawlor, K.E., Vanyai, H., Hall, C., *et al.* (2014). TNFR1-dependent cell death drives inflammation in Sharpin-deficient mice. Elife *3*.
Riffell, J.L., Lord, C.J., and Ashworth, A. (2012). Tankyrase-targeted therapeutics: expanding opportunities in the PARP family. Nat Rev Drug Discov *11*, 923-936.
Rosenthal, F., and Hottiger, M.O. (2014). Identification of ADP-ribosylated peptides and ADP-ribose acceptor sites. Front Biosci (Landmark Ed) *19*, 1041-1056.
Rowlands, D.J., Islam, M.N., Das, S.R., Huertas, A., Quadri, S.K., Horiuchi, K., Inamdar, N., Emin, M.T., Lindert, J., Ten, V.S., *et al.* (2011). Activation of TNFR1 ectodomain shedding by mitochondrial Ca2+ determines the severity of inflammation in mouse lung microvessels. J Clin Invest *121*, 1986-1999.
Saleh-Gohari, N., Bryant, H.E., Schultz, N., Parker, K.M., Cassel, T.N., and Helleday, T. (2005). Spontaneous homologous recombination is induced by collapsed replication forks that are caused by endogenous DNA single-strand breaks. Mol Cell Biol *25*, 7158-7169.
Salmena, L., Lemmers, B., Hakem, A., Matysiak-Zablocki, E., Murakami, K., Au, P.Y., Berry, D.M., Tamblyn, L., Shehabeldin, A., Migon, E., *et al.* (2003). Essential role for caspase 8 in T-cell homeostasis and T-cell-mediated immunity. Genes Dev *17*, 883-895.

Salvesen, G.S., and Duckett, C.S. (2002). IAP proteins: blocking the road to death's door. Nat Rev Mol Cell Biol *3*, 401-410.
Scaffidi, C., Medema, J.P., Krammer, P.H., and Peter, M.E. (1997). FLICE is predominantly expressed as two functionally active isoforms, caspase-8/a and caspase-8/b. J Biol Chem *272*, 26953-26958.
Scaffidi, C., Schmitz, I., Krammer, P.H., and Peter, M.E. (1999). The role of c-FLIP in modulation of CD95-induced apoptosis. J Biol Chem *274*, 1541-1548.
Schleich, K., Warnken, U., Fricker, N., Ozturk, S., Richter, P., Kammerer, K., Schnolzer, M., Krammer, P.H., and Lavrik, I.N. (2012). Stoichiometry of the CD95 death-inducing signaling complex: experimental and modeling evidence for a death effector domain chain model. Mol Cell *47*, 306-319.
Schuster, S., Roessler, C., Meleshin, M., Zimmermann, P., Simic, Z., Kambach, C., Schiene-Fischer, C., Steegborn, C., Hottiger, M.O., and Schutkowski, M. (2016). A continuous sirtuin activity assay without any coupling to enzymatic or chemical reactions. Sci Rep *6*, 22643.
Senft, J., Helfer, B., and Frisch, S.M. (2007). Caspase-8 interacts with the p85 subunit of phosphatidylinositol 3-kinase to regulate cell adhesion and motility. Cancer Res *67*, 11505-11509.
Seyrek, K., Ivanisenko, N.V., Richter, M., Hillert, L.K., Konig, C., and Lavrik, I.N. (2020). Controlling Cell Death through Post-translational Modifications of DED Proteins. Trends Cell Biol *30*, 354-369.
Sharifi, R., Morra, R., Appel, C.D., Tallis, M., Chioza, B., Jankevicius, G., Simpson, M.A., Matic, I., Ozkan, E., Golia, B., *et al.* (2013). Deficiency of terminal ADP-ribose protein glycohydrolase TARG1/C6orf130 in neurodegenerative disease. EMBO J *32*, 1225-1237.
Shen, Y., Aoyagi-Scharber, M., and Wang, B. (2015). Trapping Poly(ADP-Ribose) Polymerase. J Pharmacol Exp Ther *353*, 446-457.
Shultz, M.D., Cheung, A.K., Kirby, C.A., Firestone, B., Fan, J., Chen, C.H., Chen, Z., Chin, D.N., Dipietro, L., Fazal, A., *et al.* (2013). Identification of NVP-TNKS656: the use of structure-efficiency relationships to generate a highly potent, selective, and orally active tankyrase inhibitor. J Med Chem *56*, 6495-6511.
Silke, J. (2011). The regulation of TNF signalling: what a tangled web we weave. Curr Opin Immunol *23*, 620-626.
Silke, J., and Meier, P. (2013). Inhibitor of apoptosis (IAP) proteins-modulators of cell death and inflammation. Cold Spring Harb Perspect Biol *5*.
Silke, J., Rickard, J.A., and Gerlic, M. (2015). The diverse role of RIP kinases in necroptosis and inflammation. Nature immunology *16*, 689-697.
Silke, J., and Vucic, D. (2014). IAP family of cell death and signaling regulators. Methods Enzymol *545*, 35-65.
Slade, D., Dunstan, M.S., Barkauskaite, E., Weston, R., Lafite, P., Dixon, N., Ahel, M., Leys, D., and Ahel, I. (2011). The structure and catalytic mechanism of a poly(ADP-ribose) glycohydrolase. Nature *477*, 616-620.
Smith, S., and de Lange, T. (2000). Tankyrase promotes telomere elongation in human cells. Curr Biol *10*, 1299-1302.
Smith, S., Giriat, I., Schmitt, A., and de Lange, T. (1998). Tankyrase, a poly(ADP-ribose) polymerase at human telomeres. Science *282*, 1484-1487.
Soldani, C., and Scovassi, A.I. (2002). Poly(ADP-ribose) polymerase-1 cleavage during apoptosis: an update. Apoptosis *7*, 321-328.
Sonar, S., and Lal, G. (2015). Role of Tumor Necrosis Factor Superfamily in Neuroinflammation and Autoimmunity. Front Immunol *6*, 364.

Sordet, O., Rebe, C., Plenchette, S., Zermati, Y., Hermine, O., Vainchenker, W., Garrido, C., Solary, E., and Dubrez-Daloz, L. (2002). Specific involvement of caspases in the differentiation of monocytes into macrophages. Blood *100*, 4446-4453.
Soung, Y.H., Lee, J.W., Kim, S.Y., Jang, J., Park, Y.G., Park, W.S., Nam, S.W., Lee, J.Y., Yoo, N.J., and Lee, S.H. (2005a). CASPASE-8 gene is inactivated by somatic mutations in gastric carcinomas. Cancer Res *65*, 815-821.
Soung, Y.H., Lee, J.W., Kim, S.Y., Sung, Y.J., Park, W.S., Nam, S.W., Kim, S.H., Lee, J.Y., Yoo, N.J., and Lee, S.H. (2005b). Caspase-8 gene is frequently inactivated by the frameshift somatic mutation 1225_1226delTG in hepatocellular carcinomas. Oncogene *24*, 141-147.
Sprick, M.R., Rieser, E., Stahl, H., Grosse-Wilde, A., Weigand, M.A., and Walczak, H. (2002). Caspase-10 is recruited to and activated at the native TRAIL and CD95 death-inducing signalling complexes in a FADD-dependent manner but can not functionally substitute caspase-8. EMBO J *21*, 4520-4530.
Stephens, P.J., Tarpey, P.S., Davies, H., Van Loo, P., Greenman, C., Wedge, D.C., Nik-Zainal, S., Martin, S., Varela, I., Bignell, G.R., *et al.* (2012). The landscape of cancer genes and mutational processes in breast cancer. Nature *486*, 400-404.
Su, H., Bidere, N., Zheng, L., Cubre, A., Sakai, K., Dale, J., Salmena, L., Hakem, R., Straus, S., and Lenardo, M. (2005). Requirement for caspase-8 in NF-kappaB activation by antigen receptor. Science *307*, 1465-1468.
Sun, L., Wang, H., Wang, Z., He, S., Chen, S., Liao, D., Wang, L., Yan, J., Liu, W., Lei, X., *et al.* (2012). Mixed lineage kinase domain-like protein mediates necrosis signaling downstream of RIP3 kinase. Cell *148*, 213-227.
Sun, X., Lee, J., Navas, T., Baldwin, D.T., Stewart, T.A., and Dixit, V.M. (1999). RIP3, a novel apoptosis-inducing kinase. J Biol Chem *274*, 16871-16875.
Suzuki, S., Suzuki, T., Mimuro, H., Mizushima, T., and Sasakawa, C. (2018). Shigella hijacks the glomulin-cIAPs-inflammasome axis to promote inflammation. EMBO Rep *19*, 89-101.
Tanzer, M.C., Matti, I., Hildebrand, J.M., Young, S.N., Wardak, A., Tripaydonis, A., Petrie, E.J., Mildenhall, A.L., Vaux, D.L., Vince, J.E., *et al.* (2016). Evolutionary divergence of the necroptosis effector MLKL. Cell Death Differ *23*, 1185-1197.
Tao, P., Sun, J., Wu, Z., Wang, S., Wang, J., Li, W., Pan, H., Bai, R., Zhang, J., Wang, Y., *et al.* (2020). A dominant autoinflammatory disease caused by non-cleavable variants of RIPK1. Nature *577*, 109-114.
Teitz, T., Wei, T., Valentine, M.B., Vanin, E.F., Grenet, J., Valentine, V.A., Behm, F.G., Look, A.T., Lahti, J.M., and Kidd, V.J. (2000). Caspase 8 is deleted or silenced preferentially in childhood neuroblastomas with amplification of MYCN. Nat Med *6*, 529-535.
Tenev, T., Bianchi, K., Darding, M., Broemer, M., Langlais, C., Wallberg, F., Zachariou, A., Lopez, J., MacFarlane, M., Cain, K., *et al.* (2011). The Ripoptosome, a signaling platform that assembles in response to genotoxic stress and loss of IAPs. Mol Cell *43*, 432-448.
Thorbecke, G.J., Shah, R., Leu, C.H., Kuruvilla, A.P., Hardison, A.M., and Palladino, M.A. (1992). Involvement of endogenous tumor necrosis factor alpha and transforming growth factor beta during induction of collagen type II arthritis in mice. Proc Natl Acad Sci U S A *89*, 7375-7379.
Thornberry, N.A., and Lazebnik, Y. (1998). Caspases: enemies within. Science *281*, 1312-1316.
Thorsell, A.G., Ekblad, T., Karlberg, T., Low, M., Pinto, A.F., Tresaugues, L., Moche, M., Cohen, M.S., and Schuler, H. (2017). Structural Basis for Potency and Promiscuity in Poly(ADP-ribose) Polymerase (PARP) and Tankyrase Inhibitors. J Med Chem *60*, 1262-1271.
Thorvaldsen, T.E. (2017). Targeting Tankyrase to Fight WNT-dependent Tumours. Basic Clin Pharmacol Toxicol *121*, 81-88.

Torres, V.A., Mielgo, A., Barila, D., Anderson, D.H., and Stupack, D. (2008). Caspase 8 promotes peripheral localization and activation of Rab5. J Biol Chem *283*, 36280-36289.
Tripathi, E., and Smith, S. (2017). Cell cycle-regulated ubiquitination of tankyrase 1 by RNF8 and ABRO1/BRCC36 controls the timing of sister telomere resolution. EMBO J *36*, 503-519.
Tsuchiya, Y., Nakabayashi, O., and Nakano, H. (2015). FLIP the Switch: Regulation of Apoptosis and Necroptosis by cFLIP. Int J Mol Sci *16*, 30321-30341.
Tummers, B., Mari, L., Guy, C.S., Heckmann, B.L., Rodriguez, D.A., Ruhl, S., Moretti, J., Crawford, J.C., Fitzgerald, P., Kanneganti, T.D., *et al.* (2020). Caspase-8-Dependent Inflammatory Responses Are Controlled by Its Adaptor, FADD, and Necroptosis. Immunity *52*, 994-1006 e1008.
Ueki, Y., Tiziani, V., Santanna, C., Fukai, N., Maulik, C., Garfinkle, J., Ninomiya, C., doAmaral, C., Peters, H., Habal, M., *et al.* (2001). Mutations in the gene encoding c-Abl-binding protein SH3BP2 cause cherubism. Nat Genet *28*, 125-126.
Vanamee, E.S., and Faustman, D.L. (2018). Structural principles of tumor necrosis factor superfamily signaling. Sci Signal *11*.
Vanden Berghe, T., Kaiser, W.J., Bertrand, M.J., and Vandenabeele, P. (2015). Molecular crosstalk between apoptosis, necroptosis, and survival signaling. Mol Cell Oncol *2*, e975093.
Vandenabeele, P., Galluzzi, L., Vanden Berghe, T., and Kroemer, G. (2010). Molecular mechanisms of necroptosis: an ordered cellular explosion. Nat Rev Mol Cell Biol *11*, 700-714.
Varfolomeev, E., Blankenship, J.W., Wayson, S.M., Fedorova, A.V., Kayagaki, N., Garg, P., Zobel, K., Dynek, J.N., Elliott, L.O., Wallweber, H.J., *et al.* (2007). IAP antagonists induce autoubiquitination of c-IAPs, NF-kappaB activation, and TNFalpha-dependent apoptosis. Cell *131*, 669-681.
Varfolomeev, E., Maecker, H., Sharp, D., Lawrence, D., Renz, M., Vucic, D., and Ashkenazi, A. (2005). Molecular determinants of kinase pathway activation by Apo2 ligand/tumor necrosis factor-related apoptosis-inducing ligand. J Biol Chem *280*, 40599-40608.
Varfolomeev, E.E., Schuchmann, M., Luria, V., Chiannilkulchai, N., Beckmann, J.S., Mett, I.L., Rebrikov, D., Brodianski, V.M., Kemper, O.C., Kollet, O., *et al.* (1998). Targeted disruption of the mouse Caspase 8 gene ablates cell death induction by the TNF receptors, Fas/Apo1, and DR3 and is lethal prenatally. Immunity *9*, 267-276.
Vince, J.E., Wong, W.W., Khan, N., Feltham, R., Chau, D., Ahmed, A.U., Benetatos, C.A., Chunduru, S.K., Condon, S.M., McKinlay, M., *et al.* (2007). IAP antagonists target cIAP1 to induce TNFalpha-dependent apoptosis. Cell *131*, 682-693.
Virag, L., Robaszkiewicz, A., Rodriguez-Vargas, J.M., and Oliver, F.J. (2013). Poly(ADP-ribose) signaling in cell death. Mol Aspects Med *34*, 1153-1167.
Waaler, J., Machon, O., Tumova, L., Dinh, H., Korinek, V., Wilson, S.R., Paulsen, J.E., Pedersen, N.M., Eide, T.J., Machonova, O., *et al.* (2012). A novel tankyrase inhibitor decreases canonical Wnt signaling in colon carcinoma cells and reduces tumor growth in conditional APC mutant mice. Cancer Res *72*, 2822-2832.
Waaler, J., Machon, O., von Kries, J.P., Wilson, S.R., Lundenes, E., Wedlich, D., Gradl, D., Paulsen, J.E., Machonova, O., Dembinski, J.L., *et al.* (2011). Novel synthetic antagonists of canonical Wnt signaling inhibit colorectal cancer cell growth. Cancer Res *71*, 197-205.
Wallis, R.S. (2011). Biologics and infections: lessons from tumor necrosis factor blocking agents. Infect Dis Clin North Am *25*, 895-910.
Wang, H., Meng, H., Li, X., Zhu, K., Dong, K., Mookhtiar, A.K., Wei, H., Li, Y., Sun, S.C., and Yuan, J. (2017). PELI1 functions as a dual modulator of necroptosis and apoptosis by regulating ubiquitination of RIPK1 and mRNA levels of c-FLIP. Proc Natl Acad Sci U S A *114*, 11944-11949.

Wang, H., Sun, L., Su, L., Rizo, J., Liu, L., Wang, L.F., Wang, F.S., and Wang, X. (2014). Mixed lineage kinase domain-like protein MLKL causes necrotic membrane disruption upon phosphorylation by RIP3. Mol Cell *54*, 133-146.
Wang, L., Du, F., and Wang, X. (2008). TNF-alpha induces two distinct caspase-8 activation pathways. Cell *133*, 693-703.
Wang, W., Li, N., Li, X., Tran, M.K., Han, X., and Chen, J. (2015). Tankyrase Inhibitors Target YAP by Stabilizing Angiomotin Family Proteins. Cell Rep *13*, 524-532.
Wang, Z., Michaud, G.A., Cheng, Z., Zhang, Y., Hinds, T.R., Fan, E., Cong, F., and Xu, W. (2012). Recognition of the iso-ADP-ribose moiety in poly(ADP-ribose) by WWE domains suggests a general mechanism for poly(ADP-ribosyl)ation-dependent ubiquitination. Genes Dev *26*, 235-240.
Watt, W., Koeplinger, K.A., Mildner, A.M., Heinrikson, R.L., Tomasselli, A.G., and Watenpaugh, K.D. (1999). The atomic-resolution structure of human caspase-8, a key activator of apoptosis. Structure *7*, 1135-1143.
Williams, R.O., Feldmann, M., and Maini, R.N. (1992). Anti-tumor necrosis factor ameliorates joint disease in murine collagen-induced arthritis. Proc Natl Acad Sci U S A *89*, 9784-9788.
Wu, X., Luo, F., Li, J., Zhong, X., and Liu, K. (2016). Tankyrase 1 inhibitior XAV939 increases chemosensitivity in colon cancer cell lines via inhibition of the Wnt signaling pathway. Int J Oncol *48*, 1333-1340.
Yang, H., Wang, H., Shivalila, C.S., Cheng, A.W., Shi, L., and Jaenisch, R. (2013a). One-step generation of mice carrying reporter and conditional alleles by CRISPR/Cas-mediated genome engineering. Cell *154*, 1370-1379.
Yang, S., Wang, B., Tang, L.S., Siednienko, J., Callanan, J.J., and Moynagh, P.N. (2013b). Pellino3 targets RIP1 and regulates the pro-apoptotic effects of TNF-alpha. Nat Commun *4*, 2583.
Yao, Z., Duan, S., Hou, D., Heese, K., and Wu, M. (2007). Death effector domain DEDa, a self-cleaved product of caspase-8/Mch5, translocates to the nucleus by binding to ERK1/2 and upregulates procaspase-8 expression via a p53-dependent mechanism. EMBO J *26*, 1068-1080.
Ye, J.Z., and de Lange, T. (2004). TIN2 is a tankyrase 1 PARP modulator in the TRF1 telomere length control complex. Nat Genet *36*, 618-623.
Yeh, T.Y., Beiswenger, K.K., Li, P., Bolin, K.E., Lee, R.M., Tsao, T.S., Murphy, A.N., Hevener, A.L., and Chi, N.W. (2009). Hypermetabolism, hyperphagia, and reduced adiposity in tankyrase-deficient mice. Diabetes *58*, 2476-2485.
Yeh, T.Y., Sbodio, J.I., and Chi, N.W. (2006). Mitotic phosphorylation of tankyrase, a PARP that promotes spindle assembly, by GSK3. Biochem Biophys Res Commun *350*, 574-579.
Yeh, T.Y., Sbodio, J.I., Nguyen, M.T., Meyer, T.N., Lee, R.M., and Chi, N.W. (2005). Tankyrase-1 overexpression reduces genotoxin-induced cell death by inhibiting PARP1. Mol Cell Biochem *276*, 183-192.
Yeh, W.C., de la Pompa, J.L., McCurrach, M.E., Shu, H.B., Elia, A.J., Shahinian, A., Ng, M., Wakeham, A., Khoo, W., Mitchell, K., *et al.* (1998). FADD: essential for embryo development and signaling from some, but not all, inducers of apoptosis. Science *279*, 1954-1958.
Yeh, W.C., Itie, A., Elia, A.J., Ng, M., Shu, H.B., Wakeham, A., Mirtsos, C., Suzuki, N., Bonnard, M., Goeddel, D.V., *et al.* (2000). Requirement for Casper (c-FLIP) in regulation of death receptor-induced apoptosis and embryonic development. Immunity *12*, 633-642.
Yi, M., Dong, B., Qin, S., Chu, Q., Wu, K., and Luo, S. (2019). Advances and perspectives of PARP inhibitors. Exp Hematol Oncol *8*, 29.
Yu, J.W., Jeffrey, P.D., and Shi, Y. (2009). Mechanism of procaspase-8 activation by c-FLIPL. Proc Natl Acad Sci U S A *106*, 8169-8174.
Yu, J.W., and Shi, Y. (2008). FLIP and the death effector domain family. Oncogene *27*, 6216-6227.

Yu, P.W., Huang, B.C., Shen, M., Quast, J., Chan, E., Xu, X., Nolan, G.P., Payan, D.G., and Luo, Y. (1999). Identification of RIP3, a RIP-like kinase that activates apoptosis and NFkappaB. Curr Biol *9*, 539-542.
Zamaraev, A.V., Kopeina, G.S., Prokhorova, E.A., Zhivotovsky, B., and Lavrik, I.N. (2017). Post-translational Modification of Caspases: The Other Side of Apoptosis Regulation. Trends Cell Biol *27*, 322-339.
Zelic, M., Roderick, J.E., O'Donnell, J.A., Lehman, J., Lim, S.E., Janardhan, H.P., Trivedi, C.M., Pasparakis, M., and Kelliher, M.A. (2018). RIP kinase 1-dependent endothelial necroptosis underlies systemic inflammatory response syndrome. J Clin Invest *128*, 2064-2075.
Zhang, X., Dowling, J.P., and Zhang, J. (2019). RIPK1 can mediate apoptosis in addition to necroptosis during embryonic development. Cell Death Dis *10*, 245.
Zhang, Y., Liu, S., Mickanin, C., Feng, Y., Charlat, O., Michaud, G.A., Schirle, M., Shi, X., Hild, M., Bauer, A., *et al.* (2011). RNF146 is a poly(ADP-ribose)-directed E3 ligase that regulates axin degradation and Wnt signalling. Nat Cell Biol *13*, 623-629.
Zhong, L., Yeh, T.Y., Hao, J., Pourtabatabaei, N., Mahata, S.K., Shao, J., Chessler, S.D., and Chi, N.W. (2015). Nutritional energy stimulates NAD+ production to promote tankyrase-mediated PARsylation in insulinoma cells. PLoS One *10*, e0122948.
Zhong, Y., Katavolos, P., Nguyen, T., Lau, T., Boggs, J., Sambrone, A., Kan, D., Merchant, M., Harstad, E., Diaz, D., *et al.* (2016). Tankyrase Inhibition Causes Reversible Intestinal Toxicity in Mice with a Therapeutic Index < 1. Toxicol Pathol *44*, 267-278.